THE UNSTEADY-STATE PERFORMANCE OF AN EXPERIMENTAL THERMAL REGENERATOR

by

N. G. CUTLAND, B.Sc., A.M.B.C.S.

A Thesis presented to

THE UNIVERSITY OF YORK

for the Degree of Doctor of Philosophy

DEPARTMENT OF COMPUTER SCIENCE

March 1984

LIST OF CONTENTS

List of Figures vii

Acknowledgements x

Abstract xi

Nomenclature xiii

CHAPTER 0

INTRODUCTION 1

CHAPTER 1

THE MATHEMATICAL MODEL 12

1.1 PLANE WALL IDEALISATION 12

1.2 THE 3D MODEL 15

1.3 REDUCTION OF THE 3D MODEL TO DIMENSIONLESS FORM 17

1.4 SIMPLIFICATION OF THE 3D MODEL TO 2D 19

1.5 REDUCTION OF THE 2D MODEL TO DIMENSIONLESS FORM 21

1.6 CYCLIC EQUILIBRIUM 22

1.7 TRANSIENT BEHAVIOUR 25

1.8 THE BULK HEAT TRANSFER COEFFICIENT 27

1.9 THE RECUPERATOR ANALOGY 31

1.10 THE PASCAL MODEL 34

CHAPTER 2

LITERATURE REVIEW 35

2.1 REGENERATOR SIMULATION METHODS (OPEN METHODS ONLY) 35

2.1.1 Finite Difference Methods 35

Willmott 35

Hausen 39

Haynes 40

2.1.2 Integral Methods 42

Nusselt; Nahavandi & Weinstein; Iliffe; Hilton 42

2.2 PREVIOUS WORK ON TRANSIENT BEHAVIOUR 45

2.2.1 Theoretical Work 46

London 46

Green 49

Haynes 51

Burns 51

Heggs & Mitchell 55

2.2.2 Experimental Work 57

Chao 57

Ajitsaria 58

Hollins 60

2.3 REGENERATOR CONTROL STRATEGIES 62

Katsura & Isobe 62

Kan 66

Kwakernaak et al 68

Stikker & Broekhuis; Strausz 75

Zuidema 79

Beets & Elshout 83

Holstein & Sanna 87

Burns 90

Jeffreson 94

Smith 97

2.4 GAS-PARTICLE HEAT TRANSFER IN PACKED BEDS 100

Furnas; Saunders & Ford 100

Denton et al 102

Meek; Shearer 104

Littman et al; Gliddon & Cranfield 107

Heggs & Handley; Yoshida 108

CHAPTER 3

EXPERIMENTAL EQUIPMENT 110

3.1 BEDS 111

3.2 FLOW SYSTEM 113

3.3 HEATING SYSTEM 117

3.4 TEMPERATURE MEASUREMENT 119

3.5 CONTROL AND DATALOGGING SYSTEM 120

3.5.1 Data Input 121

3.5.2 Data Output 122

3.6 CONTROL, MEASUREMENT AND SEQUENCING SOFTWARE 123

3.6.1 Flowrate Control 125

3.6.2 Data Collection and Averaging 129

3.6.3 Sequencing of Switching 129

3.6.4 Miscellaneous Software 130

3.7 REGENERATOR PARAMETERS 131

3.7.1 Heat Transfer Coefficient, Λ, Π 131

3.7.2 Flow Distribution 133

3.7.3 Gas Dwell Time 134

3.7.4 Hausen phi-factor, $\bar{h}/h$, K/K_o 135

CHAPTER 4

EXPERIMENTAL TECHNIQUE, PROCEDURE, MODELLING AND RESULTS 137

4.1 EXPERIMENTAL TECHNIQUE 137

4.2 EXPERIMENTAL PROCEDURE 143

4.2.1 Rig Operation 143

4.2.2 Data Processing 146

4.2.3 Simulations 148

4.3 CALIBRATIONS AND ERRORS 152

4.3.1 Flowrate Calibration 152

4.3.2 Thermocouple Calibration 156

4.3.3 Miscellaneous Calibrations 158

4.4 RESULTS 159

4.4.1 Apparatus Commissioning, Early Results 159

4.4.2 Summary of Experiments 164

CHAPTER 5

DISCUSSION OF RESULTS 169

5.1 GENERAL DISCUSSION 169

5.2 STEP CHANGES IN HOT GAS INLET TEMPERATURE ($\gamma = 1$) 179

5.3 STEP CHANGES IN HOT GAS INLET TEMPERATURE ($\gamma \neq 1$) 180

5.4 STEP CHANGES IN FLOWRATE 182

5.5 SIMULTANEOUS STEP CHANGES 186

5.6 OTHER RESULTS 188

CHAPTER 6

CONCLUSIONS 191

CHAPTER 7

FURTHER WORK 196

APPENDICES

A GRAPHS OF RESULTS 202

B HEAT LOSSES 203

C CURVE FITTING 206

D RIG CONTROL SOFTWARE 210

E PASCAL SIMULATION PROGRAM 216

F PROCESSING OF EXPERIMENTAL DATA 218

References 219

LIST OF FIGURES

0.1 A Recuperator 2

0.2 Mixed Mode Exchangers 3

0.3 A Rotary Regenerator 5

0.4 A Cowper Stove 7

0.5 Bypass Main Configuration 7

0.6 Bypass Main Operation 7

0.7 Staggered Parallel Configuration 8

0.8 Staggered Parallel Flowrates 8

1.1 Plane Wall Idealisation 13

1.2 Parabola Inversion 29

1.3 Hausen's K/K_o Curves 31

2.1 Willmott's Method 38

2.2 Movement to Equilibrium of a Regenerator with Large Thermal Inertia 38

2.3 Haynes' 2D/3D Results 40

2.4 London's Results (1) 47

2.5 London's Analogue 48

2.6 London's Results (2) 48

2.7 London's Results (3) 48

2.8 Burns' Results (1) 52

2.9 Burns' Results (2) 52

2.10 Burns' Results (3) 55

2.11 Chao's Results 58

2.12 Ajitsaria's Results 60

2.13 Kan's Furnace System 67

2.14 Staggered Parallel Operation 72

2.15 Staggered Parallel: Single Stove Behaviour 74

2.16 Computerised Stove System 79

2.17 Elimination of Wall Voidage 105

3.1 Regenerator System Layout 111

3.2 Regenerator Construction 113

3.3 Regenerator System Flow Circuits 114

3.4 Failsafe Circuit 119

3.5 Thermocouple Channels 122

3.6 Heat Transfer Coefficient vs. Flowrate 132

3.7 Λ vs. Flowrate 132

3.8 Π vs. Flowrate 132

3.9 Voidage Distribution 133

3.10 Flow Distribution 134

3.11 Temperature Distribution 134

4.1 Flow 2 Calibration Plot 153

4.2 Flow 3 Calibration Plot 153

4.3 Flow 5 Characteristics 155

4.4 Flow 6 Characteristics 155

5.1 Burns & Willmott Case I 186

5.2 Burns & Willmott Case II 186

5.3 Burns & Willmott Case III 186

5.4 Run 37B $t''_{x,m}$, Simulations with f = 1.0 188

5.5 Run 37B $t'_{x,m}$, Simulations with f = 1.0 188

5.6 Thermocouple Positioning 188

5.7 Experiment Timescale 189

A.1 - A.64 Results 202

F.1 - F.2 Experiment Data Processing 218

Plate 3.1 Regenerator System General View 111

Table 3.1 Matrix Data 112

Table 3.2 Transducer Zero-Set Codes 117

Table 3.3 Multiplexer Channel Assignments (1) 122

Table 3.4 Multiplexer Channel Assignments (2) 122

Table 3.5 Butterfly Valve Addresses 122

Table 3.6 Stop Valve Addresses 122

Table 4.1 Flowrate Calibration Constants 154

Table 4.2 Flowpath Characteristic Constants 155

Table 4.3 Heater Autotransformer Settings 159

Table 4.4 Summary of Experiments 164

Table 5.1 Category 2 Results 180

Table 5.2 Category 3 Results 184

Table 5.3 Category 4 Results 186

ACKNOWLEDGEMENTS

There are many people who have contributed directly or indirectly to the completion of this thesis. My supervisor, Dr. A. John Willmott, has provided advice, guidance and encouragement throughout the period of my research. His insistence that I 'deliver the goods' provided the impetus which was required from time to time, for which I am extremely grateful. Dr. A.E. Wraith of the University of Newcastle-upon-Tyne has been very generous with the time which he has spent helping me solve problems concerning the experimental apparatus. Dr. J.B. Harness of the University of Bradford has shown much interest during many inspiring meetings, and Professor I.C. Pyle has also offered much helpful advice.

I would like to thank the Technical Staff of the Departments of Computer Science and Physics and the Staff of the Computing Service for their assistance. I would also like to thank John Galloway for his help in the typing of the thesis. The financial assistance of the S.E.R.C. must also be acknowledged.

I have spent many helpful and enjoyable hours with my friends and colleagues, who have also contributed to the thesis. My parents have continually supported and encouraged me during my time at York, and I would like to thank them especially.

Finally, I would like to thank Kathy.

ABSTRACT

This thesis presents the results of experimental and theoretical studies which have been made of the unsteady-state performance of a thermal regenerator. The response of the regenerator has been investigated for step changes in various operating parameters, in particular gas flowrates and inlet temperatures. Experimental work was carried out on a four-bed computer controlled system, originally designed by Dr. A.E. Wraith, each bed being 0.4m long by 0.3m in diameter. Flowrates varied from 0.2 std. m^3/min to 0.8 std. m^3/min, and period times were constant at 600s. The system operated between room temperature and 150^{o}C nominal.

The gas exit temperatures from experiments were compared with those from computer simulations, and it was found that by using a multiplication factor (the 'f-factor') for the model's heat transfer coefficient, good correlations between theory and experiment could be obtained. A single value of the f-factor was found which resulted in good experiment/theoretical agreement for all of the conditions investigated.

The response of the regenerator to a step change in hot gas inlet temperature was found to be independent of gas flowrate for symmetrical conditions. The response proved to be independent of the degree of imbalance for unbalanced conditions, and although, at first sight, this is contradicted by previous theoretical work, it

is argued that the results of these experiments can be fully explained. The response of the regenerator to step changes in gas flowrate was found to depend solely upon the final conditions. The response to simultaneous step changes in different operating parameters was found to be as predicted by theory.

Extensive graphs of the results have been produced, and are presented in the Appendices.

NOMENCLATURE

a	bed voidage fraction
A	surface area of packing, m^2
Bi	Biot modulus (= hw/λ)
C	specific heat of solid, J/kg^oC
d	particle diameter, m
D	bed diameter, m
E	thermal ratio, dimensionless
f	multiplication factor for heat transfer coefficient
G	superficial gas mass flowrate, kg/m^2 s
h	heat transfer coefficient, $W/m^2\,^oC$
$\bar{h}$	bulk heat transfer coefficient, $W/m^2\,^oC$
j_H	Colburn j-factor (= $St.Pr^{2/3}$)
k	gas thermal conductivity, $W/m^2(^oC/m)$
K/K_o	extent of non-linearities (Hausen)
L	length of regenerator, m
m	mass of gas resident in regenerator, kg
M	mass of packing, kg
Nu	Nusselt number (= hd/k)
P	period duration, s
Pr	Prandtl number (= $S\mu/k$)
q	'dimensionless' heat loss rate, ^oC
Q	quantity of heat, J
r	bed radius, m
Re	Reynolds number (= Gd/μ)

S	gas specific heat at constant pressure, J/kg^{o}C
St	Stanton number (= h/SG)
t	gas temperature, ^{o}C
T	solid temperature, ^{o}C
u	rate of heat flow, W
U	interstitial gas velocity, m/s
V	superficial gas velocity, m/s
w	wall semithickness, m
W	total gas mass flowrate, kg/s
x,y,z	distance, m

Greek symbols

α	solid thermal diffusivity, m^2/s
γ	degree of imbalance
ζ	dimensionless length, 3D model
η	dimensionless time, 2D model
θ	time, s
λ	solid thermal conductivity, W/m^2(^{o}C/m)
Λ	reduced length, dimensionless
μ	gas dynamic viscosity, kg/m s
ν	gas kinematic viscosity, m^2/s
ξ	dimensionless distance, 2D model
Π	reduced period, dimensionless
ρ	gas density, kg/m^3
σ	dimensionless width, 3D model
τ	temperature (gas or solid), ^{o}C
ϕ	'phi factor' (Hausen)

ω	dimensionless time, 3D model
Ω	reduced time, dimensionless

Subscripts

B	blast
f	fluid
H	harmonic mean
i	inlet
m	time mean
M	spatial mean
max	maximum
min	minimum
mux	multiplexer
o	surface
x	exit

Superscripts

'	refers to hot period
''	refers to cold period
o	optimal
^	setpoint value

CHAPTER 0

INTRODUCTION

This thesis is concerned with the physical and mathematical modelling of regenerative heat exchangers, or thermal regenerators. A small-scale computer-controlled rig is used to conduct experiments, the results of which are correlated with those from computer simulations, hence calibrating the mathematical model. Most previous work has been theoretical, to the extent where experimental experience lags seriously behind the theory, especially in the area of transient behaviour. It is via practical and simulated experiments on transient response that efficient online industrial control strategies can be developed.

Heat exchangers have obvious application in industry for the recovery of waste thermal energy, by the transfer of heat between two fluids, usually gases. For example, by transferring heat from combustion waste gases to the combustion air, considerable fuel savings can be effected, as in scrap metal melting, electricity generation and glassmaking. Relatively smaller exchangers are used in applications such as car radiators, air-conditioning plants (where 'cold' may be transferred) and solar heating installations. The most effective configuration for a heat exchanger is counterflow (or contra-flow) where the fluids flow in opposite directions, although parallel flow and crossflow configurations are also used.

In counterflow configuration, the cold gas can theoretically almost reach the inlet temperature of the hot gas, whereas in parallel flow exchangers the maximum possible is the average of the two inlet temperatures.

The commonest form of fluid heat exchanger is the continuous flow exchanger or recuperator. The two gases are separated by a partition wall (see figure 0.1) which ideally should be thin and of high conductivity (for example, steel), and heat is transferred between the gases via the wall. Recuperators are widespread due to their compactness and simplicity, but cannot be used in applications where the fluids are corrosive or at very high temperatures, due to the physical properties of the walls. In addition, if the walls are very thin recuperators cannot be used when the gases are at very different pressures. Recuperators have, however, been designed with sufficiently thick or strong walls to withstand high absolute pressures. The energy loss due to the pressure drop through a recuperator is proportional to the logarithm of the ratio of initial to final pressure, so for a given pressure drop the energy loss is less for higher absolute pressure. It is for this reason that it is desirable to operate recuperators at high pressure. A further constraint on the use of recuperators is that the gases must be clean; a continuous flow of particle-laden gas may result in deposition and eventual blockage. As will be seen, fixed bed regenerators are not subject to the constraints which limit recuperator applications.

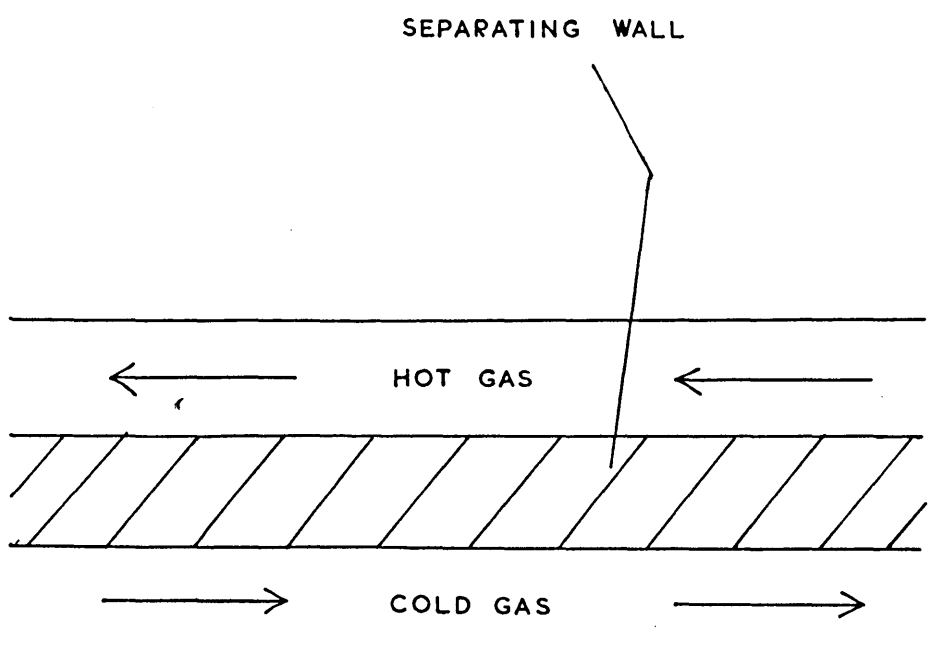

FIGURE 0.1

A RECUPERATOR

Recuperators are sometimes operated in parallel flow and crossflow configurations, as well as the more usual counterflow. Furthermore, there are various configurations which combine more than one mode in a 'mixed circuit' arrangement, such as the examples in figure 0.2. The first example combines parallel flow and counterflow, while the second is essentially counterflow with crossflow induced in the outer space by means of baffles.

Possibly the commonest form of recuperator is the shell and tube heat exchanger; tube bundle arrangements are used where the fluids are at low absolute pressure but with high flowrates, and a double tube arrangement is used for high absolute pressure with low flowrates. Very high pressure recuperators (up to 1000atm, $200^{o}C$ - $500^{o}C$) are used in the chemical industry, where reactions may actually be carried out in the exchanger. In this case, necessary catalysts may be incorporated in the recuperator walls. Recuperators can also be operated efficiently at temperatures down to $-200^{o}C$, where 'cold' is transferred from a cold gas (for example oxygen or nitrogen) to a compressed gas such as air. Heat transfer coefficients in a recuperator may be increased by the addition of fins to increase the heat transfer surface area. This is a particularly useful technique where the heat transfer coefficients are unequal on opposite sides of the wall, such as where heat is being transferred from a liquid to a gas. By adding fins to one side of the wall it is possible to balance out the heat transfer coefficients.

EX. 1

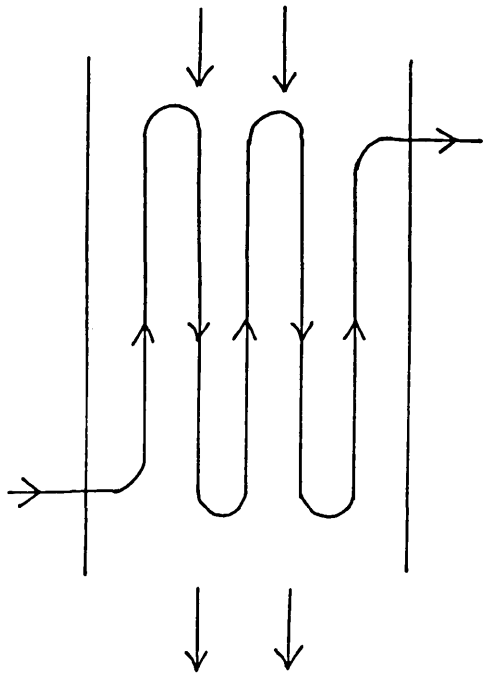

EX. 2

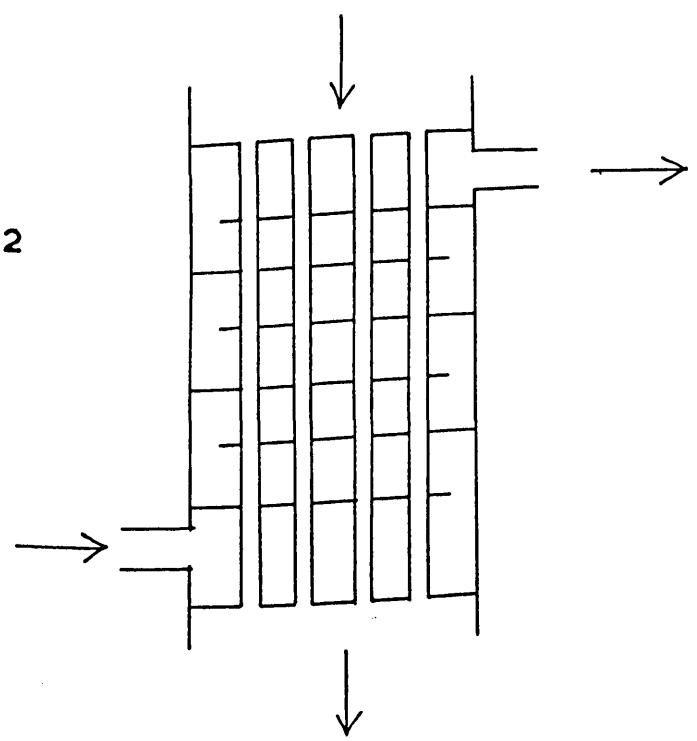

FIGURE 0.2

MIXED MODE EXCHANGERS

Thermal regenerators consist basically of a bed of solid heat-storing packing (or chequerwork) held in an insulated container, through which hot and cold gases pass alternately. Firstly the hot gas is passed over the packing, giving up its heat to the solid, for a length of time known as the hot period. After this a reversal (or changeover) takes place, and the cold gas is passed over the bed in the opposite direction, taking up heat from the solid, for the duration of the cold period. The hot period/cold period combination is termed one cycle of operation, and after several cycles the spatial distributions of gas and solid temperature in the regenerator become periodic and independent of the initial solid temperature profile. At this point the system is said to be at cyclic equilibrium, exact 'steady-state' equilibrium never being attained due to the continuous chronological variations in the temperature of the packing and the gases during the course of a cycle of operation. Because of these continuous chronological variations in the temperatures, it is often necessary in regenerator work to refer to time-mean temperatures taken over a hot or cold period.

If a change is now made to the operating conditions, such as an increase in inlet temperature or a change in flowrate, then the regenerator again enters a 'transient' phase until eventually another cyclic equilibrium state is reached. It should be noted here that the heat storage properties of regenerators may be exploited in applications such as solar heating systems, where the

diurnal variations in solar energy flux can be 'evened out' so that the delivered load matches the demand 24 hours a day. It should also be noted that due to the reversals which occur in regenerator operation, ideally no accumulation of gas-borne particles is allowed to take place and the channels remain open; the regenerator is therefore said to be 'self-purging'. Inevitably, however, deposits of solid material may be left on the packing surface although the problem is not as severe as in recuperators. Although regenerators usually operate in this counterflow configuration, parallel flow is occasionally used; no instances of crossflow regenerators are known to this author.

Regenerators are of two types, rotary and fixed bed. In the rotary regenerator the packing is arranged inside a drum, and the gases pass continuously through the packing on opposite sides while the packing rotates (see figure 0.3). The packing is sectored, and each sector experiences a period of hot gas flow followed by a period of cold gas flow, in quick sequence. Internally, therefore, the regenerator is subject to effects such as cyclic equilibrium while externally there is a continuous flow of gases as in a recuperator, with constant exit temperatures when at cyclic equilibrium. Rotary regenerators (sometimes known as rotary preheaters when in applications such as automotive gas turbines) vary in size considerably; electrical generating plants use metal plate packing regenerators with a height of 10m, a circumference of 30m and weight of typically 400 tonnes, rotating at 2-3 revolutions per minute,

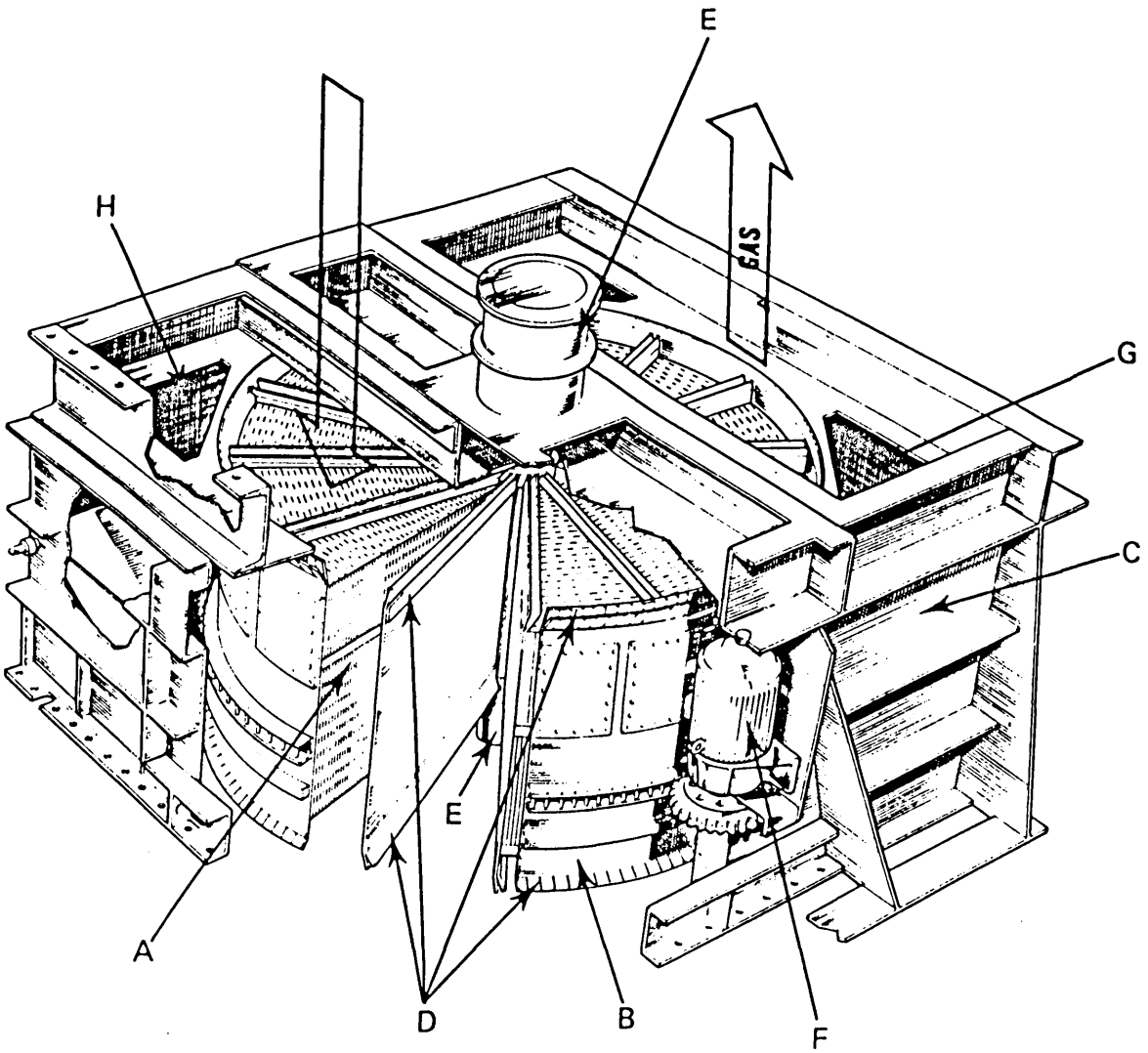

Rotary regenerator. A, Heating surface elements. B, Rotor in which the elements are packed. C, Housing in which the rotor rotates. D, Seals and sealing surfaces. E, Support and guide bearing assemblies. F, Drive mechanism. G, Gas by-pass. H, Air by-pass

FIGURE O.3

A ROTARY REGENERATOR

From Schmidt & Willmott (1981)

whereas air-conditioning applications have a diameter of as little as 1.25m. In these small regenerators the solid matrix may consist of plasticised paper or metallic wire mesh, for high area/mass ratio. The main problem associated with rotary regenerators is that of producing effective seals on the gas inlet ducts which still allow movement of the rotor while preventing gas leakage. This problem is particularly acute at high temperatures due to seal expansion and contraction, thus precluding the use of rotary regenerators in applications such as ironmaking. The other main problem, that of gas carryover into the opposite gas stream, can be overcome by incorporating a third, purging, phase into the system.

Whereas in rotary regenerators the hot and cold gases are separated spatially while the bed moves, in fixed bed regenerators the gases are separated temporally, by alternately blowing hot and cold through the one bed. For continuous operation, therefore, at least two regenerators are required, one being in the hot period while the other is in the cold period. Probably the largest fixed bed regenerators are to found in the steel industry; the ironmaking process uses three or more regenerators (Cowper stoves) to deliver heated air (or 'blast') to the furnace, at flowrates of up to 3000 m^3/min and temperatures of up to 1350^{o}C. In order to deliver such large thermal loads, the stoves may be up to 30m high, with a diameter of 7m and weight of 700 tonnes. The chequerwork, of firebrick or similar ceramic, is heated by burning the 'blast furnace gas', which is mainly carbon monoxide (a product of the

ore-reducing reaction), in excess combustion air. The combustion process, including possible enrichment of the blast furnace gas by oil, natural gas or similar fuel, is described more fully in Chapter 2. It should be noted here that, in the steel industry, the hot and cold periods may be referred to as the 'gas' and 'blast' periods respectively. A Cowper stove is shown in figure 0.4.

Two different modes of operation are used to produce blast at a constant temperature and flowrate. In the first of these, 'bypass main' operation, three stoves are usually used, with two on gas while one is supplying heated air at a temperature higher than the desired blast temperature. Two stoves are needed on gas since it is not possible to burn blast furnace gas fast enough in a single stove during the gas period to supply blast hot enough for the whole of the next blast period. Cold air flows through a bypass pipe around the stove on blast, where it is mixed with the heated air in such a proportion as to produce blast at the desired temperature. As the air exit temperature of the stove falls, the flowrate through the stove is increased (and the bypass flowrate decreased correspondingly) until eventually no cold bypass flow is being mixed with the blast, and the flowrate through the stove is equal to the blast flowrate set point. The stove is then put onto gas and another (hot) stove brought in to replace it. This is shown schematically in figures 0.5 and 0.6.

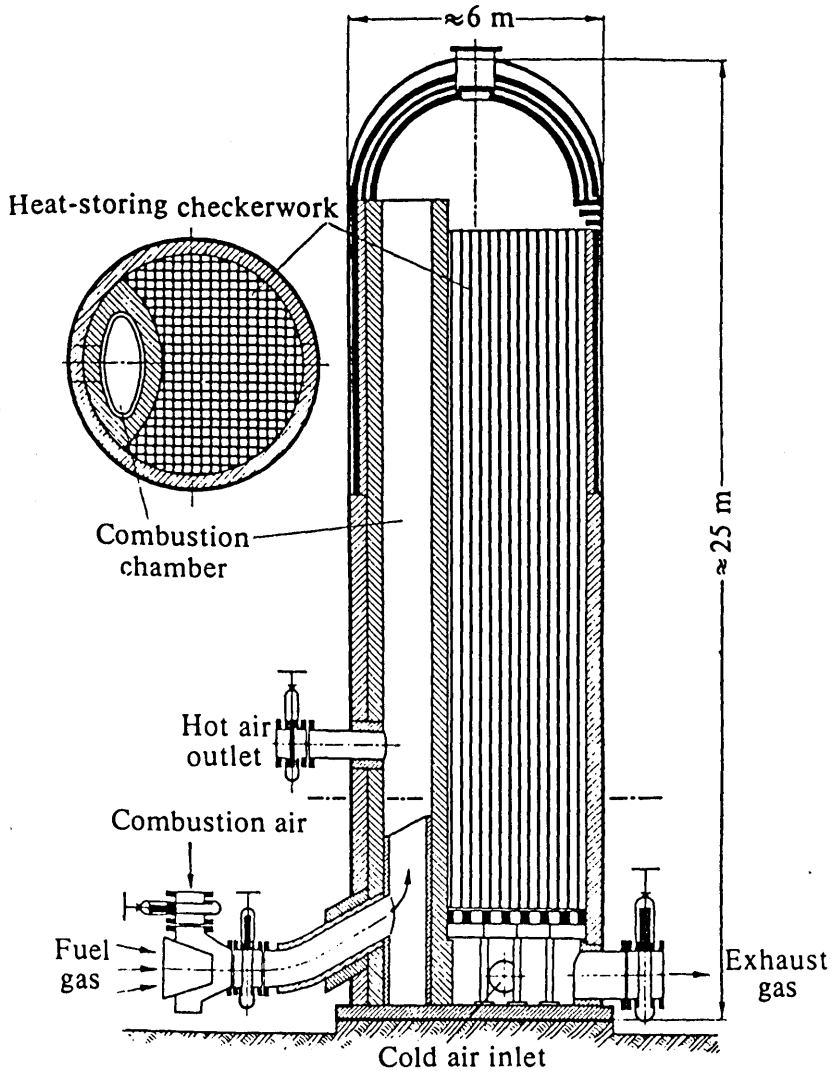

FIGURE 0.4

A COWPER STOVE

From Hausen (1983)

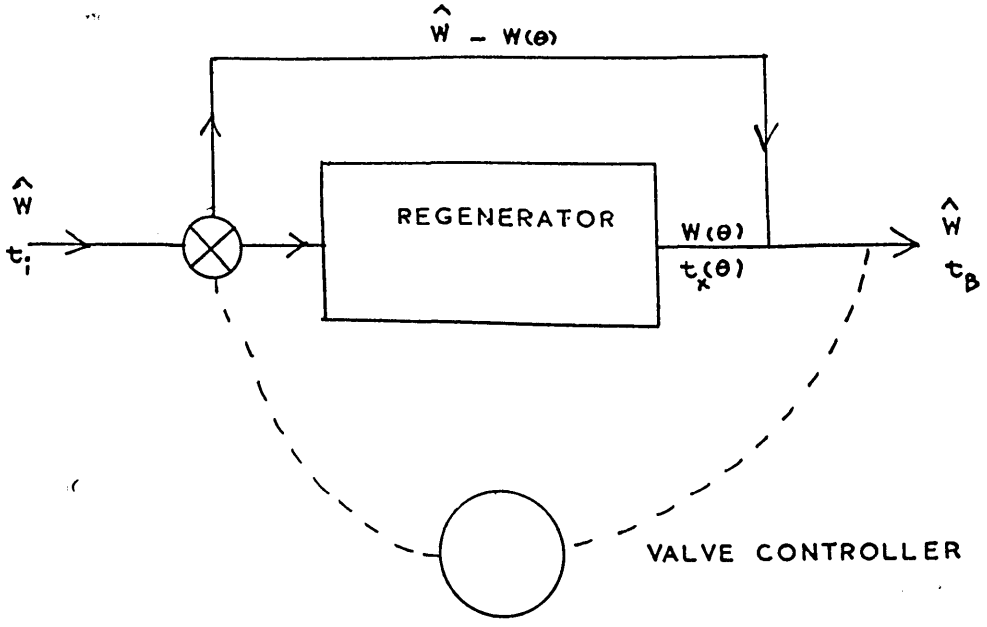

FIGURE 0.5

BYPASS MAIN CONFIGURATION

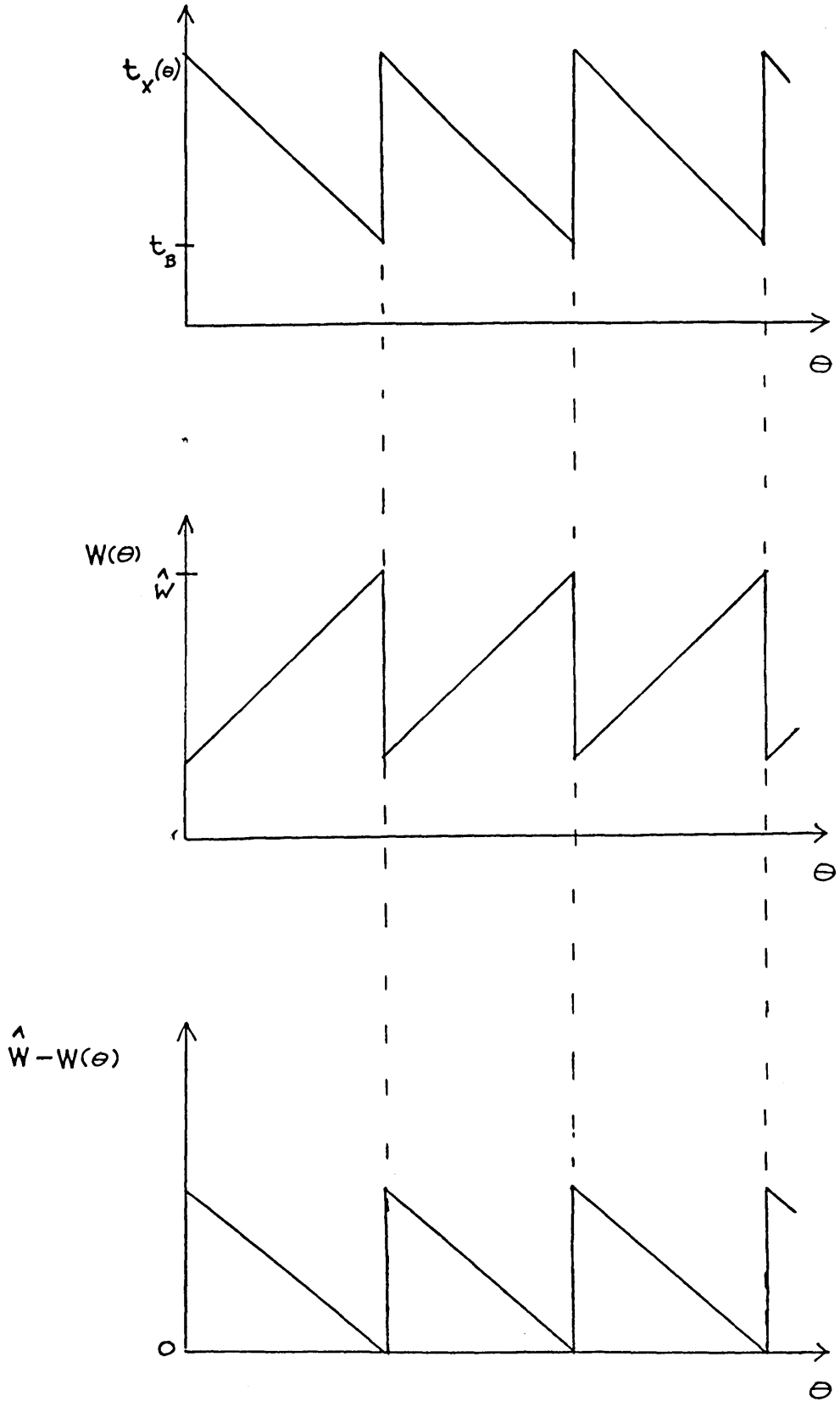

FIGURE O.6
BYPASS MAIN

The second mode of operation is known as 'staggered parallel' operation, in which four stoves are used, two of which are being heated while two supply blast. Of the two stoves on blast, the air exit temperature of one is higher than the blast temperature setpoint, and that of the other is below the same setpoint. The two output streams are then mixed in the proportion to give the desired overall blast temperature; as the air exit temperatures fall with time, the flowrates through the stoves are changed to maintain the correct mix of blast. Upon the air exit temperature of the hotter stove falling to the blast temperature setpoint (when the total blast flowrate is now being supplied by this one stove), the cooler stove is switched over onto the heating phase and a new, fully heated, stove is brought onto blast to replace it. Thus there are still two stoves on blast, with their exit temperatures lying either side of the blast temperature setpoint. Staggered parallel operation is shown in figures 0.7 and 0.8. Methods of determining and implementing the optimal operation (in terms of inlet temperatures, flowrates, changeover times, etc.) of both of these modes are described in Chapter 2.

In 1919 the Institute of Heat Economy was set up in Dusseldorf by Rummel, and much early regenerator theory emanated from the research group he established there. However, the most comprehensive mathematical theory originated with another German, Hausen, working for the Linde Company in Munich on the design of cryogenic regenerators for refrigerators. Hausen has published many papers

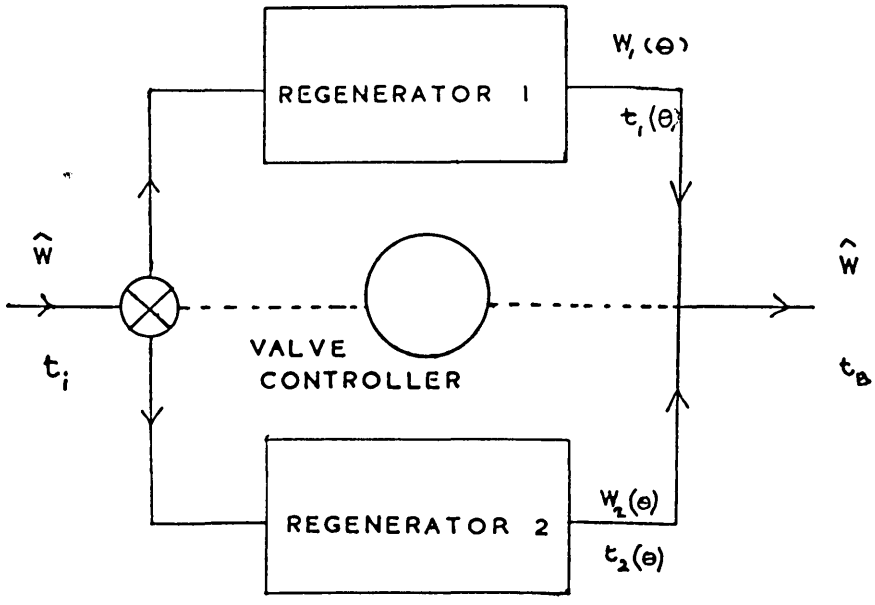

FIGURE 0.7

STAGGERED PARALLEL
CONFIGURATION

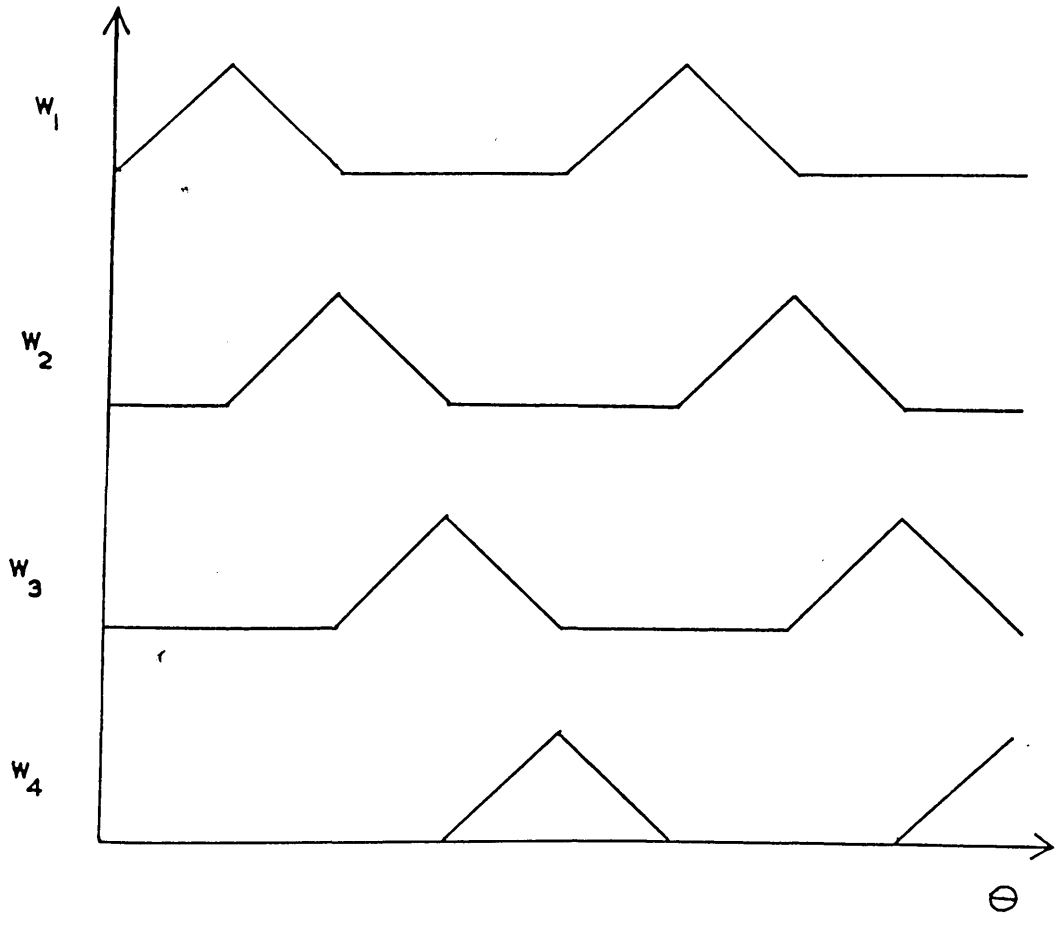

FIGURE 0.8

STAGGERED PARALLEL
FLOWRATES

and a well known book on this subject and is, more than any other single person, responsible for the foundation of regenerator theory. In Germany also, Nusselt carried out some important early work on pre-computer methods of regenerator simulation. Since the introduction of the digital computer for numerical solution of differential equations, much work has been done in England by Willmott, in particular the development of a computationally efficient regenerator model which is sufficiently general to enable study of non-linear features such as time-varying flowrates.

The majority of previous work on thermal regenerators has been theoretical, and concerned with cyclic equilibrium behaviour. This has progressed to the extent where specific methods of solution (the 'closed' methods) have been developed which provide no information about the transient state. Using 'open' methods, however, some theoretical work has been done concerning the transient behaviour of regenerators. Experimental work, on the other hand, has been extremely scarce in this area. The work carried out by the Ford Motor Company in the 1950s was the sole published work, until the University of Bradford in the 1970s and more recently the Universities of York and Leeds have sought to redress the balance.

The aims of this author have been to study the behaviour of a pilot experimental regenerator under transient conditions, with a view to developing a computer model which closely mirrors the physical model, and also with a view to gathering data which will enable

implementation of an optimal long term control strategy. Large regenerators are difficult to study directly due to the long time constants involved and the inflexibility of control; the laboratory-scale regenerator gives timescale compression of the order of tenfold, whilst retaining similarity to industrial regenerators in terms of certain dimensionless parameters (see Chapter 1). In addition the minicomputer controller/data logger provides a flexible control environment. The computer model also exhibits dimensionless parameter similarity to industrial plant, but the temperatures used correspond in scale to those on the rig and are not, therefore, expressed on the more general reduced temperature scale. It is a simple matter to change the computer model parameters and temperatures to achieve greater generality should the need arise.

The derivation of the mathematical model is described in Chapter 1 of this thesis, along with necessary definitions of terms, and the previous work in several related fields is reviewed in Chapter 2. The description of the experimental rig presented in Chapter 3 contains also an investigation into certain physical properties of the apparatus, such as heat transfer coefficients, flow distribution, gas dwell time etc. Chapter 4 contains a comprehensive discussion of the techniques employed in the work, both experimental and theoretical. Full details of the operating procedure and the results of system calibrations are also presented. The main experimental and theoretical results are discussed in

Chapter 5, and the direction which future work should take is indicated. Listings of the laboratory and mainframe computer software used in this work are presented in the Appendices, in addition to extensive graphs of the results.

CHAPTER 1

THE MATHEMATICAL MODEL

The 2D Pascal computer model of a thermal regenerator used for comparison with the experimental work undertaken in this thesis is based on a well-established mathematical model. Much previous work has been done in developing and solving the model, and its derivation and development are described in this chapter.

In developing a mathematical model, the aims are to idealise the physical system, introducing assumptions and simplifications to enable formulation of the model whilst retaining similarity to the real world. In this chapter, the development of the 3D regenerator model is described, after which further restrictions are introduced resulting in the 2D model. The 3D model is a close approximation of the physical system (the regenerator) but its solution is expensive in terms of computation time and storage requirements for both program and data. The simpler, 2D, model is much cheaper in this respect, yet can still produce an acceptable, even good, level of agreement with the 3D model.

1.1 PLANE WALL IDEALISATION

There are many different types of packing employed in regenerators; in low or moderate temperature regenerators for example, Raschig

rings (hollow cylinders), Berl saddles, randomly packed spheres or metallic honeycomb may be used. In high temperature regenerators, ceramic blocks may be used in various configurations (e.g. basket weave). A form of small rotary regenerator known as a 'heat wheel' uses plastic film wound around the central spindle. Comparisons of the various types of packing are to be found elsewhere (Hausen, 1950; Butterfield et al, 1963; Dunkle and Ellul, 1972). All of the various types can, for the purposes of analysis, be reduced to a plane wall structure. This structure is assumed to consist of a number of parallel solid walls of semithickness w and length L. The gases flow in the slots between the walls, and the edges are gas-tight with no heat transfer occurring at the wall ends (see figure 1.1). All heat transfer occurs between a wall surface and the thin layer of gas adjacent to it. For the plane wall, it is seen that

$$w = \frac{\text{Volume of solid}}{\text{Heat transfer surface area}}$$

and an equivalent w for all packing types can be evaluated; the method is described in section 1.8.

The spatial directions x, y and z are defined as in figure 1.1, with the gas flowing in the y direction. Direction x is <u>into</u> the wall so that the surfaces are at x = 0 and x = 2w, with the wall centre at x = w. Various assumptions now have to be made:

1. Longitudinal heat conduction in the solid (i.e. in the y direction) is negligible.
2. The heat transfer coefficients and other thermophysical

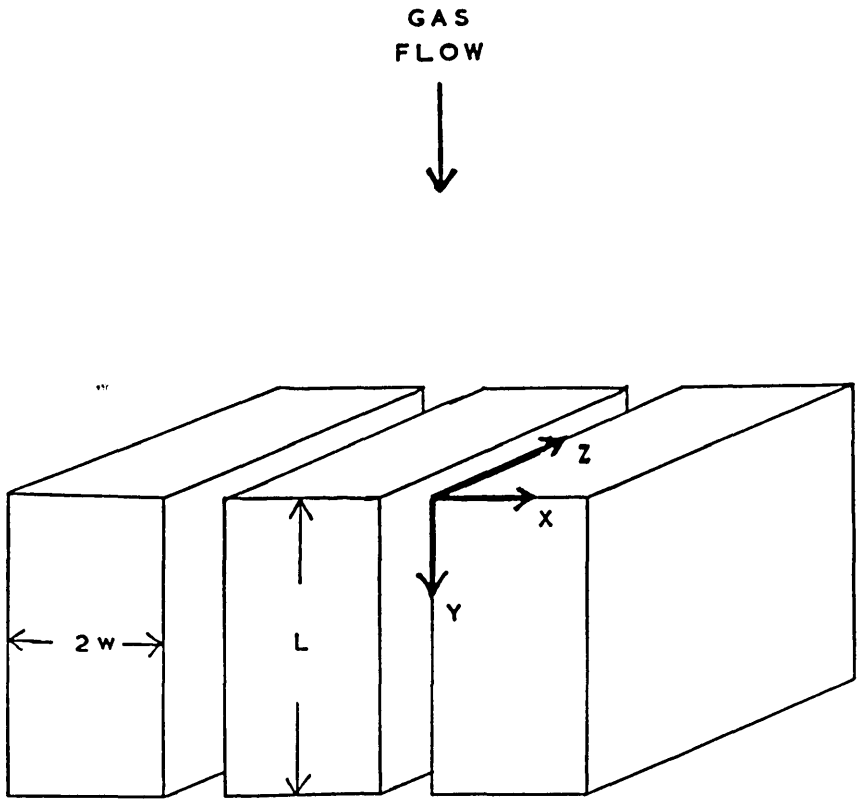

FIGURE 1.1

PLANE WALL IDEALISATION

properties of the gases and solid are constant in position and time throughout a period.

3. The gas is isothermal in the x and z direction, i.e. across the regenerator.
4. The gas inlet temperatures are constant throughout a cycle. Any changes occur at the start of a cycle.

The first assumption can be shown to be valid by considering the ratio of longitudinal conduction to heat input by the gas; for a Cowper stove this ratio is $\sim 10^{-5}$ (Willmott, 1971) and for a gas turbine regenerator it is $\sim 10^{-2}$ (Tipler, 1947). The second assumption facilitates the evaluation of numerical solutions of the differential equations. The third assumption arises from considering the geometry of the system, and implies a uniform gas flowrate distribution in the cross-section of the regenerator at all levels. As will be seen in Chapter 3, this is not always the case in some regenerators, although the assumption will be valid for most large industrial regenerators. The last assumption is made in most previous theoretical studies, but the experience of this author and also of industry suggests that the assumption is not valid in many practical cases. Where the inlet temperatures are <u>not</u> constant, they can be approximated by applying to the model a series of small step changes over the relevant time, each change occurring at the start of a period. This method is used in this author's model, as described in section 1.7. It should be noted that if a deliberate (or otherwise) change is made to the inlet temperatures of a <u>rotary</u>

regenerator, then some parts of the packing are inevitably in mid-period, so assumption four is again not strictly true (but for a different reason). Rotary regenerators can, however, be modelled under non-constant conditions by considering the individual responses of many small sections (see, for example, Burns, 1978).

1.2 THE 3D MODEL

Within the regenerator, there are two processes of heat transfer occurring:

1. Transfer within the packing.
2. Transfer via the wall surface between gas and solid

For the first process, the solid temperature is written as a function of x, y and time ($T(x,y,\Theta)$) and the gas temperature as a function of y and time ($t(y,\Theta)$). This follows directly from assumptions 3 and 4 in section 1.1. The heat transfer within the wall is given by the diffusion equation

$$\frac{\partial T}{\partial \Theta} = \alpha \left(\frac{\partial^2 T}{\partial x^2} + \frac{\partial^2 T}{\partial y^2} \right) \qquad (1.1)$$

If longitudinal conduction is neglected (assumption 1) then the second term within the brackets can be discarded. The first boundary condition is obtained by considering the fact that there is no heat transfer across the centre of the wall (from symmetry), i.e.

$$\left.\frac{\partial T}{\partial x}\right|_{x=w} = 0 \qquad (1.2)$$

Consideration of the second heat transfer process leads to the second boundary condition: the rate of heat transfer across the wall surface is given by

$$u = hA\,(T_o - t) \qquad (1.3)$$

and the rate of heat transfer from solid surface to bulk is given by

$$u = \lambda A \left.\frac{\partial T}{\partial x}\right|_{x=0,2w} \qquad (1.4)$$

Equating these expressions gives the boundary condition

$$\left.\frac{\partial T}{\partial x}\right|_{x=0,2w} = \frac{h}{\lambda}\,(T_o - t) \qquad (1.5)$$

It should be noted here that equation 1.3 allows for convective heat transfer only; radiative heat transfer becomes relevant at high temperatures, and has been incorporated and investigated in recent work by Brooks (Brooks, 1983).

The final parts of the model are evaluated by considering the second heat transfer process; the rate at which the solid is accumulating or losing heat is given by

$$u = WSL\frac{\partial t}{\partial y} + mS\frac{\partial t}{\partial \theta} \qquad (1.6)$$

Equating this expression with that for u in equation 1.3 gives

$$\frac{\partial t}{\partial y} = \frac{hA}{WSL}\,(T_o - t) - \frac{m}{WL}\frac{\partial t}{\partial \theta} \qquad \forall\ y,\theta \qquad (1.7)$$

The boundary conditions for this equation are then specified as

follows:

1. Gas inlet temperatures are given, i.e.

$$t'(0,\theta) = t'_i; \qquad 0 \leqslant \theta \leqslant P' \qquad (1.8)$$

$$t''(0,\theta) = t''_i; \qquad P' \leqslant \theta \leqslant P'' + P' \qquad (1.9)$$

2. The solid temperature distribution is the same at the start of a period as it was at the end of the preceding one, i.e. the reversal conditions are

$$T'(x,L-y,0) = T''(x,y,P'') \qquad (1.10)$$

and

$$T''(x,L-y,0) = T'(x,y,P') \qquad (1.11)$$

The complete model is thus equations 1.1 and 1.7 with the boundary conditions (1.2, 1.5 and 1.8 - 1.11).

1.3 REDUCTION OF THE 3D MODEL TO DIMENSIONLESS FORM

The equations to be reduced are

$$\frac{\partial T}{\partial \theta} = \alpha \frac{\partial^2 T}{\partial x^2} \qquad (1.1)$$

$$\frac{\partial t}{\partial y} = \frac{hA}{WSL}(T_o - t) - \frac{m}{WL}\frac{\partial t}{\partial \theta} \qquad (1.7)$$

Three dimensionless groups are introduced

$$\omega = \frac{\alpha}{w^2}\left(\theta - \frac{my}{WL}\right) \qquad (1.12)$$

$$\sigma = \frac{x}{w} \qquad (1.13)$$

$$\zeta = \frac{hAy}{WSL} \qquad (1.14)$$

and 1.1 and 1.7 become

$$\frac{\partial T}{\partial \omega} = \frac{\partial^2 T}{\partial \sigma^2} \qquad (1.15)$$

$$\frac{\partial t}{\partial \zeta} = T_o - t \qquad (1.16)$$

with boundary conditions

$$\left.\frac{\partial T}{\partial \sigma}\right|_{\sigma=1} = 0 \qquad (1.17)$$

$$\left.\frac{\partial T}{\partial \sigma}\right|_{\sigma=0,2} = \frac{hw}{\lambda}(T_o - t) = Bi\,(T_o - t) \qquad (1.18)$$

where Bi is the Biot modulus.

σ is bounded by [0,2] and upper bounds can be placed on ω and ζ by defining 'reduced length', Λ, and 'reduced time', Ω:

$$\Lambda = \zeta(y=L) = \frac{hA}{WS} \qquad (1.19)$$

$$\Omega = \omega(y=L, \theta=P) = \frac{\alpha}{w^2}\left(P - \frac{m}{W}\right) \qquad (1.20)$$

Hence a particular model can be fully and unambiguously described by specifying eight parameters: t_i, Bi, Λ and Ω for both periods.

Due to the linearity of the differential equations in temperature, it is possible to normalise all temperatures without loss of generality. A [0,1] scale is the most convenient (and most common), where all system temperatures (both solid and gases) are converted from a physical scale to the [0,1] scale. A system temperature τ is normalised using

$$\tau_{scaled} = \frac{\tau_{actual} - t''_{i\,actual}}{t'_{i\,actual} - t''_{i\,actual}} \qquad (1.21)$$

Thus the scaled hot gas inlet temperature is now equal to 1, the cold gas inlet temperature is zero, and all other system temperatures lie in between. The model used in this thesis does not, in fact, employ this temperature normalisation, all temperatures being expressed in degrees Centigrade. This is mainly due to the difficulty in predicting the extreme values of the (non-constant) inlet temperatures needed for the normalisation. The 3D model was discussed as long ago as 1927 (Nusselt, 1927) but no solutions were obtained until the advent of digital computers. In the interim, much work was done to simplify the model sufficiently to enable hand-calculated numerical solutions to be obtained.

1.4 SIMPLIFICATION OF THE 3D MODEL TO 2D

At this point, a further restriction is introduced; the solid is assumed to be isothermal in the x direction also. Hence the solid temperature is now a function of y and time only ($T(y,\Theta)$), and the heat transfer process occurring is now merely:

Transfer across the wall surface between solid and gas

The process is now dealt with by equating the rate of transfer $u = hA(T - t)$ and the rate of absorption by the wall $u = -MC\frac{\partial T}{\partial \theta}$. So the complete model is now

$$\frac{\partial T}{\partial \theta} = \frac{h A}{M C} (t - T) \qquad (1.22)$$

$$\frac{\partial t}{\partial y} = \frac{h A}{W S L} (T - t) - \frac{m}{W L} \frac{\partial t}{\partial \theta} \qquad (1.7)$$

This model was first proposed by Schumann (Schumann, 1929), who stated that it is applicable to regenerators whose solid thermal conductivity is high or whose packing consists of small particles. Schumann's 'porous prism' had a Biot modulus Bi ~ 0, implying high conductivity, i.e. $\frac{\partial T}{\partial x} = 0$ at the surface.

Schumann's model was improved by Hausen (Hausen, 1938) by rejecting the assumption that the solid is isothermal and considering instead the mean temperature across the solid:

$$T_M(y, \theta) = \frac{1}{W} \int_0^W T(x, y, \theta)\, dx \qquad (1.23)$$

A corresponding heat transfer coefficient, the bulk heat transfer coefficient $\bar{h}$, is defined such that

$$\bar{h}(T_M - t) = h(T_o - t) \qquad (1.24)$$

Equation 1.7 then becomes

$$\frac{\partial t}{\partial y} = \frac{\bar{h} A}{W S L} (T_M - t) - \frac{m}{W L} \frac{\partial t}{\partial \theta} \qquad (1.25)$$

The 'no longitudinal conduction' version of 1.1 is then integrated:

$$\frac{1}{W} \int_0^W \frac{\partial T}{\partial \theta}\, dx = \frac{\alpha}{W} \int_0^W \frac{\partial^2 T}{\partial x^2}\, dx \qquad (1.26)$$

to give

$$\frac{\partial T_m}{\partial \theta} = \frac{\alpha}{w} \left[\frac{\partial T}{\partial x}\right]_0^w \qquad (1.27)$$

The $\left[\frac{\partial T}{\partial x}\right]_0^w$ is evaluated using the boundary conditions

$$\frac{\partial T}{\partial x}\bigg|_{x=w} = 0 \qquad (1.2)$$

$$\frac{\partial T}{\partial x}\bigg|_{x=0,2w} = \frac{\bar{h}}{\lambda}(T_m - t) \qquad (1.5)$$

to give

$$\frac{\partial T_m}{\partial \theta} = \frac{\alpha \bar{h}}{w \lambda}(t - T_m) \qquad (1.28)$$

$\frac{\alpha}{\lambda}$ is equivalent to $\frac{1}{\rho C}$, and $\rho = \frac{M}{Aw}$ so 1.28 becomes

$$\frac{\partial T_m}{\partial \theta} = \frac{\bar{h} A}{MC}(t - T_m) \qquad (1.29)$$

Thus the model consists of equations 1.25and 1.29, with the same boundary conditions as before. The validity of the model obviously depends on finding an expression for $\bar{h}$. This is discussed in some detail in section 1.8.

1.5 REDUCTION OF THE 2D MODEL TO DIMENSIONLESS FORM

As before, dimensionless groups are defined for this purpose:

$$\xi = \frac{\bar{h} A y}{WSL} \qquad (1.30)$$

$$\eta = \frac{\bar{h} A}{MC}\left(\theta - \frac{my}{WL}\right) \qquad (1.31)$$

The equations now become

$$\frac{\partial T_m}{\partial \eta} = t - T_m \qquad (1.32)$$

$$\frac{\partial t}{\partial \xi} = T_m - t \qquad (1.33)$$

Limits on ξ and η are again imposed, thus defining 'reduced length', Λ, and 'reduced period', Π:

$$\Lambda = \xi(y=L) = \frac{\bar{h}A}{WS} \qquad (1.34)$$

$$\Pi = \eta(\theta=P) = \frac{\bar{h}A}{MC}\left(P - \frac{m}{W}\right) \qquad (1.35)$$

It is usual, in practical applications, for the dwell time $\frac{m}{W}$ to be small compared to P, and the reduced period is then given by

$$\Pi = \frac{\bar{h}AP}{MC} \qquad (1.36)$$

(The validity of this statement for the experimental rig is discussed in Chapter 3.) It can therefore be seen that a 2D model can be fully described by six values Λ, Π and t_i for both periods, and that the [0,1] temperature scale can still be used.

1.6 CYCLIC EQUILIBRIUM

It is necessary to know the behaviour of the model at cyclic equilibrium in order to study its transient behaviour. Much work has been done in finding the cyclic equilibrium behaviour of the 2D model, including various ways of actually determining when the state has been reached. This work is reviewed in Chapter 2.

At cyclic equilibrium, two parameters E' and E'' are defined, which give a measure of the regenerator's 'efficiency' (of heat retention) and 'effectiveness' (of heat delivery) respectively. Hausen defined the parameters thus:

$$E' = \frac{t'_i - t'_{x,m}}{t'_i - t''_i} \qquad \text{'Hot thermal ratio'} \qquad (1.37)$$

$$E'' = \frac{t''_{x,m} - t''_i}{t'_i - t''_i} \qquad \text{'Cold thermal ratio'} \qquad (1.38)$$

If the [0,1] temperature scale is used, then $t'_i = 1$, $t''_i = 0$ and $t'_{x,m}$ and $t''_{x,m}$ lie between 0 and 1, so that

$$E' = 1 - t'_{x,m} \qquad (1.39)$$

$$E'' = t''_{x,m} \qquad (1.40)$$

or, put another way, the hot gas enters at temperature equal to 1 and exits at temperature $1-E'$, while the cold gas enters at 0 and exits at E''.

Regenerators can be put into three categories,

symmetric $\quad \frac{\Lambda'}{\Lambda''} = \frac{\Pi'}{\Pi''} = 1$

balanced $\quad \frac{\Lambda'}{\Lambda''} = \frac{\Pi'}{\Pi''} \neq 1$

and unbalanced $\quad \frac{\Lambda'}{\Lambda''} \neq \frac{\Pi'}{\Pi''}$

For the symmetric and balanced regenerators, $W'S'P' = W''S''P''$, and for unbalanced regenerators, the degree of unbalance, γ, is defined as

$$\gamma = \frac{W'S'P'}{W''S''P''} \qquad (1.41)$$

for a fixed bed regenerator, and

$$\gamma = \frac{W'S'}{W''S''} \qquad (1.42)$$

for a rotary regenerator. Equations 1.41 and 1.42 are unified using the dimensionless parameters:

$$\gamma = \frac{\Pi'\Lambda''}{\Lambda'\Pi''} \qquad (1.43)$$

For the balanced case, Iliffe noted that $E' = E''$ (Iliffe, 1948), and for unbalanced regenerators, the relationship is $E' = \gamma E''$. This applies to both fixed bed and rotary regenerators. In order to specify the overall effectiveness of a regenerator therefore, it is customary to specify both E' and E'', and any unbalance in the system is thus taken into account.

Willmott carried out work on 2D/3D comparisons (Willmott, 1969a) and noted that for symmetric regenerators with $\Lambda > 5$, the agreement between 2D and 3D thermal ratios was good. The actual intra-cycle variations in exit temperature, however, did <u>not</u> agree well - although the <u>mean</u> exit temperatures over a period were in agreement. Willmott concluded that this was due to inaccuracies in the bulk heat transfer coefficient $\bar{h}$ (specifically, due to the inclusion of a single 'phi-factor', discussed in section 1.8).

1.7 TRANSIENT BEHAVIOUR

In a regenerator system, the parameters which can be varied are the inlet temperatures, the flowrates and the period times. Changes may occur due to alterations in ambient temperature or pressure (for example) or may be made deliberately in order to meet a load demand change. The system equations are still valid under transient conditions.

Consider the equations for reduced length and reduced period:

$$\Lambda = \frac{\bar{h} A}{W S} \qquad (1.34)$$

$$\Pi = \frac{\bar{h} A}{M C} \left(P - \frac{m}{W} \right) \qquad (1.35)$$

If the period duration P is changed, then only Π is affected; if, however, flowrate W is changed then both Λ and Π may also change, due to the flowrate dependence of $\bar{h}$. In most previous theoretical work, changes in W and P have been studied by affecting changes in Π alone, and assuming that $h \propto W$ (i.e. Λ is unaffected). Much work has gone into investigating the validity of this method (for example, Hausen, 1950; Schmidt and Willmott, 1981; Burns, 1978). In order to study changes in gas inlet temperatures, it has been assumed that $\bar{h}$ is constant for all temperatures so that Λ and Π are unaffected. In practice, however, the heat transfer coefficient is mildly temperature dependent and, in addition, is not quite linearly proportional to flowrate. For this reason, the model used by this author employs the correlations described in Chapter 2 to

evaluate the heat transfer coefficient (hence Λ and Π) at the prevailing temperature and flowrate for each cycle during a simulated run. This is still explicit because the temperatures and flowrates used for a cycle are those which were recorded for that cycle in the corresponding experimental run. In this way also, varying inlet temperatures (those experimentally recorded) are applied to the model.

It should be noted that if a purely theoretical run is to be conducted, then this approach to evaluating the thermophysical properties of the regenerator cannot be used. One of several methods has to be used, such as:

a) Use the prevailing temperatures from the previous cycle to evaluate the thermophysical properties for the current cycle at every point in space and time (Willmott, 1968).

b) Start as in a), integrate the regenerator equations over a period and then re-evaluate the thermophysical properties using the resulting temperatures. This is repeated until convergence occurs.

c) Using a closed method (see Chapter 2), obtain values for prevailing temperatures and use the average of the time-mean inlet and exit temperatures to evaluate the thermophysical properties once each period. Assume the properties are constant along the regenerator and throughout a period (Kulakowski and Anielewski, 1979).

These approaches are not necessary for this thesis due to the

existence of the experimental temperature profiles mentioned above.

1.8 THE BULK HEAT TRANSFER COEFFICIENT

As has been stated, it is necessary to find an expression for the bulk heat transfer coefficient $\overline{h}$ which relates the surface heat transfer coefficient h and the internal resistance to heat transfer. Hausen assumed that the temperature variation of a solid is linear with time (Hausen, 1938); after study in more depth, it is seen that, for a Cowper stove, this is a valid assumption (Knepper and Campbell, 1958). The assumption is represented by the equation

$$\frac{\partial T}{\partial \theta} = K, \text{ a constant} \qquad (1.44)$$

which, when substituted in 1.1, gives

$$\frac{\partial^2 T}{\partial x^2} = \frac{K}{\alpha} \qquad (1.45)$$

Integrating twice, and substituting the boundary conditions, gives

$$T(x) - T_o = \frac{K}{\alpha}\left(\frac{x^2}{2} - xw\right) \qquad (1.46)$$

i.e. a parabolic temperature distribution through the solid. To find an expression for the mean temperature through the solid, 1.46 is integrated again, thus:

$$\frac{1}{w}\int_o^w (T(x) - T_o)\, dx = \frac{K}{\alpha w}\int_o^w \left(\frac{x^2}{2} - xw\right) dx \qquad (1.47)$$

which yields

$$(T_M - T_o) = \frac{hw}{3\lambda}(T_o - t) \qquad (1.48)$$

Adding (t - t) to the left hand side gives

$$\frac{T_M - t}{T_o - t} = 1 + \frac{hw}{3\lambda} \qquad (1.49)$$

but since

$$\bar{h}(T_M - t) = h(T_o - t) \qquad (1.24)$$

1.49 becomes

$$\frac{1}{\bar{h}} = \frac{1}{h} + \frac{w}{3\lambda} \qquad (1.50)$$

In more general form, this expression is

$$\frac{1}{\bar{h}} = \frac{1}{h} + \frac{w}{(n+2)\lambda} \qquad (1.51)$$

with n = 1 for plane walls

n = 2 for cylinders

n = 3 for spheres

An alternate approach where the packing is not of plane wall structure is to assume that it <u>is</u> of plane wall structure and define an 'equivalent thickness' for the packing shape. This is then used in equation 1.50. The equivalent thickness, TH, is given by

$$TH = \frac{\text{Volume of solid}}{\text{Surface area}} + \frac{TH_{ch}}{2} \qquad (1.52)$$

where TH_{ch} is what Hausen terms the 'characteristic thickness' of the shape. This is not defined but is evidently, for a sphere or a cylinder, the diameter. In the case of a sphere,

$$TH = \frac{4\pi r^3}{3.4\pi r^2} + r = \frac{4}{3}r \qquad (1.53)$$

so the equivalent semithickness is $\frac{2}{3}r$. If this is substituted for w in equation 1.50, we obtain

$$\frac{1}{\bar{h}} = \frac{1}{h} + \frac{2r}{9\lambda} \qquad (1.54)$$

This is approximately equivalent to

$$\frac{1}{\bar{h}} = \frac{1}{h} + \frac{r}{5\lambda} \qquad (1.55)$$

which is the form of equation 1.51 when n = 3 (spheres). The surface heat transfer coefficient h depends upon many things (as described in Chapters 2 and 3), and for a high solid thermal conductivity λ (when the solid tends to an isothermal state) it is seen that $\bar{h} \sim h$. In this instance the Schumann and Hausen models converge.

The assumption that $\partial T/\partial\Theta$ is constant (1.44) is, in fact, <u>not</u> true at the start of a period; the parabolic temperature profile inverts, as shown in figure 1.2. Hausen introduced a factor Φ (Hausen, 1942) to average out the effect of the inversion through the period. Equation 1.51 now becomes

$$\frac{1}{\bar{h}} = \frac{1}{h} + \frac{w\Phi}{(n+2)\lambda} \qquad (1.56)$$

Φ can be found from the expressions below:

First, let

$$\beta = \frac{2w^2}{\alpha}\left(\frac{1}{P'} + \frac{1}{P''}\right)$$

Then

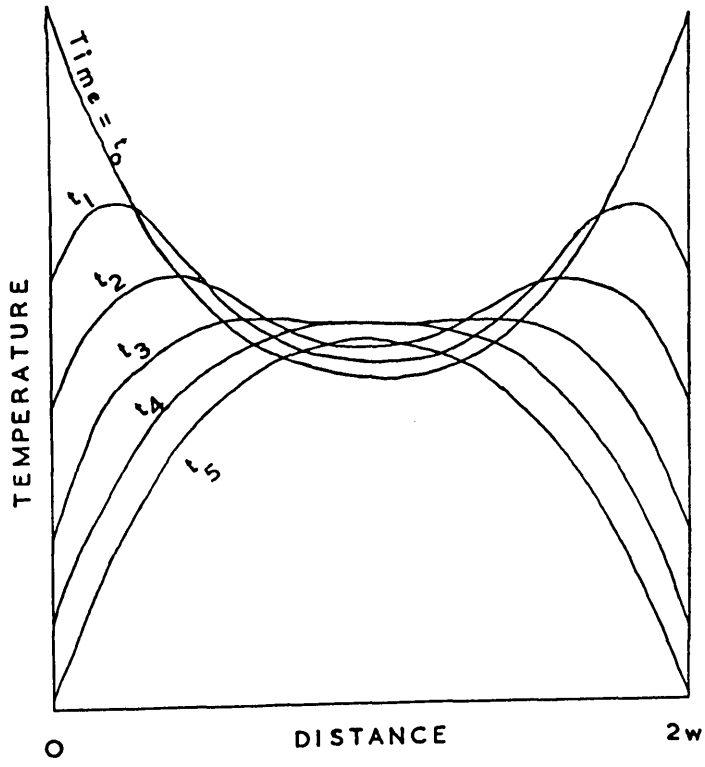

FIGURE 1.2

PARABOLA INVERSION :

(ACTUAL SCALES ARE

APPLICATION-SPECIFIC)

plates: $\Phi = 1 - \frac{1}{30}\beta$ if $\beta \leqslant 10$

cylinders: $\Phi = 1 - \frac{1}{48}\beta$ if $\beta \leqslant 15$

spheres: $\Phi = 1 - \frac{1}{70}\beta$ if $\beta \leqslant 20$

otherwise

$$\Phi = \frac{2.142}{\sqrt{\varepsilon + \beta}} \qquad \begin{array}{l} \varepsilon = 0.3 \text{ plates} \\ \varepsilon = 1.1 \text{ cylinders} \\ \varepsilon = 3.0 \text{ spheres} \end{array} \quad (1.57)$$

It should be noted here that some confusion has existed in the past over the definition of Φ. The expressions used in this chapter (equation 1.57) are following the form of most modern work (for example, Schmidt and Willmott, 1981), but originally (Hausen, 1950) equation 1.50 was written with w equal to the thickness (not semithickness) and without the 3 in the denominator. The expressions then given by Hausen for Φ (c.f. equation 1.57) give values equal to one-sixth of the values yielded by the expressions quoted here. Both methods are equivalent provided consistency is observed.

As stated earlier, Willmott suggested that a single phi-factor throughout a period is unsatisfactory, leading to discrepancies between the intra-cycle exit temperatures of the 2D and 3D models. In fact, recent work (Hinchcliffe and Willmott, 1981) has included a time-dependent Φ, and hence produced good agreement between 2D and 3D intra-cycle (as well as time-mean) temperatures.

Another important effect observed by Hausen is that the non-linearity of the solid temperature with time at the reversals is more prominent at the entrance to the regenerator. The constant inlet temperature can be seen to propagate the effect along the regenerator, where the intensity of the effect gradually diminishes. The extent of this phenomena can be measured by a factor K/K_o which is given by

$$\frac{K}{K_o} = \frac{E'}{1-E'}\left(\frac{1}{\Lambda'} + \frac{1}{\Lambda''}\right) \qquad (1.58)$$

K/K_o is bounded by [0,1] the effect being less significant as it approaches 1. Curves for K/K_o are shown in figure 1.3.

The parameters λ, Φ, $\bar{h}/h$ and K/K_o for the experimental rig are evaluated and discussed in Chapter 3.

1.9 THE RECUPERATOR ANALOGY

It is necessary to mention briefly that periodic flow regenerators can be successfully simulated, with high computational efficiency, by continuous flow recuperators. For a recuperator to have the same dynamic characteristics as a regenerator, several parameters must be identical. Specifically, the partition wall of the recuperator should have the same heat capacity as the packing of the regenerator (hence 'thick-walled' recuperators); the hot and cold gas flowrates should be the same for the recuperator as for the regenerator; the regenerator heat transfer coefficients should also apply to the

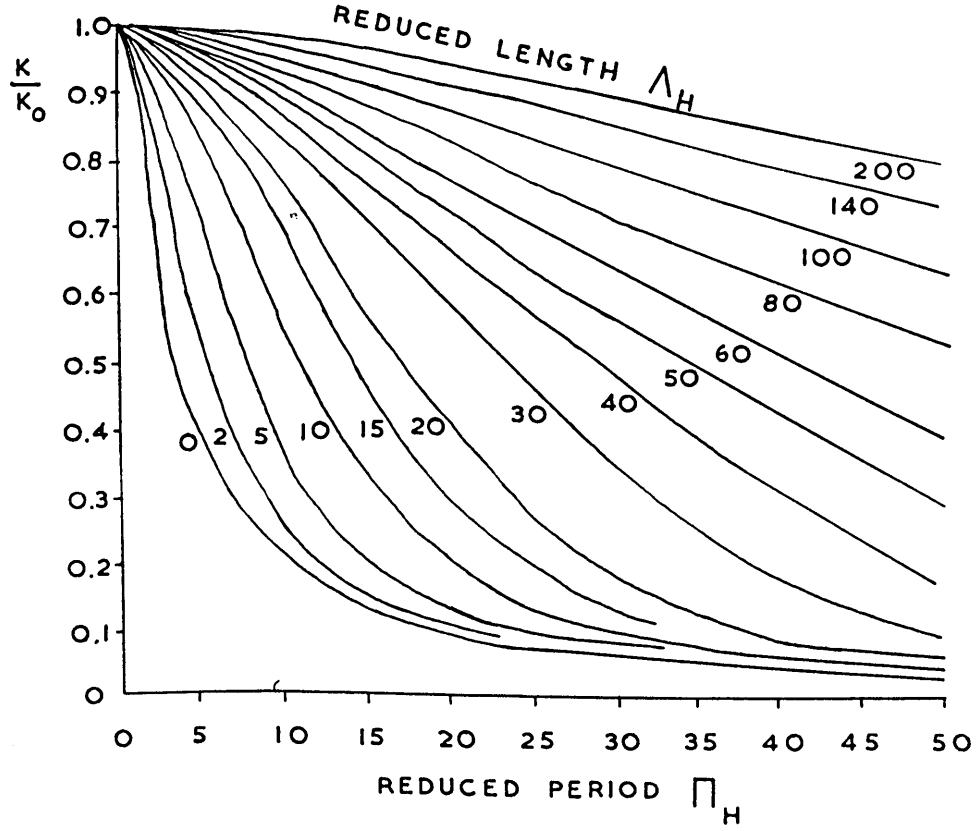

FIGURE 1.3

HAUSEN'S $\frac{K}{K_o}$ CURVES

equivalent recuperator; and the heat transfer surface area of the regenerator should be replicated by the area of the recuperator wall exposed to the hot gas and by the area exposed to the cold gas. This last point implies that the total heat transfer surface area of a regenerator is half that of the equivalent recuperator.

The recuperator model is derived by considering the temperature behaviour of the two (counterflow) gas streams and the dividing wall, and by making assumptions similar to those made in the regenerator model concerning conductivity etc. If the heat capacity of the gases is assumed negligible compared to that of the wall, and if similar dimensionless replacements to before are made, then the equations describing recuperator performance become

$$\frac{\partial T}{\partial \eta} = \gamma_1 (t'' - T) + (t' - T) \qquad (1.59)$$

$$\frac{\partial t'}{\partial \xi} = T - t' \qquad (1.60)$$

$$\frac{\partial t''}{\partial \xi} = \gamma_2 (t'' - T) \qquad (1.61)$$

where

$$\gamma_1 = \bar{h}''/\bar{h}'$$

$$\gamma_2 = \Lambda''/\Lambda'$$

and

$$\Lambda' = \bar{h}'A/W's'$$

$$\Lambda'' = \bar{h}''A/W''s''$$

It can be seen that these equations form a very similar system to the dimensionless regenerator equations (1.30 - 1.36) although, due

to the continuous nature of recuperator operation, there is no concept of reduced period. The effect produced by the gases which pass alternately in time $\eta = \Pi' + \Pi''$ in a regenerator occurs in time $\eta = \Pi'$ in a recuperator. Therefore in order to map the recuperator timescale on to the regenerator timescale, a factor $\Pi'/(\Pi' + \Pi'')$ must be used. The time-mean gas exit temperatures over a cycle of regenerator operation then correspond to the gas exit temperatures of the recuperator at a time (on the new timescale) equivalent to the end of the regenerator cycle in question.

A particularly useful application of the recuperator analogy is in the modelling of the transient performance of unbalanced regenerators. An equivalent symmetric recuperator ($\gamma_1 = \gamma_2 = 1$) is defined using the same approach as that recommended by Hausen (1950) for regenerators, that is the use of harmonic mean reduced lengths and reduced periods:

$$\frac{2}{\Pi_H} = \frac{1}{\Pi'} + \frac{1}{\Pi''} \qquad (1.62)$$

$$\frac{2}{\Lambda_H} = \frac{1}{\Pi_H}\left(\frac{\Pi'}{\Lambda'} + \frac{\Pi''}{\Lambda''}\right) \qquad (1.63)$$

The response of a regenerator to step changes in gas inlet temperatures and flowrates can be successfully modelled using this approach, and a full treatment of the methods of solution and comparisons of recuperator/regenerator results can be found in Willmott and Burns (1979).

1.10 THE PASCAL MODEL

The model used in this thesis for the simulation of experimental runs is a 2D model which uses the average of the experimentally-recorded time mean inlet and exit temperatures as the temperature at which to evaluate the thermophysical properties, hence h, and Λ, Π etc. The heat transfer coefficients are evaluated every period, and the correlations used and method of solution of the model (open solution of equations 1.32 and 1.33) are described in Chapter 2. Various parameters such as Φ and K/K_o are examined in Chapter 3. It is also possible to incorporate the effect of heat losses in the model, and the method is described later.

The model is coded in Pascal to run on a DECsystem-10.

CHAPTER 2

LITERATURE REVIEW

2.1 REGENERATOR SIMULATION METHODS (OPEN METHODS ONLY)

2.1.1 Finite Difference Methods

The equations to be solved are those stated in Chapter 1,

$$\frac{\partial t}{\partial \xi} = T - t \qquad (2.1)$$

$$\frac{\partial T}{\partial \eta} = t - T \qquad (2.2)$$

The gas and solid temperatures t and T are to be computed spatially at either end of the regenerator and at equally spaced intermediate positions, and also chronologically at equal time intervals.

Willmott

Willmott's method (Willmott, 1964) is described here in some detail since it is the basis for the model used in this thesis.

The number of distance steps used is m, and the number of time steps p. Let the distance interval be $\Delta\xi$ and the time interval $\Delta\eta$, so that $m\Delta\xi = \Lambda$ and $p\Delta\eta = \Pi$. Applying the trapezoidal approximation to equations 2.1 and 2.2 gives:

$$t_{r+1,s} = t_{r,s} + \Delta\xi/2 \left(\left.\frac{\partial t}{\partial \xi}\right|_{r,s} + \left.\frac{\partial t}{\partial \xi}\right|_{r+1,s} \right) \qquad (2.3)$$

$$T_{r,s+1} = T_{r,s} + \Delta\eta/2 \left(\left.\frac{\partial T}{\partial \eta}\right|_{r,s} + \left.\frac{\partial T}{\partial \eta}\right|_{r,s+1} \right) \qquad (2.4)$$

where suffix $r \Rightarrow \xi = r\Delta\xi$

and suffix $s \Rightarrow \eta = s\Delta\eta$

Substituting $\alpha = \frac{\Delta\xi}{2}$ and $\beta = \frac{\Delta\eta}{2}$, and also

$$\left.\partial t/\partial \xi\right|_{r,s} = T_{r,s} - t_{r,s} \qquad (2.5)$$

$$\left.\partial T/\partial \eta\right|_{r,s} = t_{r,s} - T_{r,s} \qquad (2.6)$$

gives

$$t_{r+1,s} = \frac{(1-\alpha)}{(1+\alpha)} t_{r,s} + \frac{\alpha}{(1+\alpha)}\left(T_{r+1,s} + T_{r,s} \right) \qquad (2.7)$$

$$T_{r,s+1} = \frac{(1-\beta)}{(1+\beta)} T_{r,s} + \frac{\beta}{(1+\beta)}\left(t_{r,s+1} + t_{r,s} \right) \qquad (2.8)$$

Boundary conditions are (i) $t_{0,s} = t_i$ for both periods and (ii) $T_{r,o}$ known $\forall r$ initially, and subsequently found at each changeover by

$$T_{r,o} = T_{m-r,p} \qquad (2.9)$$

Replacing

$\frac{1-\alpha}{1+\alpha}$ by A_1 , $\frac{\alpha}{1+\alpha}$ by A_2

$\frac{1-\beta}{1+\beta}$ by B_1 , $\frac{\beta}{1+\beta}$ by B_2

2.7 and 2.8 become

$$t_{r+1,s} = A_1 t_{r,s} + A_2\left(T_{r+1,s} + T_{r,s} \right) \qquad (2.10)$$

$$T_{r,s+1} = B_1 T_{r,s} + B_2\left(t_{r,s+1} + t_{r,s} \right) \qquad (2.11)$$

These are mutually implicit, so it is necessary to substitute for

$t_{r,s+1}$ in 2.11 from 2.10, obtaining

$$T_{r,s+1} = B_1 T_{r,s} + B_2 \left[A_1 t_{r-1,s+1} \quad A_2 \left(T_{r,s+1} + T_{r-1,s+1} \right) + t_{r,s} \right] \qquad (2.12)$$

Rearranging:

$$(1 - A_2 B_2) T_{r,s+1} = B_1 T_{r,s} + B_2 t_{r,s} + A_2 B_2 T_{r-1,s+1} + A_1 B_2 t_{r-1,s+1} \qquad (2.13)$$

Hence the final form of the equations used in the solution are 2.10 and a rearrangement of 2.13 :

$$t_{r+1,s} = \ddot{A}_1 t_{r,s} + A_2 (T_{r+1,s} + T_{r,s}) \qquad (2.10)$$

$$T_{r,s+1} = K_1 T_{r,s} + K_2 t_{r,s} + K_3 T_{r-1,s+1} + K_4 t_{r-1,s+1} \qquad (2.14)$$

for all r = 0..m

s = 0..p

where

$$K_1 = \frac{B_1}{1 - A_2 B_2} \quad , \quad K_2 = \frac{B_2}{1 - A_2 B_2}$$

$$K_3 = \frac{A_2 B_2}{1 - A_2 B_2} \quad , \quad K_4 = \frac{A_1 B_1}{1 - A_2 B_2}$$

Hence the integration procedure is as follows:

1. From known $T_{r,0}$ $\forall r$ at start of period, and given $t_{0,0}$, calculate $t_{r,0}$ $\forall r$ using 2.10
2. Evaluate $T_{0,s}$ $\forall s$ using 2.11
3. Evaluate $T_{r,s}$ then $t_{r,s}$ for r = 1..m, s = 1, by applying 2.14 and 2.10 repeatedly.
4. Repeat step 3 for all intervening time steps until the end of the

period (s = 2..p)

5. Apply reversal condition (2.9) and continue from step 1 above.

This is shown diagramatically in figure 2.1, in the space-time mesh. The process is continued until cyclic equilibrium is attained. This, according to Willmott, is when the difference in the values of the final cold gas exit temperature of two successive cycles is less than a pre-specified amount, ε. In order to calculate the time-mean exit temperature, Gregory's formula (Hartree, 1958) is used:

$$\frac{1}{\Pi}\int_0^{\Pi} t_x(\eta)\,d\eta = \frac{1}{p}\left[t_{m,0} + \sum_{s=1}^{p-1} t_{m,s} + \frac{1}{2}t_{m,p} - \frac{1}{12}(\nabla t_{m,p} - \Delta t_{m,0}) - \frac{1}{24}(\nabla^2 t_{m,p} + \Delta^2 t_{m,0}) - \frac{19}{720}(\nabla^3 t_{m,p} - \Delta^3 t_{m,0})\right] \quad (2.15)$$

where Δ and ∇ are the forward and backward differences respectively.

The criterion for cyclic equilibrium used by Willmott is inadequate when the regenerator being simulated is slow to reach equilibrium. Burns (1978) states that this is when $\Lambda > 10$, $\Lambda/\Pi > 3$. It can be seen that in this case, whilst the condition $|t''_{x,n} - t''_{x,n-1}| < \varepsilon$ may be true, $|t''_{x,final} - t''_{x,n}|$ may be much greater than ε and therefore cyclic equilibrium is not, in fact, attained. This is shown graphically in figure 2.2. To overcome the fact that $t''_{x,final}$ is unknown, in Burns' modification of Willmott's method, an estimate for t''_x is extrapolated using Aitken's' formula (Henrici, 1964) and the true equilibrium criterion can then be employed where necessary. The author has also applied this method.

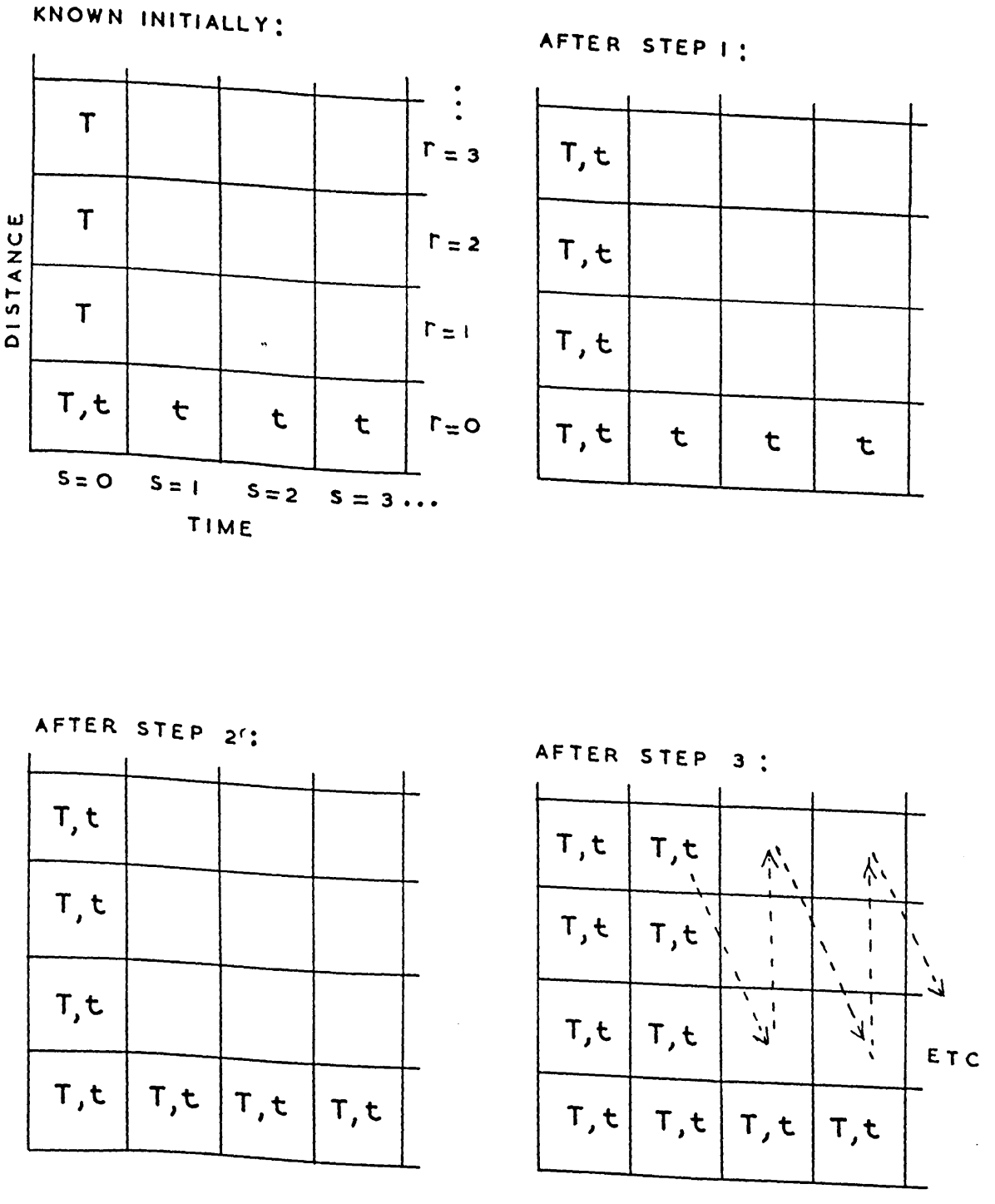

FIGURE 2.1

WILLMOTT'S METHOD

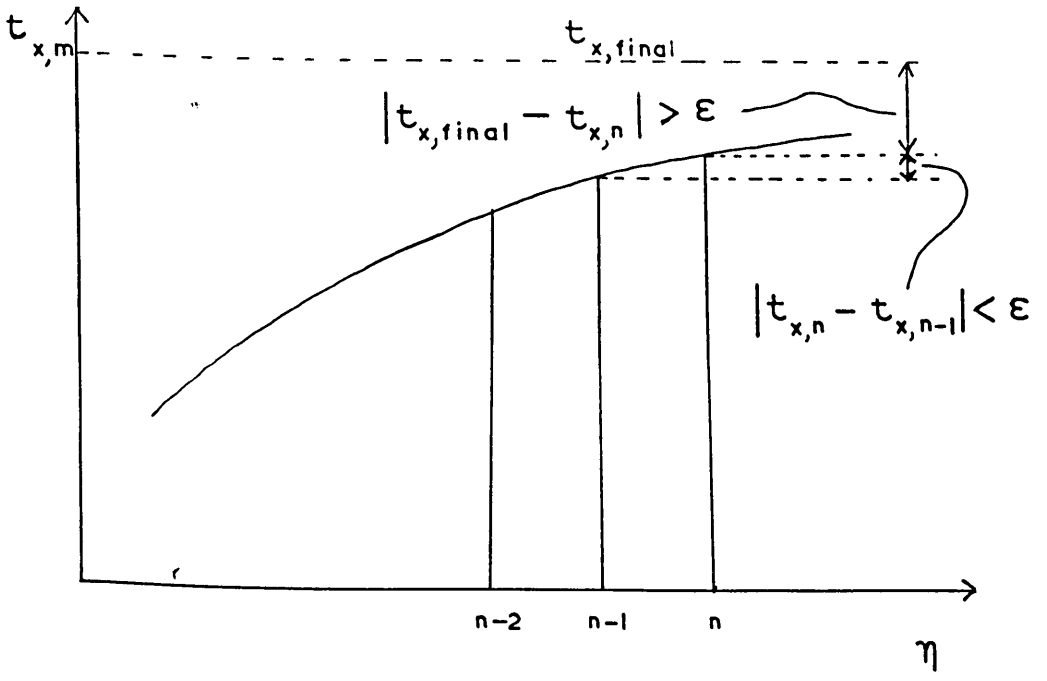

FIGURE 2.2

MOVEMENT TO EQUILIBRIUM OF A REGENERATOR WITH LARGE THERMAL INERTIA

Hausen

This method (Hausen, 1950), originally a graphical method, lends itself also to digital computer implementation. Allen published a similar yet independently developed method shortly afterwards (Allen, 1952); Hausen's method is described below, followed by the ways in which Allen's method differs.

Gas temperature is eliminated from equations 2.1 and 2.2 giving

$$\frac{\partial^2 T}{\partial \xi \, \partial \eta} + \frac{\partial T}{\partial \xi} + \frac{\partial T}{\partial \eta} = 0 \qquad (2.16)$$

The solution is considered in the space-time mesh below

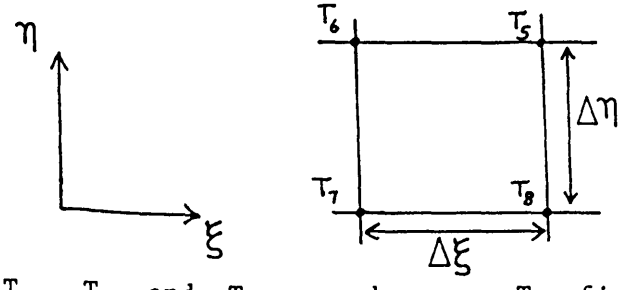

where T_6, T_7 and T_8 are known. To find T_5, the following substitutions are made in 2.16 :

$$\frac{\partial T}{\partial \xi} = \left((T_5 - T_6)/\Delta\xi + (T_8 - T_7)/\Delta\xi \right) / 2 \qquad (2.17)$$

$$\frac{\partial T}{\partial \eta} = \left((T_6 - T_7)/\Delta\eta + (T_5 - T_8)/\Delta\eta \right) / 2 \qquad (2.18)$$

$$\frac{\partial^2 T}{\partial \xi \, \partial \eta} = \left((T_5 - T_6)/\Delta\xi + (T_8 - T_7)/\Delta\xi \right) / \Delta\eta \qquad (2.19)$$

giving

$$T_5 = T_8 \frac{(2 + \Delta\xi - \Delta\eta)}{(2 + \Delta\xi + \Delta\eta)} - T_7 \frac{(2 - \Delta\xi - \Delta\eta)}{(2 + \Delta\xi + \Delta\eta)} + T_6 \frac{(2 - \Delta\xi + \Delta\eta)}{(2 + \Delta\xi + \Delta\eta)} \qquad (2.20)$$

For the case $\Delta\xi = \Delta\eta$, this reduces to

$$T_5 = T_7 \frac{(\Delta\xi - 1)}{(\Delta\xi + 1)} + \frac{T_8 + T_6}{(\Delta\xi + 1)} \qquad (2.21)$$

Once values of the solid temperature T have been found, the gas temperature t is found directly by substitution in 2.2

The important difference in Allen's method is his use of successively finer 'nets' (space-time meshes). The solutions found using the first net (5 distance and 2 time steps, for example) are used as initial guesses for the second net (with more steps), and so on. Using three nets, Allen reports accuracy of $\pm \frac{1}{2}\%$ in thermal ratios, and greatly accelerated convergence, since the coarser nets converge extremely quickly and also provide close initial guesses for the finer nets.

Haynes

Haynes (1973) used a modification of Willmott's method to compare two-dimensional and three-dimensional models of a regenerator, with special reference to the mapping of 2D onto 3D for transient operation of the regenerator.

He considered the cold side gas exit temperature, in response to a step change in hot gas inlet temperature, and noted that the two-dimensional values were consistently lower than those of the three-dimensional model. (See figure 2.3)

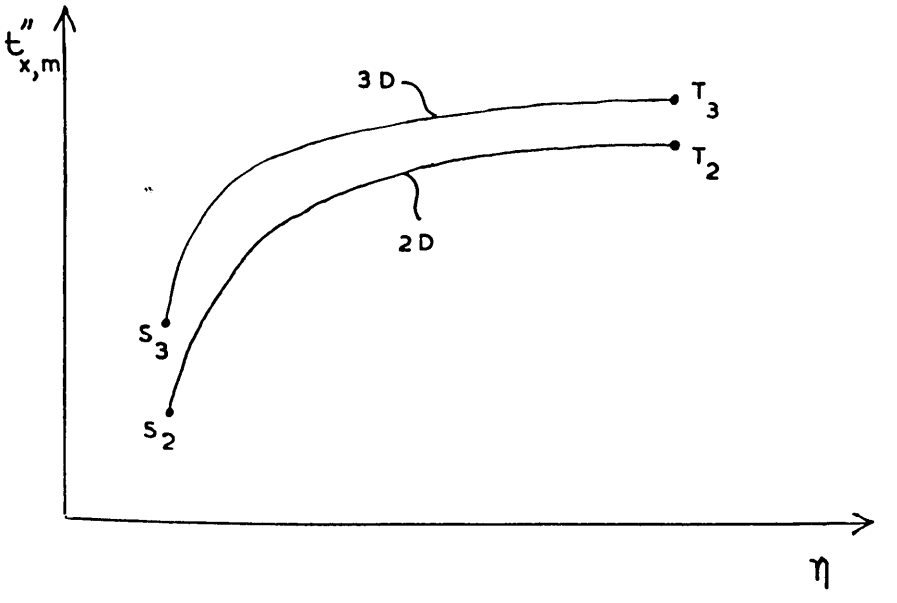

FIGURE 2.3

HAYNES' 2D/3D RESULTS

In order to translate the two-dimensional curve onto the three-dimensional curve, a simple transformation is formulated using the end points of the curves, thus :

$$S_3 = E\,S_2 + F \qquad (2.22)$$

$$T_3 = E\,T_2 + F \qquad (2.23)$$

E and F are therefore found, and Haynes proved that these constants are independent of the size of the step change in t_i'. Specifically, for the case where $t_i'' = 0$, $t_i' = 1$ and $t_i'^{*} = 1.5$ ($t_i'^{*}$ = temperature after step),

$$E = S_3 / S_2 \quad , \quad F = 0$$

that is, the transformation is not only linear, but is also mere scalar multiplication.

Haynes concludes that this transformation gives a good agreement between two-dimensional and three-dimensional models of transient response, and proposes that an approximate three-dimensional transient model can be efficiently implemented given (i) this transformation, (ii) a two-dimensional transient temperature distribution and (iii) a three-dimensional cyclic equilibrium temperature distribution. This is more efficient than implementing an open method three-dimensional model directly, since there exist very fast closed three-dimensional methods for computing the three-dimensional equilibrium temperatures, and two-dimensional open methods are considerably more rapid than three-dimensional open methods. Hence this procedure would be faster overall than applying

an open three-dimensional method.

2.1.2 Integral Methods

Nusselt, Nahavandi and Weinstein, Iliffe, Hilton

Nusselt's now famous paper (Nusselt, 1927) described the state of regenerator theory at the time of it's publication. He identified five different cases, arising from different assumptions concerning various parameters (for example, thermal conductivity of packing), each case giving rise to a different three-dimensional model. The five cases are summarised in Thomas (1972). The most applicable case to this thesis is that where the thermal conductivity of the packing is assumed to be zero in the direction parallel to the gas flow, and infinite in the perpendicular direction. The reasons for choosing this particular Nusselt model arise from consideration of factors such as Hausen's phi factor, and these are discussed in Chapter 3. In the case of the model adopted, the isothermal (across the regenerator) solid gives rise to a two-dimensional model. Nusselt, and subsequent authors (Nahavandi and Weinstein, 1961), represented the solution of equations 2.1 and 2.2 in integral form:

$$T''(\xi,\eta) = e^{-\eta} F''(\xi) - \int_0^{\xi} \frac{i J_1 2i\sqrt{(\xi-\varepsilon)\eta}}{\sqrt{(\xi-\varepsilon)\eta}} \eta\, e^{-(\eta+\xi-\varepsilon)} F''(\varepsilon)\, d\varepsilon \qquad (2.24)$$

for the cold period, and

$$T'(\xi,\eta) = 1 - e^{-\eta}(1 - F'(\xi)) + \int_0^{\xi} \frac{i J_1 2i\sqrt{(\xi-\varepsilon)\eta}}{\sqrt{(\xi-\varepsilon)\eta}} \eta e^{-(\eta+\xi-\varepsilon)}(1 - F'(\varepsilon))\,d\varepsilon \qquad (2.25)$$

for the hot period, where J_1 is the first order Bessel function and the initial solid temperature distribution is given by

$$F'(\xi) = T'(\xi, 0) \qquad (2.26)$$

$$F''(\xi) = T''(\xi, 0) \qquad (2.27)$$

The solid temperature distribution at the end of each period ($\eta = \Pi''$(cold), $\eta = \Pi'$(hot)) is given by:

$$T''(\xi,\Pi'') = e^{-\Pi''}F''(\xi) + \int_0^{\xi} K''(\xi-\varepsilon)\,F''(\varepsilon)\,d\varepsilon \qquad (2.28)$$

and

$$T'(\xi,\Pi') = 1 - e^{-\Pi'}(1 - F'(\xi) + \int_0^{\xi} K'(\xi-\varepsilon)(1 - F'(\varepsilon))\,d\varepsilon \qquad (2.29)$$

which uses a further simplifying notation

$$K(\xi-\varepsilon) = -\frac{i J_1 2i\sqrt{(\xi-\varepsilon)\Pi}}{\sqrt{(\xi-\varepsilon)\Pi}}\,\Pi\, e^{-(\Pi+\xi-\varepsilon)}$$

Alternate application of 2.28 and 2.29 represents an open method of simulating a regenerator. Careful use must be made of the reversal conditions, these assuming that distance is always measured from the gas inlet, in both periods. For counterflow operation, and where $\Lambda' = \Lambda'' = \Lambda$, the reversal conditions are:

$$T''(\xi,\Pi'') = T'(\Lambda-\xi, 0) \qquad (2.30)$$

$$T'(\xi,\Pi') = T''(\Lambda-\xi, 0) \qquad (2.31)$$

hence the initial solid temperature distributions for equations 2.28 and 2.29 are:

$$F''(\Lambda-\xi) = T'(\xi,\Pi') \qquad (2.32)$$

$$F'(\Lambda-\xi) = T''(\xi,\Pi'') \qquad (2.33)$$

Iliffe (1948) simplified Nusselt's method by firstly representing temperatures on a 0-1 scale so that the hot gas inlet temperature has the value unity and the cold gas inlet temperature the value 0. All other system temperatures then fall between these two values. Secondly, Iliffe proposed representing the integrals 2.28 and 2.29 approximately, using Simpson's rule, and then, given an initial solid temperature distribution, 'jumping' to the end of the period via this Simpson integral. Then, since the temperatures at the end of one period are equal to those at the start of the next, the process can be repeated in an open fashion.

Nahavandi and Weinstein's approach represents the initial solid temperature distribution as a polynomial:

$$F'(\xi) = \sum_{k=0}^{n} a_k(\xi)^k \qquad (2.34)$$

$$F''(\xi) = \sum_{k=0}^{n} b_k(\xi)^k \qquad (2.35)$$

These are substituted into the integral equations and the problem now involves determining the values of a_k and b_k. Gaussian quadrature is used to evaluate the integrals.

The Nusselt equations 2.28 and 2.29 have recently been considerably simplified (Hilton, 1983) using a radical change in notation. Hilton represents the gas temperatures on the reduced 0-1 scale, but the originality of his method lies in taking the gas inlet temperature to be 0 in both periods, the inlet temperature in the alternate period being 1. Then the function $G(\xi)$ is defined to be

$$G(\xi) = 1 - F(\xi) \qquad (2.36)$$

and so the two complex Nusselt equations can be reduced to the more elegant

$$T''(\xi,\eta) = e^{-\eta} F(\xi) + \int_0^{\xi} K''(\xi-\varepsilon)\, F(\varepsilon)\, d\varepsilon \qquad (2.37)$$

with F being replaced by G for the hot period.

2.2 PREVIOUS WORK ON TRANSIENT BEHAVIOUR OF REGENERATORS

The response of regenerator systems to a change in operating conditions has been investigated

1. Theoretically - a) analytically
   b) numerically

2. Experimentally - a) analogue e.g. electrical
   b) 'true' e.g. small scale rigs

In this review, case 2(a) is considered as a theoretical approach and is thus discussed in the following section.

2.2.1 Theoretical Work

London

Between 1958 and 1964, London published much work on the continuous flow exchanger (recuperator) which, as has been seen in Chapter 1, is directly analogous to a periodic flow regenerator. Considering the exchanger as part of a gas-turbine system, Cima and London (1958) formulated an involved mathematical model which incorporated the idea of heat capacity, C, and resistance to heat transfer, R. The mathematical model was derived by studying the heat transfer rate equation between the exchanger wall and the hot and cold gases, the thermal energy excess inflow over outflow, and the rate of energy storage in the wall. The analytical solution for the model is very complex and Cima and London went to great lengths to non-dimensionalise the model, choosing their parameters with extreme care (listing several criteria for good parameter choice) to give graphical compactness and a general idealisation of the system. This led to a model where the system temperatures and efficiencies are given as a function of eight dimensionless parameters. General solutions to this model are impossible, due to the complexity of the differential equations, boundary and initial conditions, and the large number of parameters. In order to find special solutions by an analogue method, the number of parameters was therefore reduced to give

$$\varepsilon'^{*},\ \varepsilon''^{*} = f\,(NTU, \theta^{*}, \theta_d^{*}, C^{*}) \qquad (2.38)$$

where

$$\varepsilon''^{*} = \frac{C_G''\,(t_x'' - t_i'')}{C_{min}\,(t_i' - t_i'')} \qquad (2.39)$$

$$\varepsilon'^{*} = \frac{C_G'\,(t_i' - t_x')}{C_{min}\,(t_i' - t_i'')} \qquad (2.40)$$

and NTU (number of transfer units) is a function of heat transfer area, conductance, C_{min}

θ^{*} = dimensionless time, $\theta / \theta_{d\,min}$

θ_d^{*} = dimensionless gas dwell-time ratio, $\theta_{d\,min}/\theta_{d\,max}$

C^{*} = wall capacity ratio, C_w / C_{min}

subscript G refers to gas, W refers to wall.

For the compact graphical representation which Cima and London sought, the number of parameters had to be reduced to three, so they chose to study the special cases

1) ε''^{*} as a function of time, after a step in t_i' (NTU, θ_d^{*}, C^{*} constant)
2) ε''^{*} as a function of time, after a step in the capacity rate of the gases (NTU varies, others constant)

Their results, shown in figure 2.4, indicate that the '90% response time', θ_{90}^{*} is ~70 for a step in t_i', and ~1 for a step in NTU (≡ flowrate). The conclusion is, therefore, that under the

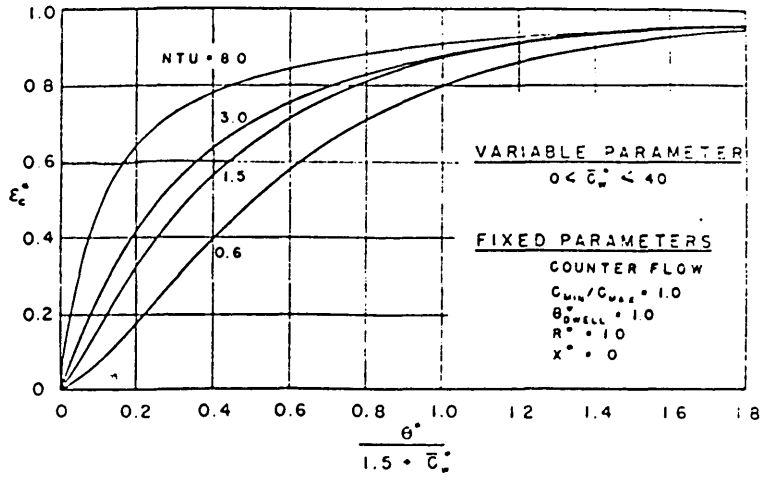

ϵ_c^* response to a step-function change $\Delta t_{A\ in}$.

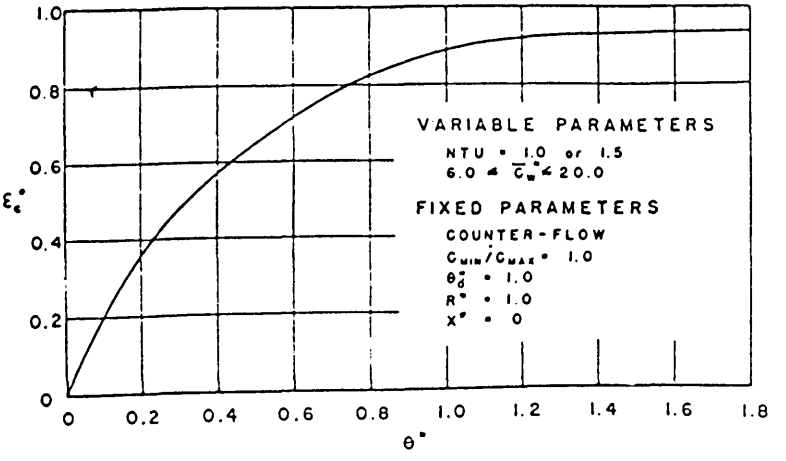

ϵ_c^* response to a step-function change in NTU.

FIGURE 2.4

LONDON'S RESULTS (1)

From Cima & London (1958)

operating conditions considered, the response is dominated by changes in t_i' .

(Note that, in figure 2.4, $\frac{\theta^*}{1.5 + C_w^*} = 1.4 \Rightarrow \theta^* = 70$)

The analogue apparatus used by London consisted of a C-R circuit with synchronous motors controlling switches via gear chains and pulleys, the effect being that of rolling capacitors ('gas') carrying charge ('heat') down an exchanger, transferring it via resistors. (See figure 2.5)

Further work (London et al, 1959) confirmed the work described above, and also looked at the behaviour of the gas turbine precooler, intercoolers and ducting. Some analytical work was also carried out and the analytical/analogue results are compared in figure 2.6. A 3% error in the analogue was deduced.

In a third paper (London et al, 1964) solutions were found by digital computer and periodic flow exchangers were also considered. Two continuous dimensionless parameters (normalised 0-1) were defined, to describe the gas temperature responses to step changes:

$$\varepsilon_{f1} = \frac{t_x'(\theta) - t_x'(0)}{t_x'(\infty) - t_x'(0)} \qquad (2.41)$$

$$\varepsilon_{f2} = \frac{t_x''(\theta) - t_x''(0)}{t_x''(\infty) - t_x''(0)} \qquad (2.42)$$

where time $\theta = 0$ is the instant when the step occured and time $\theta = \infty$ is when the system has re-attained a cyclic equilibrium state.

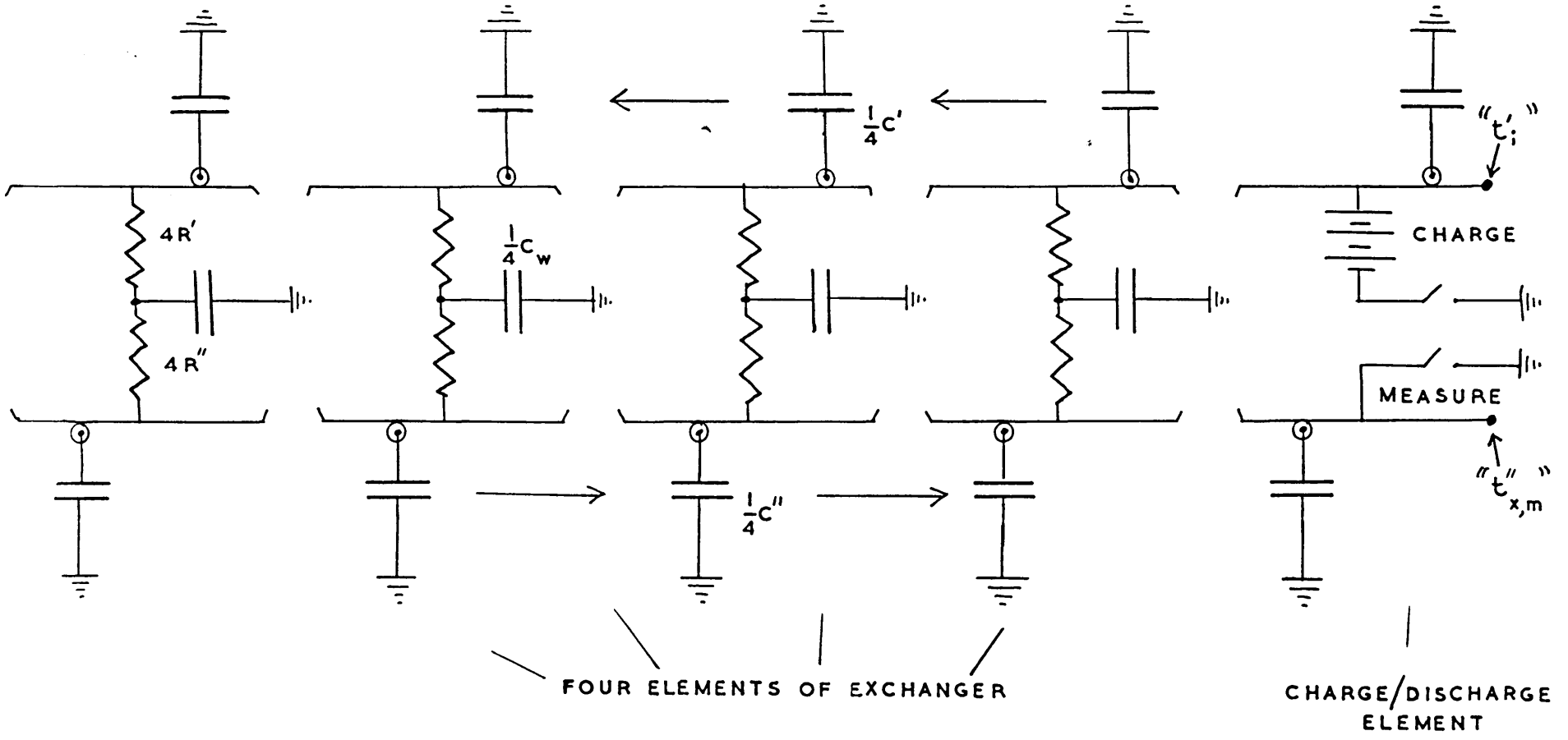

FIGURE 2.5: LONDON'S ANALOGUE

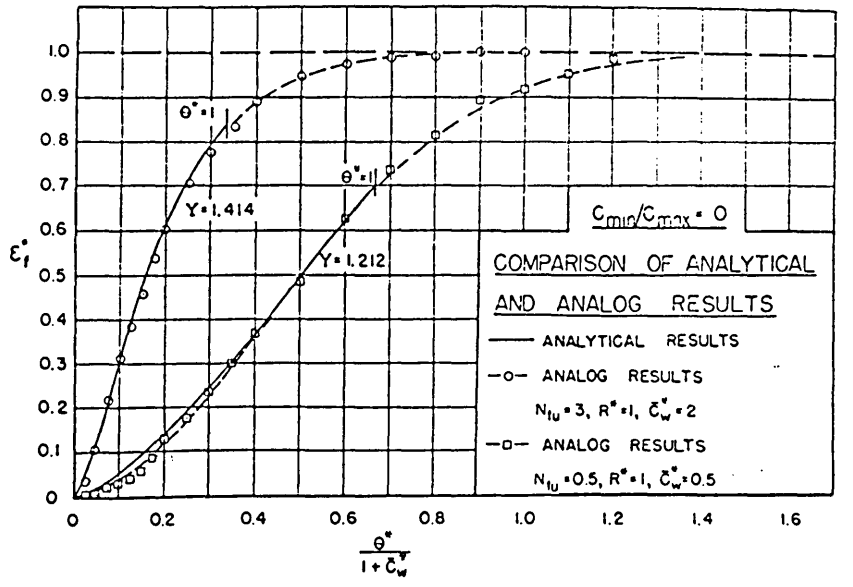

FIGURE 2.6: LONDON'S RESULTS (2)

From London et al (1959)

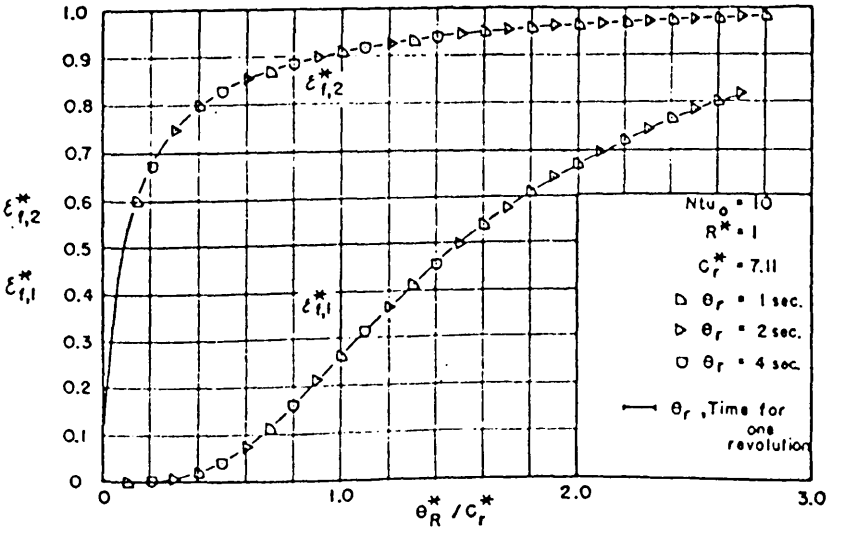

FIGURE 2.7: LONDON'S RESULTS (3)

From London et al (1959)

It should be noted that London's 1964 paper was the first work to consider the response of the hot gas exit temperature as well as that of the cold gas; that is, responses were investigated on both the opposite and the same sides as the step change. The results of this work are shown in figure 2.7.

An error is quoted of 6% on the y-axis, this being due to oscilloscope errors; no mention is made of errors due to component and/or switching timing inaccuracies. The important finding of this work is that the 90% response time for ε_{f2} is considerably less than that for ε_{f1}, due to a 'lag' between the two curves. It was also observed that the response ε_{f2} was ten times as fast in periodic flow exchangers as in equivalent continuous flow exchangers.

Green

Green (1967) investigated the length of time taken by a regenerator to re-attain an equilibrium state after a change in operation. Green used the finite difference method of Willmott, and studied symmetric regenerators ($\Lambda'/\Lambda'' = \Pi'/\Pi'' = 1$) subjected to steps in inlet gas temperature and flowrate. His approach was to cycle a two-dimensional model to cyclic equilibrium, effect a step change in the desired parameter, then observe the number of cycles to re-attain equilibrium. For a step in t'; his results were that the total reduced time to equilibrium, Θ, is independent of reduced period, Π; for shorter Π more cycles are needed and vice versa.

For given Λ, $\Theta = 2\Pi n = k$ (constant) (2.43)

Next, Green investigated the relationship

$$\Theta = f(\Lambda) \qquad (2.44)$$

and many simulations led to the explicit formula

$$\Theta = 0.524\Lambda^2 + 3.76\Lambda + 9.432 \qquad (\Lambda > 30) \quad (2.45)$$

The main fault in Green's work is that the point of equilibrium is dependent upon the criterion used which, in this case, is not a good one. Use of Aitken's formula, as described in section 2.1.1, leads to a better formula for $\Theta(\Lambda)$ and this work was carried out by Burns, as described later. Green's work did, however, illustrate the relationship between the regenerator's thermal inertia (represented by time to equilibrium) and the fundamental parameter Λ.

Whereas the size of a step in temperature is irrelevant due to equations 2.1 and 2.2 being linear in temperature, for steps in flowrate the size of the step is relevant. Green reported surprising results in this area; that the total time to re-establish equilibrium initially increases with size of step and, after a maximum, decreases for larger steps. The maximum time results from a ten per cent increase in flowrate, this also being a realistic figure for industrial Cowper Stoves. Green estimates that since two to three weeks would be required for a Cowper Stove to re-attain equilibrium, many stoves continually operate under transient conditions. Further work was undertaken by Burns (discussed below) who also pointed out that Green's findings indicate the importance

of understanding the transient behaviour of regenerators.

Haynes

Haynes undertook work on the relationship between results from the two-dimensional and three-dimensional models, specifically the response of the cold gas to a step change in hot gas inlet temperature (Haynes, 1973). This work has already been discussed in section 2.1.1 and will not, therefore, be reiterated here.

Burns

Burns, in his D.Phil thesis, used a model based on Willmott's method to investigate extensively the transient behaviour of regenerators (Burns, 1978). Having cycled the model to equilibrium, a step change is effected and then two parameters, ε_{g1} and ε_{g2} (being discrete adaptations of London's continuous ε_{f1} and ε_{f2}) are studied until equilibrium is re-attained. ε_{g1} and ε_{g2} are defined as:

$$\varepsilon_{g1} = \frac{t'_x(n) - t'(0)}{t'_x(\infty) - t'_x(0)} \qquad (2.46)$$

$$\varepsilon_{g2} = \frac{t''_x(n) - t''_x(0)}{t''_x(\infty) - t''_x(0)} \qquad (2.47)$$

at the end of the nth period after the step.

It should be noted that $t'_{x,m}(\infty)$ can be calculated in advance from the definitions of the thermal ratios, since the ratios do not change, and thus ε_{g1} and ε_{g2} can be evaluated as the simulation

proceeds.

Burns investigates ε_{g1} and ε_{g2} as a function of Λ and Π for several different regenerator operating configurations (symmetric, balanced, unbalanced), in addition to bypass main configuration, rotary regenerators etc. Step changes in either temperature or flowrate are considered and then simultaneous steps in both temperature and flowrate. Burns' results for a single step in t_i' are similar to those of London et al (see figure 2.8). Using a rigorous convergence criterion for detecting equilibrium (the Aitken criterion), Burns proposes a more accurate version of Green's equation for time to equilibrium (2.45). The Burns equation, using a convergence criterion $\varepsilon = 10^{-4}$, is:

$$\Theta = 0.622\Lambda^2 + 4.144\Lambda + 6.464 \qquad (2.48)$$

Further, for another criterion, $\varepsilon = E$ (say 10^{-2}), the time to equilibrium is now given by

$$\Theta_E = \Theta \ln E / \ln \varepsilon \qquad (2.49)$$

In order to obtain explicit formulae for ε_{g1} and ε_{g2}, Burns plotted $\log (1-\varepsilon_{g1})$ and $\log (1-\varepsilon_{g2})$ against dimensionless time, resulting in graphs such as figure 2.9. These led to a first approximation:

$$\varepsilon_{g1} = 1 - e^{-(\eta_H - C_1)/\eta_c} \qquad (2.50)$$

$$\varepsilon_{g2} = 1 - e^{-(\eta_H - C_2)/\eta_c} \qquad (2.51)$$

where C_1, C_2, η_c are positive real constants, and η_H is the

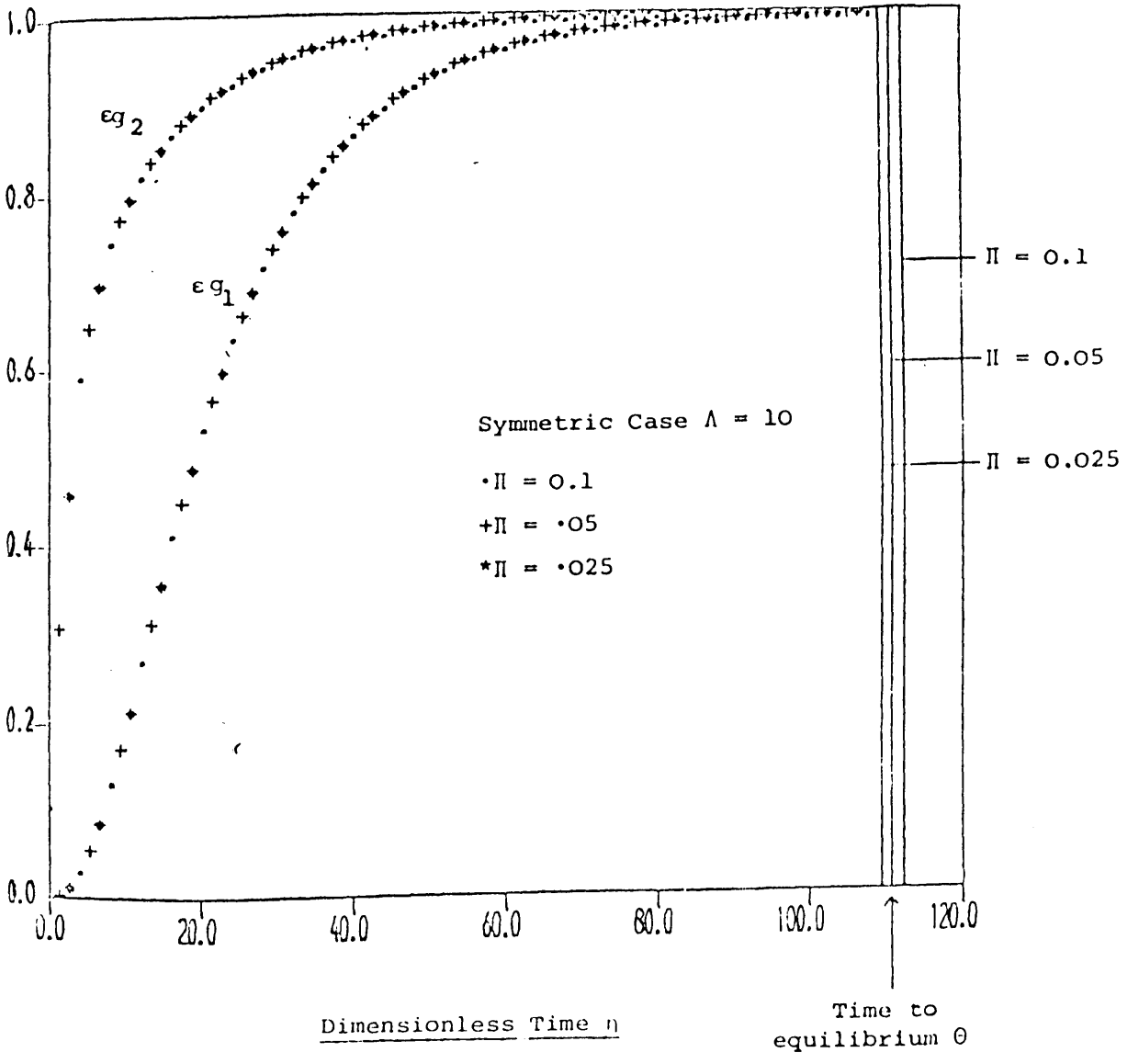

FIGURE 2.8

BURNS' RESULTS (I)

From Burns (1978)

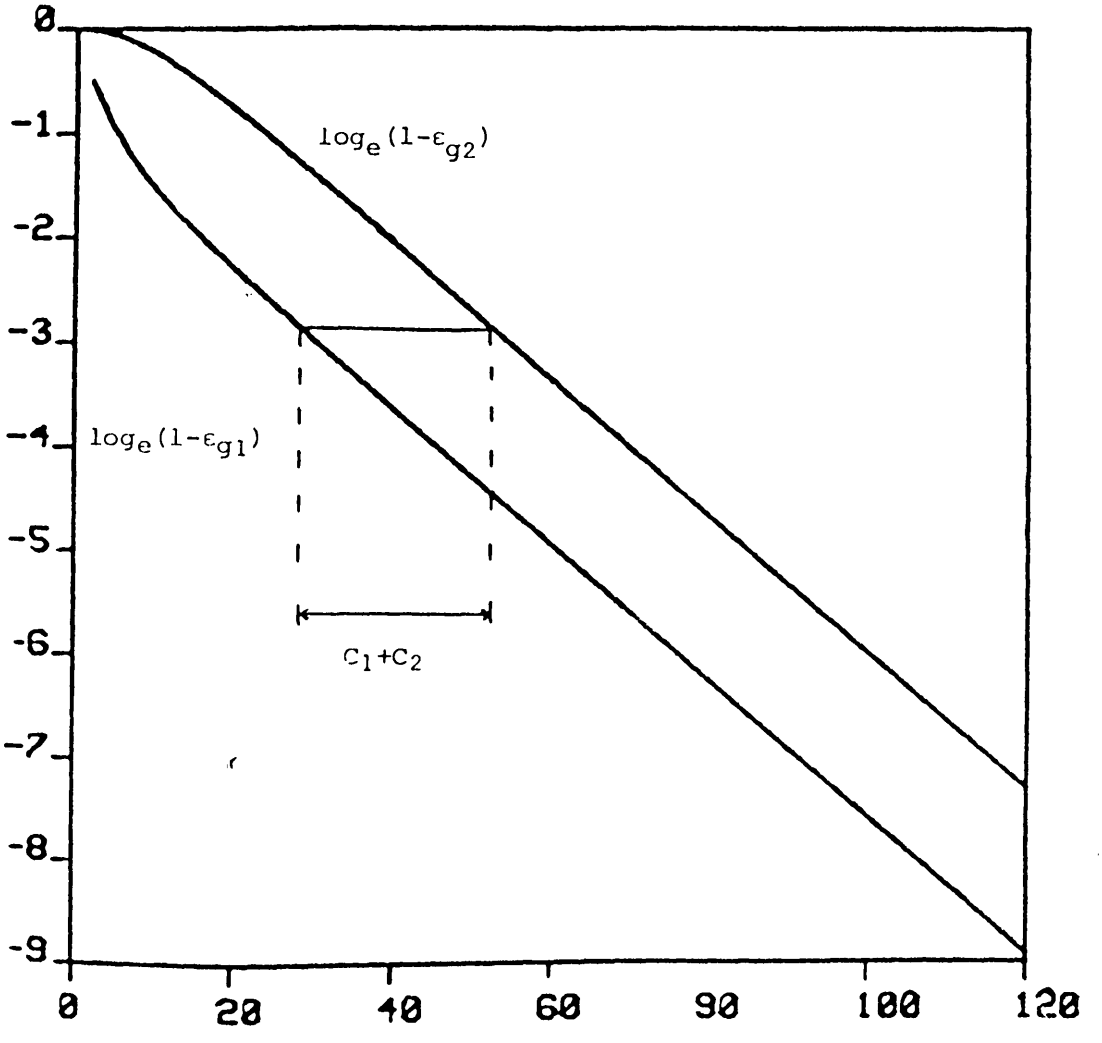

FIGURE 2.9

BURNS' RESULTS (2)

From Burns (1978)

dimensionless harmonic time (= $(2\Pi_H)n$) which provides a measure of time over successive cycles. Burns suggests that further exponential terms should be added to improve the approximation in the initial (non-linear) region of the $\log_e$ curves.

The observed lag between hot and cold side responses is parameterised by

$$lag_H = C_1 + C_2 \qquad (2.52)$$

and the time constant, η_c, using least squares fitting, was found to be given by

$$\eta_c = 0.0922\Lambda_H^2 + 0.498\Lambda_H + 0.928 \qquad (2.53)$$

Burns extended Green's work on flowrate step changes by effecting changes in Π (as did Green); this method is satisfactory since, as discussed in Chapter 1,

$$\Lambda \propto h \quad \text{and} \quad \propto 1/W$$

$$\Pi \propto h \qquad (2.54)$$

and $h \propto W$, hence changing W merely changes Π. ε_{g1} and ε_{g2} are again used to trace the regenerator's behaviour, but since the thermal ratios will be different at the second equilibrium, $t_{x,m}(\infty)$ will not be known until equilibrium is re-established and, hence, ε_{g1} and ε_{g2} cannot be computed until such time.

Burns' explanation of Green's findings rests on the fact that the time to equilibrium depends upon the final state of the system. If the regenerator is initially balanced, for a small step in flowrate, the final state is still ~ balanced, so the time to equilibrium increases with size of step. For larger steps, however, the final state of the regenerator becomes increasingly unbalanced and Θ decreases. Thus there is a point beyond which the effect of imbalance dominates the response.

The findings are summarised thus:

1. For any regenerator, ε_{g1} and ε_{g2} have identical time constants.
2. The constants η_c, C_1, C_2, and hence lag_H, are independent of reduced period Π for $\Lambda_H/\Pi_H > 3$ (i.e. for most practical systems).
3. The time constant η_c depends upon Λ_H and the degree of imbalance, and is independent of the magnitude of the step change in flowrate (or period duration).
4. C_1 and C_2 increase with reduced length, and for changes in flowrate or period duration, the lag is also dependent upon the step size. For larger steps in flowrate the value of the lag (and C_1, C_2) approaches that obtained for changes in t'_i.

In his work on simultaneous step changes, Burns stresses that the response of a system to two simultaneous steps, or indeed to many steps spaced out in time, may be studied by looking at the

superposition of the individual responses to each change. Figure 2.10 shows the success of this method - for a simultaneous increase in t'_i and decrease in W', the responses obtained by superposition map exactly onto those obtained by direct simulation of the simultaneous step.

A conclusion of the work on simultaneous steps is that the possibly unexpected curves which may result (such as initial dips and/or overshoot) can be explained as follows. The response of a regenerator to a single change in operating conditions in one period is considerably more rapid in the opposite period than that in which the step occurs (as previously stated). Hence superposition considerations, with this in mind, result in 'strange' curves. Burns subsequently applies this knowledge of transient behaviour in discussing feedforward control methods for meeting load changes in a practical regenerator system. This is covered in section 2.3.

Heggs and Mitchell

Studying symmetric regenerators only, Heggs and Mitchell (1981) carried out simulations mapping the response of the system to a step change in hot gas inlet temperature alone. Their main finding was that, in contradiction to all previous work, the total time to equilibrium was a function of the size of the step change. It was also noted that the time to equilibrium depended upon reduced period, Π, and, for changes in t'_i of > 50%, the following equation

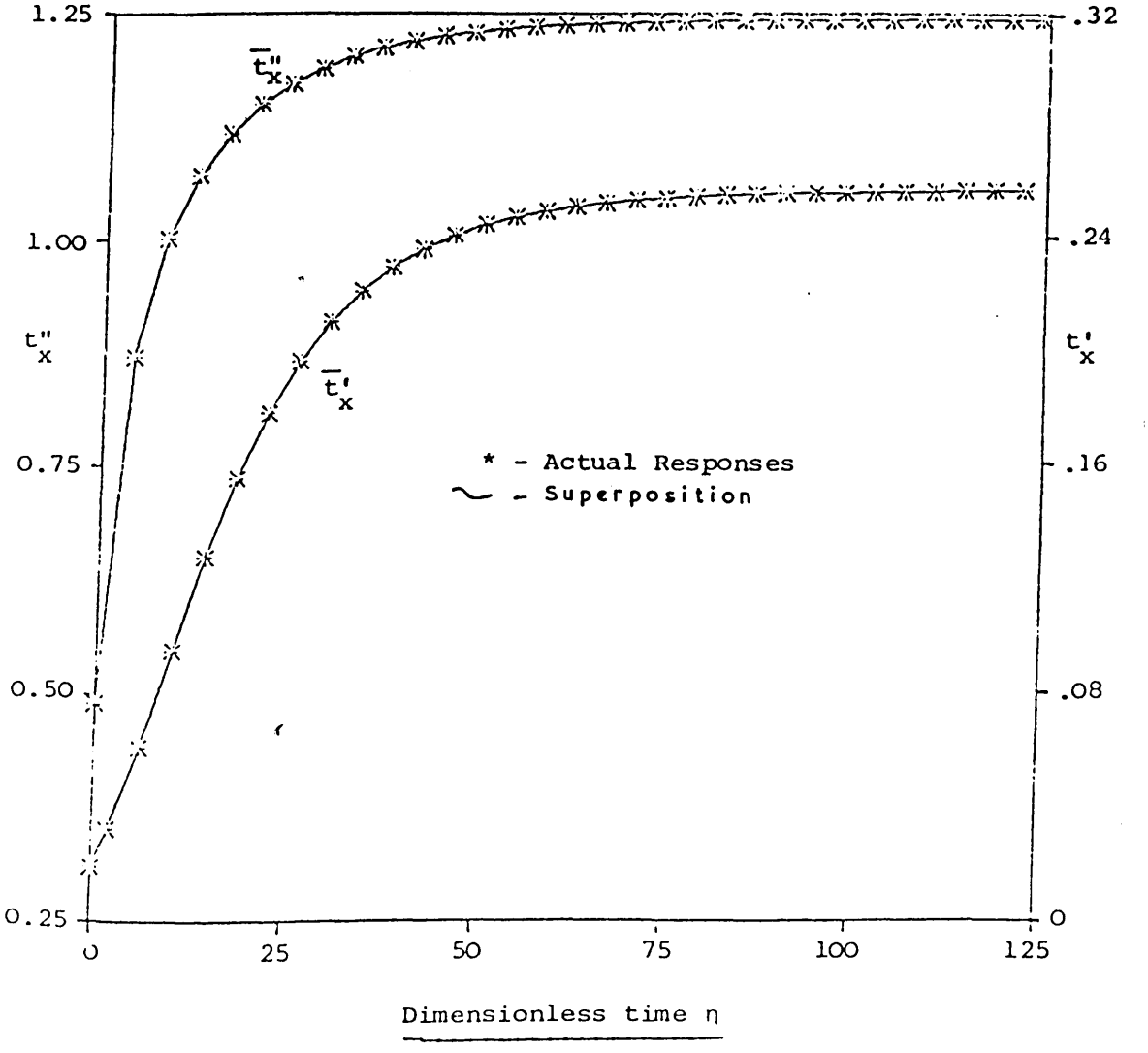

FIGURE 2.10

BURNS' RESULTS (3)

From Burns (1978)

was presented:

$$\Theta = (0.313 + 0.043\Pi + 0.0013\Pi^2)\,\Lambda^2 + (11.504 - 1.156\Pi + 0.0130\Pi^2)\,\Lambda + (-10.778 + 4.663\Pi + 0.0478\Pi^2) \qquad (2.55)$$

The size of step change was defined as a percentage of the final temperature, and a graph showing the dependence of Θ upon the percentage change, for changes of < 50%, was presented by Heggs and Mitchell. No quantification of the curve was given. It should be noted that the implication of this finding is that if the size of a step change is measured in degrees Centigrade, the time to equilibrium is different to that resulting from the same step measured in degrees Kelvin, for example. This is clearly not so. The error in the work, which explains the findings of Heggs and Mitchell, is as follows. For subsequent exit temperatures $t''_x(n)$ and $t''_x(n-1)$, the convergence of the regenerator to equilibrium is given by

$$\varepsilon = \frac{t''_x(n) - t''_x(n-1)}{t'_i - t''_i} \qquad (2.56)$$

normalised on a $t'_i - t''_i$ scale.

If a step change to $t'_i = t'^*_i$ is then made, the convergence is now given by

$$\varepsilon^* = \frac{t''_x(n) - t''_x(n-1)}{t'^*_i - t''_i} \qquad (2.57)$$

on the $t'^*_i - t''_i$ scale, so that

$$\varepsilon^* = \frac{t'_i - t''_i}{t'^*_i - t''_i}\,\varepsilon \qquad (2.58)$$

It can therefore be seen that for a larger t'^*_i, the convergence ε^*

decreases w.r.t. ε , and so the value of the criterion used should be reduced. It is apparent that Heggs and Mitchell used a single value of the criterion for all values of percentage change, resulting in longer times to equilibrium for larger changes.

Mitchell (1982) re-stated this work, and attempted to verify it experimentally, but the few results which were obtained were not sufficient for comparison.

2.2.2 Experimental Work

Very little experimental work has been published concerning transient behaviour of regenerator systems, but it is encouraging to note that the situation is changing due to the realization that theory far outstrips practical experimentation in this area. Industrial experience has tended to lack a reasoned approach to investigation of phenomena.

Chao

The Ford Motor Company (Chao, 1955) published work concerning the design and testing of an experimental rotary regenerator for gas turbines. Chao describes the performance of the regenerator in terms of its efficiency, pressure drop, air loss, bed temperature distribution etc., using reduced length and reduced period as previously defined. The importance of studying transient behaviour

is noted, due to automotive applications requiring rapid start-up and frequent load changes, but very little quantification of the system responses is undertaken.

Using a Hausen/Allen scheme, the predicted reduced air exit temperature (time mean), defined as

$$\varepsilon(\theta) = \frac{t''_{x,m}(\theta) - t''_i}{t''_{x,m}(\infty) - t''_i} \qquad (2.59)$$

is computed and plotted against time for regenerator start-up from cold, and experimentally observed points are plotted on the same graph; the agreement appears to be excellent and is reproduced in figure 2.11.

No investigation is made of the hot side response to a change in air inlet temperature (the application not requiring this knowledge). Furthermore, no analysis of the curves is undertaken, so no equations for the responses are available for comparison with previously described theoretical work.

Ajitsaria

In Ajitsaria's Ph.D. thesis, the response of a small regenerator to changes in flowrate and period duration were studied (Ajitsaria, 1973). The regenerator consisted of four beds 45cm long by 10cm diameter, containing 5mm diameter steel ball bearings. The gas used was air in both periods, the air temperature in the hot period being controlled by varying the flowrate of steam through a steam heat

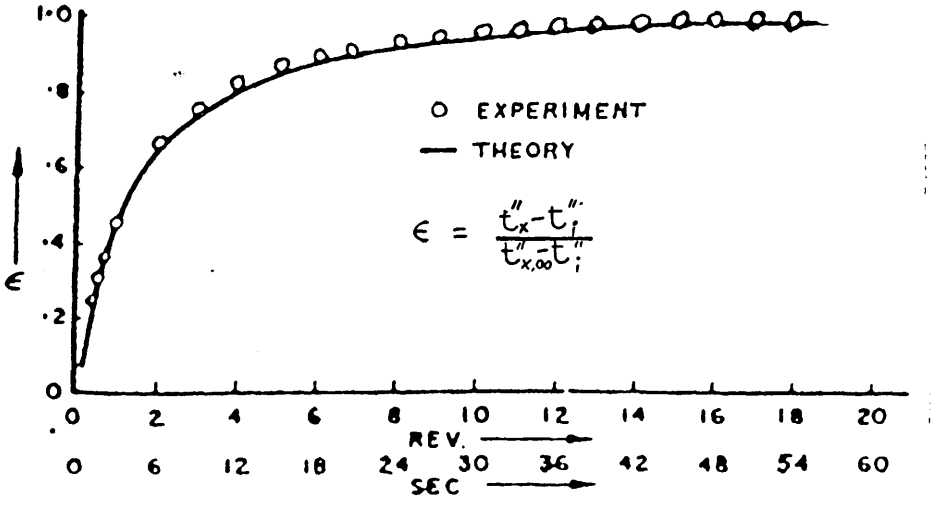

FIGURE 2.11

CHAO'S RESULTS

From Chao (1955)

exchanger. System temperatures were measured using homemade copper/constantan thermocouples linked to chart recorders, the cold junction being immersed in melting ice. Air flowrates were measured using rotameter flowmeters and controlled using 'visual feedback' by manually adjusting needle valves. The integration technique used for evaluating time-mean temperatures was to cut along the thermocouple trace on the chart and then weigh the remaining paper. Electro-mechanical timers operated the needle-valve solenoids to effect changeovers, this being the only truly automatic part of this otherwise manual system.

The efficiencies of the system, and the number of steps to re-establish equilibrium after a step change were studied, for various Λs and Πs, for steps in flowrate and period length. Changes in Λ can be effected by changing the diameter and/or material of the bed particles, and similarly Π. One of the chief difficulties Ajitsaria reports is the problem of conducting a 'constant Λ and Π' experiment; the heat transfer coefficient is flowrate dependent, so changing the flowrate alters Π. As previously discussed, Hausen and others proposed that a linear relationship $h \propto W$ is a valid assumption (i.e. changing W has no effect on Λ) but in practice it is found by both Ajitsaria and the author of this thesis that changing W changes Λ as well (although by a small amount).

Ajitsaria produced many graphs, such as figure 2.12, showing the number of cycles to equilibrium as a function of the size of the step, for many different Λs and Πs and for steps in the two quantities mentioned above. A Willmott method model was used to simulate the experiments.

Ajitsaria's conclusions were mainly concerned with the experimental/theoretical discrepancies; for a step in flowrate the discrepancies decrease as Π decreases, and are less with step increases than with step decreases. The maximum discrepancies in thermal ratio are 2% and the error in the number of cycles to equilibrium ranges from zero to 52% as Λ/Π ranges from 2 to 27. Ajitsaria attributes the errors to non-constant inlet temperatures (a problem also observed by this author); to errors in the model (interestingly); and to the fact that heat losses have larger effect at large Λ/Π.

Hollins

Hollins, at the University of Leeds, worked on the response of a regenerator to a step change in period duration (Hollins, 1981). The apparatus consisted of a packed bed section of variable length (15cm - 35cm) and diameter 8cm, and experiments were conducted with particles of various different materials and sizes (diameter range 5mm - 12mm). Platinum resistance thermometers were used, with orifice plate/transducer flow measurement. Bed pressure drop was

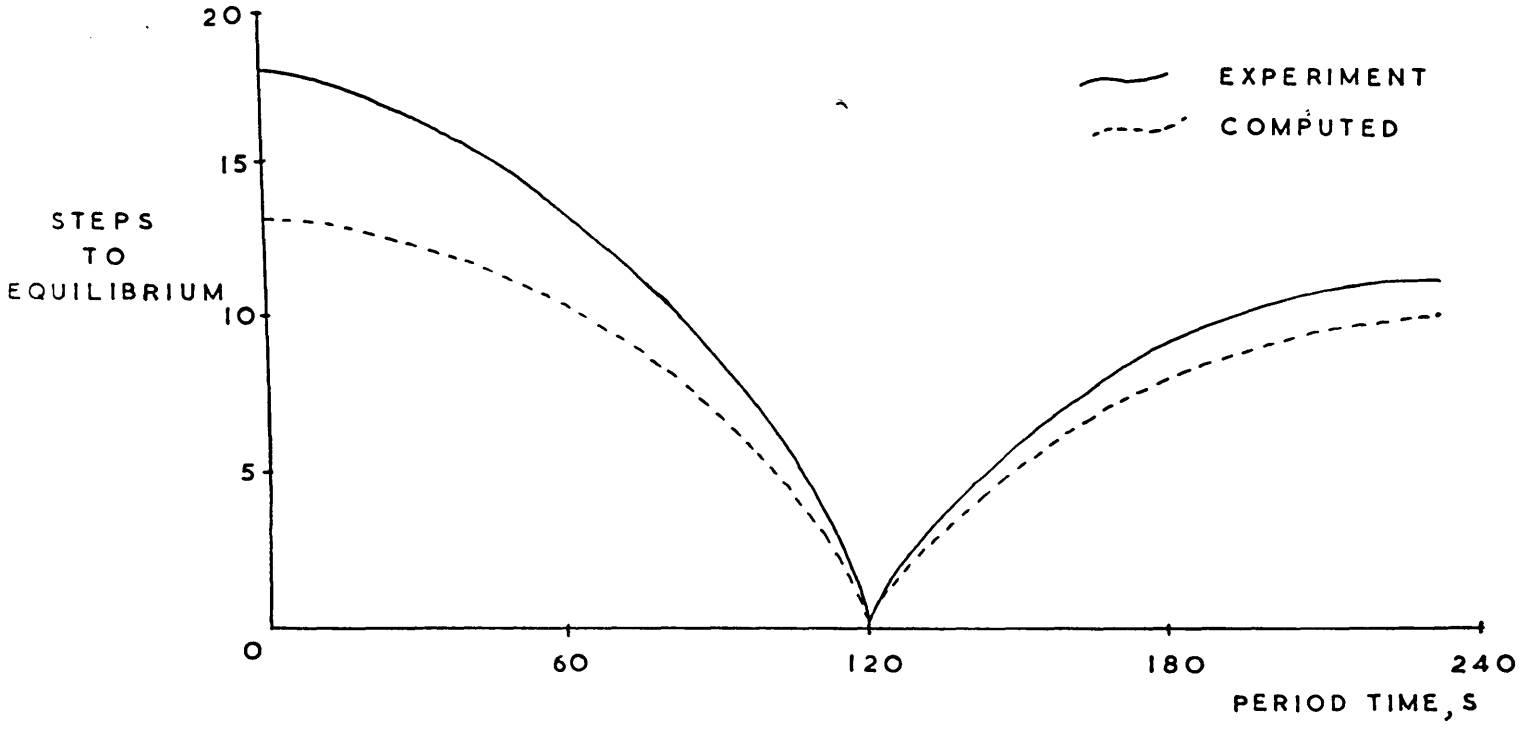

FIGURE 2.12: AJITSARIA'S RESULTS

indicated by manometer, and the whole rig controlled by minicomputer. Hollins reported the effects of heat losses to container, pipes, atmosphere etc.; non-constant inlet temperatures were observed, due to the source and/or sink effects of the pipework, this problem not being resolved. The capacity effects of the container were reduced by insulating the inside with 1mm ceramic wool, and Hollins comments on the useful side effect this has in reducing excess wall voidage. It seems, however, that with a container/particle diameter ratio of ~7 in the worst case, the wall voidage would be very large indeed, and 1mm insulation would have very little effect in reducing it. This is especially so considering the compaction qualities of the Kaowool used. It is therefore to be assumed that, while wall capacity effects were reduced, wall voidage effects were still manifest.

In order to reduce heat losses to atmosphere, Hollins' apparatus worked at temperatures little above ambient, $t_i'' = 30^{\circ}C$ and $t_i' = 40^{\circ}C$. This, obviously, gives a maximum temperature differential of $10^{\circ}C$ at around ambient temperature and it is to be presumed, as a result, that the experiments were very susceptible to fluctuations in ambient temperature. Further, the difficulties associated with observing such small changes in temperature, even with constant ambient conditions, are obvious.

The work done (all under balanced conditions, constant flowrate) studying cycles to equilibrium after a change in period duration produced discrepancies with simulations. Hollins attributed the discrepancies to (i) not allowing sufficient time to equilibrium before effecting a step; (ii) heat losses (less relevant at high flowrates since Q_{loss}/Q_{total} is reduced); and (iii) packing intraconduction (stated to be negligible if $\Lambda/Bi < 60$). Hollins found it necessary to shield the thermometers because of radiation, although it is well known that radiation effects are negligible at such low temperatures. Flow jetting was reported as occuring, in addition to the wall effects, and shields placed in the beds to produce flow 'shadows'. The pipework capacity effects were successfully incorporated in the computer model.

2.3 REGENERATOR CONTROL STRATEGIES

Previous work in this field again falls into two categories:

a) Qualitative experimental and/or industrial descriptions

b) Theoretical analysis and predictions.

These categories are not reviewed separately, but the entire field is considered chronologically.

Katsura and Isobe

In this summary of Japanese methods for automatic stove control and changing (Katsura and Isobe, 1965), the authors identify the four

kinds of control which are necessary:

1. Temperature control of the stove top (hot gas inlet temperature) - protect the packing and, in addition, obtain the greatest possible heat accumulation.
2. Fuel/air ratio control - linked with (1) to obtain optimum combustion and maximum heat accumulation.
3. Flow control of blast furnace gas - keep flowrate at its setpoint and ensure stable combustion, hence controlling the heat accumulation required for the cold period of the next cycle.
4. Temperature control of hot blast (cold gas exit temperature) - necessary for successful furnace operation.

In the first category, Katsura and Isobe mention the criticallity of positioning of the temperature measurement thermocouples; considerable differences in temperature readings were obtained for different insertion depths. Stove top temperature is controlled by adjusting the amount of excess combustion air (i.e. changing the fuel/air ratio). The fuel and air flowrates are typically measured by orifice plate devices and the ratio of the two controlled by signals based on the temperature of the stove top. The physical means of control vary from plant to plant but usually involve a butterfly valve driven by either an electric motor or a cylinder (hydraulic or pneumatic) linked, via a suitable converter, to an electronic controller.

The flowrate of blast furnace gas is usually controlled to a fixed value, or adjusted by remote manual control. Alternately, the heat accumulated during the hot period is controlled by varying the blast furnace gas setpoint depending on the product (blast temperature x blast flowrate). Thus the stove accumulates heat according to the demand of the furnace.

The control of the blast temperature is obviously one of the most important parts of blast furnace operation. Several aspects of this control are therefore indicated by Katsura and Isobe, such as positioning, structure and quality of thermocouples, and the effect of heat losses between measuring point and furnace. The inevitable conclusion from this last point is that blast temperature and flow velocity must be measured as close to the furnace as possible.

In the conclusion to the first part of their report, Katsura and Isobe comment on the performance of the above control system; stove top temperature is controlled to $\pm 10^{o}C$, excess air control (evaluated by waste gas analysis) to $\sim 1\%$ at time of optimum combustion, and blast temperature to $\pm 5^{o}C$. The control system has a response time of, typically, one minute mainly due to thermocouple lag. It will be seen in later chapters that this physical system is similar in many respects to the model regenerator used in this thesis.

The second part of the paper describes methods of automatic changing of the stove system. Two factors determine changing time, the 'consumption' of stored heat in the cold period and the storage of heat in the hot period. In the cold period, three areas are used to determine changing:

i) changeover when (blast temperature - setpoint) < 0

ii) changeover when proportion of bypass flow in the blast is less than a specified amount

iii) changeover when the limit switch fitted on the bypass flow butterfly valve indicates that the valve is closed beyond a certain point .

The third condition is a 'belt and braces' situation in conjunction with (ii), to ensure that errors or failure in the flow measuring devices do not result in complete system failure. As the bypass valve closes to reduce the proportion of bypass flow in the blast, it eventually closes a switch, this then effecting a changeover if one has not been signalled by conditions (i) or (ii). Limit switches are fitted as safety devices on the experimental rig used in this thesis (see Chapter 3).

In the hot period, the exhaust gas temperature is monitored and when it rises above a specified value, combustion is halted.

Displays are provided of the condition of each stove ('on blast', 'on gas' or 'boxed up') and the valve openings and closings are also indicated. Various safety devices are employed, such as ignition

confirmation indication, changeover failure indication and failsafe devices to close butterfly valves upon loss of air flow, air pressure, electrical power etc.

Katsura and Isobe summarize several problem areas in the automatic control and changing of hot blast stoves. These are:

1. Short life and inaccuracy of dome thermocouple.
2. Disturbances introduced by changes in gas and air pressure.
3. The inadequacy of the product (blast flowrate x blast temperature) for determining heat flow.
4. A number of problems involving the butterfly valves, such as slipping of the limit switches and shearing of the valve driving levers.

Some of these problems have been encountered by this author, as described in Chapter 3.

Kan

The aims of the Fuji Electric furnace/stove control system (Kan, 1968) are to improve heating efficiency and reliability, with the associated hardware being an automatic switching (changeover) device, the actual valves, and combustion control/blast temperature control devices. The staggered parallel operating configuration (an early implementation of this method), together with the control computer used are considered to contribute to the improvement of heating efficiency, whilst a contactless (semiconductor-based)

automatic switching system together with electronic measuring devices provides greater reliability.

Kan describes the details and features of the staggered parallel scheme in some depth, pointing out that a dedicated electronic controller handles flowrate mixing proportions etc. The function of the digital computer in the system is overall control and monitoring of the entire furnace/stoves system as opposed to low-level control of the stove flowrates etc. Specifically, the computer performs the following:

1. Realtime analysis of furnace behaviour
2. Control of furnace charging, dependent upon 1.
3. Stove system control.

Only the third point is of relevance here. A general system is shown in figure 2.13, where the dedicated electronic controllers are now replaced by additional computers. The sequencing and switching of the stoves, in this case, can be performed in four different modes: completely automatic (all decisions taken by computer); semi-automatic (operator issues switching commands which the computer carries out, opening and closing valves in the correct sequence); manual remote (operator issues commands to each valve, in the correct sequence); manual local (valves opened and closed by hand winch). Not surprisingly, perhaps, Kan reports that the fully automatic system gives the best results in terms of optimum heat efficiency, speed of decision making, efficiency of stove

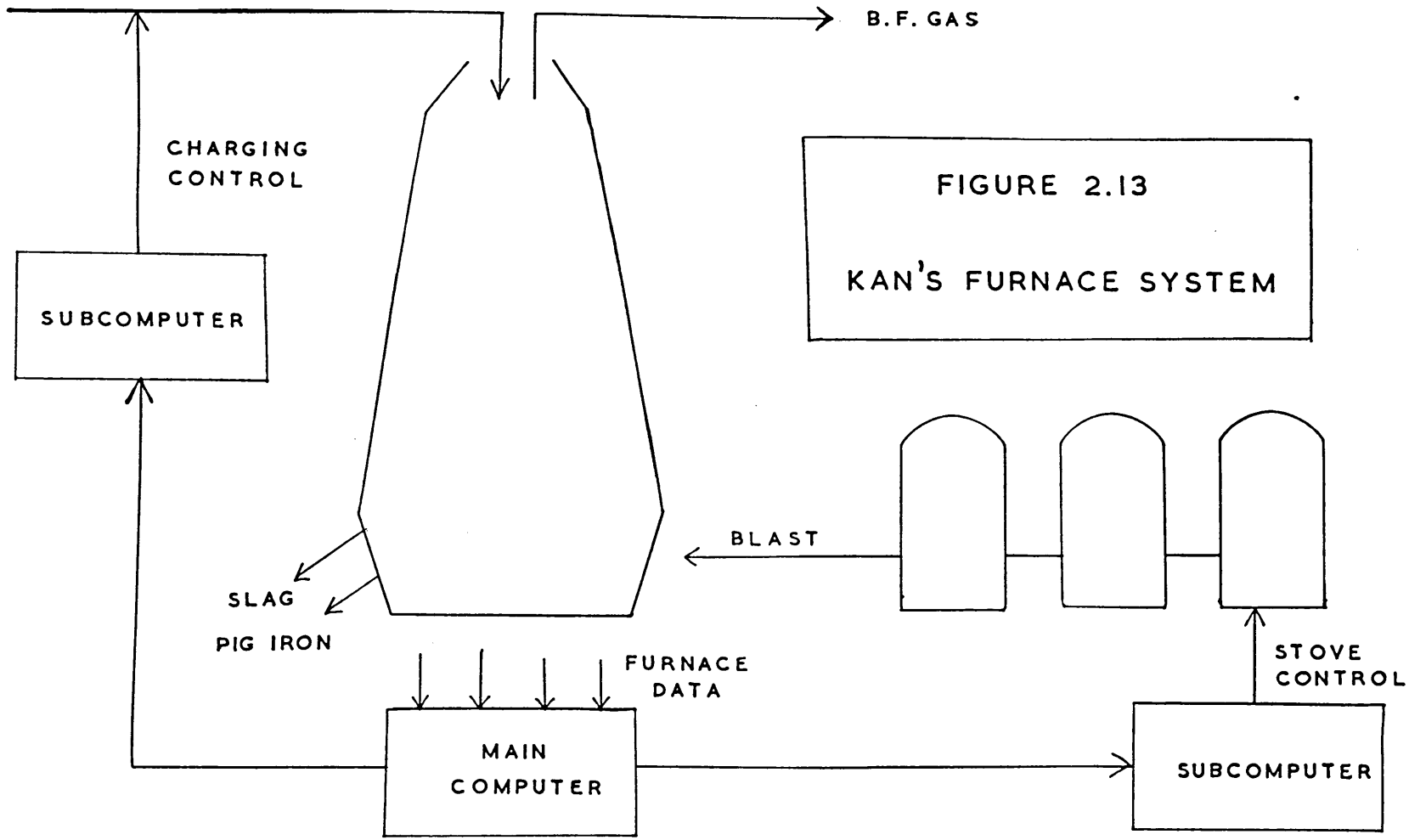

FIGURE 2.13

KAN'S FURNACE SYSTEM

scheduling, etc.

The combustion control unit also improves efficiency by ensuring that there are no heat deficiencies, and minimising the amount of enriching fuel used. Its manipulated variables are the fuel/blast furnace gas ratio and the excess air/gas ratio, and the controlled variables are the dome temperature and waste gas temperature. In this respect, the system is very similar to Katsura and Isobe's system.

Kwakernaak, Strijbos and Tijssen

In two papers, published in the late 1960s/early 1970s, Kwakernaak et al presented detailed mathematical analyses of conditions for optimal operation of thermal regenerators. The first paper (Kwakernaak et al, 1969) treats the problem in some detail by considering only the heating period, then briefly includes the cooling period as being an integral part of regenerator operation.

The basic regenerator equations are stated in the following (dimensional) form:

$$\frac{\partial T}{\partial \theta} = \frac{hA}{MC}(t - T) \qquad (2.60)$$

$$\frac{\partial t}{\partial y} = \frac{hA}{WSL}(T - t) \qquad (2.61)$$

During the heating period, the gas leaving the regenerator has a

non-zero heat content, and inefficiency is thus introduced. The efficiency of the hot period is defined as:

$$\eta = \frac{Q_s}{Q_h} \tag{2.62}$$

where Q_s is the heat stored and Q_h is the total heat supplied. Q_s and Q_h are given by

$$Q_s = \frac{M}{L} \int_0^L \left[CT\big|_{\theta=P'} - CT\big|_{\theta=0} \right] dy \tag{2.63}$$

$$Q_h = \int_0^{P'} W'(\theta)\, St\big|_{y=0}\, d\theta \tag{2.64}$$

The optimisation problem is formulated as follows:

Given a fixed initial solid temperature distribution $T(y,0) = T_o(y)$, and given a fixed amount of heat which must be stored during the hot period, how should the inlet gas temperature $t'(0,\theta) = t'_i(\theta)$ and mass flowrate $W'(\theta)$ be chosen as functions of time to maximise the thermal efficiency η?

Since Q_s is fixed, maximising η amounts to minimising Q_h. A constraint

$$t'_i(\theta) < t'_{i\,max} \quad \forall\, \theta \tag{2.65}$$

is imposed due to practical limits. The complete analytical solution is only possible with the assumptions

1. Specific heats C and S are constant, and
2. Heat transfer coefficient h depends on W only.

The system equations 2.60 and 2.61 become, with these assumptions and after substitution of one into the other,

$$\frac{\partial T(y,\theta)}{\partial \theta} = -\alpha h(\theta) T(y,\theta) + \alpha h(\theta) \exp\left\{-\frac{\beta h(\theta)}{W(\theta)} y\right\}$$

$$+ \frac{\alpha\beta h^2(\theta)}{W(\theta)} \int_0^y \exp\left\{-\frac{\beta h(\theta)}{W(\theta)}(y-\psi)\right\} T(\psi,\theta)\, d\psi \qquad (2.66)$$

where $\alpha = A/MC$, $\beta = A/SL$, $h(\theta)$ means $h(W(\theta))$

Since the distribution $T_o(y)$ is fixed, the condition that heat to be stored is fixed can be written

$$\int_0^L T(y, P')\, dy = Q_{s,g} \qquad (2.67)$$

where $Q_{s,g}$ is a given quantity. This is a constraint on the final state of the system 2.66. The condition that heat supplied must be minimised amounts to minimising

$$\int_0^P W'(\theta)\, t_i'(\theta)\, d\theta \qquad (2.68)$$

(c.f. 2.64)

The optimisation problem is now :

Transfer the parameter system (2.66) from a fixed initial state $T_o(y)$, in a fixed time P', to a terminal state $T(y,P')$ which satisfies 2.67 (heat to be stored is fixed) so that 2.68 (heat supplied) is minimised yet 2.65 (t_i' maximum value) is not violated. Kwakernaak et al achieve this via the use of Hamiltonians, upon inspection of which they reach the initial conclusion that $t_i'(\theta)$ must be set equal to its maximum value $t_{i\,max}'$ for the whole period. Under this assumption, they evaluate the Hamiltonian and using Laplace transforms conclude that the optimal gas flowrate W' does not depend upon time.

The overall conclusion is, therefore, that the maximum thermal efficiency arises from using the maximum allowed hot gas inlet temperature and constant flowrate. The actual value of optimal flowrate $\dot{W}^o$ must be chosen so as to store the desired amount of heat. Kwakernaak et al also state that (by a similar argument) the period duration should be set to its maximum allowed value, although this is certainly not the case; if P'_{max} were sufficiently large, the solid would become isothermal along the regenerator and, as the heating period continues, no more heat would be stored and the efficiency η would start to fall. In order to avoid this the constant flowrate W^o would have to be zero, which cannot be the case.

In considering the cooling phase as well, the overall objective (to minimise heat supplied) remains the same, and embedding the heating cycle in a complete problem merely affects the initial solid temperature distribution. This must now be linked to conditions in the cooling period, but since most of the arguments previously employed are independent of the initial and final conditions, it is not surprising that the same conclusions are reached; that is, $t'_i(\theta) = t'_{i\,max}$ and $W'(\theta)$ = constant, W^o. The authors state that the first of these conditions cannot, now, be rigorously proved yet 'it seems highly unlikely' that $t'_i(\theta)$ should be chosen less than $t'_{i\,max}$. In conclusion, it is proposed that the above conditions (and the dubious condition $P' = P'_{max}$) be used as a starting point for developing numerical procedures for optimising stove operation, and

this is done in the second paper.

The second paper (Kwakernaak et al, 1970) applies the above results to the optimisation of a four stove staggered parallel system. The assumption made are as follows:

1. A constant blast flowrate is demanded.
2. The operation is periodic (i.e. cyclic equilibrium is attained).
3. The four stoves are operated identically apart from a time shift.
4. The non-zero changeover time is taken from the hot period.

Figure 2.14 shows this diagramatically.

Certain generally accepted assumptions are also made, such as negligible heat loss, gas heat capacity small compared to packing, transversal heat conduction allowed for in heat transfer coefficient, etc. Similar system equations as before are used (2.60, 2.61) and the usual reversal conditions are applied. In addition, the conditions that each stove operates identically and that the desired rate of blast W_B is always supplied, give rise to the equation

$$W''(\theta) + W''(\theta + \tfrac{1}{2}P'') = W_B \qquad 0 \leq \theta \leq P'' \tag{2.69}$$

and to obtain the desired blast temperature, the following condition must also be imposed:

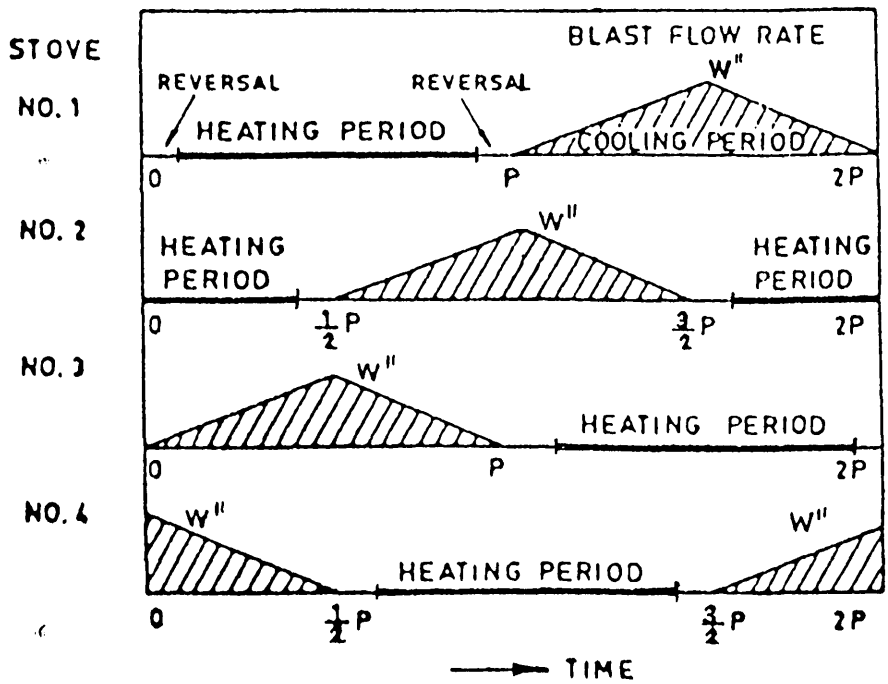

FIGURE 2.14

STAGGERED PARALLEL OPERATION

From Kwakernaak et al (1970)

$$\frac{W''(\theta).t_x''(\theta) + W''(\theta+\tfrac{1}{2}P'').t_x''(\theta+\tfrac{1}{2}P'')}{W_B} = t_B \qquad (2.70)$$

where t_B is the blast temperature setpoint. The heat supplied to the regenerator is given by a similar equation to 2.64:

$$Q_h = S\int_0^{P'} W'(\theta)\left[t_i'(\theta) - t_i''\right] d\theta \qquad (2.71)$$

where t_i'' is used as a reference temperature.

The heat given up by a stove in the cold period is given by

$$Q_c = \tfrac{1}{2} S W_B (t_B - t_i'') P'' \qquad (2.72)$$

and the efficiency is defined as

$$\eta = Q_c/Q_h \qquad (2.73)$$

Since Q_c is fixed, Q_h has to be minimised, as before.

The optimisation procedure involves considering the above system of equations and manipulating $W'(\theta)$, $t_i'(\theta)$, $W''(\theta)$, P' and P'' so that Q_h is a minimum. The technological constraint 2.65 is again imposed. P'' is considered fixed, and its optimal value determined by repeated optimisations at different values of P''. The starting point is the set of conclusions reached in the first paper and a numerical procedure is used to find the minimal hot period flowrate (W^o) which satisfies the equations. The Willmott 1964 method (with p time and m distance steps) is used to solve the basic equations; for given W^o, t_i' and $W''(\theta)$, the final solid temperature distribution is calculated (and, via the reversal conditions, the initial

distribution for the next period). Hence the initial solid temperature distribution T(y,0) can be considered as a function of hot period flowrate W^o, and cold period flowrate $W''(\theta)$, $0 \leqslant \theta \leqslant P''$. After rearranging 2.69 and 2.70 in discrete form, a series of p equations is obtained for W^o and the p variables W''_1, $W''_2 \ldots W''_p$ which constitute $W''(\theta)$. A quasi-Newton algorithm coded in Algol-60 is used for their solution, and the cold gas flowrate profile obtained is a slightly skewed version of that shown in figure 2.14, this being consistent with other work (Willmott, 1969b; Razelos and Benjamin, 1978), shown in figure 2.15.

The quantitative results are specific to the industrial site which was chosen for analysis and are, as such, of little interest here but the generalised conclusions <u>are</u> relevant and are as follows:

1. The efficiency of the four stove staggered parallel system is not very sensitive to variations in the duration of the cooling period P'', and
2. For any given duration of cooling period, there is only a very small range of admissible solutions for optimal operation.

These conclusions suggest that the operation of the system is not very critical, in the sense that very little can be gained by sophisticated refinements. A more involved mathematical method enabling more precise choice of period durations would only result in a fraction of a percent change in efficiency. This represents a negligible financial saving to an industrial company and is

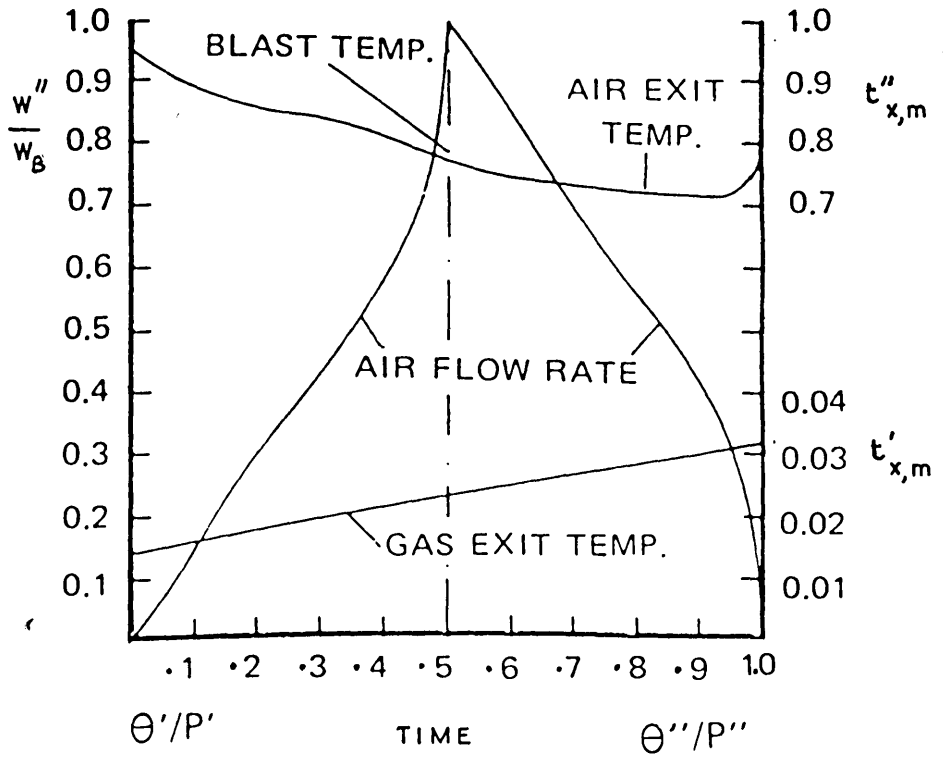

FIGURE 2.15

STAGGERED PARALLEL:
SINGLE STOVE
BEHAVIOUR

From Schmidt & Willmott (1981)

therefore not worthwhile.

Stikker and Broekhuis ; Strausz

The control system for bypass main and staggered parallel operation implemented at an industrial site in Ijmuiden was developed by studying the behaviour of Willmott-type models, and is described in two identical papers (Stikker and Broekhuis, 1970; Strausz, 1970). Similar assumptions to those made by Kwakernaak et al concerning heat conduction, losses, etc. are made and detailed quantitative results are again specific to the site. A more general discussion of the results reveals that, firstly, the system performance, measured in terms of maximum blast temperature, is better in staggered parallel than in bypass main and, secondly, that a similar performance can result from a smaller volume of packing if the height is increased. This is due to the gas velocity, and hence convective heat transfer coefficient, increasing with decreasing cross-section. Unfortunately, however, the pressure drop also increases so no overall performance improvement is achieved.

Interesting parallels with this thesis are observed when Stikker and Broekhuis discuss the correlation between real and simulated results. They note the difficulties encountered by this author; namely, that over the period required by the system to reach equilibrium, in practice at least one of the variables (e.g. cold gas inlet temperature) will change. To overcome this, Stikker and

Broekhuis suggest that either the model predictions should be corrected or else a 'retrospective simulation' should be done using the actual conditions. The latter, as will be seen, is the method adopted in this thesis. Using this procedure, where the gas and air flowrates and inlet temperatures applied to the model were those measured during an actual run, good agreement (±10% max.) was obtained between actual and simulated period durations. It should be noted at this point that termination of the heating period in the model occurs when the lower part of the chequerwork reaches that temperature observed in the 'real' case, and the cooling period is terminated when the chequerwork at around half-height falls to the observed value. This is in contrast to the work of this thesis where the actual periods are used and gas temperatures are compared.

A similar agreement (±10% max.) is obtained for waste gas temperature, although it is stated that this involves a correction to the convective heat transfer coefficient; a constant term is added to the value calculated by Hausen's method. It is also stated that attempts to correct the heat transfer coefficient by a constant multiplication factor were not successful, and a possible cause of error in the shape of the flues is proposed. The solid temperature agreement is reported to be good at the lower end of the regenerator in the heating period, becoming progressively worse along the length of the regenerator. For the blast period, the agreement is said to be good at all points, so it is deduced that discrepancies are introduced during the heating period, possibly due to flow

maldistribution in the upper part of the chequerwork, or non-uniform flame temperature.

The analysis of control principles by Stikker and Broekhuis is, in its nature, 'trial and error'. The problem of non-constant operating conditions means that the maximum allowable waste gas temperature (to minimise losses yet optimise performance) has to be recalculated if the cold gas inlet temperature changes. For this reason the control strategy is based on principles other than that of effecting a changeover when waste gas temperature rises to a preset level. Specifically, the principles used were:

1. A fixed amount of heat is delivered to the stoves in the heating period (c.f. Kwakernaak et al), based upon required blast flowrate, temperature and period, and on stove efficiency and mode of operation.
2. This heat is supplied in a calculated time interval, based on the mode of operation and the blast period minus changeover time.
3. The blast period is ended as soon as a certain thermal level is reached, determined by the position of the bypass valve (if in bypass main mode) or by a prefixed difference between dome and blast temperature.

Thus there is always a fully heated stove available at changeover. If the stoves are kept on a minimum thermal level, then when a disturbance such as a sudden increased blast temperature demand

occurs, the increase in heat output required may be as large as the total heat supplied in the period. Thus a choice has to be made between incurring extra losses by having excess heat stored, not allowing sudden changes in demand or temporarily decreasing the blast period.

As mentioned earlier, Stikker and Broekhuis also worked on the computer controlled implementation of staggered parallel operation in a practical system. The basic instrumentation (per stove) consisted of gas and air flowmeters, waste gas temperature meters, a dome temperature meter and a combustion control device. The central computer (a PDP-8) was not very powerful (in terms of speed and flexibility) by today's standards, yet still performed the following functions:

1. Direct digital control (P.I.D.) of the air and gas inlet valves - operator can change control coefficients via switches.
2. Sequencing of changeovers, such that there is always a 'full stove' available on time.
3. Calculation of gas flowrate set point depending on blast flowrate and temperature demand etc.
4. Control of the gas flowrate and termination of heating when a preset amount of gas has been burnt (with override if waste gas temperature rises too far).
5. Control of air/gas ratio.
6. Monitoring of various analogue and digital signals.

Stikker and Broekhuis then discuss the ways in which the system handles non-stationary conditions. If the blast temperature setpoint is lowered, the cooler stove is taken off blast and the system automatically switches to three stove bypass main operation. This prevents any stove being cooled too far, and staggered parallel is resumed when the on-blast stove has cooled to a suitable level. If blast temperature or flowrate setpoints are raised then combustion control ensures that the change in demand is met by increasing gas flowrate, and also (for temperature increases) shortening periods. If for any reason the computer detects that the demand change cannot be met, an alarm is raised. Single stove failure (e.g. a stuck valve) results in automatic switching to bypass main, while multiple stove failure produces an alarm and cessation of automatic control. However, data is still collected to enable a swift return from manual operation, upon repair.

The plant schematic for the system described by Stikker and Broekhuis and Strausz is shown in figure 2.16.

Zuidema

Based on the work of Kwakernaak et al, this work is a theoretical analysis of non-stationary operation of a staggered parallel system (Zuidema, 1972). The aims are to conduct the system after a load change such that

1. The duration of the upset is minimised, and

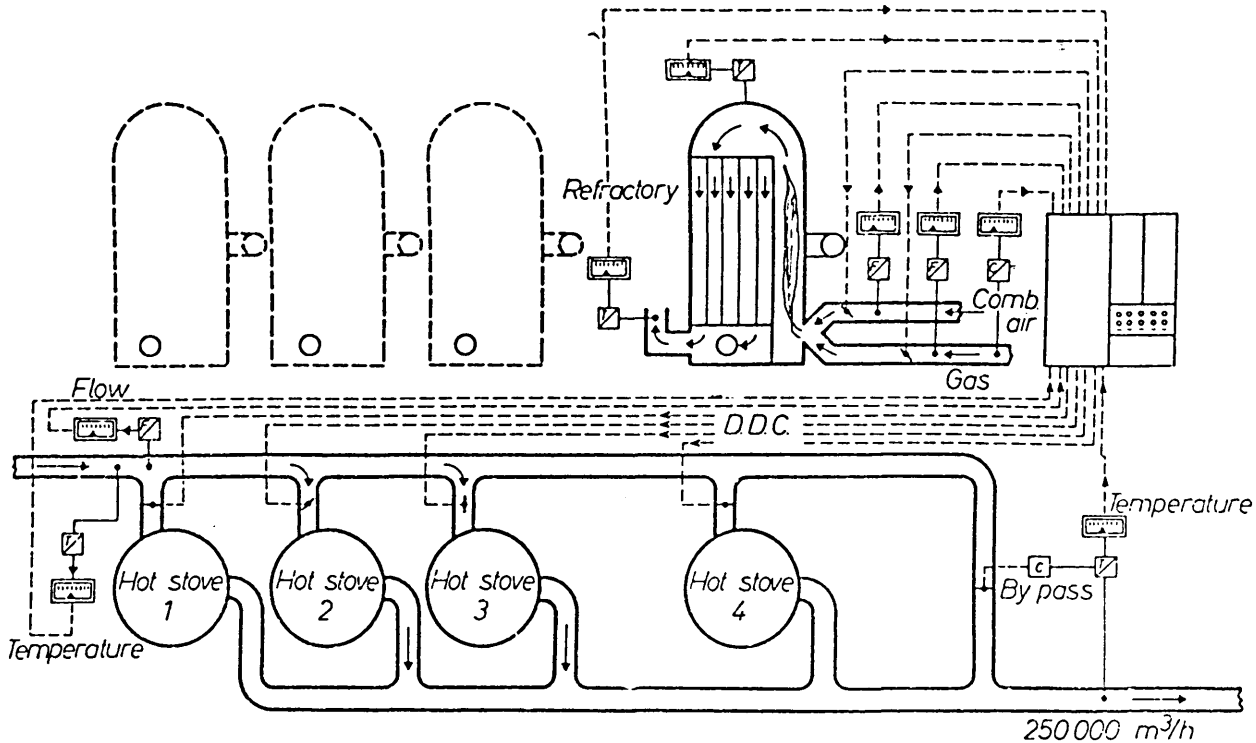

FIGURE 2.16

COMPUTERISED STOVE SYSTEM

From Stikker & Brockhuis (1970)

2. If the load change cannot be met immediately, the period of the shortfall of demand is minimised.

Load changes which fall into this latter category are known as 'large' changes, 'small' changes being those which can be met immediately. Large changes imply that either the flowrates cannot be adjusted to compensate, or the system period durations decrease so far that the demanded load cannot be satisfied; this is known as 'collapse'. It is evident that load decreases are always small changes.

As in Kwakernaak's work, the system is operated according to principles such as $W' =$ constant, $t'_i = t'_{i\,max}$ etc. and, importantly, load changes only occur at the start of a period. A Willmott-type model is used with the numerical approach employed previously in order to solve the problem. It should be noted that, in Zuidema's terminology, there are two 'periods' in the heating or cooling 'phase', the end of a period being when one stove is brought onto blast and another put onto heating. This point will correspond to midway through the blast phase of another stove. Five basic timewise profiles are used. These are:

P[i], i = 1,2... , the duration of the ith period after a load change

t_g[i], the blast temperature delivered in the ith period

W_g[i], the blast flowrate in the ith period

W'_1[i], the gas flowrate for the stove which is in the first period of its heating phase, and

$W_2'[i]$, the gas flowrate for the stove which is in the second period of its heating phase.

Input to the program consists of the initial solid gas temperature distributions and also $t_B[i]$, $W_B[i]$, $W_1'[i]$, $W_2'[i]$ and the most important independent variable P[i]. Obviously P[i] will also be a function of the profiles which have occurred before the demand change, and since $W' =$ constant within a heating phase, then $W_2'[j+1] = W_1'[j]$ $(j = 1..i)$ which considerably reduces the number of variables.

When a small load change occurs to the stationary system, it is assumed that the load then remains constant long enough for a new stationary state to be established. To minimise the time to equilibrium, $t_B[i]$ and $W_B[i]$ are set to the desired values for all i, and then the gas flowrates $W_1'[i]$ and $W_2'[i]$ are chosen such that the periods P[i] are made as close as possible to the values which will prevail at the new stationary state. Thus the system is forced to operate with the steady state period durations, which makes it fast to settle to that state. Typical solutions for the Hoogovens plant indicate that a 2% increase in blast temperature setpoint requires maximum gas flowrate for four periods, after which stationary state is attained in three periods.

When a large load change occurs, it is detected during the computation since the required blast temperature is not delivered despite maximum heating flowrates. Associated with this is a steady

decrease in the period duration. It is then necessary to adopt a two-stage strategy: (i) lower the aim of the system and accept a lowered output for a certain time (n cycles); (ii) during this time the heat content of the system builds up to the point when the demand can again be met and a steady state re-attained using the small change approach. In detail, for stage (i) the gas flowrates are kept at W'_{max} and the manipulated variables are the loads delivered in each period. Assuming the demanded blast flowrate is always delivered, the manipulated variables become the blast temperatures $t_B[i]$. The technique used by Zuidema is to satisfy the conditions

$$t_B[n+1] = \hat{t}_B \quad \text{(demanded value)} \qquad (2.74)$$

$$P[n+1] = P_{ss} \quad \text{(steady state value)} \qquad (2.75)$$

whilst also minimising

$$\sum_{i=1}^{n} (\hat{t}_B - t_B[i])^2 \qquad (2.76)$$

These three conditions are incorporated in the expression

$$\sum_{i=1}^{n} (\hat{t}_B - t_B[i])^2 + \lambda (P[n+1] - P_{ss})^2 \qquad (2.77)$$

which is minimised using a standard computer package, with λ sufficiently large. The overall method is to repeat the minimisation with different values of n to find the best value, then follow the small change approach adjusting the heating gas flowrates so that P[i] is always equal to P_{ss} . Numerical results indicate that as the value of n increases the square root of the criterion 2.76 steadily decreases; also as n increases, the time taken for the system to respond to a load change increases (by definition) but the

response is smoother. For a small n there is a large initial shortfall followed by a jump to the new load temperature. The choice of n is therefore dependent upon the particular system requirements in a practical installation.

Zuidema concludes that this procedure can be used in an online situation, specifically when information about future load changes is available, when the method enables stove content to be built up beforehand. It is apparent that it is more valuable to use the qualitative findings for improving control loops, as opposed to refining the equations sufficiently to achieve accurate predictions.

Beets and Elshout

The Hoogovens Company developed an offline mathematical model for the design and development of a blast furnace stove system and its control scheme (Beets and Elshout, 1976). This includes optimisation of capital expenditure as well as thermal performance, and is used for improving existing systems as well as designing new ones. A series of control strategies was studied in a staggered parallel environment with bypass main as a stove failure backup (c.f. Stikker and Broekhuis), and the best strategy implemented at the practical plant.

The usual Willmott-type model is used, but when considering overall control performance, the novelty of Beets and Elshout's work becomes apparent. Only one figure is used to represent the thermal condition of a stove, that is the total amount of heat integrated over the whole chequerwork. (This is in contrast to the usual approach where the complete distribution is considered as many values.) This method is also well suited to an online control model. The heat content is considered at two points in time: at the end of the blast phase, the 'residual heat' provides information regarding the level of equilibrium characteristic of the current operating conditions; and at the end of the gas phase the 'accumulated heat' provides information regarding the capacity of the system and its ability to meet changes in conditions. It should be noted that under static conditions, the same level of residual heat is observed at the end of each blast period. Additionally, after a temporary disturbance, this same level of residual heat is eventually re-attained whereas if a disturbance is permanent the residual heat level changes. The blast volume and temperature setpoints, dome temperature and blast period setpoints all affect the residual heat level.

In studying the dynamic behaviour of the system, Beets and Elshout consider an increase in blast volume (an example of 'a disturbance'), an increase in blast temperature ('a serious disturbance') and an unexpected change to bypass main ('a very large disturbance'). In all of these disturbances, the heat supplied

during the heating period must be increased, in order to raise the residual heat level, after which the system will stabilize around the new level. (The change to bypass main requires this since the capacity of a three-stove bypass main system is much less than that of a four-stove staggered parallel system). Blast flowrate setpoint changes are accommodated by allowing the blast period duration to change and then stabilizing around a new residual heat level after adjusting the heating rate. Changes in blast temperature setpoint are largely self-controlling; the period duration is allowed to change, hence the residual heat level changes. The difference between this residual heat level and the accumulated heat level is later adjusted by altering the heating rate.

Beets and Elshout considered it most important to investigate and develop a control model for the heating phase, since the main control variables in the stove system are the gas flowrates. As an example of the complicated interactions which can occur, a case is cited wherein one stove acquires extra heat, once, by remaining on gas longer than usual; hence another stove is forced to remain on blast longer than normal, after which the normal amount of heat is supplied to it. In the next cycle, this stove is short on accumulated heat, so the blast period is shorter than usual. It is thus seen that an excess of heat in one stove can lead to a shortage in another. The basic control model for the heating phase is used to calculate the amount of heat to be supplied and the time available to do so. In a stable situation this is trivial, and when

a disturbance occurs the aim of the model is to restore a stable operation, without overshoot (to avoid further disturbances). This is usually easily achieved, unless the disturbance is so large that collapse is threatened; in this case three stoves are put on heating while only one remains on blast, thus raising the accumulated heat level sufficiently. During this time, as with Zuidema's scheme, the drop in blast temperature is accepted. An expected change to bypass main can be accomodated by increasing the accumulated heat level steadily beforehand, but Beets and Elshout's model also allows a smooth transition after a large unexpected change such as this. Little detail is given, except to state that the scheme is better than manual control in practice.

The errors arising from the 'total heat content' approach only become apparent when equilibrium is being restored after a large change in operating conditions. This is due to a resultant change in the way in which heat is distributed along the chequerwork. According to Beets and Elshout, however, relatively good results are still obtainable using their method. In addition, their method is still useable in the situation where optimal control is not possible due to minimisation of time to stable state resulting in impractically high gas flowrates. This scheme can still produce control within constraints, albeit not optimal.

The Hoogovens implementation of Beets and Elshout's work uses a digital computer rather than analogue devices, in order to achieve greater flexibility of the controller. This is necessary due to the control characteristics of the plant being dependent upon the mechanical characteristics of valves, maximum gas flowrates, required blast volume, etc. and these installation-dependent constants are easily altered in a digital computer controller. Additionally, adaptive control is possible as the stoves cool.

Holstein and Sanna

The main aim of this system (Holstein and Sanna, 1978) is to monitor and control the behaviour of the gas burner in order to achieve as high a blast temperature as possible. In particular, the rate of enrichment of the furnace gas is to be maintained constant, the combustion air is to be monitored and controlled by analogue methods and the dome temperature must be held close to its setpoint by adjusting either the rate of enrichment or the proportion of excess combustion air. Changeovers are sequenced, as usual, according to the fall of exit temperature during the cooling phase, but also taking into account the heating rate of the burners. During the heating period, the heat to be delivered to the stove is assumed to be equal to the amount given up during the preceding blast period, this having been calculated at the time. In addition, the dome and waste gas temperatures of the previous heating period are used to make predictions concerning the operation of the burner during the

current period. Hence the 'calorific debit' which the burner has to supply can be calculated, and hence the burner controlled to minimise heat wastage.

The calorific debit, Q_B, is given by

$$Q_B = P'S'W't_o = k\,\frac{W''P''(t''_{x,m} - t''_i)}{1 - t'_{x,m}/t_{dome}} \qquad (2.78)$$

where t_o = theoretical temperature of combustion at burner.

In order to correct for theoretical/real discrepancies, the constant k is written as the product of two factors

$$k = k_o c \qquad (2.79)$$

where k_o (stored in the computer) takes account of the insulation of the stove (i.e. heat losses) and the specific heat of the blast, and c is a corrective term to account for drifts in the thermal balance, such as the difference between blast setpoint $\hat{t}_B$ and the actual temperature at the end of the period, t''_{xo}. c is thus given by

$$c = 1 + \alpha(\hat{t}_B - t''_{xo}) \qquad (2.80)$$

The coefficients k_o and α are determined by experiment at system testing time.

The computer monitors and controls the enrichment of the gas by fuel gas (and so controls the flame temperature) so as to achieve the required dome temperature whilst also minimising the rate of enrichment. Knowing the calorific debit to be supplied, the

calorific values of the two gases and the rate of enrichment, the overall heat content of the gas mixture can be calculated and the correct amount of heat delivered. If the dome setpoint is attained before the end of the heating period, the supply of fuel gas is shut off and the excess air adjusted to maintain a constant dome temperature.

The two methods of controlling the dome temperature (enrichment or excess air) can obviously only be used once the dome temperature setpoint has been determined. Holstein and Sanna outline two means of determining the setpoint, depending upon whether maximum thermal yield or minimum cost of blast is required. In the former case, the dome setpoint is merely determined by the limiting factors introduced by the chequerwork properties. In the latter case, the combustion control becomes more involved; good costs, realised by low waste gas temperatures, can only be obtained by enriching the furnace gas with expensive fuel gas. This can be seen from the heat balance equation:

$$W'S'P'(t_i' - t_{x,m}') = W_B S_B P_B (t_B - t_i'') \qquad (2.81)$$

Consider the RHS to be constant (the desired heat output per blast period) and the LHS equal to the same constant (the heat to be supplied to the regenerator per heating period). If t_i' were forced to rise to a given value (i.e. if flame temperature were increased by enrichment) and also the waste gas temperature $t_{x,m}'$ were somehow made to fall, then the balance could be maintained by reducing W' to a lower value. Similarly, if t_i' were raised to the higher value and

W' deliberately reduced to its lower value, then $t'_{x,m}$ would be forced to fall (assuming constant P'). Now, clearly, the saving realised by reducing the waste gas temperature is counterbalanced by the cost of fuel gas, so an optimal flame temperature must be found which results in a minimal cost per unit of delivered heat. The overall cost equation must also incorporate the 'price' assigned to blast furnace gas; this will vary from site to site due to surpluses (where the gas may be flared off, hence given a zero 'price') or shortages (where the 'price' will be considerably higher). Holstein and Sanna simulated runs with different rates of enrichment to find the optimal flame temperature and hence the optimal enrichment rate. During practical industrial running the control model calculates the 'price of heat' after each cycle of operation and, after correction for theoretical/actual discrepancies, maintains an optimal enrichment rate.

Burns

Burns' work on transient response (Burns, 1978) has been described in section 2.2 and his application of the work to feedforward regenerator control strategies is described here.

Burns considers first the case where a regenerator at cyclic equilibrium with known thermal ratios E' and E'' (given by

$$E' = \frac{t'_i - t'_{x,m}}{t'_i - t''_i} \qquad (2.82)$$

$$E'' = \frac{t''_{x,m} - t''_i}{t'_i - t''_i} \qquad) \qquad (2.83)$$

is required to deliver an increased load of temperature mean value t_B. In addition, the constraint is imposed that the waste gas temperature t'_x must not exceed a certain maximum. As usual, the increased load is to be met by increasing the hot gas inlet temperature, and it is the knowledge of the responses ε_{g1} and ε_{g2} that is applied to achieve this. The responses are given by:

$$\varepsilon_{g1} = \frac{t'_{x,m}(n) - t'_{x,m}(0)}{t'_{x,m}(\infty) - t'_{x,m}(0)} \qquad (2.46)$$

$$\varepsilon_{g2} = \frac{t''_{x,m}(n) - t''_{x,m}(0)}{t''_{x,m}(\infty) - t''_{x,m}(0)} \qquad (2.47)$$

If the new load is to be met in the first cycle then $t''_{x,m}(1)$ must be equal to t_B. The final cold gas exit temperature which would result from constant operation from this point on is, from 2.47,

$$t''_{x,m}(\infty) = \frac{t_B - t''_{x,m}(0)}{\varepsilon_{g2}(1)} + t''_{x,m}(0) \qquad (2.84)$$

and since the thermal ratios are unchanged then at steady state, for $t''_i = 0$ (normalised scale):

$$t''_{x,m}(0) = E'' t'_i \qquad (2.85)$$

$$t''_{x,m}(\infty) = E'' t'^{*}_i \qquad (2.86)$$

where t'^{*}_i is the new hot gas inlet temperature. This is calculated directly by combining 2.84, 2.85 and 2.86 to give

$$t'^{*}_i = \frac{t_B - E'' t'_i}{E'' \varepsilon_{g2}(1)} + t'_i \qquad (2.87)$$

In order to ensure that the constraint upon the waste gas

temperature is observed, the following equations are used:

$$t'_{x,m}(\infty) = t'^{*}_{i}(1 - E') \tag{2.88}$$

$$t'_{x,m}(0) = t'_{i}(1 - E') \tag{2.89}$$

hence, using 2.46,

$$t'_{x,m}(n) = \varepsilon_{g1}(n)(t'^{*}_{i} - t'_{i})(1 - E') + t'_{i}(1-E') \tag{2.90}$$

Thus can the controller predict all future values of the waste gas temperature and take steps to avoid violation of the constraint.

Burns shows that if, as above, the load increase is met in the first cycle (and thereafter all operating conditions remain constant), the temperature $t''_{x,m}$ will, after the first cycle, continually overshoot the required t_B. To prevent this, a further step change in t'_i is used to hold t''_x at the required t_B in the second cycle, and so on. The equations representing the superposition of responses are

$$t'_{x,m_2} = t'_{x,m_1} + \varepsilon_{g1}(t'^{*}_{x,m} - t'^{o}_{x,m}) \tag{2.91}$$

$$t''_{x,m_2} = t''_{x,m_1} + \varepsilon_{g2}(t''^{*}_{x,m} - t''^{o}_{x,m}) \tag{2.92}$$

where subscript 1 denotes the response due to one step alone

subscript 2 denotes the overall response due to both steps

$t^{*}_{x,m} = t_{x,m}(\infty)_2$

$t^{o}_{x,m} = t_{x,m}(\infty)_1$

Application of the equations leads to evaluation of the overall responses, the responses due to the initial step alone being given by 2.90 and its equivalent for the cold side. Thus equations 2.91

and 2.92 are used to ensure that the required load is delivered in the second period, this process being repeated at each subsequent cycle until cyclic equilibrium is re-established.

Burns' work is sufficiently general to enable multiple changes of load, t_B, and it is noted that the possibility of unexpected convergence of $t'_{x,m}$ to its maximum allowed value requires the 'look ahead' technique described. In discussing the implications of his work to practical stove control, Burns suggests that the method be developed to incorporate changes in flowrate; since the operation would then be non-linear, the resulting (imperfect) system would require feedback correction to tune the model. It does seem however, from this author's experience, that feedback compensation would be necessary anyway, to correct the usual discrepancies, so incorporating flowrate changes would not result in any great decrease in efficiency. Burns also suggests that, due to the dependence of this control method on many simulations to obtain the responses, a more computationally economic method must be found than those employing Willmott's two-dimensional model. Burns carried out some work using the 'recuperator analogy' to this end but, beyond quoting his figures of computing times approximately 25% of the Willmott two-dimensional model and relative errors of 5% in exit temperatures, description of the work is outside the scope of this thesis.

Jeffreson

Jeffreson's work describes a method of formulating feedforward control models for stove systems (Jeffreson, 1979). The method is sufficiently general to enable it to be used with any operating configuration, although most of the description concerns bypass main. As usual the load variables are blast temperature t_g and flowrate W_g, the manipulated variables being bypass flowrate, hot gas inlet temperature and hot gas flowrate. Constraints imposed include those upon t_i' (maximum possible), combustion gas flowrate (maximum available) and hot gas exit temperature (maximum allowed). Jeffreson adopts Zuidema's terminology in defining a load change as 'large' if collapse occurs following it, and 'small' if it is met in the short and long term.

The stove simulation model used by Jeffreson is derived using the usual physical assumptions, and after normalisation of the system equations, standard computer packages (University of Adelaide) are used for their solution. (Specifically, fourth order Runge-Kutta is used for integration and the process continued until the cold gas flowrate equals the blast demand, at which point a changeover is effected).

In a 1-N system (one stove on blast, N on gas), the regenerator equations become

$$\frac{\partial t''}{\partial y} = \frac{h''A}{W_B S''}(T - t'') \qquad (2.93)$$

$$\frac{\partial t'}{\partial y} = \frac{Nh'A}{N W'S'}(t' - T) \qquad (2.94)$$

and since $P' = NP''$, the heat balance equation becomes

$$Q = N W'S'(t'_i - t'_{x,m}) = W_B S''(t''_{x,m} - t''_i) \qquad (2.95)$$

The solution is well-known, especially when written in the 'logarithmic mean temperature difference' form:

$$Q = U A (LMTD) \qquad (2.96)$$

where

$$U = h''(Nh') / (h'' + Nh')$$

$$LMTD = (\Delta_1 - \Delta_2) / \ln(\Delta_1/\Delta_2)$$

$$\Delta_1 = t'_i - t''_{x,m}$$

$$\Delta_2 = t'_{x,m} - t''_i$$

Thus, using 2.95 and 2.96, the minimum allowable hot gas flowrate W'_{min} can be predicted for a given load $t_B (= t''_{x,m})$ and W_B. Alternately, for a given set of operating conditions, the equations can be used to determine whether or not collapse will occur, providing the flowrate dependence of heat transfer coefficients is known. As the duration of of the blow shortens (near-collapse), the hot gas flowrate must be increased and, provided the <u>average</u> flowrate over the period is maintained above W'_{min}, the load change is kept 'small'. Obviously, to maximise efficiency, the average value of W' must be kept as close as possible to W'_{min} before the load change, and then W' or t'_i adjusted as necessary.

In practice, the changeover time P is finite, and taken from the heating period, so that

$$P' = P_c + P'_{actual} = NP'' \qquad (2.97)$$

and therefore the shortest possible cold (blast) period is of duration P_c/N. Jeffreson points out that a given amount of heat can be delivered to a stove by two different flowrate time profiles, providing their average value is the same; it is necessary, therefore, for a feedforward controller merely to ensure that the required <u>average</u> flowrate over several cycles is fed forward, irrespective of changeover time. Collapse will still occur, however, if the blast period duration is reduced to P_c/N or less.

Jeffreson observed, for finite changeover times, the existence of two cyclic equilibrium states for a given hot gas flowrate, the cold period durations being different. Computer simulations showed that a system perturbed by, for example, rounding errors will move from the equilibrium with shorter cold period duration to that with longer period duration (and lower thermal efficiency) if the cold period duration is allowed to be unconstrained. This complicates the feedforward control over <u>average</u> hot gas flowrate, but feedforward action is still possible by integrating the average hot gas flowrate and feeding it back to adjust the required hot gas flowrate for the next cycle. Required flowrate in cycle k+1 depends upon the average flowrate measured during cycle k as follows:

$$\hat{W}'_{k+1} = W'_k \cdot (W'_{avg} / W'_{k\,avg}) \qquad (2.98)$$

where W'_{avg} is the desired value of average hot flowrate calculated by the feedforward controller; $W'_{k\,avg}$ is the integrated flowrate measured during cycle k; and $\hat{W}'_k$ is the setpoint in the previous cycle.

Jeffreson compares his method to that of Zuidema and concludes that the two methods would produce similar results and would both be limited by similar criteria, such as constraints on gas flowrate and the effects of changeover time.

Smith

Recent work carried out on the computer-controlled experimental regenerator at the University of York (Smith, 1983) has produced extremely good results in terms of 'tightness of control' although no results are available for thermal efficiency. Using the apparatus described in Chapter 3 of this thesis, Smith considered the steady state operation of staggered parallel and bypass main configurations, using a 'time varying scaling factor' as a form of feedback compensation. In staggered parallel operation the predicted (feedforward) flowrate through the warmer of the two on-blast regenerators is given by

$$W''_w = W_B \frac{t_B - t''_{x,c}}{t''_{x,w} - t''_{x,c}} \qquad (2.99)$$

where subscript w refers to the 'warmer' stove

c refers to the 'cooler' stove.

Then obviously

$$W''_c = W_B - W''_w \qquad (2.100)$$

It is, as described earlier, necessary that the stoves produce blast at temperatures which straddle the blast setpoint, i.e.

$$t''_{x,c} < t_B < t''_{w,c} \qquad (2.101)$$

and, as usual, changeover is effected when this is no longer true. Smith observed that the feedforward flowrate (2.99) is not satisfactory due to heat losses resulting in a temperature drop between regenerator and temperature measurement points, so the setpoint is multiplied by a scaling factor S_f so that

$$W''_w = S_f W_B \frac{t_B - t''_{x,w}}{t''_{x,w} - t''_{x,c}} \qquad (2.102)$$

Since the heat losses from the gas to the system pipework become less as the pipework heats up, the scaling factor and hence the feedforward setpoint is constantly re-calculated during a cycle using

$$S_f = \frac{t''_{x,w} W''_w + t''_{x,c} W''_c}{t_{B,a} (W''_w + W''_c)} \qquad (2.103)$$

where $t_{B,a}$ is the blast temperature achieved last cycle.

This enables control of t_B to within $\pm 2\%$ of its setpoint; even better control is achieved using a form of differential control which arises from calculating S_f using

$$S_{f,n+1} = \frac{3}{2} \frac{t''_{x,w} W''_w + t''_{x,c} W''_c}{t_{B,a} (W''_w + W''_c)} - \frac{1}{2} S_{f,n} \qquad (2.104)$$

Control of t_B to $\pm \frac{1}{2}\%$ is reported using this approach.

Two main practical problems are noted by Smith, both involving changeovers. Firstly, changeovers are found to occur immediately after the previous changeover, possibly due to gas carryover effects and thermocouple lag producing a falsely low reading of temperature; this was simply overcome by automatically disabling changeovers for a short time following a changeover. Secondly, and similarly, immediately after a changeover, the hotter regenerator may be supplying virtually no blast, resulting in the exit thermocouple experiencing a large drop in temperature which causes the control program to make decisions based on incorrect data. This problem Smith overcame by forcing the hotter regenerator to operate with a certain minimum cold flowrate (thus, incidentally, causing a negligibly small step decrease in the flowrate through the cooler regenerator). The tightness of control produced by Smith's method in bypass main is not as good as in staggered parallel, this apparently being due to the discontinuous operation. The flowrate through a regenerator in bypass main operation jumps from zero to its initial blast period value then, after a steady increase to W_B, jumps back to zero (followed by the regenerator's heating phase). In contrast, the flowrate through a regenerator in staggered parallel operation increases steadily from zero to W_B, then decreases steadily back to zero. This flowrate profile is much more amenable to automatic control.

An alternative to Smith's use of the time varying scaling factor is to evaluate the feedforward setpoints as per theory then add a conventionally calculated feedback term. Good results are, however, produced using Smith's method.

2.4 GAS-PARTICLE HEAT TRANSFER IN PACKED BEDS

The final section of this literature review forms a brief summary of some of the various coefficients for heat transfer between gas and packing in a packed bed. An extensive summary and comparison of nearly 250 correlations has previously been carried out (Barker, 1965). It should be noted that the experimental work presented in this thesis is not concerned with experimentally determining heat transfer coefficients; rather, correlations reported in the literature have been assumed and applied, hence the inclusion of this present section.

Furnas, Saunders and Ford

These classic papers (Furnas, 1932; Saunders and Ford, 1940) contain much early experimental and resultant analytical work on methods of finding heat transfer coefficients, but due to the work being highly specific to the conditions and materials used in the experiments, correlations are of doubtful relevance to this thesis.

Furnas's correlation, for iron spheres, is

$$h_g = (0.0059\, V^{0.7}\, t^{0.3}\, 10^{(1.68-3.56a^2)}) / d^{0.9} \qquad (2.105)$$

where h_g = heat transfer correlation (cal/sec ^{o}c) per cm^3 of overall bed volume

V = gas velocity, standard litres/sec per cm^2 of bed cross-sectional area

t = gas temperature ABSOLUTE

a = voidage fraction

d = particle diameter, cm.

Saunders and Ford used a constant flowrate technique, passing heated gas over a bed of spheres for a given period then cooling the bed, whilst continually recording the inlet and exit temperatures, manually. Much care was taken over lagging, minimising the heat capacity of the container and obtaining uniform incident temperature distributions across the bed; an anulus of higher flowrate was, however, observed within 1 ball diameter from the container wall, where the flowrate was observed to be 50% higher than elsewhere. (This problem was eventually overcome by Meek, as is described later). The ratio of bed diameter to particle diameter, D/d, was typically 32 and the voidage fraction typically 0.38. The inlet piping was kept at the same temperature as the inlet air by independent heaters, and the experiment was repeated for three different container/particle sizes. No explicit formula for the heat transfer coefficient is given, but many curves of the variation of gas temperature through the bed versus a form of dimensionless

time are shown:

$$\frac{t_x - T_o}{t_i - T_o} \text{ vs. } \frac{V \theta S_{vol}}{d C_{vol}}$$

where T_o = bed initial temperature

V = superficial gas velocity

S_{vol} = gas specific heat (volume basis)

C_{vol} = solid specific heat (volume basis)

The heat transfer also depends upon another dimensionless group which accounts for the internal temperature distribution in the packing, but for high conductivity packing and/or small d, Saunders and Ford state that this can be safely ignored, although no threshold figures are quoted. Whilst Saunders and Ford's techniques and observations are of interest, their quantitative results are not presented in a way which facilitates application to the work of this thesis.

Denton, Robinson and Tibbs

The work of Denton et al (1963) on heat transfer and pressure loss in beds of spheres is used as the basis for part of the theoretical model used in this thesis. The experimental approach adopted by Denton et al is to construct a 1.5cm diameter 'test sphere' of copper which contained within itself a spiral-wound heating element and several thermocouples. It was configured to run at a constant surface temperature T_s whilst suspended either alone in an air stream at room temperature t_o or as a member of a packed bed. The

air stream velocity is measured with a pitot tube and orifice plate with water manometer, and controlled by adjusting the speed of the blower. The temperature difference $\Delta t = T_s - t_o$ was measured directly using the sphere's integral thermocouple with its cold junction in the air stream at t_o, and t_o was measured using another thermocouple. With T_s maintained constant, the electrical energy supplied to the heater was measured, and then corrected for losses along the suspension wires. The correlation obtained was

$$h = \frac{(w/4.2)}{\pi d^2 \Delta t} \qquad (2.106)$$

(where w = corrected watts supplied)

this being valid for a range of Δt up to 46°C and t_o = 300K.

For a packed bed the method was identical, except that the test sphere was surrounded by randomly packed glass spheres or similarly heated copper spheres. With Reynolds number defined as

$$Re = Gd/\mu = \rho V d/\mu = V d/\nu \qquad (2.107)$$

the heat transfer coefficient is given (in terms of Stanton number) by

$$St\ (= h/SG) = 0.72\, Re^{-0.3} \qquad (2.108)$$

$$\text{for } Pr\ (= S\mu/k) = 0.73\text{, i.e. air}$$

Alternately, expressed as the heat transfer coefficient per unit volume of bed,

$$h_s/SG = 4.32\left(\frac{1-a}{d}\right) Re^{-0.3} \qquad (2.109)$$

The wall effects were considered and it was concluded that for

D/d = 11..42, the voidage of the wall was ~0.45/0.37 of that of the bulk of the bed, averaged over an anulus of width 2d. The dependence of h upon Re was studied, and it was found that despite a maximum (independent of Re) for Re > 5000, for Re < 3000 the h versus Re curve for D/d = 17 is identical to that for D/d = 34.

Meek, Shearer

Very meticulous study has been undertaken at the N.E.L. on heat transfer (Meek, 1962; Shearer, 1962). Meek's work is specifically aimed at regenerator applications of packed sphere beds, and was conducted with great attention to detail in the experimental method. Shearer, using the same apparatus and method, extended Meek's work to low conductivity beds and confirmed the same results. The method used is to employ a 'cyclic' transient technique based on the solution of the heat transfer equations

$$m_f \rho S (\partial t/\partial \theta + \bar{U}\, \partial t/\partial y) = h(T - t)$$

$$= - m_s \rho_{solid} C\, \partial T/\partial \theta \qquad (2.110)$$

where m_f = hydraulic radius (fluid volume/surface area of bed)

$\bar{U}$ = mean fluid interstitial velocity

m_s = volume/surface area ratio for bed.

Meek observed the gas exit temperature for a sinusoidally varying inlet temperature, thus reducing the number of measurements needed if a step increase were used.

The apparatus contained turning vanes and screens to ensure uniform flow across the pipe cross section around all bends (see Chapter 3). A blower ($14m^3/min$) supplied the air, with flowrates measured by orifice plates and controlled by flat plate damper and butterfly valve. A two kilowatt electric heater warmed the air to around 10^oC above ambient, the voltage being varied sinusoidally by a moving coil regulator driven by a crank on a constant speed electric motor. The period of power oscillation ranged from 0.75 seconds to 6 minutes, and the corresponding temperature oscillations were measured by platinum resistance thermometers. A thermometer is used as one arm of a Wheatstone bridge and the out of balance current is recorded from a moving spot galvonometer on a roll of photographic paper.

The beds, (horizontally oriented) consisted of randomly packed 10mm diameter steel balls, the end plates being comprised of similar balls welded together. Bed porosity was determined by filling the voids with water and, to ensure uniform porosity - i.e. eliminate wall effects - an ingenious solution was used; the beds were immersed in epoxy resin at the edges, as shown in figure 2.17. To investigate the effectiveness of these measures, beds were constructed without the resin and with wire mesh endplates, and comparisons undertaken.

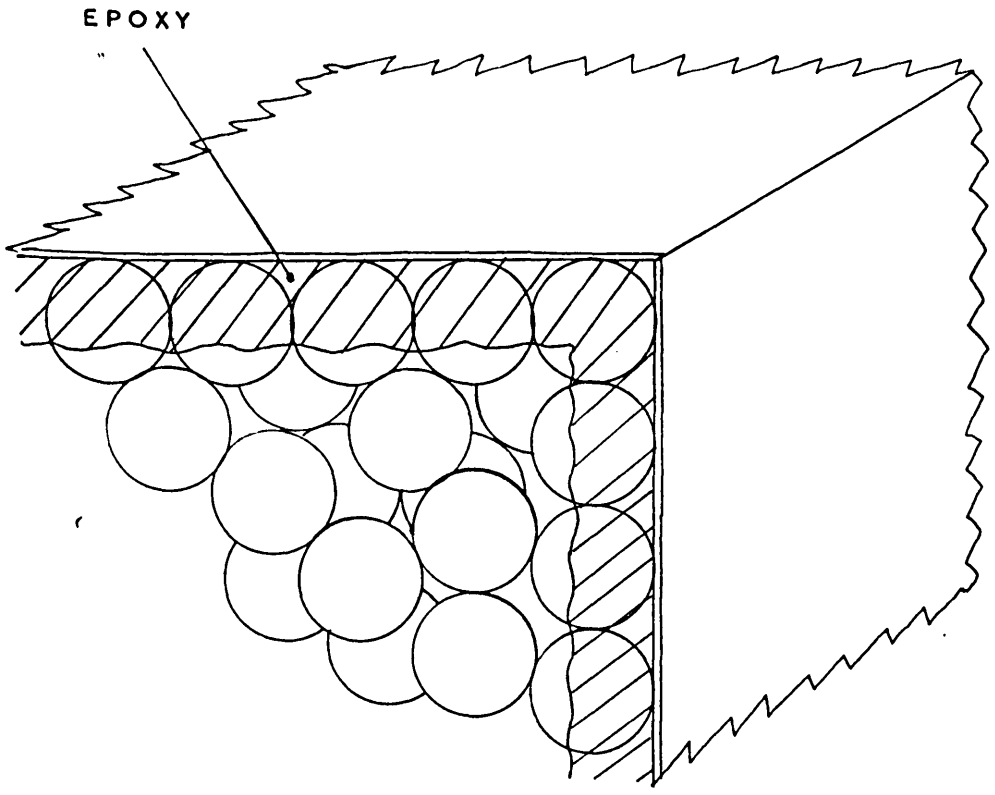

FIGURE 2.17

ELIMINATION OF WALL VOIDAGE

Meek discusses the validity of the established ways of presenting the results, and suggests that the usual definitions of Stanton number (2.108) and Reynolds number (2.107) place undue emphasis on the effect of bed porosity; if porosity is changed, V and d remain constant while interstitial velocity changes, hence for constant Re, h (and so St) would alter. For this reason Meek redefines the above parameters as

$$St_1 = h / (S \rho \bar{U}) \qquad (2.111)$$

$$Re_1 = 4 \rho \bar{U} m_f / \mu \qquad (2.112)$$

and then plots the experimental data as $St_1 Pr^{2/3}$ versus Re_1. Results are generally higher than other reported work due to a) elimination of wall effects and b) Meek's use of 'true' random packing as opposed to the more usual packing where a degree of order occurs 'accidentally'. Meek states that wall effects only become negligible for $D/d > 100$, although Denton et al reported significance of wall effects only for $D/d < 10$. The correlation arrived at by Meek is, for large D/d,

$$St_1 Pr^{2/3} = 0.22 Re^{-0.31} \qquad (2.113)$$

or, alternatively,

$$St = 0.72 Re^{-0.3} \text{ for } Pr = 0.73 \qquad (2.114)$$

which is identical to the correlation of Denton et al.

Littman, Barile and Pulsifer; Littman and Sliva;

Gliddon and Cranfield

The work of the first paper (Littman et al, 1968) concentrates on low Reynolds number conditions, $2 < Re < 100$, using a cyclic method on packed beds of spheres with diameter range 0.5mm to 2mm. The apparatus consisted of the usual setup of manometers, rotameters, thermocouples and electrical heaters. Nusselt number, defined as

$$Nu = h d / k \qquad (2.115)$$

is plotted versus Reynolds number on log-log paper; no quantification of the curve is quoted, but geometrical analysis of the curve by this author has yielded the equation

$$Nu = 0.53 Re^{0.75} \qquad (2.116)$$

For $Re < 100$ this yields values of h very close to those of Denton et al.

In the second paper (Littman and Sliva, 1970), the work of the first paper is extended down to Re = 0.3 which, although outside the scope of this thesis, is interesting because it was found that Nu increased with increasing bed voidage; this seems to be in opposition to the work of Denton et al, who reported increased voidage leading to a decrease in heat transfer coefficient (see equation 2.109). Littman and Sliva suggest, as explanation, that friction effects have a serious effect on fluid flow at such low Reynolds numbers, and the effect could be expected to vanish as Re

increases.

Gliddon and Cranfield produced results specific to beds of alkalised alumina (Gliddon and Cranfield, 1970) and concluded that the correlation

$$Nu = 0.36\,Re^{0.94} \pm 30\% \qquad (2.117)$$

encompasses both their results and those of Littman. The large quoted error is a good indication of the general lack of precision obtainable in the area of heat transfer in packed beds, this being due to the complexity of fluid flow through channels of non-constant diameter, and the associated difficulty in defining Re.

Heggs and Handley; Yoshida

The correlations produced by these authors (Heggs and Handley, 1968; Bird et al, 1960) are in a similar form, and attempt to improve the definition of Reynolds number to obtain more accurate heat transfer coefficients. The Colburn j-factor is defined as

$$j_H = St\,Pr^{2/3} \qquad (2.118)$$

A modified Reynolds number, Re_m, is defined in each paper, and a correlation of the form

$$j_H = C_1\,Re_m^{C_2} \qquad (2.119)$$

is then used to calculate j_H, hence h.

Heggs and Handley define Re_m, based on the hydraulic diameter of the particles, thus:

$$Re_m = \frac{2}{3}\frac{d\rho V}{(1-a)\mu} = \frac{2}{3}\frac{dV}{(1-a)\nu} \qquad (2.120)$$

and then use 2.119 in the form

$$j_H = \frac{0.26}{a} Re_m^{-0.33} \qquad (2.121)$$

Likewise, Yoshida defines Re_m as

$$Re_m = G / (AVR.\mu.\psi) \qquad (2.122)$$

where AVR = area/volume ratio per unit volume of bed (= 6/d (1-a))

ψ = shape factor (= 1 for spheres)

and then

$$j_H = 0.91\ Re_m^{-0.51} \quad \text{if } Re_m < 50$$
$$j_H = 0.61\ Re_m^{-0.41} \quad \text{if } Re_m > 50 \qquad (2.123)$$

It will be seen that the Heggs and Handley correlation yields values of h very slightly lower than those of Denton et al, whilst the Yoshida correlation gives values of h ~1.5 times those of Denton et al at low flowrates, gradually changing slope to give values ~0.9 of Denton's at higher flowrates ($1.0 m^3$/min). Both of these correlations have been closely investigated by this author, and are applied in Chapter 3.

CHAPTER 3

EXPERIMENTAL EQUIPMENT

The apparatus used for this thesis was designed by Dr. A.E. Wraith of the University of Newcastle-upon-Tyne. This chapter describes the apparatus in its final form as used for the experiments discussed in Chapter 5. The original state of the apparatus and the changes made by this author to achieve the final form are described in section 4.4.1.

The experimental thermal regenerator consisted of several distinct elements: a) thermally active matrices, scaled for similarity with industrial plant; b) the valve and flow system; c) the air heating system,, incorporating various failsafe devices; d) the temperature measuring system; e) the controller, a minicomputer whose function was to sequence regenerator operation and to control flowrates according to an experimental strategy. Associated with the control computer were various pieces of software which, in addition to sequencing and control, performed data collection and averaging. In this chapter each of the above elements is described, and in addition various parameters, both dimensional and dimensionless, are evaluated and discussed for the experimental regenerator system (or 'rig').

The rig consisted of four air-blown matrices (or 'beds') composed of glass spheres enclosed by stainless steel vessels 300mm in diameter, 750mm long, mounted vertically. The beds were coupled so as to operate in any cyclic mode with or without bypass, with a maximum flowrate of 2. 0 std. m^3/min per regenerator. The beds, the air ducting, the air heater and process instrumentation devices were mounted on a free-standing 'coat-rack' frame, the resulting unit occupying a space 1m x 1.5m x 2.5m high, which was easily accomodated in a small laboratory (see figure 3.1 and plate 3.1). Remote from this frame was a 19" rack containing the control computer and datalogging equipment, and the laboratory also housed a general control and indication cubicle. This cubicle contained the heater power supplies and control autotransformers, the heater failsafe circuitry, chart recorders indicating the regenerator dome pipe temperatures, and various lamps providing a visual indication of the system flowpaths. The air blower was housed in a separate room, and plastic ducting laid through the ceiling void. An outlet from the in-house 80 p.s.i. instrument air network was installed in the laboratory, close to the rig, and a 24 p.s.i. supply obtained in addition, by use of a reducing valve on the 80 p.s.i. supply. A drier and two filters were installed in line to ensure a clean, dry compressed air supply.

3.1 BEDS

The cylindrical stainless steel containers (300mm x 750mm) were

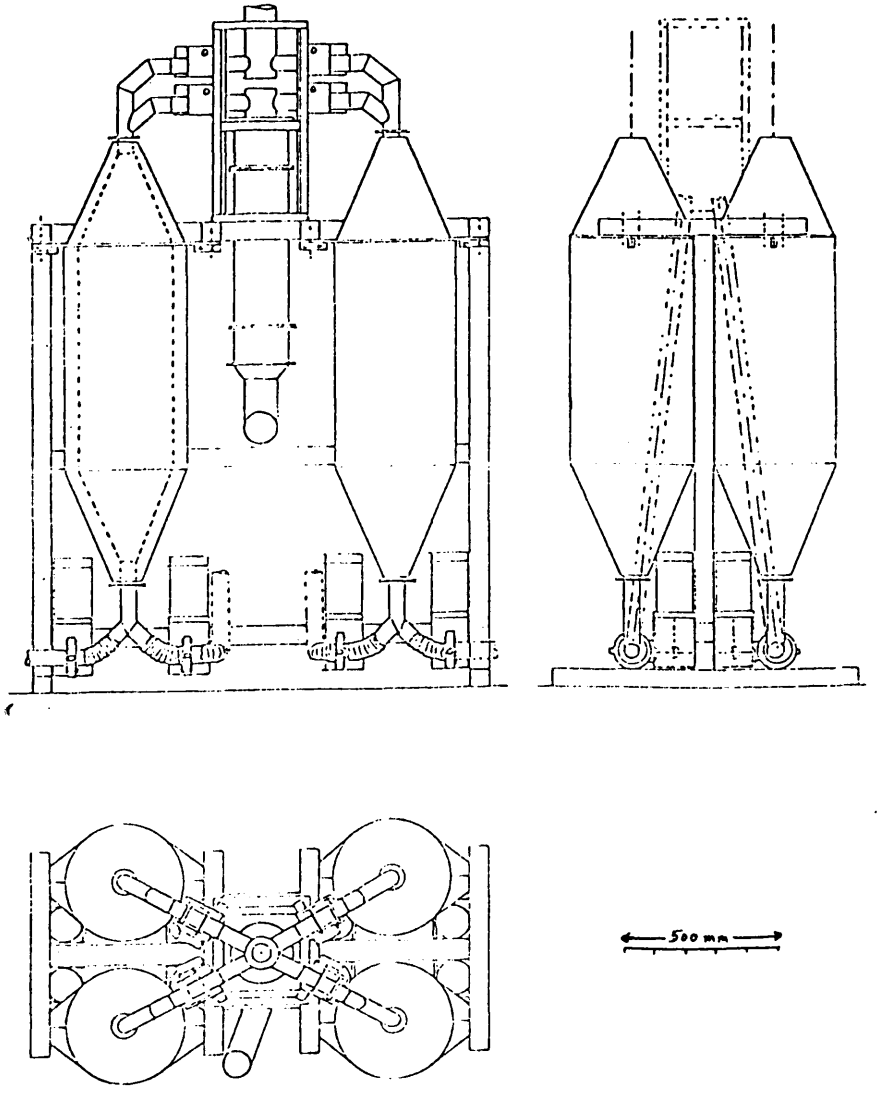

FIGURE 3.1

REGENERATOR SYSTEM LAYOUT

From Willmott & Wraith (1982)

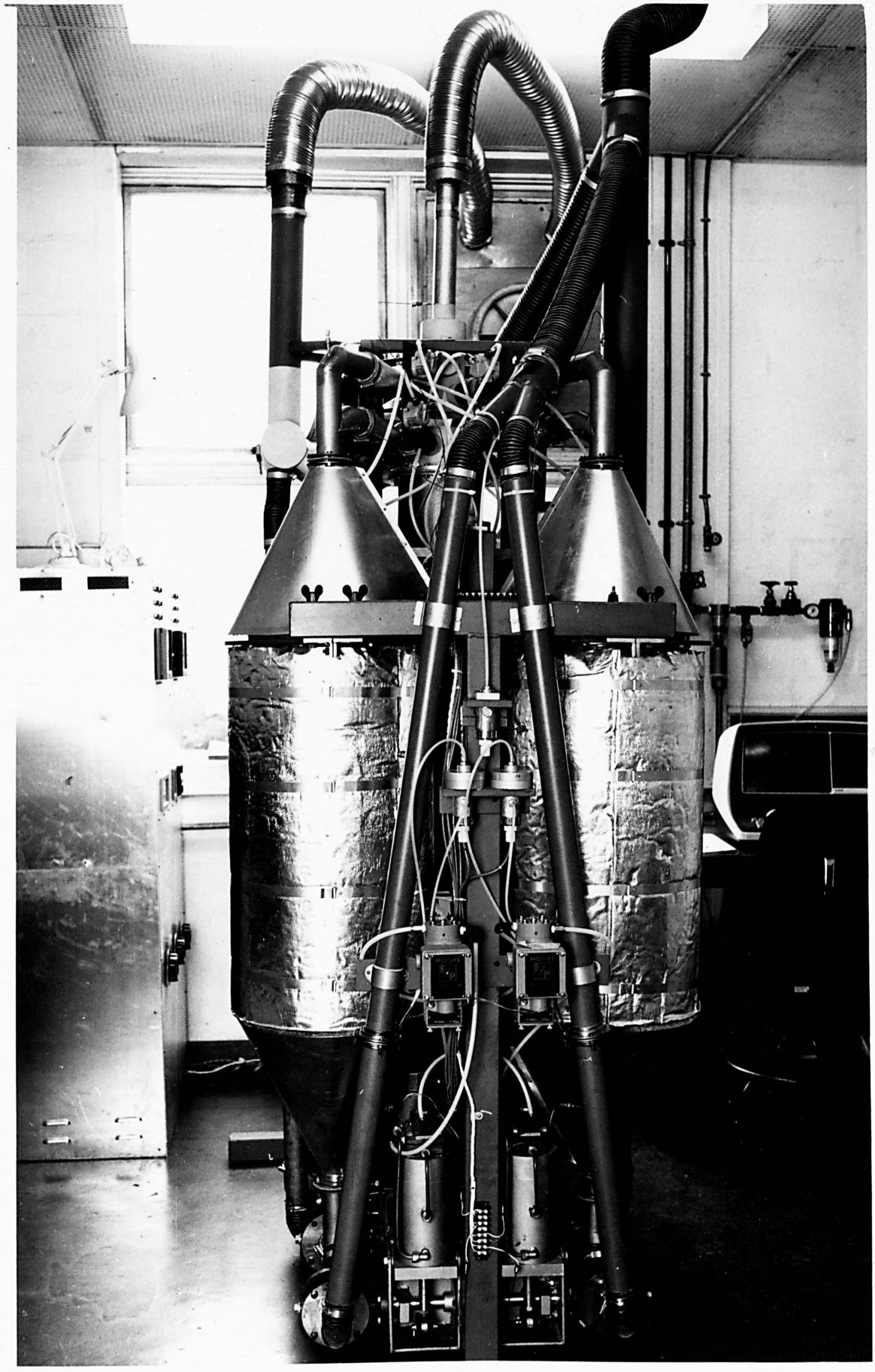

Plate 3.1

Regenerator System
General View

suspended vertically from a flange, and insulated externally using a 25mm thickness of foil-backed lamellar-mat insulation. A wire mesh provided the bottom endplate upon which the packing rested, and steel cones were bolted to either end with a sealing gasket, to provide the diameter reduction necessary for connection to the pipework. The packing was, initially, 12mm gravel which was used for early commissioning of the rig. It was subsequently realised that this packing resulted in an unrealistically high value of reduced length Λ and so, in order to retain similarity with industrial plant, the packing was replaced with 17mm diameter soda glass spheres. To achieve a value of Λ of around 15-25 at the flowrates considered, the containers were filled to a depth of approximately 40cm, the spheres being weighed as they were installed. The mass of packing per regenerator was in the region of 40kg; the exact figures are shown in table 3.1 along with the thermal and physical parameters of the packing. The mass of insulation per regenerator was ~1.6kg.

The figure for voidage (a = 0.41) is an overall figure, being calculated from the mass of packing and the expected mass (with no voids) based on the manufacturer's figure for density. In fact, the voidage of a packed bed is known to vary considerably across the bed, with a theoretical figure of 0.37 in the bulk (Spiers, 1962). The flow distribution resulting from this non-constant voidage is discussed in section 3.7.

Material	Soda Glass Spheres
Particle Diameter, d	17mm
Particle Density, ρ	2480 kg/m^3
Particle Specific Heat, C	1130.4 $J/kg^{\circ}C$
Particle Thermal Conductivity, λ	0.72 $W/m^2(^{\circ}C/m)$
Particle Thermal Diffusivity, α	2.57×10^{-7} m^2/s
Voidage (overall), a	0.41
Heat Transfer Surface Area, A (per Reg.)	5.9 m^2
Mass of Packing, M Reg. 1	40.48 kg
Reg. 2	42.03 kg
Reg. 3	41.80 kg
Reg. 4	40.25 kg

Table 3.1

As a result of operating the regenerator shells half-full, a sluggish temperature response at reversals was observed. This was due to the time required for the gas brought to rest in the deadspace to mix and disperse with the new flow, and so was especially manifest at low flowrates. In order to solve this problem, internal flowguides were inserted; the guides were thin aluminium cones which rested on the packing, fitting closely to the container walls, being linked to the exit/entry pipework by flexible glass hose, adjustable to any depth of packing. In this way the deadspace was bypassed and, as a useful side-effect, the heat leak from the gas to surroundings was reduced by removing the gas from direct contact with the supporting yoke, a thermal sink of considerable capacity. Figure 3.2 shows the construction of a single regenerator.

3.2 FLOW SYSTEM

The common source for the hot and cold gas flows was a 7.5 h.p. blower, providing a total of 5 std. m^3/min at a pressure of 0.2 bar gauge. The common source was intended to stabilise blower duty. Two empty oil drums were placed in series at the blower outlet, to act as reservoirs to even out rapid flow fluctuations. The air was ducted from the remote compressor room to the rig via 4" o.d. plastic sewerage pipe, and at the rig the flow could be diverted several ways; a) directly to the cold (bottom) end of any regenerator; b) via the electrical heater to the hot (top) end of

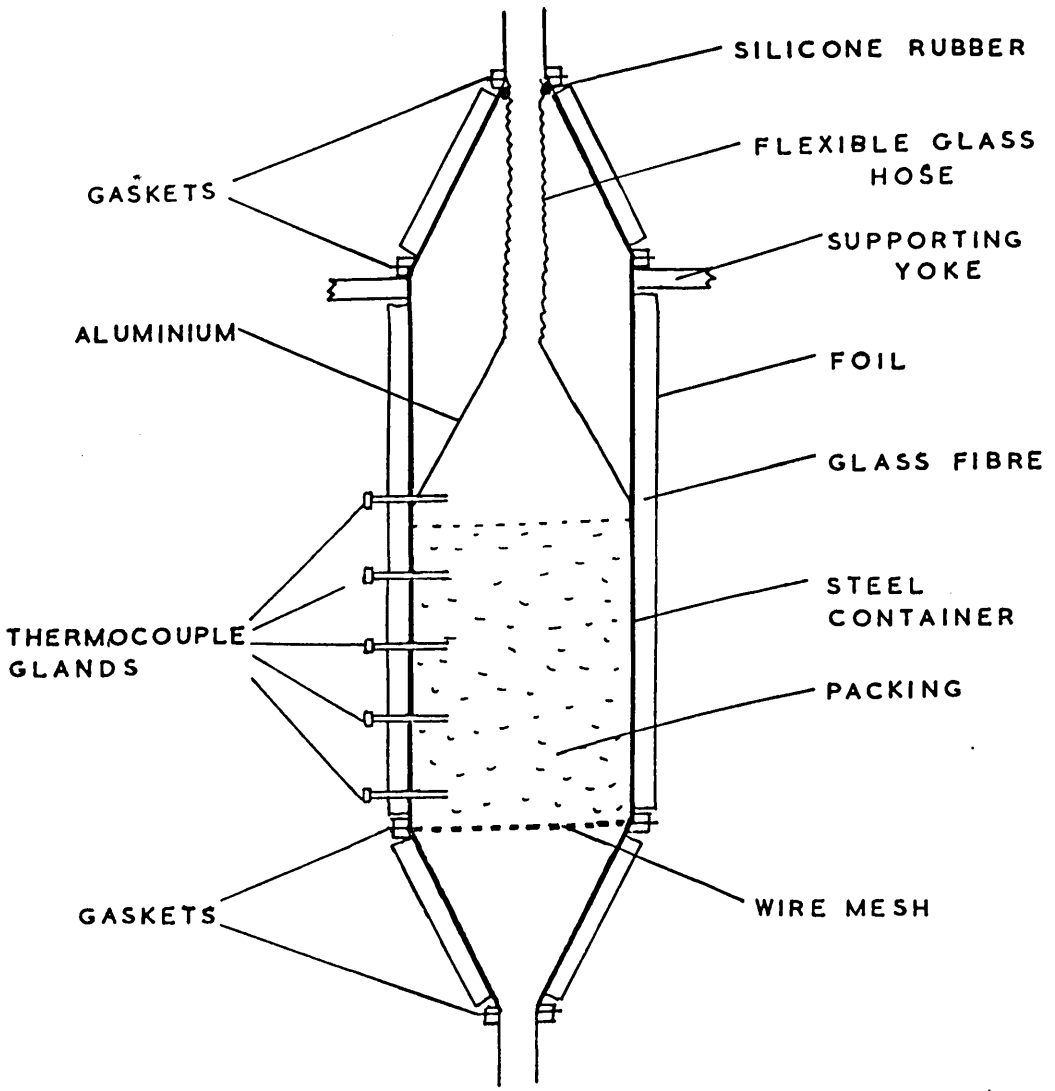

FIGURE 3.2

REGENERATOR CONSTRUCTION

APPROX. 1/10 SCALE

any regenerator; c) through the bypass pipe to the mixing chamber on the cold gas exit circuit. The heater system is described in section 3.3 and the flow circuits are shown schematically in figure 3.3. Where the pipework had sharp bends, especially near the heater, constant flow velocity across the pipe section was achieved by inserting clusters of smaller diameter flexible hoses within the larger pipe.

Flowrate measurement was achieved by use of corner tap orifice meters (conforming to B.S.1042) positioned on the cold side of the regenerators, i.e. on the cold inlet flow and hot outlet flow, as well as on the bypass. Experiments were carried out on a range of orifice meters, and the final configuration used was a mixture of 16mm and 20mm diameter orifice plates. Each meter had an associated diaphragm strain gauge type differential pressure transducer (Pioden type UP1) with 0-250mm w.g. range. Similar transducers (type UP3) provided absolute line pressure measurements for meter correction, and each meter had an associated thermocouple (see section 3.4) for line temperature corrections. According to B.S.1042, the room temperature mass flowrate, W, of gas at temperature t K is given by

$$W \propto \sqrt{\frac{\Delta P . PR}{t / t_r}} \qquad (3.1)$$

where ΔP = pressure drop across orifice plate

PR = pressure ratio (line pressure/atmospheric pressure)

t_r = room temperature (K)

Then, knowing the various constants associated with orifice plate,

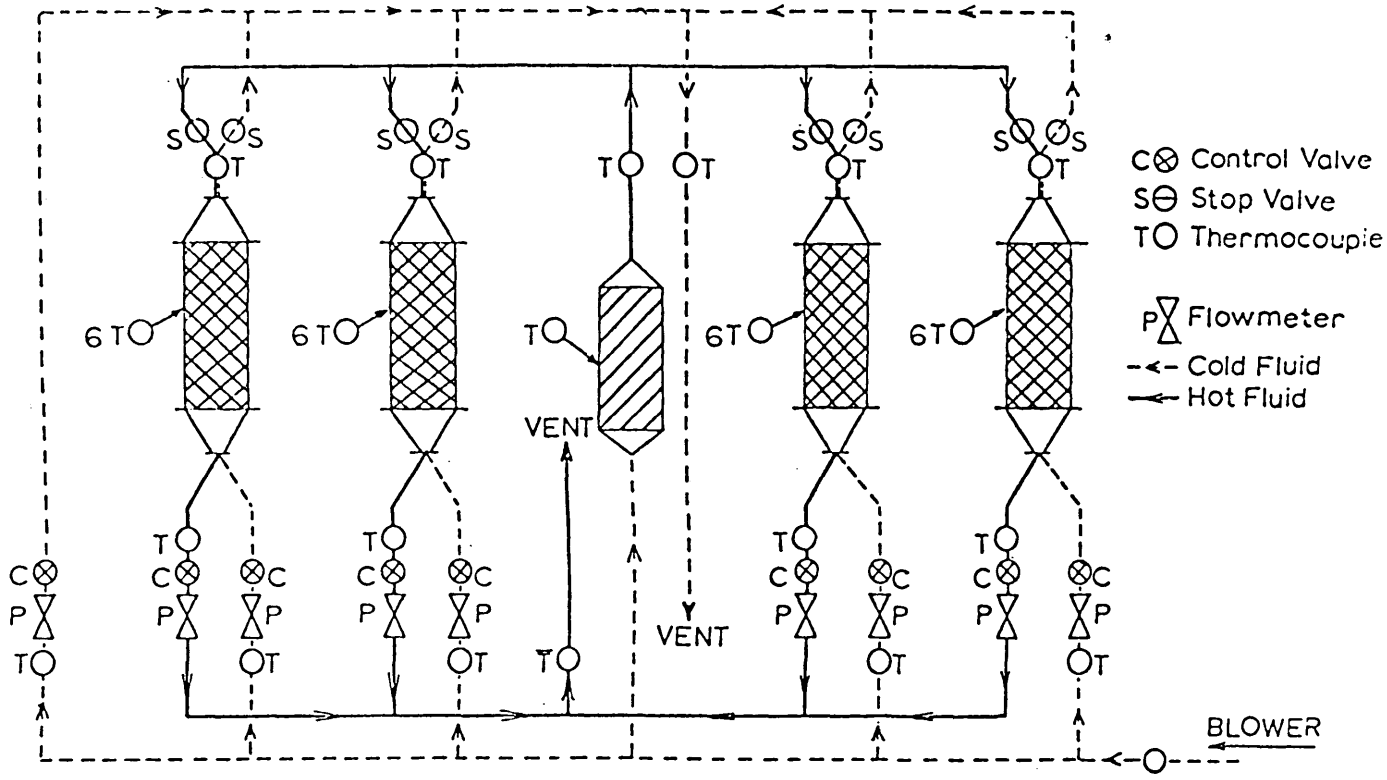

FIGURE 3.3

REGENERATOR SYSTEM FLOW CIRCUITS

From Willmott & Wraith (1982)

differential pressure transducer, etc., the constant of proportionality can be found and incorporated in the control software. It was found, however, that a better form of equation 3.1, for the rig meters, was

$$W \propto \left(\frac{\Delta P . PR}{t/t_r} \right)^m \qquad (3.2)$$

where $m \sim 0.5$ but $\neq 0.5$.

Calibration of the meters was therefore undertaken by use of a Rotameter, as described in Chapter 4. In fact, the various constants were amalgamated by measuring transducer output millivoltage for several Rotameter flowrates, and obtaining an equation of the form

$$W = c \left(\frac{V_T . PR}{t/t_r} \right)^m \qquad (3.3)$$

where V_T = transducer output (mV).

The constants c and m for each of the nine flowmeter/transducer combinations were incorporated in the software, as described in section 3.6. The values of the constants are given in Chapter 4. The pressure ratio PR is related to the absolute pressure transducer output millivoltage V_A by the equation

$$PR = 1 + 0.0142\, V_A \qquad (3.4)$$

and the ratio t/t_r is obtainable directly from the meter thermocouple voltage, knowing the characteristics of the thermocouple (see section 3.4).

The flows were controlled by means of two valves per flowpath: 'stop' valves (on/off) for primary routeing and sealing, and 'control' valves (proportional) for rate control. The stop valves were specially designed by Dr A.E. Wraith of the Department of Metallurgy, University of Newcastle, and constructed to have a low thermal mass. Similar commercially available 50mm bore valves are comparatively massive. The valves worked on a peristaltic principle, and consisted of a length of silicone rubber tubing which was gripped by a PTFE roller connected to a quarter-turn Kinetrol vane-type actuator. The actuators were served by the 80 p.s.i. instrument air system, routed by Martonair M1741/152 solenoid valves. Thus an analogue 10V signal from the computer would cause a stop valve to close, and a zero signal would cause it to open.

The control valves were commercial flange-type seal seat butterfly valves (MonoValve 6110). Their relatively high thermal capacity (although still small by commercial standards) was irrelevant due to the fact that they were positioned on the cold end of the flow paths. The valves were actuated by a piston and con rod, the piston position being determined by the proportion of the instrument air passed by an E/P converter (Moore 77-16, 0-10V). Thus a 0-10V signal would cause a proportional opening of the valve. The flowrate versus input signal characteristics of each valve/actuator/converter assembly were calibrated and, as with the flowmeters, the associated constants were incorporated in the control software (see section 3.6).

The pressure transducers each had a zero-set circuit incorporated in the computer front panel; the identifying numbers and the associated transducers are shown in table 3.2.

3.3 HEATING SYSTEM

The maximum design temperature and flowrate indicated that a 9kW heater was required. The cylindrical heater chamber was mounted centrally in the nest of regenerator vessels, with the pipework connecting heater to regenerators kept as short as possible. Three wire-wound heating coils on ceramic formers were installed in the chamber, with swirl chambers and disc and doughnut baffles at top and bottom to ensure uniform heating of the air flow. Each coil was connected to a 240V a.c. 30A supply via an autotransformer, with coil number 3 also connected via a West-Gardian Q3X hardware three-term controller. In this way a gas temperature setpoint could be maintained with good accuracy; the three autotransformers were set to the pre-tabulated settings for the flowrate and temperature required (see section 4.3) and the Q3X controller (thyristor-based), in conjunction with a chromel/alumel thermocouple, switched coil 3 in such a way as to maintain the setpoint.

In order to ensure safe unattended operation of the rig overnight, it was considered necessary to install various failsafe devices. The areas which were identified as being failure-critical were as follows:

Pressure Transducer Zero-Set Code	Transducer
1	Reg. 2 cold flow
2	Reg. 1 cold flow
3	Reg. 1 hot flow
4	Reg. 2 hot flow
5	Bypass flow
6	Reg. 3 hot flow
7	Reg. 4 hot flow
8	Reg. 4 cold flow
9	Reg. 3 cold flow
a	Absolute pressure Regs. 1 & 2
b	Absolute pressure waste confluence
c	-
d	Absolute pressure Regs. 3 & 4

Table 3.2

a) Main blower failure

b) High-pressure instrument air failure

c) Low-pressure instrument air failure

d) Failure of all hot gas exit butterfly valves

e) Failure of all hot gas inlet stop valves

Failure of all hot gas inlet or exit valves simultaneously (d or e) could result from mechanical failure or, more likely, from the failure of the control computer. The situation to be trapped was where all inlet or exit valves were closed at the same time, resulting in no airflow over the heater and subsequent overheating of the coils. A third possibility was that the control software deliberately 'boxed up' the regenerators, in which case the heater should cut out but subsequently cut in when at least one regenerator is switched back to hot period. All other failure conditions resulted in heater cut-out requiring manual operator reset.

Failure conditions a, b and c were trapped using pressure switches, normally open at atmospheric pressure and calibrated to close at 50 per cent of the relevant pressure. Condition d was detected using four limit switches, normally closed and wired in parallel, positioned so that when the butterfly actuating piston was at the bottom of its travel (valve closed) the switch was opened. Condition e was detected using the relays which powered the indicator lamps on the control and indication cubicle. As a final 'belt and braces' check, a copper/constantan thermocouple was placed

in the heater chamber and, using a comparator circuit, a switch was opened if the heater temperature reached 210°C. A relay in the circuit ensured that conditions a, b, c or heater overtemperature resulted in isolation of the heater until the operator pressed a reset button. The switches detecting valve closure were placed in the circuit such that the relay remained closed (heater on) if these switches re-opened. This is shown schematically in figure 3.4.

3.4 TEMPERATURE MEASUREMENT

Gas temperatures throughout were measured using 1.5mm o.d. MI copper/constantan thermocouples, inserted through PTFE glands which were tightened by screwthread. The couples were connected to the computer's datalogger (which served as the cold junction) using self-wire compensating cable. The temperature-voltage characteristics of the couples was incorporated in the experiment processing software (see Chapter 4) and calibration was carried out as described in section 4.3.

When measuring gas temperatures, it was necessary merely to insert a thermocouple in the gas stream, the couples being self-supporting and of low thermal capacity. To enable measurement of packing internal temperatures, 2mm diameter holes were drilled ultrasonically in several of the 17mm glass spheres, for the insertion of thermocouple tips. These were to be fixed with an epoxy resin with similar thermophysical properties as the glass. It

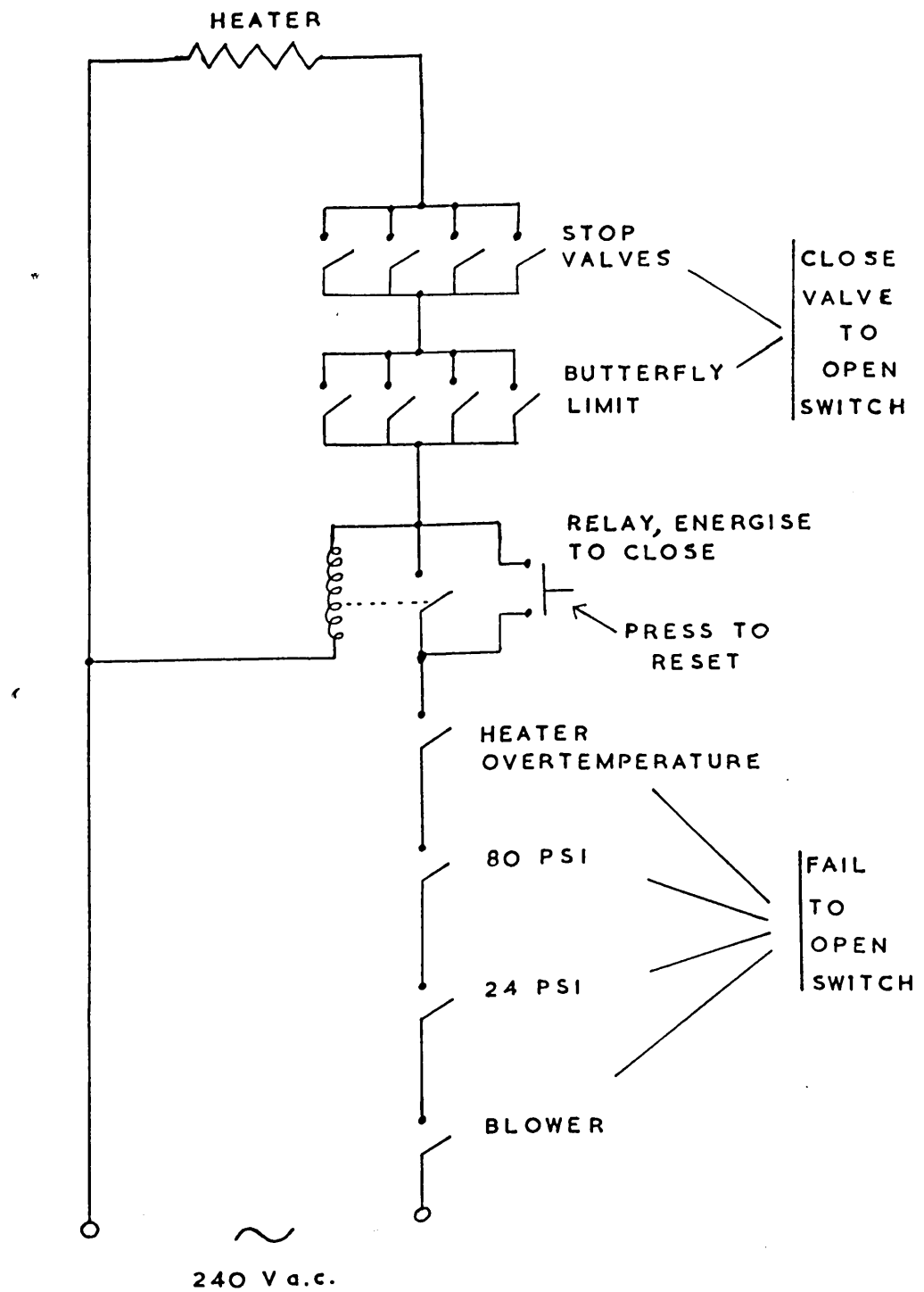

FIGURE 3.4

FAILSAFE CIRCUIT

was not, however, subsequently necessary to measure internal solid temperatures and so the drilled spheres were not installed. The positioning of the thermocouples is described in section 3.5.1.

The temperature, in degrees Centigrade, of the cold junction enclosure (the datalogging rack) was continuously measured during a run using a Fluke 80T/150 temperature to millivolts converter. The output of the device was recorded by the computer and used in the experiment processing software. Subsequently, a MicroConsultants compensating card was installed; the output of this device is the millivoltage to be added to that recorded from a thermocouple, in order to give a direct reading of thermocouple temperature (as opposed to temperature difference).

For temperature correction of flowrates, the ratio t/t_r is given by

$$t / t_r = 1 + 0.0798\ V_{Tc} \qquad (3.5)$$

where V_{Tc} = thermocouple output (mV) for copper/con couples, and t_r = 293 K; t/t_r is then given as a ratio of absolute temperatures.

3.5 CONTROL AND DATALOGGING SYSTEM

The computer system used was a MicroConsultants 'Dialogue' system, comprising a Computer Automation Alpha LSI-2/20 16-bit processor with 32K core memory; a multiplexed analogue input rack with 15-bit ADC; a digital I/O rack with 8-bit DAC/ADC; a paper tape punch and fast paper tape reader. In addition, Servoscribe and J.J. X-Y

plotters were connected to the system. Note: the analogue input rack is also referred to as 'the logger' and 'the multiplexer'. The three main functions of the control computer were:

a) control of flowrates to a given setpoint

b) collection and averaging of temperature and flowrate data, and

c) sequencing of regenerator switching.

The methods of achieving the above functions are fully described in section 3.6, and the current section is mainly concerned with a description of the analogue I/O system.

3.5.1 Data Input

The analogue input rack comprised a series of card-mounted reed relays, each of which formed an input channel to the computer for analogue data. The card manufacturers quoted the reed life as 10^8 operations, implying continuous use for 6.4 years (at 0.5 Hz) before failure. The input amplifier gain range, and hence input data range, was software selectable between 10mV and 1.28V. There were four input channels per card, numbered from the bottom up when inserted in the rack. The three connections to the card edge connector for each channel were, from the bottom up, +ve, -ve and ground; for unipolar input signals (i.e. all signals in the work reported here) the -ve and ground signals were connected together.

The rack connections (i.e. channel assignments) as per the original design are summarised in tables 3.3 and 3.4. Various alterations were made to thermocouple channels, in an attempt to minimise losses and measure 'mixed' temperatures (see Chapter 4), and the final assignments are shown diagramatically in figure 3.5. These alterations were made only on regenerators 1 and 2, and since no readings were taken on regenerators 3 and 4, channels 29 to 33 and 41 to 45 were, in fact, not connected. Channels 0, 12, 24 and 36 were not connected, due to the thermocouples being connected to the chart recorders in the control and indication cubicle. Channels 51 and 55 were also not connected.

3.5.2 Data Output

Output control signals could be sent to butterfly valve or stop valve actuators via the I/O rack using the software commands DWOUT and DBOUT. The command

DWOUT (I,J)

output to channel I an integer in the range 0-255, i.e. 8 bit resolution. After conversion by a DAC, a 0-10V signal resulted. This signal was applied to the E/P converter on a butterfly valve resulting in movement of the valve such that J = 0 corresponded to fully closed and J = 255 corresponded to fully open. The channel addresses (I) are given in table 3.5. Channel 18 was not connected in this work.

Multiplexer Channel No.				Assignment
Regenerator				
1	2	3	4	
0	12	24	36	Warm gas out t/c } at dome
1	13	25	37	Hot gas in t/c } pipe
2	14	26	38	Cold gas in t/c } at orifice
3	15	27	39	Waste gas out t/c } plate
4	16	28	40	Stack pipe t/c
5	17	29	41	Bottom bed t/c
6	18	30	42	Next to bottom bed t/c
7	19	31	43	Centre bed t/c
8	20	32	44	Next to top bed t/c
9	21	33	45	Top bed t/c
10	22	33	46	Cold flow diffrl. transducer
11	23	34	47	Hot flow diffrl. transducer

Note: see also accompanying text

Table 3.3

Multiplexer Channel No.	Assignment
48	Bypass flow differential transducer
49	Absolute transducer, Regs.1 & 2 cold in
50	Absolute transducer, Regs.3 & 4 cold in
51	Absolute transducer, waste confluence
52	Waste confluence t/c
53	Bypass t/c
54	Warm gas confluence (blast temp) t/c
55	Gas heater t/c
56	Cold junction $^{\circ}C \rightarrow mV$ converter

Table 3.4

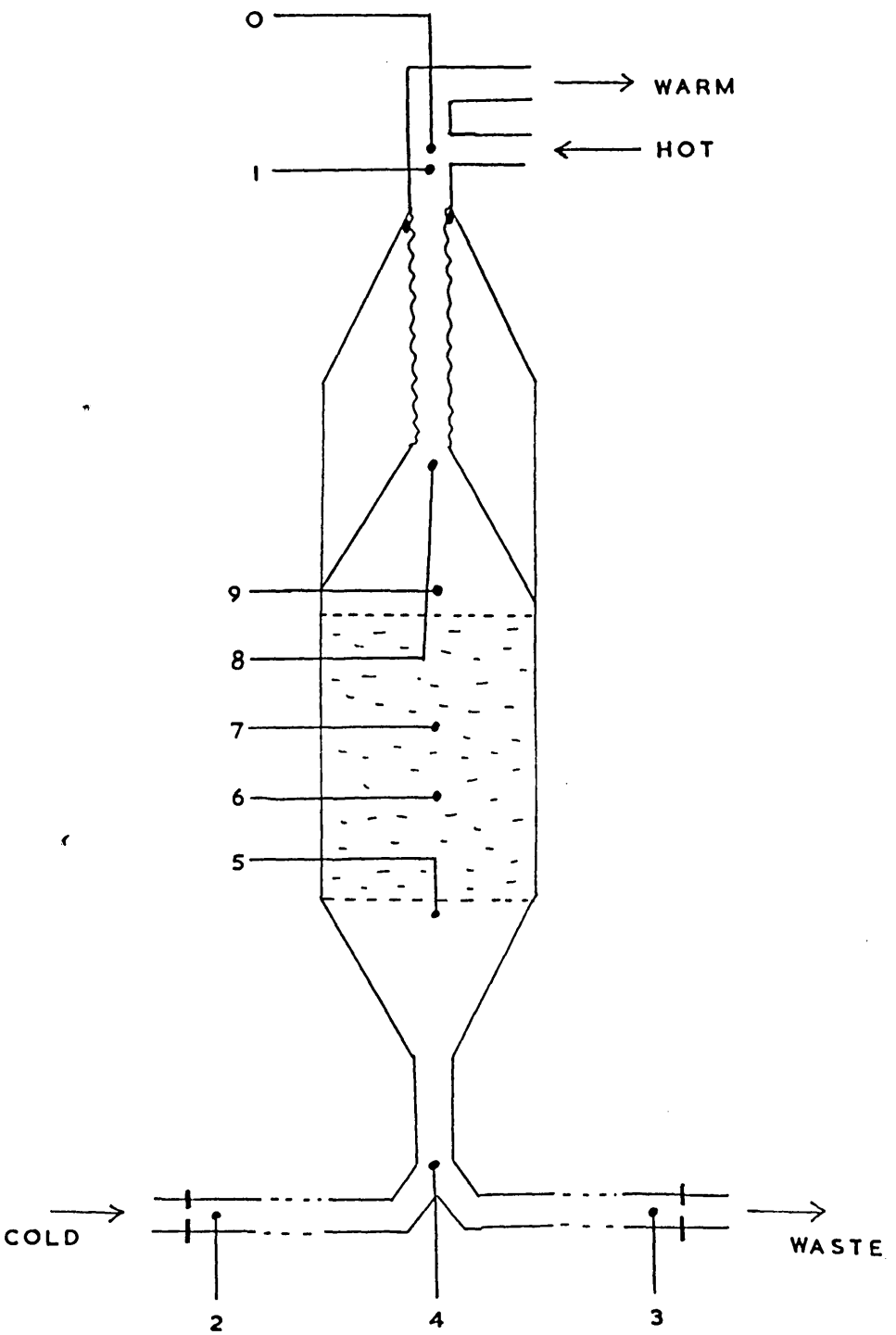

FIGURE 3.5

THERMOCOUPLE CHANNELS

Butterfly valve	Address
Reg. 1 cold in	0
waste out	2
Reg. 2 cold in	4
waste out	6
Reg. 3 cold in	8
waste out	10
Reg. 4 cold in	12
waste out	14
Bypass	16
Gas heater	18

Table 3.5

Stop Valve	Address
Reg. 1 warm out	32
hot in	33
Reg. 2 warm out	34
hot in	35
Reg. 3 warm out	36
hot in	37
Reg. 4 warm out	38
hot in	39

Table 3.6

The stop valves were similarly controlled, but by a single-bit output command

DBOUT (I,J)

where an output J = 0 corresponded to open and J = 1 corresponded to closed. The channel addresses for the stop valves are given in table 3.6. The commands DWOUT and DBOUT are part of the MUSIC system, described in the next section.

3.6 CONTROL, MEASUREMENT AND SEQUENCING SOFTWARE

The software system used on the Dialogue system was a realtime datalogging executive and user-language known as DLX/MUSIC. The user-language MUSIC is a realtime BASIC derivative which allows analogue or digital output via the DWOUT and DBOUT commands described earlier. MUSIC also has standard features such as FOR loops, function definitions, arithmetic tests and branching, and hardcopy output. In addition, through interaction with DLX, multitasking is possible. MUSIC has an interactive interpreter for program entry, yet also stores a compiled version of the program. In this way an increase in speed of two orders of magnitude is achieved over conventional BASIC-like languages. The primary interaction between DLX and MUSIC is via the sharing of data; values of input signals read by DLX (see below) are placed directly in an array which is accessible by MUSIC. It is in this way that a user-program can measure and act upon conditions which exist at the controlled apparatus (in the case of this thesis, the regenerator

rig).

The executive, DLX, handles the data input via the use of 'scanning groups'. These groups, defined by the user, directly access the multiplexer which in this work formed the interface with the rig instrumentation. The easiest way to describe the operation of DLX groups is by way of an example. A group definition has the form

$G6 C16-25 I0:2:30 R6 M0 J37

This defines Group number 6; the group, when 'enabled' under user or program control, will scan channels 16 to 25 of the multiplexer, placing the measured data in the array V. (In fact, elements V(0) to V(9) will contain the data since the first addressed data channel is read into V(0), etc.) The next field in the definition is the interval between scans; in the above example, 2 minutes 30 seconds elapse before the next scan commences. The amplifier gain range is specified as 6 (640mV) and the data is to be measured in integrating mode (mode 0). This mode provides maximum interference rejection, and a sampling rate of 33 channels per second. In free-run mode (no interference rejection) a sampling rate of 200Hz can be achieved, but in this work integrating mode was used throughout. The final field in the definition is the 'jump line'; this specifies the line number (37) of the MUSIC program to which control is passed upon completion of a scan. The code at line 37 and thereafter may then access the data in the array V.

DLX groups may be enabled and halted by the user either directly from a VDU or from within a MUSIC program. Moreover, the definitions of a group can be changed under program control, providing a facility for, say, changing the duration of a regenerator period by altering a group interval field. The groups may also be scheduled relative to a time-of-day clock, enabling actions to be performed at a given time after a certain condition occurs.

A detailed description of the MUSIC software and DLX group definitions used in the work is presented in Appendix D, and only the underlying principles are discussed below.

As previously stated, the functions of the computer (and hence the software) were

a) control of flowrates to their setpoints

b) collection and averaging of experimental data, and

c) sequencing of regenerator switching.

3.6.1 Flowrate Control

A three term controller was written in MUSIC. The basic equation is

$$u(\theta) = k_c\left[e(\theta) + \frac{1}{T_i}\int_0^{\theta} e(\theta)\,d\theta + T_d\,\frac{d\,e(\theta)}{d\theta}\right] \qquad (3.6)$$

where u = manipulated variable (output to valve),

k_c = controller gain

e = error signal

T_i = integral time constant

T_d = differential time constant

The error signal is defined as

$$e(\theta) = r(\theta) - W(\theta) \qquad (3.7)$$

where r = set point

W = controlled variable (mass flowrate)

Equation 3.6 is discretised using a trapezoidal summation and a two point difference form to give

$$u(n) = k_c\left[e_n + \frac{1}{T_i}\left(\tfrac{1}{2}(e_0 + e_1) + \cdots + \tfrac{1}{2}(e_{n-1} + e_n)\right)\Delta\theta + T_d\left(\frac{e_n - e_{n-1}}{\Delta\theta}\right)\right] \qquad (3.8)$$

Using a 'velocity algorithm', i.e. making the output equal to $\Delta u = u_n - u_{n-1}$, and also substituting $e_n = r_n - W_n$ and assuming $r_n = r \ \forall n$,

$$\Delta u = k_c\left[W_{n-1} - W_n + \frac{\Delta\theta}{T_i}\left(r - \frac{W_n + W_{n-1}}{2}\right) + \frac{T_d}{\Delta\theta}(2W_{n-1} - W_{n-2} - W_n)\right] \qquad (3.9)$$

In the MUSIC program, k_c was stored in the variable G, k_c/T_i in F, $k_c T_d$ in P, and $\Delta\theta$ in T. The expression for output u_n ($= \Delta u_n + u_{n-1}$) is then

$$u_n = u_{n-1} + G(W_{n-1} - W_n) + FT\left(r - \frac{W_n + W_{n-1}}{2}\right) + \frac{P}{T}(2W_{n-1} - W_{n-2} - W_n) \qquad (3.10)$$

The controller constants G, F and P were determined experimentally (see Chapter 4) and the time interval T was two seconds, the interval between scans of the data required by the controller. A function FNG evaluated u from equation 3.10. The array Z was used to store setpoints r and previous values of u and W which are required in equation 3.10.

The quantity W (mass flowrate) was evaluated using equation 3.3, with the constants c and m for each flow being stored in the array X. A function FNC performed this task.

In order to find the relevant channel addresses for transducer/thermocouple input and control signal output, a function FNF was written. Using the convention

cold gas flow for reg. 1 = flow 1

hot gas flow for reg. 1 = flow 2

cold gas flow for reg. 2 = flow 3

hot gas flow for reg. 2 = flow 4

etc, and

bypass = flow 0,

it is apparent that, for regenerator n,

hot gas flow = flow 2n and

cold gas flow = flow 2n-1

Examination of tables 3.4 and 3.5 then yields a set of generalisations; for flow number i ($i \in \{0..8\}$):

butterfly valve output channel = 16 $\quad i = 0$

	2(i-1)	$i \in \{1..8\}$
stop valve output channel =	n/a	i = 0
	i + 31	$i \in \{1..8\}$
correction thermocouple input channel =	53	i = 0
	6i-4	i odd
	6i-9	i even
differential transducer input channel =	48	i = 0
	6i+4	i odd
	6i-1	i even
absolute transducer input channel =	n/a	i = 0 or even
	49	i odd and $i \leqslant 4$
	50	i odd and $i > 4$

The reason for the last generalisation is that for even numbered (hot) flows, the flow meter is immediately before the vent to atmosphere, so PR = 1 and no absolute pressure correction is necessary.

The MUSIC routine called after every scan of the multiplexer (i.e. every 2 seconds) consisted of a FOR i = 0 TO 8 loop containing code which, for each flow i, (1) assigned the relevant channel addresses, (2) measured the mass flowrate, (3) evaluated the feedback term for valve position and then (4) made the correct output to the stop valves and control valves. Finally, the array W was assigned to contain the same data as V, so that other DLX groups need do no multiplexer accesses.

3.6.2 Data Collection and Averaging

This was performed by a section of MUSIC code which was executed every two seconds, execution being started by a 'dummy' DLX group which did no scanning. The MUSIC routine accessed various arrays which the flowrate control routine set to contain temperature and flowrate data. For each execution, a counter was incremented and the values of flowrate for flows 1-4 were added to accumulator variables. In addition, the thermocouple millivoltages for six couples on each of regenerators 1 and 2 were similarly accumulated. The recorded couples were channels 1-4, 8 and 9 (see figure 3.5) and their equivalents on regenerator 2. This provided temperature data from three different measuring points at the dome and three points at the stack of each regenerator. Upon the termination of a regenerator period, the accumulated variables were divided by the value of the counter, providing a time-mean value of the data over the period. This averaging was carried out by the routine which performed the regenerator switching (see below).

3.6.3 Sequencing of Switching

This was performed by MUSIC routines called by two DLX groups, denoted by A and B. Both groups were defined as having an interval equal to the sum of the desired hot and cold period durations, and then group A was enabled at the start of the run. Group B was set to be enabled after P seconds. When group A performed a (dummy)

scan, the MUSIC routine which was called changed the flowrate setpoints to those pertaining to the cold period . Similarly, the routine for group B assigned the setpoints for the hot period. The flowrate controller then performed the necessary valve switching automatically. Next, the sequencing software averaged the temperature and flowrate data as described previously, output it to the papertape punch and displayed an information message on the VDU. Finally, the accumulator variables and counter were zeroed for the start of the next period. The scheduling of groups A and B is shown below:

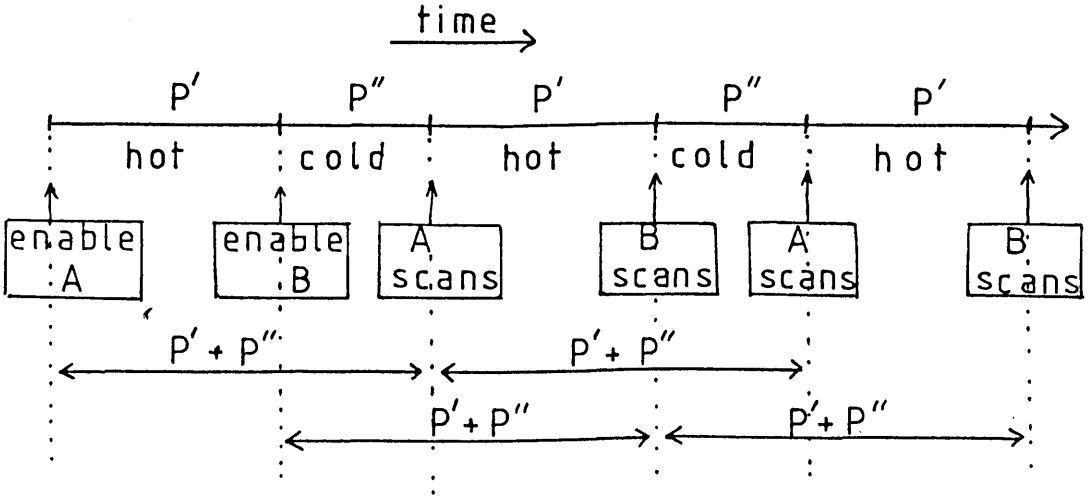

It can be seen that the three separate functions which the computer performed in controlling the rig were, in fact, very closely related.

3.6.4 Miscellaneous Software

Also involved in the rig control software was a startup section, which enabled the user to input various experiment parameters such as period times and flowrates, and which, after error checking, set

group intervals and enabled relevant DLX groups.

The multiplexer temperature was averaged and recorded on papertape in a similar way to the gas temperature and flowrate data; this required the use of a group which scanned only the single channel connected to the temperature/mV converter, once per minute.

Functions were written to evaluate approximate temperatures from thermocouple voltages and to enable and disable groups relative to the time of day.

3.7 REGENERATOR PARAMETERS

In this section, where figures are referred to as 'typical', the prevailing conditions are 0.5 std. m^3/min flowrate, with an average gas temperature of 58°C (i.e. (inlet temperature + exit temperature) / 2 = 58°C).

3.7.1 Heat Transfer Coefficient, Λ, Π

The principal parameter affecting the correlation between experiment and theory is the gas/solid heat transfer coefficient. This is because the results obtained from the computer simulation are directly dependent upon Λ and Π, hence upon the heat transfer coefficient, $\bar{h}$. The purpose of this work was <u>not</u> to determine empirically the value of heat transfer coefficient but rather to

apply existing correlations to the simulation and thus determine an agreement with the experiments.

Figure 3.6 shows graphs of heat transfer coefficient versus mass flowrate for the range of flowrates considered in this thesis and for four different heat transfer coefficient correlations. These are (i) Denton/Meek/Shearer (Denton et al, 1963; Meek, 1962; Shearer, 1962), (ii) Litmann (Litmann et al, 1968; 1970), (iii) Heggs and Handley (1968) and (iv) Yoshida (Bird et al, 1960). It is seen from the graphs that the Heggs and Handley correlation is consistently the lowest of the four, that the Denton correlation is approximately the average of the four, and that the Yoshida correlation is slightly higher than Denton at low flowrates. Yoshida's correlation has a lower slope, and becomes 0.95 of Denton's at high flowrates. Litmann's correlation is only applicable to the lower part of the flowrate range. For these reasons, and also due to its widespread acceptance, the correlation of Denton/Meek/Shearer was chosen as the main correlation to use in the simulations undertaken in this work.

The values of reduced length Λ and reduced period Π resulting from the different correlations are shown plotted against flowrate in figures 3.7 and 3.8. It can be seen that Λ is typically 14 and Π typically 1.8.

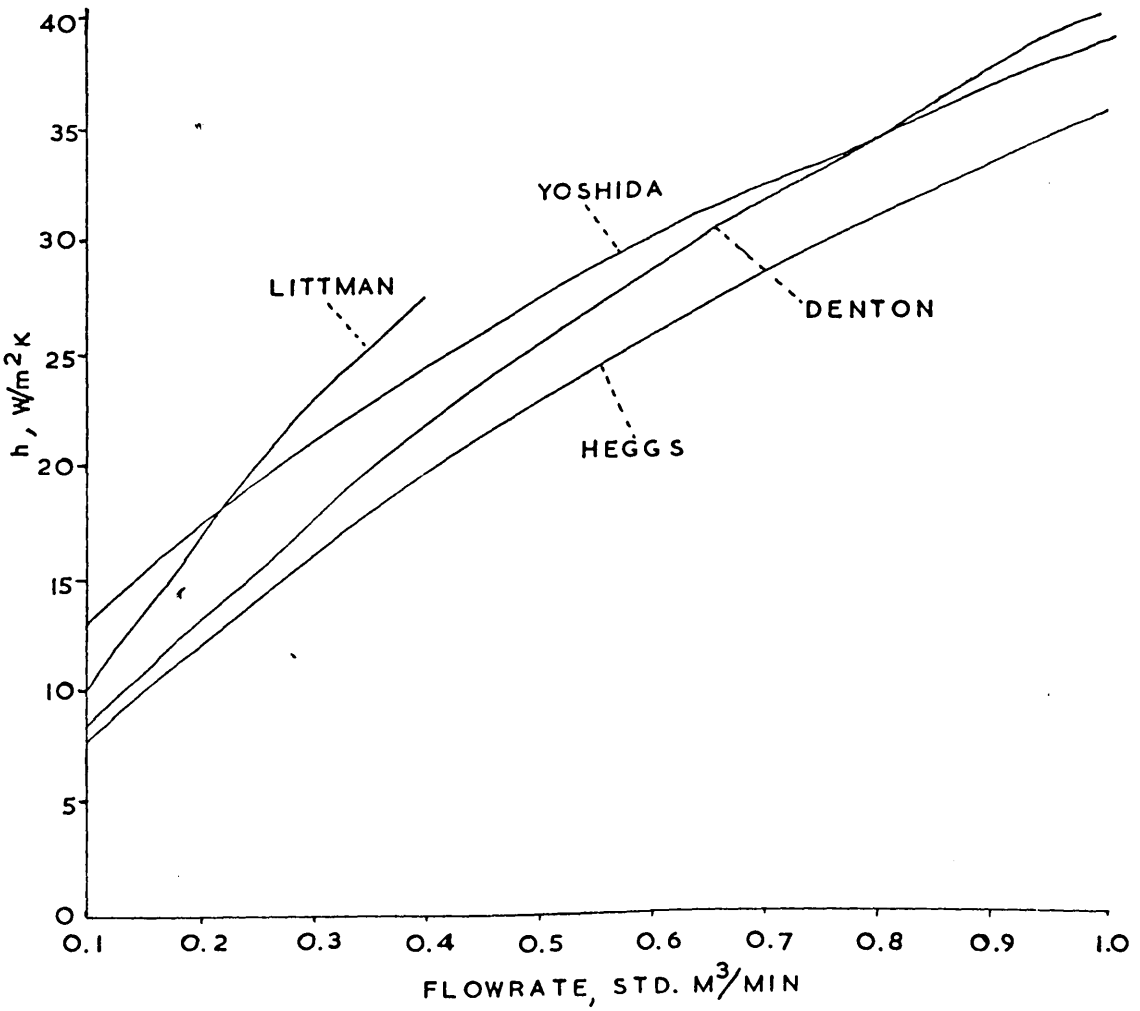

FIGURE 3.6

HEAT TRANSFER COEFFICIENT
VS.
FLOWRATE

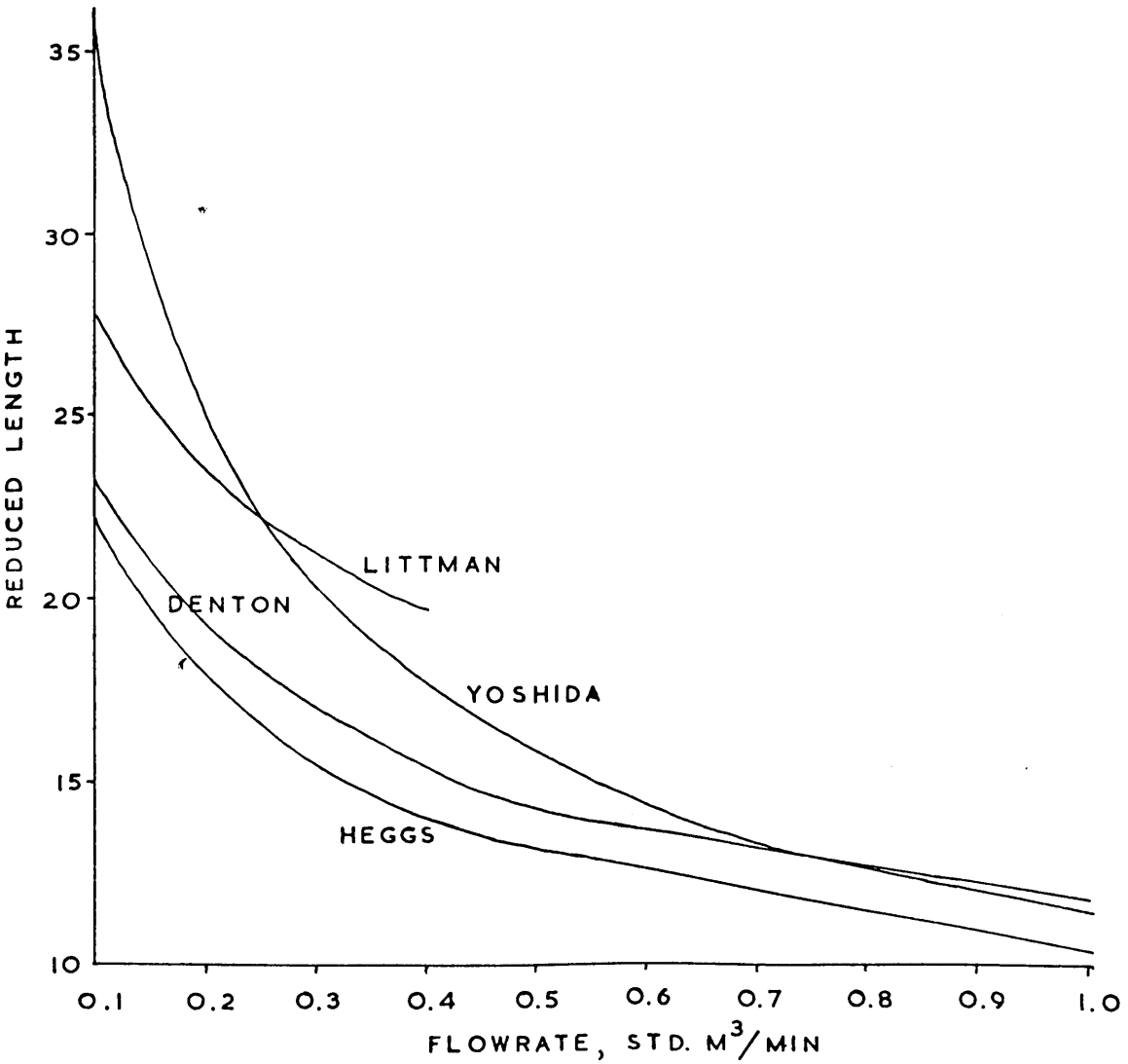

FIGURE 3.7

REDUCED LENGTH VS. FLOWRATE

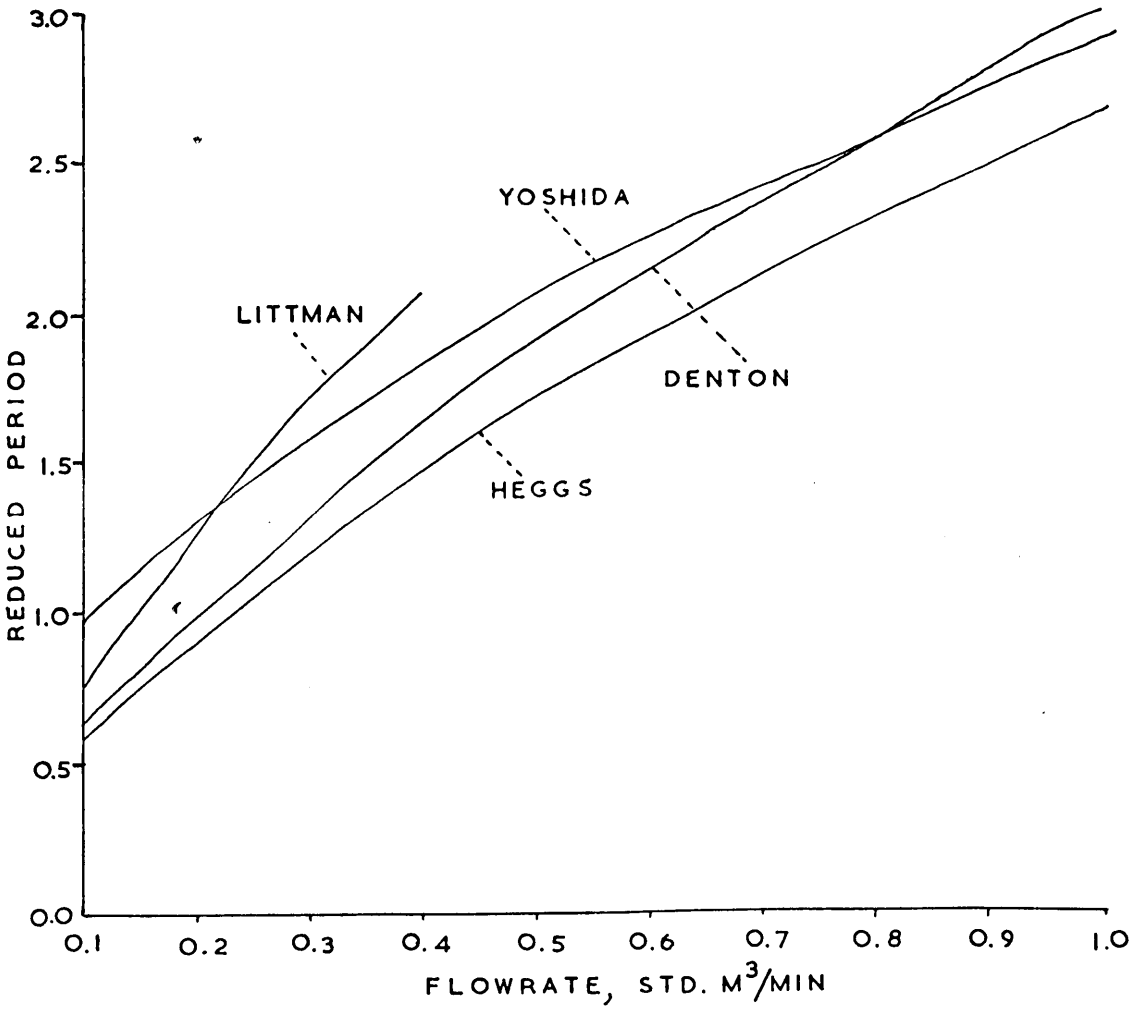

FIGURE 3.8

REDUCED PERIOD VS. FLOWRATE

3.7.2 Flow Distribution

It is well known that the void fraction is larger near the walls of the container of a packed bed than in the central region. Experimental work by Benenati and Brosilow (1962) showed that, for $D/d \sim 20$, the void fraction oscillates close to the wall, in such a way that the voidage can be approximated by an average value of 0.5 within half a sphere diameter of the edge, and an average value around 0.4 over the bulk. Figure 3.9 is reproduced from Schlunder (1978), based on the results of Benenati and Brosilow. As D/d was increased from 20 to ∞, very little change occurred in the voidage distribution. The implication is that $D/d = 20$ is the critical value below which wall effects are significant and above which the effects, although still manifest, are negligible.

Work on flow distribution by Schwartz and Smith (1953), however, produced a figure of $D/d = 30$ as the critical value. (It should be noted here that D/d for the regenerator rig is equal to 17.65). Schwartz and Smith's results show that, for $D/d = 17.65$, the velocity within one sphere diameter of the wall is 60 per cent higher than that in the centre. Analysis of Schwartz and Smith's experimental data by Afgan and Schlunder (1974) yielded the equation

$$\frac{V}{\overline{V}} = \frac{K + \frac{P+2}{2}\left(\frac{r}{R}\right)^P}{K+1} \qquad (3.11)$$

where r = distance from centre

R = container radius

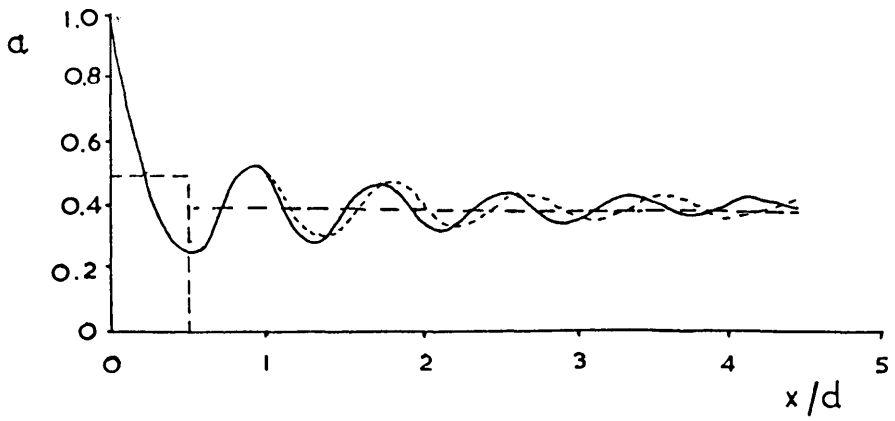

FIGURE 3.9

VOIDAGE DISTRIBUTION

V = superficial velocity at distance r

$\bar{V}$ = mean superficial velocity

$K = 1.5 + 0.0006(D/d - 2)^3$

$P = 1.14\sqrt[3]{(D/d - 2)}$

For the regenerator rig, R = 0.15m, D/d = 17.65, giving K = 3.80 and P = 2.85. The resulting theoretical flow velocity profile is shown in figure 3.10.

An experiment was conducted to investigate the effect of the non-uniform velocity upon cold gas exit temperature. The regenerator was cycled to equilibrium (see Chapter 4) and the cold gas exit temperature was measured immediately above the bed at various points across the bed.The results are shown in figure 3.11. No analysis of the curve was undertaken, but it is apparent that wall effects are significant in the experiments reported in Chapters 4 and 5. The problem was overcome by measuring a 'mixed' temperature, not immediately above the bed, as described in Chapter 4.

3.7.3 Gas Dwell Time

The gas dwell time is important in its effect at changeover; the time taken to purge the regenerator of gas from the previous period (assuming plug flow) should be small with respect to the period duration. This affects the accuracy of the computer simulation, as can be seen from equations 1.35 and 1.36.

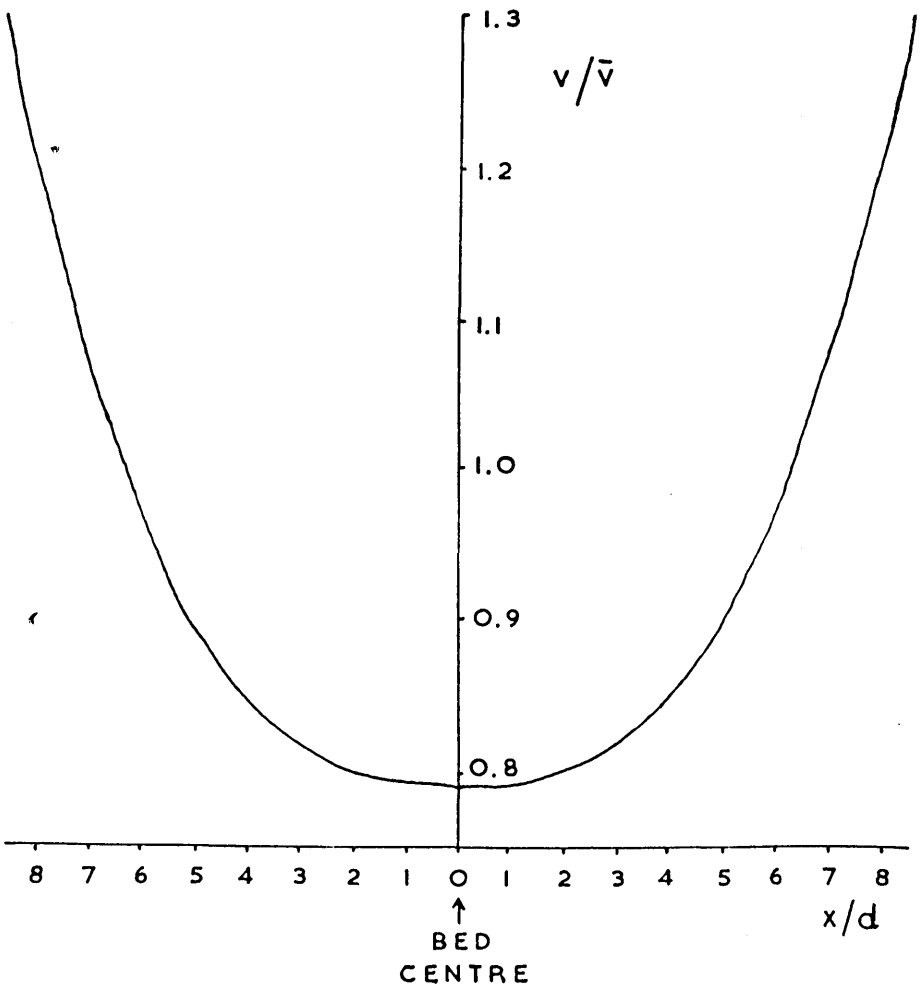

FIGURE 3.10

FLOW DISTRIBUTION

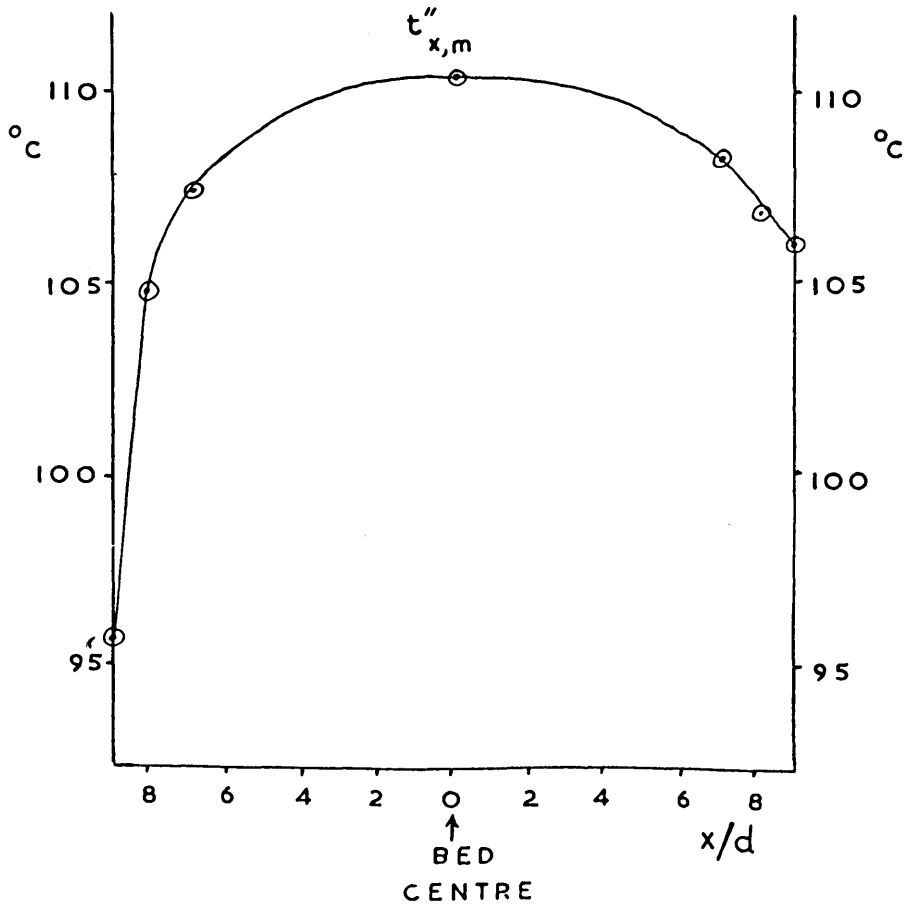

FIGURE 3.11

TEMPERATURE DISTRIBUTION

For the rig, the mass of gas, m, resident in a regenerator vessel at any time is found from the equation

$$m = \pi/4 . D^2 . L . a . \rho \qquad (3.12)$$

$$= 0.012 \text{ kg} \quad \text{at } 58^\circ C$$

The mass flowrate range considered in this work was from 0.1 std. m^3/min to 1.0 std. m^3/min, a range of W of 0.002 kg/s to 0.02 kg/s. This gives a range of dwell times, m/W, of 6.20 s to 0.62 s, typically 1.24 s. The period durations used in this work were constant at 10 minutes (= 600 s) so even in the worst case the dwell time is only ~1% of the period duration. The shortest period duration which could be used with the above flowrate range, using the criterion (dwell time $\leq$ 10% of the period duration), is 1 minute.

3.7.4 Hausen phi-factor, $\bar{h}/h$, K/K_o

For the purposes of simulation, the bulk heat transfer coefficient, $\bar{h}$, is related to the surface heat transfer coefficient, h, by the expression

$$\frac{1}{\bar{h}} = \frac{1}{h} + \frac{w \Phi}{5 \lambda} \qquad (1.56)$$

The factor Φ, which averages out the effect of the parabola inversion through the period, is found from equation 1.57. The expression $2w^2/\alpha.(1/P' + 1/P'')$ evaluates to 1.87 for typical operating conditions on the experimental rig, so the first form of equation 1.57 is used. This yields a value of $\Phi = 0.97$, indicating

that the effect of parabola inversion is very small.

The heat transfer coefficient $\bar{h}$ used in the simulations reported in Chapter 5 was a factor, f, times the Denton correlation. f was found to have the value 0.85 (reported in detail in Chapter 5), and in order to evaluate $\bar{h}/h$ it is assumed that h can be expressed as another factor, f_2, times the same correlation. $w\phi/5\lambda$ evaluates to 2.29×10^{-3} so that, for typical operating conditions,

$$\frac{1}{0.85 \times 24.51} = \frac{1}{f_2 \times 24.51} + 2.29 \times 10^{-3}$$

This gives $f_2 = 0.89$, hence $\bar{h}/h = 0.95$. The proximity of this figure to 1 implies that, for the rig, a Hausen-type (mean solid temperature) 2D model is approximately equivalent to a Schumann-type (isothermal solid) 2D model. (Note: over the entire range of rig flowrates, the factor $\bar{h}/h$ varies from 0.98 at low flowrates to 0.92 at high flowrates).

The parameter K/K_o, quantifying the effect of temperature non-linearities at the regenerator entrance, can be found from the curve for $\Lambda = 15$ (typical) in figure 1.3. At $\Pi = 2.0$ (typical) it is seen that $K/K_o \sim 1$, implying negligible effect. A more accurate figure can be obtained using the equation

$$\frac{K}{K_o} = \frac{2}{\Lambda_H}\left(\frac{E}{1 - E}\right) \qquad (3.13)$$

For typical conditions on the rig, this expression yields a value $K/K_o = 0.95$, confirming that the effect is negligible.

CHAPTER 4

EXPERIMENTAL TECHNIQUE, PROCEDURE, MODELLING AND RESULTS

This chapter describes the experimental methods used to study the transient behaviour of fixed bed regenerators and the particular conditions studied. Described are the procedure used in conducting a experiment, and the subsequent methods of data analysis. The techniques employed in the computer simulation are discussed, as are the methods and results of the various system model calibrations which were undertaken. A summary of the early experiments carried out and their results is presented. The experiments carried out for the main discussion in the next chapter are then described.

4.1 EXPERIMENTAL TECHNIQUE

In the work presented here, measurements were taken on regenerators 1 and 2 only. Regenerators 3 and 4 were used as 'receivers' for the hot flow while regenerators 1 and 2 were in the cold period. This was necessary since it was not possible (and also undesirable) to turn the gas heater off during the cold period. Regenerator 3 operated with the same flowrates as regenerator 2 but one period out of phase, and regenerator 4 was similarly paired with regenerator 1. In this way two experiments, with different flowrates, could be conducted simultaneously provided that the period times were the same. Since all experiments were simple cyclic operating mode with

$P' = P'' = 600$ seconds, this was possible. At the end of a period, thermocouple and flowrate data corresponding to both of the measured regenerators was output to the papertape punch.

It was not possible to conduct more than two experiments simultaneously. In order to ensure a constant hot gas inlet temperature, it was necessary that the total gas flowrate over the heater remained constant during successive cycles. The pairing technique ensured that this condition was met for the main part of the experiments. There was, however, a 'warmup' period of 1800s (= 30 mins) at the start of an experiment, when hot gas was passed continuously through regenerators 1 and 2; this reduced considerably the time taken for the regenerators to reach cyclic equilibrium. The (total hot gas flowrate = constant) criterion meant that it was not possible to supply a warmup period to regenerators 3 and 4. The criterion does not preclude the use of operating methods such as staggered parallel because at any one time two regenerators are on hot, with constant flowrates (see section 2.3, Smith (1983)). For simple cyclic operation, however, only two regenerators can be measured simultaneously unless:

a) the other two regenerators do not receive a warmup period, or

b) regenerators 1 and 2 are 'boxed up' after their warmup period while regenerators 3 and 4 receive a warmup period, or

c) the heater is controlled from the computer (see Chapter 7), or

d) another gas heater is installed

None of these techniques were used in this work, so only two

experiments were conducted at any one time.

For each of regenerators 1 and 2 the following quantities were measured and recorded:

In the hot period:

a) hot gas flowrate

b) gas inlet temperature at regenerator dome pipe (channel 1 in figure 3.5)

c) gas inlet temperature at top of guide cone (channel 8 in figure 3.5)

d) gas inlet temperature immediately above bed (channel 9 in figure 3.5)

e) gas exit temperature at regenerator stack pipe (channel 4 in figure 3.5)

f) gas exit temperature at orifice plate (channel 3 in figure 3.5)

In the cold period:

a) cold gas flowrate

b) gas inlet temperature at orifice plate (channel 2)

c) gas inlet temperature at regenerator stack pipe (channel 4)

d) gas exit temperature immediately above bed (channel 9)

e) gas exit temperature at top of guide cone (channel 8)

f) gas exit temperature at regenerator dome pipe (channel 1)

Items (b) to (f) in each period were actually recorded as thermocouple millivoltage outputs and subsequently converted to temperatures by the experiment processing software (see section 4.2.2.). Moreover, the millivoltages recorded were the time-mean of the readings taken every two seconds during the period, as described in Chapter 3. The importance of time-mean temperatures in regenerator work has been discussed in Chapters 0 and 1. In order to avoid false readings of temperature after a changeover, the first ten seconds of every period were ignored by the temperature measuring software. This allowed for flushing of the gas from the previous period, even assuming some mixing of the gases (i.e. non-plug flow). The period 10 seconds represents 1.7% of the total period duration. A similar period was ignored at the end of each period, to allow data output. This ignored period is referred to as the 'integration chopoff' period.

The temperatures actually studied were (c) and (e) in both periods, these representing the gas temperatures in a 'mixed' area. The flow distribution described in section 3.7 resulted in a non-uniform temperature distribution across a bed immediately above it. The measurement points chosen represent a compromise between minimising heat losses (i.e. measuring close to the bed) and obtaining mixed gas temperatures (i.e. measuring at a smaller diameter pipe remote from the bed). The temperatures (b), (d) and (f) were recorded for the purposes of comparison, but do not represent valid temperatures. The severity of this effect is discussed in Chapter 5.

The flowrates for all nine flowpaths in the system were controlled by the software three-term controller described in section 3.6. Denoting k_c by K_p, k_c/T_i by K_i, and $k_c T_d$ by K_d, the coefficients chosen were K_p(proportional) = 1.5, K_i(integral) = 9.0 and K_d(derivative) = 0. These were determined empirically by trial and error, and represent the best trade-off between instantaneous accuracy of control and speed of response to a setpoint change. During tests, it was observed that with K_i = 0, a constant offset resulted, and as K_i was increased to around 9.0 (with K_p = 1.5), the time taken for the flowrate to settle to a new setpoint became progressively less. As K_i was increased beyond 9.0, oscillations in the flowrate started to appear, and the response time lengthened as a result. With K_i = 9.0, the effect of increasing K_p beyond about 5 was to introduce more and more 'noise' onto the flowrate, so that the instantaneous deviation of flowrate from its setpoint was sometimes quite large. K_d was chosen as zero since it was found that introducing any derivative control at all resulted in severe overshoot and undershoot when setpoints were changed. The controller was strictly, therefore, Proportional plus Integral only.

The response time of the controller was improved greatly by using a form of feedforward control; as the output, O, to a valve was increased, the flowrate, W, in the pipe increased as shown below:

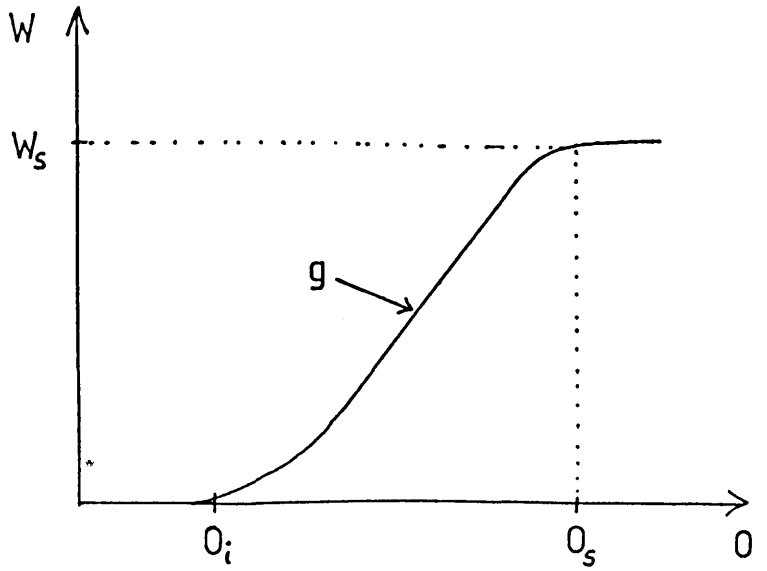

The flowrate W_s is the saturation flowrate corresponding to output O_s beyond which any further opening of the valve resulted in no increase in flowrate; this was due to the pipework and orifice meter geometry etc. The intercept O_i is the minimum valve output necessary to allow flow passage. The gradient g and intercept O_i were evaluated for each flowpath, and for a setpoint $\hat{W}$ the initial output to the valve was $O_{FF} = \hat{W}/g + O_i$. After this, the three-term controller took over to evaluate the feedback term O_{FB} and the subsequent output to the valve was $O = O_{FF} + O_{FB}$. The values of g and O_i for each flowpath are tabulated in section 4.3.1.

The hot gas inlet temperatures were controlled by the dedicated hardware controller, the user setting the three autotransformers to the necessary positions for the temperature and flowrate required.

4.2 EXPERIMENTAL PROCEDURE

4.2.1 Rig Operation

The procedure outlined below assumes that the computer system has been previously loaded with DLX/MUSIC and the control software version TRNS15.MUS. The procedure for system loading is described in the DLX/MUSIC manual situated in the regenerator laboratory.

In order to conduct an experiment it was first necessary to power up the computer and peripherals, open the three valves on the instrument air supply, and turn on the main blower at the slave switch. The 240 V a.c. supplies (13A and 30A) to the control and indication cubicle were then switched on at the junction boxes, providing power to various indicating devices and the heater coils. The Chessel chart recorders recording heater outlet temperatures were then turned on, and the timebases set to 1 hr/cm. The timebase of the J.J. chart recorder which monitored flowrates was then set to 1 mm/sec, with the $\div 100$ circuit switched in, and the pens were inserted. The Fluke '^{o}C to mV' converter was switched on, and the final preparation necessary was to press the 'DC ON' rocker switch on the papertape punch and ensure that a header of blank tape was fed through.

The next action was to type RUN at the VDU to initiate a dialogue in which the period durations, integration chopoff, warmup duration and flowrates were specified. The computer subsequently took over control of the regenerator system and started flow routeing and control. At this stage it was necessary to press the heater manual reset button, adjust the West-Gardian controller to the required setpoint, and turn up the three autotransformers. In order to achieve a fast settling of the heater outlet temperature it was found that a 'visual feedforward/feedback' technique was most successful: the autotransformers were turned fully on, and as the temperature started to overshoot its setpoint, they were gradually backed off until the temperature was stable. At this point the autotransformers were set to the pre-tabulated values. The variable 'A' was set, via the VDU, to the number of the regenerator whose flowrates were to be recorded on the J.J. plotter. For example, setting A = 2 resulted in flows 3 and 4 being recorded (regenerator 2 cold flow - black pen; regenerator 2 hot flow - red pen).

Cyclic equilibrium was attained, under the conditions studied in this work, a maximum of 12 hours after the start of an experiment. A step change was then made, either in hot gas inlet temperature, gas flowrate or both simultaneously. A step change in hot gas inlet temperature was made as follows: firstly the autotransformer settings corresponding to the flowrate and new temperature were found from tables. As soon as regenerators 1 and 2 switched to cold period, the West-Gardian setpoint was turned up to its new value and

the autotransformers turned full up then backed off as before. In this way, the time during which the gas was slowly attaining its new temperature fell in the hot period of regenerators 3 and 4, so that, upon a changeover, regenerators 1 and 2 (the measured regenerators) experienced a 'true' step change at the beginning of the hot period, that is as exact a step change as possible.

Step changes in flowrate were made by changing the values of the variables Y(1) to Y(4) which stored the setpoints (in std. m^3/min) for flows 1 to 4. This was done via the VDU, but the facility existed for changing the variables under program control at a given time of day or depending upon various experimental conditions. Y(1) to Y(4) were only referenced upon a changeover, so that changing (say) Y(1) at any time resulted in a change in regenerator 1 cold gas flowrate at the beginning of the next cold period. If flowrate step changes resulted in any change in the total hot gas flow over the heater, then it was necessary to adjust the heater controls to maintain a constant hot gas inlet temperature. As before, this was always done at such time as to result in a 'true' step change, with constant temperature, being delivered to regenerators 1 and 2.

Simultaneous step changes in inlet temperature and flowrate were carried out in a similar manner to that described above, but instead of adjusting the heaters to maintain a constant temperature they were adjusted to effect a step increase in temperature. Again this was done so that regenerators 1 and 2 experienced a 'true' step

change. Where a simultaneous change involved a change in cold gas flowrate, the change in flowrate occurred at the start of the cold period after the hot period temperature change.

At the end of a run, typically 12 hours after a step change, the procedure for halting the system was as follows: firstly the INTerrupt button on the computer console was pressed, causing all DLX/MUSIC processing to halt. Next, the heater autotransformers and mains switches were turned off, followed by the main blower. The papertape containing the experimental data was removed (with a blank trailer), as were the temperature and flowrate charts. This was followed by the powering-down of all apparatus, as listed in the startup procedure.

4.2.2 Data Processing

A suite of programs was written in Pascal to run on a DECsystem-10, to convert the papertape millivoltage data to a form suitable for analysis, as temperatures. The papertape contained data for both regenerators 1 and 2, the data consisting of (for each period) the cycle number; the logger internal temperature; the flowrates recorded; and the various inlet and exit thermocouple millivoltages as itemised in section 4.1. This was copied to a disk file named Rnnmm.DAT where nn and mm were two-digit numbers identifying the run. Initially, this file was split into two files such that one contained the data for regenerator 1 and the other regenerator 2.

This was done using a program SPLIT.PAS which also split the data from different thermocouples into separate files. The naming convention was as follows. Taking runs 37 and 38 as an example, the rig data file R3738.DAT was split into 6 files such that

RES37A.DAT was regenerator 1 data with t'_i and $t''_{x,m}$ measured immediately above the bed, and $t'_{x,m}$ and t''_i measured at the regenerator stack pipe

RES37B.DAT was regenerator 1 data with t'_i and $t''_{x,m}$ measured at the top of the gas guide cone, and $t'_{x,m}$ and t''_i measured at the regenerator stack pipe

RES37C.DAT was regenerator 1 data with t'_i and $t''_{x,m}$ measured at the regenerator dome pipe, and $t'_{x,m}$ and t''_i measured at the hot and cold flow orifice meters respectively.

RES38A.DAT, RES38B.DAT and RES38C.DAT were the corresponding files for regenerator 2 data. Subsequently, each of the 6 files was treated as a separate input file to the remaining steps of the processing, and the runs referred to as 'run 37A' etc. The remaining steps were:

1. Convert millivoltages to temperatures (see section 4.3.2) using PRELIM.PAS, and produce a user-readable data listing and a plotting file
2. Using data from 1., conduct a simulation using EXPSIM.PAS (see section 4.2.3), and produce a data listing and plotting file
3. Evaluate ranges of data using RANGE1.PAS
4. Plot data from 1. and 2. on a CALCOMP plotter or graphics

VDU using PLOT1.PAS, PLOT3.PAS or PLOT4.PAS

Various quantities could be plotted on each graph, from either experiment, simulation or both. In order to simplify the procedure, and to ensure a consistent naming convention for the files produced, a series of MIC (Macro Interpreted Command) files and a HELP file were produced. The help file, and a diagram showing the data processing procedure, are reproduced in Appendix F.

4.2.3 Simulations

The simulations of experiments which were used for the correlations discussed in Chapter 5 were produced using a Pascal program running on a DECsystem-10 computer. The program employed Willmott's method for solution of equations 1.32 and 1.33 (see section 2.1, Willmott (1964)), and a listing of the program and its description are presented in Appendix E. The general methods used are described below.

The fundamental difference between the model used in this thesis and those generally used is that this model did not assume constant inlet temperatures but used the profiles recorded during an experimental run. This improved the accuracy of the simulations in two ways. Firstly, the accuracy was improved merely by using the observed temperatures as inlet temperatures, and secondly the observed inlet and exit temperatures provided a means of evaluating Λ and Π for the model at the start of each period. For a given

cycle, the Pascal simulation evaluated the mean of the inlet and exit temperatures recorded for that cycle in the experiment. This mean temperature was passed to a procedure which evaluated the heat transfer coefficient, and hence Λ and Π, at that temperature. The user decided, at the start of the simulation run, which of four heat transfer coefficient correlations would be used. It was established that the temperature dependence of gas specific heat was negligible over the temperature range considered in this work. The temperature dependence of gas density, viscosity and thermal conductivity was, however, taken into account.

The Pascal model was also capable of handling a warmup period at the start of a run. The user specified the warmup duration, in multiples of the hot period duration, and also the initial (uniform) solid temperature. The program then used the experimental hot gas inlet temperature from cycle number 1 for the warmup. It should be noted that the actual gas temperatures during the experimental warmup period were not, in fact, likely to be equal to the cycle 1 temperatures for the entire duration; the initial discrepancies between simulated and observed exit temperatures are attributable to this. The fact that initial solid temperatures were possibly not uniform also contributed to the discrepancies. For the simulations reported in this thesis, the initial solid temperatures were assumed to be a uniform 20^{o}C, and the warmup duration to be of 3 hot periods (= 30 mins) duration .

Heat losses were incorporated in the model, and the detailed method is presented in Appendix B. The principle was to evaluate the thermal energy excess inflow over outflow for a hot-cold cycle at cyclic equilibrium, then assume that this, spread over the cycle, gave the heat loss rate. The user of the program specified the cycle number at which the loss rates were to be evaluated. The technique was to pick a cycle where the regenerator was at equilibrium in the experiment and then apply this loss rate to all preceding cycles. To allow for the possibility that a different heat loss rate existed at the second (post-step) equilibrium, the loss rate was evaluated again and applied to all cycles between the step change and this equilibrium. For example, if the regenerator reached cyclic equilibrium at cycle 20, and a step change occurred at cycle 35, then the heat loss rate was evaluated at cycle 20 and applied to cycles 1 to 34. If the subsequent equilibrium was attained at cycle 60 and the experiment stopped at cycle 74, then another heat loss rate was evaluated at cycle 60 and applied to cycles 35 to 74. The facility also existed in the Pascal program for the user to specify the actual heat loss rates to be used, rather than specifying the cycles at which the loss rates would be automatically evaluated. This facility was not used in the work presented here, since the automatic heat loss rate evaluation proved to be entirely adequate.

In summary, the simulations proceeded as follows:

1. Read t'_i , $t'_{x,m}$, t''_i , $t''_{x,m}$, W' and W'' for the current cycle from experimental data
2. Evaluate h' at temperature $(t'_i + t'_{x,m})/2$ and flowrate W'
3. Evaluate h'' at temperature $(t''_i + t''_{x,m})/2$ and flowrate W''
4. Evaluate Λ', Λ'', Π' and Π'' using h' and h''
5. Multiply Λs and Πs by f (see below)
6. Solve the regenerator equations for one hot-cold cycle with inlet temperatures t'_i and t''_i as read at 1.
7. Increment cycle number and goto 1, unless end of experimental data

A program, TUNER.PAS, was written to 'fit' simulated results to experimental results. The entire simulation program described above was packaged as a procedure and called repeatedly, with various multiplication factors for the heat transfer coefficients. The object was to find a multiplication factor, f, which a) minimised the mean square difference between simulated and experimental exit temperatures, and b) was consistent and applicable to all experiments. The method used is described in detail in Appendix C. The program user specified the convergence criterion, the maximum allowed change in f between iterations, and whether the fitting was to be done for the hot or cold side. The curve fitting done for the experiments reported in this thesis was done on the cold side gas exit temperatures, with the first 10 cycles ignored to allow for the expected initial discrepancies. The resulting values of the

f-factor are discussed in Chapter 5.

4.3 CALIBRATIONS AND ERRORS

4.3.1 Flowrate Calibration

Early commissioning work on the rig by Dr. S.A.H. Smith suggested that the relationship between the differential pressure transducer (d.p.t.) voltage and the mass flowrate of gas through an orifice meter could be established from first principles. A square root relationship (see equation 3.1) was therefore assumed, and the constant of proportionality found from known quantities such as transducer sensitivity, supply voltage, orifice diameter, etc. It was decided at an early stage of the research for this thesis, however, that a more accurate calibration could be obtained: the voltage-flowrate relationship was established via direct measurement of both quantities and the constants c and m (see equation 3.3) were evaluated from graphs on log v. log paper. The calibration was undertaken with the help of Dr. A.E. Wraith, using a 47E Rotameter gap flowmeter for flowrate measurement. Firstly, all d.p.t.s were zero-set to within +0.01 mV of 0V with the main blower off. Next, with the blower on, the E/P valve actuators were zero-set so that the valve just closed (i.e. no flow could be felt by hand) for a zero output from the computer. Then, for each flowpath and typically 20 flowrates per flowpath, the following were recorded:

a) Rotameter reading (cm)

b) Flowrate (l/min) from (a) and manufacturers calibration curve

c) Uncorrected d.p.t. reading (mV)

d) Uncorrected absolute pressure transducer (a.p.t.) reading (mV), for cold flows only

e) A.p.t. reading from (d) corrected for zero-offset, for cold flows only

f) Pressure ratio PR, from (e), for cold flows only

g) D.p.t. reading from (c) corrected for PR, for cold flows only

It should be noted that line pressure correction was not necessary for hot flows since the flow meters were downstream of the regenerators and butterfly valves, so there was no flow constriction before the discharge to atmosphere. Hence PR = 1.0

Equation 3.3, after taking logs of both sides, becomes

$$\log W = \log c + m \log V_T^* \qquad (4.1)$$

where V_T^* = pressure-corrected d.p.t. millivoltage

Thus, if d.p.t. millivoltage (item (c) for hot flows or (g) for cold flows) is plotted on the x-axis of log v. log graph paper, and flowrate (item (b)) is plotted on the y-axis, the constant m is found from the gradient and the constant c is evaluated from a (W, V_T^*) pair of values. Calibration curves for flows 2 and 3 are shown in figures 4.1 and 4.2. There is a point beyond which an increase in flowrate produced no further increase in transducer output. This point, known as the saturation flow, arises from the geometry of the orifice flow meters, and the MUSIC rig control

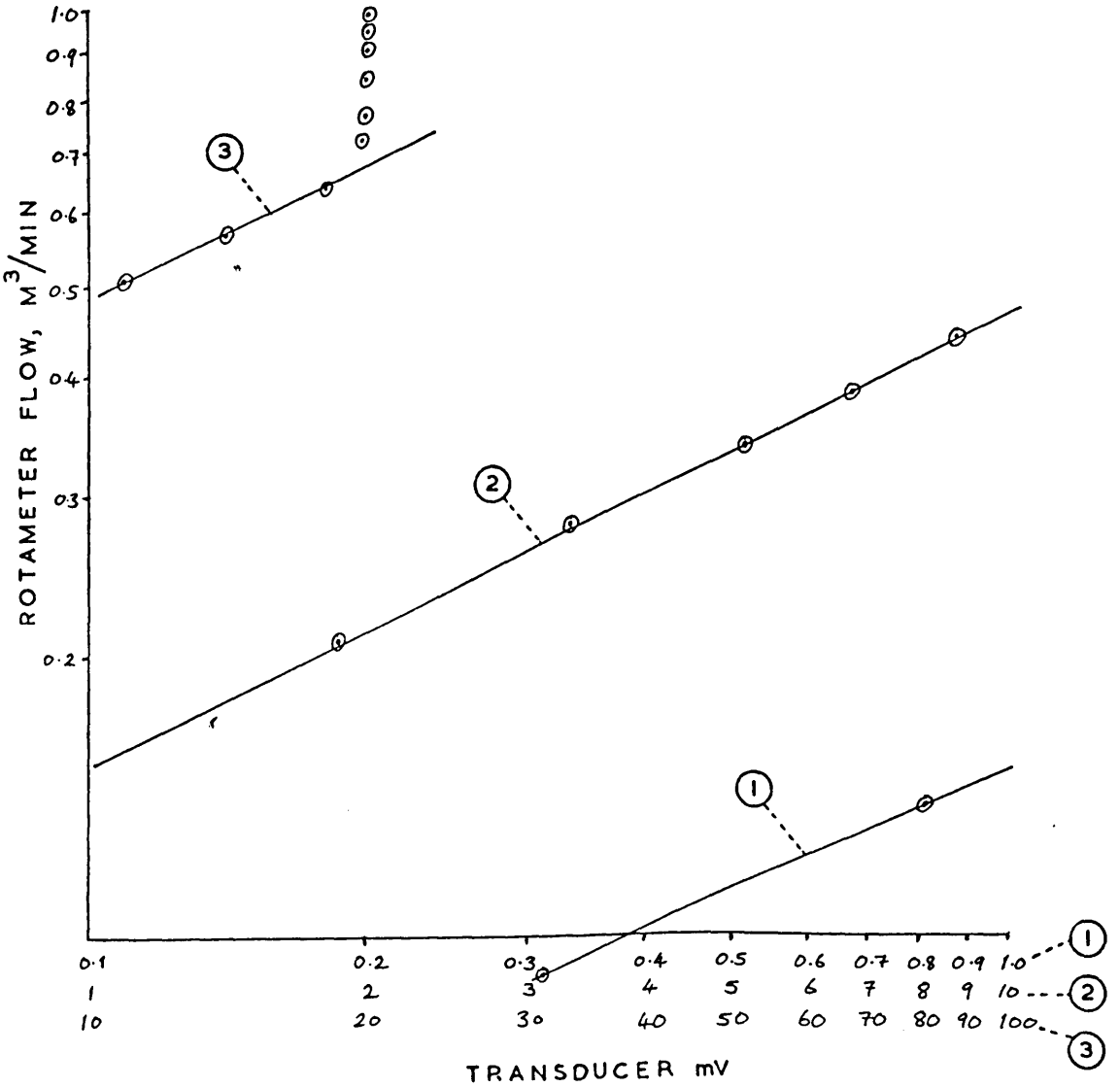

FIGURE 4.1

FLOW 2 CALIBRATION PLOT

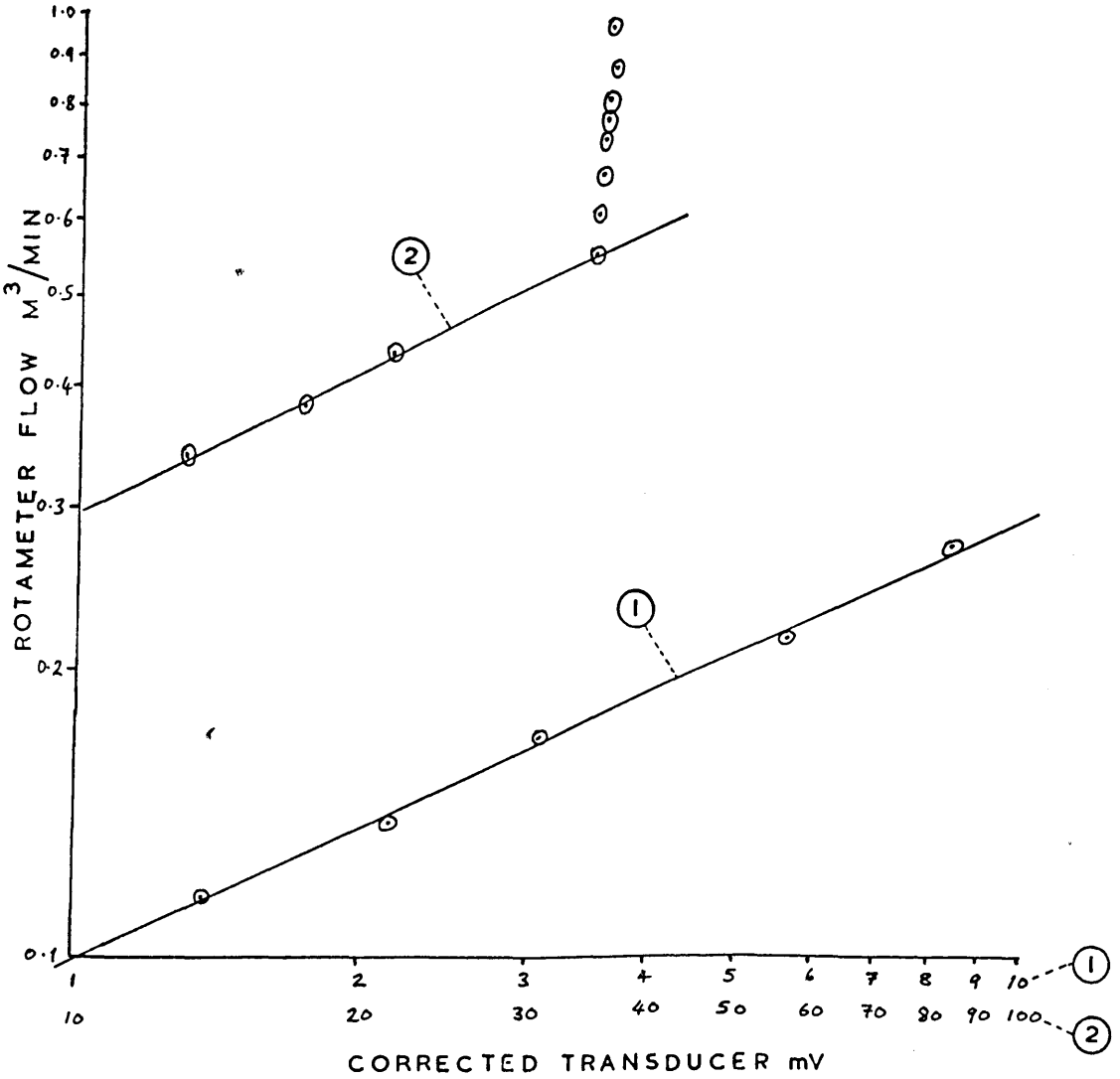

FIGURE 4.2

FLOW 3 CALIBRATION PLOT

software incorporated traps to prevent the user requesting a flowrate setpoint greater than the saturation flow.

Analysis of the calibration curves yielded the values of c and m shown in table 4.1. These values were incorporated in the MUSIC software as described in section 3.6.

The values of flowrate calculated from transducer voltages (using the c and m values) deviated from the actual (Rotameter-measured) flowrates by a very small amount. For regenerator 1, the calculated cold flowrate was found to be ~2% high at 0.2 std. m^3/min, and < 1% high at 0.8 std. m^3/min. The calculated hot flowrate was found to be ~5% high at 0.15 std. m^3/min and 1.5% low at 0.65 std. m^3/min. For regenerator 2 the calculated cold flowrate was < 1% low at 0.15 std. m^3/min, and ~2.5% low at 0.5 std. m^3/min. The hot flowrate was ~5% high at 0.15 std. m^3/min and ~1.8% high at 0.9 std. m^3/min. These errors were deemed to be acceptable, and a definite improvement on the 'first principles' approach, which gave errors as large as 30 or 40%. It was assumed for the purposes of temperature correction of flowrate that the thermocouple cold junction temperature was constant at 20°C; this gave a worst-case error in flowrate of < 1%, and a typical figure of close to zero.

The disadvantage of the adopted approach to calibration is that whenever an orifice flowmeter or d.p.t. is replaced, the flow must be re-calibrated and c and m evaluated again. In the 'first

Flow No.	c	m	Saturation Flowrate m^3/min	Orifice Plate Diameter (mm)
0	0.0914	0.515	0.5	16
1	0.1928	0.493	0.75	20
2	0.1621	0.476	0.65	20
3	0.0957	0.489	0.5	16
4	0.1641	0.505	0.9	20
5	0.1623	0.493	0.8	20
6	0.0927	0.510	0.55	16
7	0.1595	0.498	0.8	20
8	0.1547	0.501	0.8	20

Table 4.1

principles' approach it is merely necessary to substitute the new orifice diameter and/or transducer sensitivity in the relevant equations. It can be seen, however, that the advantages, in terms of accuracy, outweigh the disadvantage in convenience.

The flow characteristics of each flowpath were examined to obtain values of g and O_i for the flowrate controller (see section 4.1). The method was to record (on a chart recorder) the flowrate measured by the computer against the 8-bit integer output to the valve, both ascending and descending. Typical plots are shown in figures 4.3 and 4.4. The hysteresis effect was due to slack (both mechanical and electrical) in the various linkages between computer and valve. The gradients and x-axis intercepts were found from these plots, and their values, stored in the MUSIC software, were as shown in table 4.2. Further flowrate errors were introduced when a flowrate was placed under the control of the three-term controller. It was observed that the maximum instantaneous deviation of a flowrate from its setpoint was $\pm$10%, but the average of the flowrate over the duration of a period was exactly equal to its setpoint. This source of errors was therefore ignored. The response time of the controller to a 50% change in flowrate was found to be typically 6 seconds, this period being spent in overshoot. This was due to adding feedforward and feedback terms, and was considered to be negligible, if not actually useful in aiding flushing at changeovers.

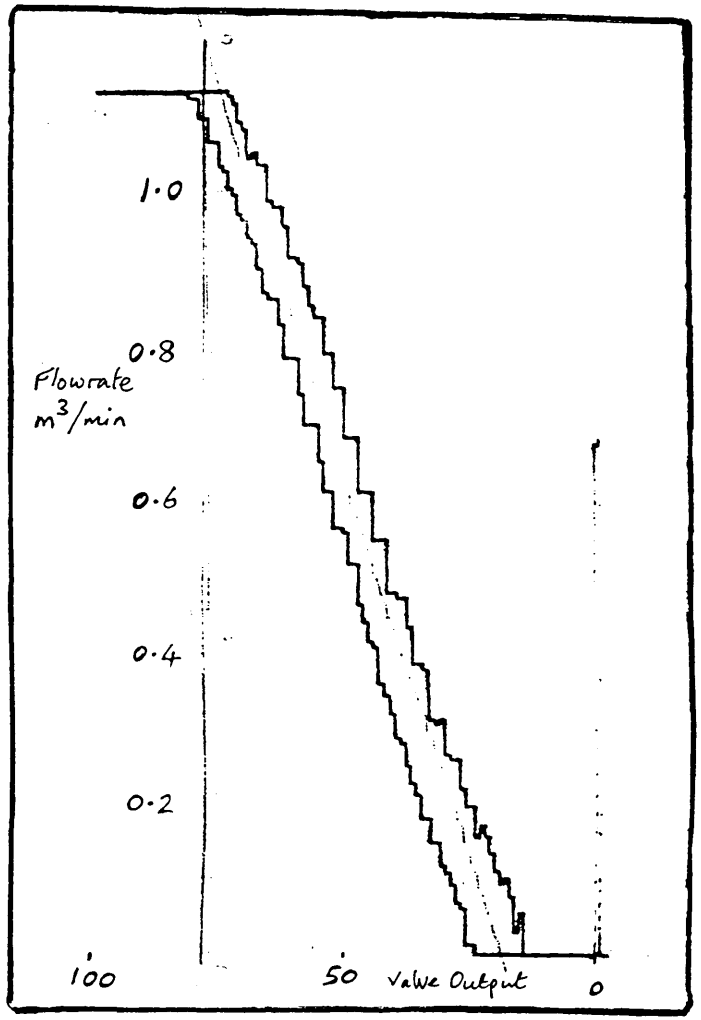

FIGURE 4.3
FLOW 5 CHARACTERISTICS

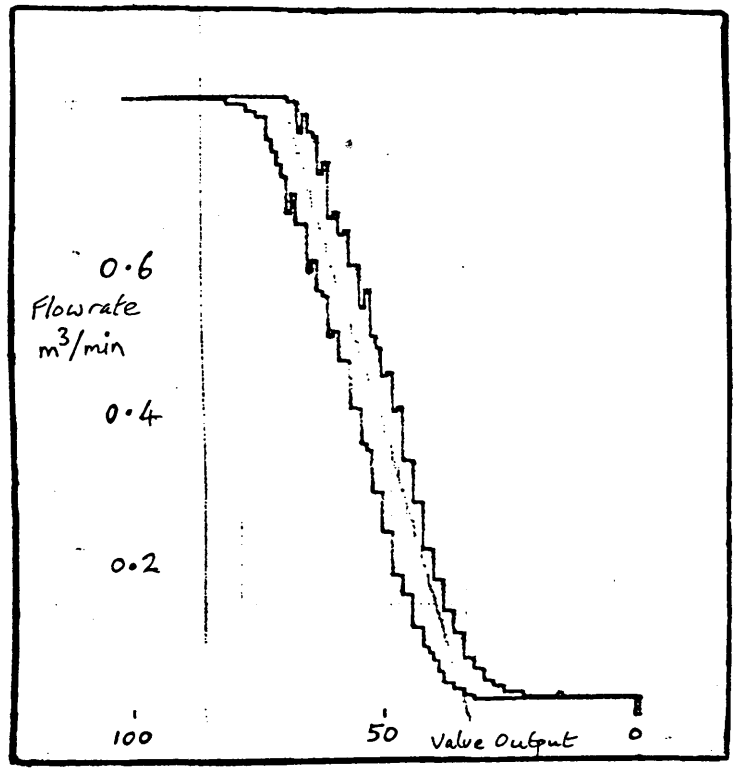

FIGURE 4.4
FLOW 6 CHARACTERISTICS

Flow No.	Gradient g	Intercept O_i
0	0.01462	11.76
1	0.02074	4.41
2	0.01921	22.06
4	0.01949	10.29
5	0.01553	19.12
6	0.02057	33.82
7	0.02331	8.82
8	0.01972	14.71

Table 4.2

It was attempted, at one time, to calibrate the distribution of flowrate across a bed as the gas emerged from the bed. These attempts were made by Dr. J.B. Harness, using a platinum wire bridge anemometer, and were unsuccessful due to the physical construction of the regenerator rig. No further attempts were made by this author.

4.3.2 Thermocouple Calibration

Standard data for the e.m.f. produced by a copper/constantan thermocouple suggested that the temperature-voltage relationship was not quite linear. Using the NAG routine E02ACF, a polynomial was found:

$$V_{TC} = 3.24\times10^{-5}(\Delta t)^2 + 3.998\times10^{-2}(\Delta t) + 2.543\times10^{-2} \qquad (4.2)$$

where V_{Tc} = thermocouple voltage (mV)

Δt = temperature difference (^oC)

Applying the formula for solution of a quadratic,

$$\Delta t = \frac{-3.998\times10^{-2} + \sqrt{3.998\times10^{-2} + 4\times3.24\times10^{-5}\times(2.543\times10^{-2} + V_{Tc})}}{2 \times 3.24\times10^{-5}} \qquad (4.3)$$

This equation was used by the data processing program PRELIM.PAS to evaluate system temperatures from recorded millivoltage data. In order to give temperatures in degrees Centigrade (as opposed to temperature differences) it was necessary to add the value of the multiplexer temperature measured every cycle by the Fluke temperature to voltage converter. Using equation 4.3 resulted in a maximum error of 0.02mV at 300°C. This corresponds to 0.5°C at

300°C, or < 0.2% error, so it was deduced that errors from this source could be ignored.

All of the thermocouples used on the rig were commercial devices, so it was not expected that they would be much in error. However, to account for errors produced from all elements concerned with temperature measurement (i.e. couples, connecting blocks, compensating cables, logger input cards and logger input amplifiers), each couple was calibrated 'in situ' using melting ice and steam end points. This was done by holding the thermocouple tip in either melting ice or the spout of a vigorously boiling kettle, whilst recording the millivoltage measured by the computer. The logger temperature was simultaneously recorded. The regenerator 1 thermocouples (numbered 1-4, 8 and 9 on figure 3.5) were at worst 2.6°C in error with a temperature difference of 84°C, and at worst 1.1°C in error with a temperature difference of 16°C. Typical figures were 2.0°C at 82°C and 0.5°C at 19°C. This represented a percentage error of ~2.5% (typical) across the range of temperature applicable to this thesis. For regenerator 2 (thermocouples 13-16, 20 and 21), the errors were: worst case 2.2°C at 80°C, 0.4°C at 17°C; typically 1.8°C at 84°C, 0.4°C at 17°C. This again represented a percentage error of 2.5% (typical) across the whole range.

As a further check, the regenerator system was left blowing cold for 7 hours, and the measured outlet temperatures were compared. All thermocouples on regenerators 1 and 2 indicated 18.8°C, within ±0.2°C of each other.

4.3.3 Miscellaneous Calibrations

The accuracy of the computer's internal clock, which determined the accuracy of the period durations, was checked and found to have negligible error. Over 12 hours the clock gained a maximum of 10 seconds over a quartz watch with known accuracy of +1 second per week. This represents negligible timing error in a 600s period duration.

The Fluke '°C to mV' converter was calibrated by holding the probe in either melting ice or steam from a vigorously boiling kettle, whilst measuring the output of the device on a digital voltmeter. At 0°C the device measured between 0.0 and 0.1mV, and at 100°C it measured between 99.9 and 100.0mV. It was therefore deduced that the cold junction temperatures recorded during experiments introduced no further error in the measurement of gas temperatures.

Manufacturer's figures for the accuracy of the 15-bit ADCs on the multiplexer were ±2 bits in 10mV, corresponding to less than 1μV in 10mV. The ADCs were regularly calibrated and adjusted by MicroConsultants engineers, and in any case, errors in ADCs and/or

input amplifiers were included and accounted for in the calibrations of other equipment (flow meters and thermocouples). These possible errors could therefore be ignored.

The gas heaters were calibrated merely to enable adjustment of the autotransformers to give a fast response to setpoint changes. It was not necessary to know the accuracy of the West-Gardian controller since it was the inlet temperatures recorded by system thermocouples which were used for simulations. The autotransformer settings were found and tabulated for various nominal temperatures (at the heater outlet) between $50^{o}C$ and $150^{o}C$ over a range of flowrates from 0.2 to 1.2 std. m^3/min. The settings are shown in table 4.3. The accuracy of the hot gas inlet temperatures is seen to be determined by the thermocouple accuracies, discussed in the previous section. A typical figure for the temperature drop between the heater outlet and the guide cone inlet thermocouple was $15^{o}C$ for nominal temperature in the range $100^{o}C$ to $150^{o}C$.

4.4 RESULTS

4.4.1 Apparatus Commissioning, Early Results

The initial commissioning of the rig was carried out by Drs. S.A.H. Smith and A.E. Wraith, but there were still several problems to be overcome by this author when research commenced. The work done by this author (in addition to the calibrations and software

Flow-rate m^3/min	Temperature ^oC										
	50	60	70	80	90	100	110	120	130	140	150
0.2	50 50 60	60 60 70	70 70 70	70 70 80	70 80 80	70 80 90	80 90 100	80 90 100	90 90 100	90 100 100	90 100 110
0.3						80 90 90					100 110 120
0.4	60 60 60	70 70 80	80 80 90	80 90 90	80 90 100	90 90 100	90 100 100	90 100 110	110 110 110	110 110 120	110 120 130
0.5						100 110 120					120 130 140
0.6	70 70 70	80 90 90	90 100 100	100 100 110	100 110 110	120 120 130	110 120 135	120 130 140	130 130 140	140 140 150	140 150 155
0.7						125 125 135					155 160 165
0.8	90 90 90	90 100 100	110 110 110	110 120 120	110 120 130	130 130 140	130 135 140	140 150 150	150 150 160	160 160 170	170 170 170
0.9						140 140 145					
1.0						150 150 150					
1.1						165 165 180			180 180 190		195 200 220
1.2						180 180 180					200 220 220

Heater Autotransformer Settings in order Heater 1, 2, 3

Table 4.3

design described above and in Chapter 3) is described below.

A recurring problem was that of the butterfly valve linkages. The square-section shaft of the valve was held in a round collar by four grubscrews, and it was found that these screws constantly worked loose, resulting in a large hysteresis effect. After dismantling all nine valve assemblies and tightening the screws, the system would operate for approximately one week ($\equiv$ 60 hours running time) before re-tightening was necessary. In order to remedy the problem, hardened steel 'D's were inserted between shaft and collar, but it was found that when the screws were tightened down, the brittleness of the Ds caused them to crack. The final remedy was to re-design the collar with a close-fitting square section hole into which the shaft located. No re-tightening of the screws was necessary after installation of these collars, even after several hundred hours of operation.

The gas heaters were switched by a relay-operated mercury switch, and it was found that the rocking motion caused fatigue and eventual failure of the 30A wires. The heater circuitry was rewired twice in the period of research by this author.

There was initially a problem with water in the compressed air supply causing corrosion etc., and this was overcome by installing several filters and driers in the supply lines. Subsequently a drier failed, resulting in the deposition of dessicant drying agent

throughout the instrument air system. This necessitated the dismantling and cleaning of all valve actuators.

Various other modifications and repairs were made to the hardware, to achieve the final form of the apparatus as described in the previous chapter. Specifically, the packing was changed; the gas guide cones were installed; the heater failsafe circuitry was installed; and thermocouples were frequently re-positioned. The re-positioning involved dismantling the regenerator domes and stacks, and the final positions were as shown in figure 3.5.

The original packing, around which the apparatus was commissioned and software designed by Dr. S.A.H. Smith, consisted of 3/8 - 5/8 inch washed river gravel, to a depth of 40cm. Early experiments by this author, with a single regenerator cycling to equilibrium under symmetric conditions, indicated that the thermal ratios were extremely high; $E' = 0.98$, $E'' = 0.95$. It should be noted that these experiments were conducted with a) uncalibrated, erroneous flowrates and b) badly positioned thermocouples, and this may explain the findings. However, the magnitude of the figures led to the decision to replace the packing with particles of larger diameter, in order to achieve similarity with industrial plant in Λ and Π (hence E).

It was originally intended to study the parameters ε_{g1} and ε_{g2} (equations 2.46 and 2.47) as the regenerator responded to a step change in hot gas inlet temperature, but experiments proved that

this was not viable. It is theoretically possible to predict the final gas exit temperatures as described in section 2.2, and hence evaluate ε_{g1} and ε_{g2} as the run proceeds; in practice, however, the predicted values proved to be extremely unreliable. Large fluctuations in the dimensionless parameters resulted, especially in the hot side responses. The hot side responses were also extremely susceptible to non-constant cold gas inlet (i.e. ambient) temperatures. This resulted in difficulties when attempting to quantify the curves for ε_{g1} and ε_{g2}; plots of $\ln(1 - \varepsilon_{g1})$ and $\ln(1 - \varepsilon_{g2})$ were far from the straight lines required to evaluate the constants lag_H and η_c. It was for this reason that the emphasis of the research was changed. As discussed in Chapter 5, it was decided to work on producing a good correlation between experimental and simulated results for transient behaviour, rather than trying to quantify the responses of the rig.

Early attempts at producing the correlation were reasonably successful but, due to errors in both experiment and simulation, no importance can be attached to the results. Several experiments were conducted consisting of a step change in hot gas inlet temperature under symmetric conditions, for a range of flowrates; the resulting value of the f-factor was 1.56. Later, more accurate, work (as presented in Chapter 5) yielded a value of f less than 1, and the early value can be safely ignored because:

a) thermocouples were not positioned to minimise wall effects

b) flowrates were uncalibrated and inaccurate

c) simulations assumed constant cold junction temperature and constant Λ and Π for each half of a run

By (c), what is meant is that Λ and Π were held constant from the beginning of a run to the step change (1st half) and then changed and held constant until the end of the run (2nd half). Items (a) and (b) were subsequently rectified as already described, and the simulation program was modified to evaluate Λ and Π each cycle (also previously described).

Early work on simultaneous step changes revealed that the rig was not obtaining a heat balance at the equilibrium after the change. A typical run was with $W' = W'' = 0.4$ std. m^3/min, and $t_i' = 100^oC$ nominal. At the step change, t_i' was increased to 130^oC nominal, and W'' to 0.6 std. m^3/min. It was to be expected that

$$W'S'P'(t_i' - t_{x,m}') = W''S''P''(t_{x,m}'' - t_i'') \qquad (4.4)$$

or, since $S' = S''$ and $P' = P''$,

$$W'(t_i' - t_{x,m}') = W''(t_{x,m}'' - t_i'')$$

In fact, allowing for the existence of heat losses,

$$W'(\Delta t)' > W''(\Delta t)'' \qquad (4.5)$$

This was not, in fact the case; typical figures were $(W'\Delta t')/(W''\Delta t'') = 0.74$ to 0.97. The worst case figures were improved upon positioning the thermocouples in the gas guide cones and typical figures were then 0.94 to 0.97. This represented an error in temperature measurement of 2^oC, or an error in flowrate of only $\sim 3\%$, and so was considered acceptable. The later work

(presented in Chapter 5) used a nominal post-step inlet temperature of 150°C, and it is apparent that the imbalance problem was reduced further by making the higher percentage change in gas thermal capacity rate at a step change.

4.4.2 Summary of Experiments

This section describes the operating conditions which were studied to obtain the results presented and discussed in the next chapter. The experiments are summarised in table 4.4. Four categories of experiment were considered, and four experiments from each category appear in Chapter 5. In all experiments, hot and cold period durations were equal, $P' = P'' = 600s$. In addition, since the temperature dependence of the specific heat of air is negligible at experimental temperatures, $S' = S''$, so that the degree of imbalance, γ, could be expressed as

$$\gamma = \frac{W'}{W''} \qquad (4.6)$$

In the cases where a step change in hot gas inlet temperature was made, the change was a step increase from 100°C nominal to 150°C nominal. All step changes were made at the beginning of a period, and when a simultaneous change involved a change in cold gas flowrate, it occurred after the temperature change.

Run No.	Pre-step			Post-step			Category
	W'	W''	t_i'	W'	W''	t_i'	
37B	0.4	0.4	100	0.4	0.4	150	1
38B	0.3	0.3	100	0.3	0.3	150	1
39B	0.6	0.6	100	0.6	0.6	150	1
40B	0.5	0.5	100	0.5	0.5	150	1
41B	0.35	0.7	100	0.35	0.7	150	2
42B	0.8	0.4	100	0.8	0.4	150	2
43B	0.48	0.64	100	0.48	0.64	150	2
44B	0.6	0.4	100	0.6	0.4	150	2
45B	0.6	0.6	100	0.3	0.6	100	3
46B	0.3	0.3	100	0.6	0.3	100	3
47B	0.35	0.35	100	0.35	0.7	100	3
48B	0.5	0.5	100	0.5	0.25	100	3
49B	0.6	0.3	100	0.6	0.6	150	4
50B	0.5	0.5	100	0.5	0.25	150	4
51B	0.3	0.6	100	0.6	0.6	150	4
52B	0.6	0.2	100	0.4	0.2	150	4

Flowrates in m^3/min

Temperatures in ^oC

Table 4.4

Category 1 experiments (runs 37B-40B) were concerned with the response of a regenerator to a single step change in hot gas inlet temperature. All experiments were under symmetric conditions ($\gamma = 1$), and had different flowrates.

Category 2 experiments investigated the effect of imbalance on category 1. The degree of imbalance was kept constant throughout a run, and four different values of γ were studied. If a category 1 experiment is included in this category, then the response of a regenerator to a step change in hot gas inlet temperature was studied for $\gamma = 0.5$, 0.75, 1.0, 1.5 and 2.0. This corresponds to runs 41B, 43B, 37B-40B, 44B and 42B respectively.

Category 3 experiments were conducted with t_i' constant, with a single step in either hot or cold flowrate. Four conditions were investigated: W' increased, W' decreased, W'' increased and W'' decreased. All step changes resulted in a change from $\gamma = 1.0$ to either $\gamma = 0.5$ or $\gamma = 2.0$. The $\gamma = 0.5$ (final) condition was reached by either (i) decreasing W' (run 45B) or (ii) increasing W'' (run 47B). Similarly the $\gamma = 2.0$ (final) condition was achieved by either (i) increasing W' (run 46B) or (ii) decreasing W'' (run 48B). Time did not permit the study of experiments with $\gamma \neq 1$ (initial).

Category 4 experiments were intended to study complex situations by effecting simultaneous step changes in flowrate and hot gas inlet temperature. Control strategies for industrial Cowper stoves with

minimal fuel consumption may well involve simultaneous step changes, and it is for this reason that an understanding of the responses is necessary. Theoretical work by Burns and Willmott (1978) investigated three specific cases of simultaneous step changes, and observed that a 'superposition' principle can be applied. The effect of multiple step changes can be evaluated by combining linearly the effects of each individual step change; this can be thought of as a 'transient rescaling' of temperatures from the old $[t_i', t_i'']$ scale to the new $[t_i'^*, t_i'']$ scale. Assuming that the normalised responses ε_{g1} and ε_{g2} (see section 2.2, Burns (1978)) to a single step in t_i' are known, and the exit temperatures $t'_{x,m}$ and $t''_{x,m}$ following a single step change in gas flowrate are also known, then the effect $\overline{t'_{x,m}}$, $\overline{t''_{x,m}}$ of a simultaneous step change in the two quantities is given by

$$\overline{t'_{x,m}} = t'_{x,m} + \varepsilon_{g1}(t_x'^* - t_x'^o) \qquad (4.7)$$

$$\overline{t''_{x,m}} = t''_{x,m} + \varepsilon_{g2}(t_x''^* - t_x''^o) \qquad (4.8)$$

where t_x^* and t_x^o represent the cyclic equilibrium exit temperatures for the new and old temperature scales respectively. Figure 2.10 illustrates the success of the method. Burns and Willmott state that initial dips or overshoot in the exit temperatures may occur when an increase in inlet temperature is accompanied by either (i) a decrease in flowrate in the same period, or (ii) a change in any parameter in the opposite period. The initial part of an exit temperature curve is due to the 'opposite side' response which is considerably more rapid than the 'same side' response; subsequently the 'same side' response becomes felt and may 'pull back' the first

response. Burns and Willmott successfully applied the superposition principle to such cases.

The problem in studying the superposition principle experimentally is how the principle should be applied to cases where inlet temperatures are not constant, as for the experimental rig. Constant inlet temperatures are necessary for application of Burns and Willmott's method, and so it is not clear how an experimental study should proceed. Due to the importance of simultaneous step changes to industrial control strategies, however, it is most desirable that at least a tentative investigation be made, and the experimental and theoretical results compared qualitatively. For this reason, the Category 4 experiments were designed to be as similar as possible to Burns and Willmott's cases I - III. A fourth experiment was also included, for completeness.

Burns and Willmott's work was conducted with $\Lambda' > \Lambda''$ for some cases, and step changes were made by changing t_i' and Π' or Π''. Translating these conditions to the rig, it was necessary to conduct experiments with $\Lambda' \sim \Lambda''$ and to make step changes in t_i' and W' or W''. Therefore these experiments were similar, but not identical, to Burns and Willmott's cases. The conditions studied were as follows:

(i) $W' = 0.5W''$ ($\gamma = 0.5$) changing to $W' = W''$ ($\gamma = 1.0$) by increasing W'; Burns and Willmott case I, run 51B

(ii) $W' = 3W''$ ($\gamma = 3.0$) changing to $W' = 2W''$ ($\gamma = 2.0$) by decreasing W'; Burns and Willmott case II, run 52B

(iii) $W' = 2W''$ ($\gamma = 2.0$) changing to $W' = W''$ ($\gamma = 1.0$) by increasing W''; Burns and Willmott case III, run 49B

(iv) $W' = W''$ ($\gamma = 1.0$) changing to $W' = 2W''$ ($\gamma = 2.0$) by decreasing W''; run 50B

It is seen that experiments (i) and (iii) were equivalent in that the final conditions were $\gamma = 1.0$, but the means of achieving the final conditions were different. This similarly applies to experiments (ii) and (iv). All permutations of hot and cold flowrate increases and decreases were studied.

The results of the experiments in all four categories are presented and discussed in the next chapter.

CHAPTER 5

DISCUSSION OF RESULTS

In this chapter the results of the experiments and simulations summarised in section 4.4.2 are presented and discussed in detail. Preceding the discussion specific to each category of experiment is a general discussion of the results as a whole.

5.1 GENERAL DISCUSSION

Graphs of all results are presented in Appendix A. For each of the experiments there are four graphs, all plotted with cycle number ($\equiv$ time) on the x-axis:-

1) cold gas inlet temperature (^{o}C) from experiment
2) hot gas inlet temperature (^{o}C) from experiment
3) cold gas exit temperature (time-mean) (^{o}C) from experiment and simulation
4) hot gas exit temperature (time-mean) (^{o}C) from experiment and simulation

The main interest lies with the correlation between experimental and simulated exit temperatures, but the inlet profiles (in fact time-mean as well) are reproduced for completeness and to enable analysis by future workers.

As discussed earlier, the exit temperatures are presented in ^{o}C rather than the dimensionless form used by previous workers. It is, in fact, generally possible to non-dimensionalise the cold side responses for the results presented, but it is not possible for the hot side responses. This is because

a) the hot gas exit temperature was usually close to the ambient temperature, so that changes in ambient temperature affected the exit temperature directly, and

b) changes in input conditions on one side have a more immediate effect on exit behaviour on the opposite side (see Chapter 2). This means that changes in cold gas inlet (= ambient) temperature affect the hot gas exit temperature immediately. The non-constant cold gas inlet temperatures observed during the experiments (see graphs) can be seen to severely affect the hot gas exit temperatures, whereas on the opposite side the 'filter' effect of the regenerator smooths such variations and no influence is seen. As a result, the hot side sometimes appears not to reach equilibrium (although the variation over 10 cycles is typically only $3^{o}C$), and so $t'_{x,m}(\infty)$ cannot be determined. The dimensionless parameter ε_{g1}, given by

$$\varepsilon_{g1}(n) = \frac{t'_{x,m}(n) - t'_{x,m}(0)}{t'_{x,m}(\infty) - t'_{x,m}(0)} \qquad (2.46)$$

cannot, therefore, be determined either. Since the main aim of this work was to obtain good experiment/simulation agreement rather than to obtain an equation for the responses, this is not considered serious.

Earlier work by the Ford Motor Co. (see section 2.2, Chao (1955)), concerned with an experimental rotary regenerator, made no attempt to reproduce the hot gas responses, presumably for similar reasons to those discussed above. The conclusion from Chao's work and the work in this thesis is that, in practice, little can be learned about the transient state of a regenerator system by studying the hot side response, so long as the inlet temperature of the cold gas varies chronologically with the ambient temperature.

The simulated results shown on the graphs were obtained using 10 time and 10 distance steps for solution of the model. Early simulations were undertaken using only 5 steps, and an investigation into the number of steps required for sufficient accuracy revealed that the difference between exit temperatures using 20 steps and those using 5 steps was only $0.1^{o}C$ in $50^{o}C$. Five steps are therefore sufficient (although 10 steps were actually used).

The theory behind the heat loss treatment used in the simulations is presented in Appendix B. In order to determine the points in time where equilibrium was established (hence the points at which to evaluate heat loss rates), the exit temperature curves for each experiment were examined; the cycle numbers chosen and the values of heat loss rate are reported in the following sections. The effect of including heat losses in the simulations was investigated by merely comparing the exit temperatures of simulations with and without heat losses. For a typical run, with an experimental cold

gas exit temperature of 111°C, a simulation with no heat losses gave an exit temperature of 114.7°C. With losses included, this figure was reduced to 112.5°C. The agreement between experiment and simulation was therefore improved, although it is apparent from these figures, and from the values given later for heat loss rates, that losses played relatively little part in the accuracy of the simulations. Typically, the heat input to a regenerator during the hot period was 550kJ and the loss rate was 17W. The total heat loss in both periods was therefore 20kJ; this represents 3.6% of the total heat input, lost over the entire hot-cold cycle.

In five of the simulations, the heat loss rate was assigned the value zero; this is indicated in the text where necessary, and was done because of there being a small apparent heat gain at equilibrium. Comparison of the quantities $W'(t'_i - t'_{x,m})$ and $W''(t''_{x,m} - t''_i)$ in these cases gives a typical imbalance of 1.5 in 35 (with W = 0.6 std. m^3/min), implying that a 2.5°C error in a thermocouple reading or a 1.7% error in flowrate would account for the imbalance. Another contributory factor is the choice of cycle number for heat loss rate evaluation. The cycles chosen were those where $t''_{x,m}$ was judged to be stable and constant, with no reference to $t'_{x,m}$. Where $t'_{x,m}$ was close to ambient temperature and varying greatly, a few cycles either way could cause a 2.5°C change in $(t'_i - t'_{x,m})$. A similar argument applies to $(t''_{x,m} - t''_i)$, and the imbalance could be reduced (if not removed) by averaging the quantities $W'\Delta t'$ and $W''\Delta t''$ over the whole of the portion of the

experiment spent at equilibrium.

The only factor common to the five experiments where the imbalance occurred is that they were all conducted on regenerator 1. Not all regenerator 1 experiments exhibit the imbalance and, more importantly, no regenerator 2 experiments exhibit it. This further points to thermocouple and/or flowrate errors. The accuracy of these quantities has been discussed in Chapter 3. The heat flow imbalance, $(W'\Delta t' - W''\Delta t'')$, is considered to be negligible within the accuracy of the experiments and choice of cycle for heat loss rate evaluation.

The magnitude of the loss rates was generally small, and this is explained as follows. Large heat losses to atmosphere occurred on the rig between the gas heater and the gas guide cones on the regenerators, but these losses were irrelevant since the inlet temperatures were measured at the tops of the cones. The path from the cone top to the regenerator exit cone was well-insulated externally, and so losses to atmosphere would be expected to be small. Heat lost from gas and/or packing to the regenerator container (and consequently to pipework etc.) was regenerated upon a changeover, and was therefore not strictly lost at all. At rig commissioning time, large losses were observed from the containers to their (thermally massive) supporting yokes, but installation of the guide cones removed the gas from direct contact with the containers in this region, so the problem was no longer manifest.

All of the simulations shown on the graphs use the Denton heat transfer coefficient correlation (Denton et al, 1963; Meek, 1962; Shearer, 1962), and incorporate the constant multiplication factor discussed below. The reason for using the Denton correlation is that whichever correlation is used, the factor is found to be less than 1.0, and the correlations which give the lowest values of heat transfer coefficient are those of Denton and Heggs (Heggs and Handley, 1968). Thus to keep the factor as close to 1.0 as possible, either of these (very close) correlations should be used. The Denton correlation is used here for historical reasons and also because of its more widespread acceptance, although the Heggs correlation actually gives f-factors marginally closer to 1.0. Examples of simulations using these correlations (and the others discussed in Chapter 2) are shown in section 5.6.

In some cases, discrepancies between experiment and simulation can be seen in the initial few cycles of a run. The discrepancies are due to the fact that various quantities were not accurately known, as has been indicated in Chapter 4. Specifically, the hot gas inlet temperature during the initial warmup period of an experiment was not recorded, and in addition, and indeed more importantly, the initial solid temperature distribution at the start of an experiment was not known. The discrepancies arise from the assumptions and estimates which have to be made as a result of this lack of data; the actual assumptions and estimates have been discussed in section 4.2.3. Because of the discrepancies, the initial 10 cycles were

ignored when evaluating the mean square differences in the curve fitting procedure (see Appendix C).

The values of multiplication factor, f, which minimise the mean square difference (m.s.d.), and the values of the m.s.d. itself, are reported in the sections pertaining to each experiment. The fitting was done for the cold gas exit temperatures, and so the values of m.s.d. represent typically 1.9°C (at worst 3.2°C) in ~100°C. The average of the f-factors which minimise the m.s.d. for each experiment is 0.85, and the use of this value of f gives an average m.s.d. over all experiments of 3.48. This is compared to an average m.s.d. of 2.03 if the best f for each experiment is used. The simulations shown on the graphs in Appendix A were therefore all carried out using Denton's correlation and an f-factor of 0.85.

The reasons for the existence of the f-factor (i.e. the reasons why $f \neq 1.0$) are many, and are also somewhat irrelevant. Most previous work on the empirical determination of heat transfer coefficients has reported correlations applicable only to the actual apparatus used in the work. Since the aim of the work in this thesis was <u>not</u> to determine empirically a heat transfer coefficient, it is valid to merely state here that the heat transfer coefficient applicable to the packed beds in the regenerator system was approximately 0.85 times the Denton correlation. It is postulated that the f-factor was necessary because of:

(i) wall-flow effects and/or backflow; work is in progress to determine the severity of the effect for the rig (Penney, 1984)

(ii) the regenerative effect of the containers and pipework, which is not included in the simulations

(iii) the inherent uncertainty in heat transfer coefficient correlations for packed beds

and

(iv) experimental errors in general (e.g. thermocouple and flowrate errors)

It has been established (in Chapter 3) that the computer model used was applicable to the rig in terms of Hausen's Φ and K/K_o factors, and so no further errors were introduced in this respect. Longitudinal conduction in the beds is also unlikely to be relevant since spheres in a packed bed are in point contact only.

Where, in the text below, the phrase 'cycles to equilibrium' is used, this refers to the number of hot-cold cycles which were required before the difference in consecutive values of $t''_{x,m}$ was $\leqslant 0.5^{o}C$. It is easy, in theoretical work, to apply strict equilibrium criteria such as Aitken's criterion (see section 2.2.1). In experimental work such as that reported here, such equilibrium criteria are not meaningful, due to the effect of variations in ambient conditions and to the large (relative to theory) errors in temperature measurement. It can be seen from some of the graphs in Appendix A that even approximately 40 cycles after a step change,

the cold gas exit temperatures were still rising slowly. Criteria such as Aitken's would not, therefore, judge the system to be at equilibrium, even after 40 cycles. The 0.5°C criterion, however, leads to equilibrium apparently being attained after ~7 cycles. This criterion is, at first sight, unsatisfactory, but no other criterion can usefully be applied in these circumstances. The 0.5°C criterion is valid, considering the accuracy of temperature measurement and the stability of ambient conditions.

It should be made clear that the complete representation of transient behaviour is contained in the actual chronological variations in exit temperatures, both in terms of the magnitude of the temperatures and the shape of the curves. The number of cycles taken to re-attain cyclic equilibrium is only one parameter, which attempts to summarise the response and which is not particularly useful in experimental work. The complete representation of the response of the system is available from the experimental graphs, and was also incorporated into the simulations; the whole of an exit temperature curve (except the very beginning) was taken into account when evaluating the f-factor which gives rise to the good level of experimental/theoretical agreement reported below. As an example, it will be seen that the degree of imbalance has no effect on the system's response to a step change in t_i', if the number of cycles to equilibrium alone is considered. If, however, the actual chronological temperature variations are considered, then it is seen from the graphs in Appendix A that the degree of imbalance does have

an effect on the response of the regenerator.

Previous theoretical work, therefore, is useful in providing a guide to transient behaviour in terms of temperature variations, but is of less value in predicting the number of cycles to equilibrium. This is due to the fact that theoretical work has always imposed ideal conditions upon the model, in particular constant flowrates and inlet temperatures. This enables the use of a rigorous equilibrium criterion. For an improved experiment/simulation agreement (in terms of temperature magnitude, curve shape and cycles to equilibrium), the computer model must incorporate the timewise variations in flowrates and inlet temperatures, and must use an equilibrium criterion applicable to the experimental work. This was done by this author, and it will be seen that an excellent level of agreement results, in terms of all aspects of transient behaviour.

Previous theoretical work (Burns, 1978; Green, 1967) produced correlations for the total reduced time to equilibrium, Θ, of the form

$$\Theta = a\Lambda^2 + b\Lambda + c$$

where a,b,c are real constants.

Due to the small variations in Λ over the range of flowrates considered, it was not possible to produce such a correlation for the experiments discussed here, even for the convergence criterion discussed above which was found to be applicable to experimental work. As a result, the number of cycles to equilibrium is simply

reported separately for each experiment.

5.2 STEP CHANGES IN HOT GAS INLET TEMPERATURE ($\gamma = 1$)

The four examples of step changes in t_1' show extremely good agreement between experiment and simulation, on both the cold and hot sides. The hot side exit temperatures were very close to ambient temperature and so, for the reasons outlined previously, are of no importance. Step changes were typically from 90°C to 125°C, and the results were as follows. For a flowrate of 0.3 std. m^3/min (run 38B), 8 cycles were taken to re-establish equilibrium, using the 0.5°C criterion. The heat loss rates, evaluated at cycles 35 and 70, were 3.5W and 14.2W respectively, and the minimum m.s.d. is 1.44 using f = 0.88. With f = 0.85, the m.s.d. is 1.56. For a flowrate of 0.4 std. m^3/min (run 37B), 7 cycles were taken to equilibrium (0.5°C criterion), and the heat loss rates (cycles 35 and 70) were 3.6W and 18.5W. The minimum m.s.d. is 1.18 (with f = 0.80) and using f = 0.85 the m.s.d. is 1.50. For 0.5 std. m^3/min and 0.6 std. m^3/min (runs 40B and 39B), 8 cycles were taken to equilibrium. The minimum m.s.d.s are 0.80 (run 40B) and 0.89 (run 39B), both obtained using f = 0.85. Heat loss rates for run 40B were 1.1W (cycle 25) and 17.8W (cycle 72). For run 39B, heat loss rates were assigned the value zero, because of the imbalance discussed previously. The difference between $W''\Delta t''$ and $W'\Delta t'$ is 1.3 at cycle 27 and 0.2 at cycle 72. This represents either a maximum temperature error of 2.2°C or maximum flowrate

error of 3.3%, or a combination of smaller errors in both quantities. This is acceptable, to the degree of accuracy reported in Chapter 4.

The number of cycles to equilibrium and also the qualitative shapes of the curves indicate that there was very little, if any, variation of the cold side responses with flowrate. The experiment/simulation agreement for the cold side is excellent (within $\sim 1^{o}C$ average), and it is also good for the hot side, taking into account the temperature scales on the graphs. It can be seen that the exit temperature curves for runs 37B and 38B are similar, as are those for 39B and 40B. This is because runs 37B and 38B were conducted simultaneously on regenerators 1 and 2 (and similarly runs 39B and 40B) hence the t_i'' profiles were similar. This observation lends further weight to the statement that hot side responses were influenced greatly by ambient conditions, including t_i''.

5.3 STEP CHANGES IN HOT GAS INLET TEMPERATURE ($\gamma \neq 1$)

The degree of imbalance, defined as $\gamma = (W'S'P')/(W''S''P'')$, can be expressed as W'/W'' in this work, since $S' = S''$ and $P' = P''$ for all experiments. The values of γ studied were 0.5 (run 41B), 0.75 (run 43B), 1.5 (run 44B) and 2.0 (run 42B). The results are summarised in table 5.1.

γ	Run No.	Cycles to Eqbm.	Heat losses (cycle, rate (W))	Minimum m.s.d. and corresponding f	M.s.d. with f = 0.85
0.5	41B	7	-	6.36, 1.36	9.42
0.75	43B	7	-	1.18, 0.99	4.81
1.5	44B	8	30, 30.6 55, 63.5	1.44, 0.72	4.45
2.0	42B	9	35, 56.1 71, 84.3	2.21, 0.61	4.81

Table 5.1

It is seen from the table (and the graphs) that run 41B has a particularly bad experiment/simulation agreement. The minimum value of m.s.d. is obtained with f = 1.36, which is by far the highest f-factor found for any experiment. For this reason, run 41B was excluded when averaging the f-factors to find the overall figure of 0.85. (The effect of including this run is to raise the average to 0.88). However, applying a factor of 0.85 to run 41B gives an m.s.d. of 9.42, corresponding to only ~3°C. Moreover, the hot side agreement is seen from the graphs to be exceptionally good with f = 0.85. For these reasons it is concluded that even for this run, an acceptable correlation results from using f = 0.85.

The heat loss figures for runs 41B and 43B are omitted from table 5.1, again because of a small apparent heat gain. The figures for $(W''\Delta t'' - W'\Delta t'')$ for run 41B are 1.8 at cycle 25 and 1.9 at cycle 52. Again, this represents a very small error in W and/or Δt, so is not considered serious. Figures for run 43B are 1.5 at cycle 35 and 0.8 at cycle 74.

By including in this category any of the category 1 experiments, it can be seen that the response of the regenerators to step changes in t_i' exhibits no dependence on the degree of imbalance for the range $0.5 \leqslant \gamma \leqslant 2.0$. The responses appear to be independent of γ both in terms of the number of cycles to equilibrium and in terms of the (qualitative) shape of the curves. Theory states, however, that the total time to equilibrium should be reduced by introducing imbalance

into the regenerator operation (see, for example, Burns (1978)). The equilibrium criterion used in the analysis of these experiments gives ~7 cycles to equilibrium. It is postulated that this time to equilibrium is so short that changes due to the effect of imbalance cannot be detected; a change would only be observed if a rigorous equilibrium criterion were to be applied, and this is not possible in experimental work, as discussed earlier.

Typical figures for the number of cycles to equilibrium from Burns' theoretical work are 58 cycles with $\gamma = 1.0$, 30 cycles with $\gamma = 2.0$ and 15 cycles with $\gamma = 0.5$. A considerable reduction in the total time to equilibrium is therefore observed as imbalance is introduced. If Burns' results are subjected to equilibrium criteria such as that used in this thesis, however, then < 10 cycles are taken to equilibrium for all values of γ. The change in time to equilibrium as a result of imbalance is therefore no longer manifest. It is for this reason that the experimental responses appear to independent of γ.

The experiment/simulation agreement is seen from the graphs to be very good on both the hot and cold sides, for a value of f = 0.85, at all values of γ.

5.4 STEP CHANGES IN FLOWRATE

For this category of experiment, two cases were considered, with the

final conditions being reached by different methods. The two cases were (1) $\gamma = 1.0 \rightarrow 0.5$ by (a) decreasing W' (run 45B) and (b) increasing W'' (run 47B); (2) $\gamma = 1.0 \rightarrow 2.0$ by (a) increasing W' (run 46B) and (b) decreasing W'' (run 48B). Step changes in both directions in both hot and cold flowrates were thus studied.

During these experiments, minor computer crashes occurred; the processor hung for the order of one minute during cycle 9 in runs 45B and 46B, and during cycle 14 in runs 47B and 48B. This caused the hot gas flowrates to remain at a slightly high value for a short time, resulting in the dips in hot gas inlet temperature profiles seen in graphs A.34, A.38, A.42 and A.46. The dips are small enough (in terms of both magnitude and duration) to be ignored.

These dips aside, it appears from the same graphs that t_i' was generally not constant during the experiments. If note is taken of the scales, however, then it is seen that the variations are in fact quite small. The variation in t_i' for runs 47B and 48B is only $\sim 1.5^{\circ}C$, i.e. so small as not to appear if t_i' were plotted on similar scales as the runs which involved step changes in temperature. The t_i' profiles for runs 45B and 46B show a slightly larger variation, which occurred around the time of the flowrate step change. The total gas flowrate over the heater theoretically remained constant throughout the experiment; before the step, W' (regenerator 1) was 0.6 std. m^3/min and W' (regenerator 2) was 0.3 std. m^3/min, and after the step the figures were 0.3 and 0.6

respectively. No adjustment was therefore made to the heater settings. However, due to the change in capacity rate of the gas entering each individual regenerator, the constant heater settings resulted in a change in inlet temperatures. For run 45B, t_i' dropped by $\sim 4^oC$, and for run 46B, t_i' rose by $\sim 9^oC$. Considering the magnitude of the effect of a step change in t_i' of 50^oC (see section 5.2 or 5.3), the effect of these small changes in t_i' can be expected to be small. The effect of the flowrate step changes can therefore be expected to dominate the results, and so the changes in t_i' can be ignored.

The timescale (x-axis) of runs 45B and 46B should be noted. All experiments except for these two ran for ~24 hours (~ 72 cycles in total), but an overnight malfunction in the control computer caused runs 45B and 46B to terminate after 63 cycles. The x-axis scales are therefore somewhat expanded in relation to all other runs.

The results of these experiments are summarised in table 5.2. Due to the hot gas exit temperature magnitudes for this group of experiments, the hot side responses were not greatly affected by ambient variations (with the possible exception of run 47B). It was therefore possible to apply the 0.5^oC criterion to the hot side responses, and obtain figures for 'time to equilibrium' for both hot and cold responses. The $(W''\Delta t'' - W'\Delta t')$ figures for run 45B are 0.4 (cycle 35) and 2.0 (cycle 62).

Stepchange Conditions	Run No.	Cycles to Equilibrium		Heat Losses (cycle, rate (W))	Minimum m.s.d. and corresponding f	M.s.d. with f = 0.85
		Cold Side	Hot Side			
γ = 1.0 → 0.5 by W' ↓	45B	12	7	-	1.70, 0.93	2.07
γ = 1.0 → 0.5 by W'' ↑	47B	11	6	30, 4.3	2.76, 0.83	2.78
γ = 1.0 → 2.0 by W' ↑	46B	6	15	34, 5.7 63, 31.8	0.81, 0.80	0.99
γ = 1.0 → 2.0 by W'' ↓	48B	6	15	25, 1.6 63, 26.1	1.15, 0.92	1.36

Table 5.2

It can been seen from table 5.2 and the graphs of exit temperatures (figures A.35/36, A.39/40, A.43/44, A.47/48) that, as in the theory, the response of the regenerator to a step change in flowrate depended solely upon the final conditions. The initial conditions and the method used to achieve the final conditions had no bearing on the responses. For a final condition $\gamma = 0.5$, the hot side responded faster than the cold side, and the responses were independent of whether W' or W'' was changed; in both cases the exit temperatures followed the same decreasing curves. For a final condition $\gamma = 2.0$, the cold side responded faster, and again the responses were independent of whether W' or W'' was changed.

The m.s.d.s for all four experiments in this category are seen to be extremely small for $f = 0.85$. The graphs show the agreement to be excellent for the hot side; even run 47B, which at first sight appears bad, is good when the y-axis scale is taken into account. For the cold side, the agreement is also good, with the possible exception of the final part of run 45B. However, this discrepancy is only of the order of $2.5^{\circ}C$ and therefore deemed to be acceptable. The fact that the size of the discrepancy changes after the step change implies that the value of f should change; this is attributed to the $W\Delta t$ imbalance, which is seen to change magnitude after the step change.

The conclusion of this part of the work is that a good experiment/simulation correlation is obtained for flowrate step changes using f = 0.85.

5.5 SIMULTANEOUS STEP CHANGES

For this category of experiment, the criterion used to determine equilibrium" is not applicable; the combined effect of two step changes may cause the response due to one to be 'pulled back' by the other. This means that successive cycles may be within 0.5°C of each other at the minimum or maximum of a curve, as the second response takes over. This is obviously before equilibrium is attained, and figure A.64 illustrates this well. The aim of these experiments was

a) to verify that the f = 0.85 correlation is applicable to complex multiple-change situations, and
b) to qualitatively verify Burns and Willmott's results (1978) for a practical regenerator.

Temperature step changes were as for runs 37B-44B, and the results are shown in table 5.3. For run 51B, $(W''\Delta t'' - W'\Delta t') = 1.8$ at cycle 34 and 1.6 at cycle 74; again this is a sufficiently small discrepancy to allow heat loss rates to be taken as zero.

Burns and Willmott's curves for their cases I-III are shown in figures 5.1-5.3. By comparing these curves with figures A.59/60 (case I), A.63/64 (case II) and A.51/52 (case III) it can be seen

Stepchange conditions	Run No.	Burns Case	Heat Losses (cycle, rate (W)	Minimum m.s.d. and corresponding f	M.s.d. with f = 0.85
$\gamma = 0.5 \rightarrow 1.0$	51B	I	-	4.88, 1.09	10.80
$\gamma = 3.0 \rightarrow 2.0$	52B	II	34, 37.4 74, 50.6	3.18, 0.60	5.02
$\gamma = 2.0 \rightarrow 1.0$	49B	III	37, 41.3 55, 0.6	4.56, 0.83	4.60
$\gamma = 1.0 \rightarrow 2.0$	50B	-	37, 2.9 73, 49.9	2.75, 0.99	4.16

Table 5.3

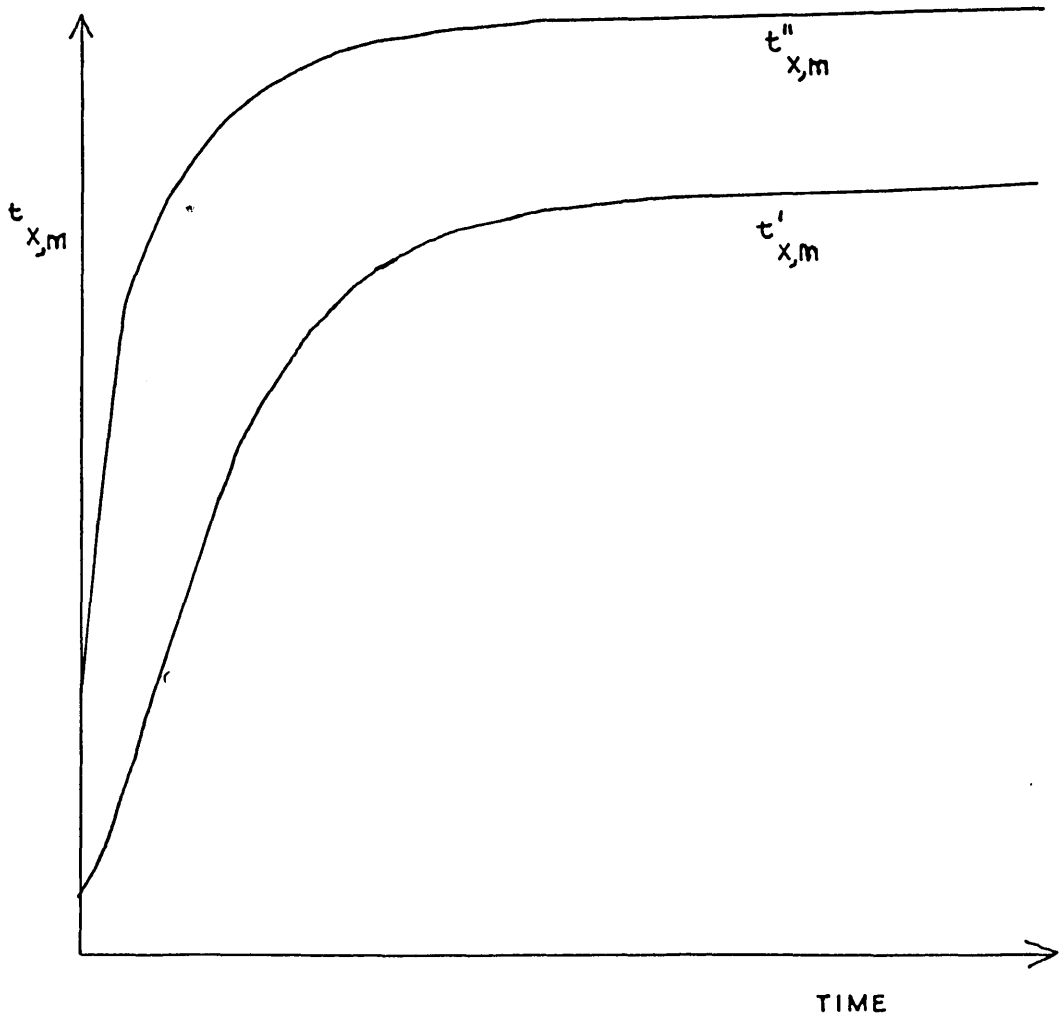

FIGURE 5.1

BURNS CASE I

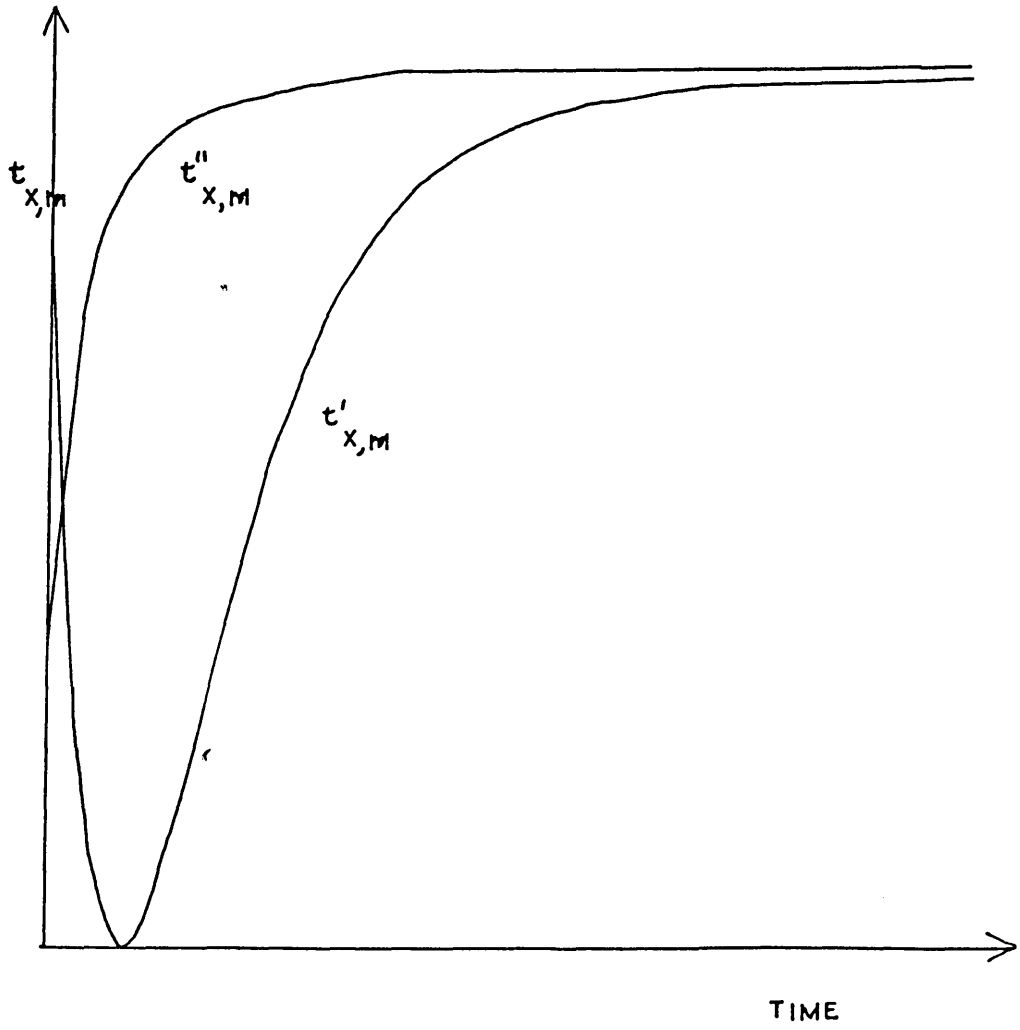

FIGURE 5.2

BURNS CASE II

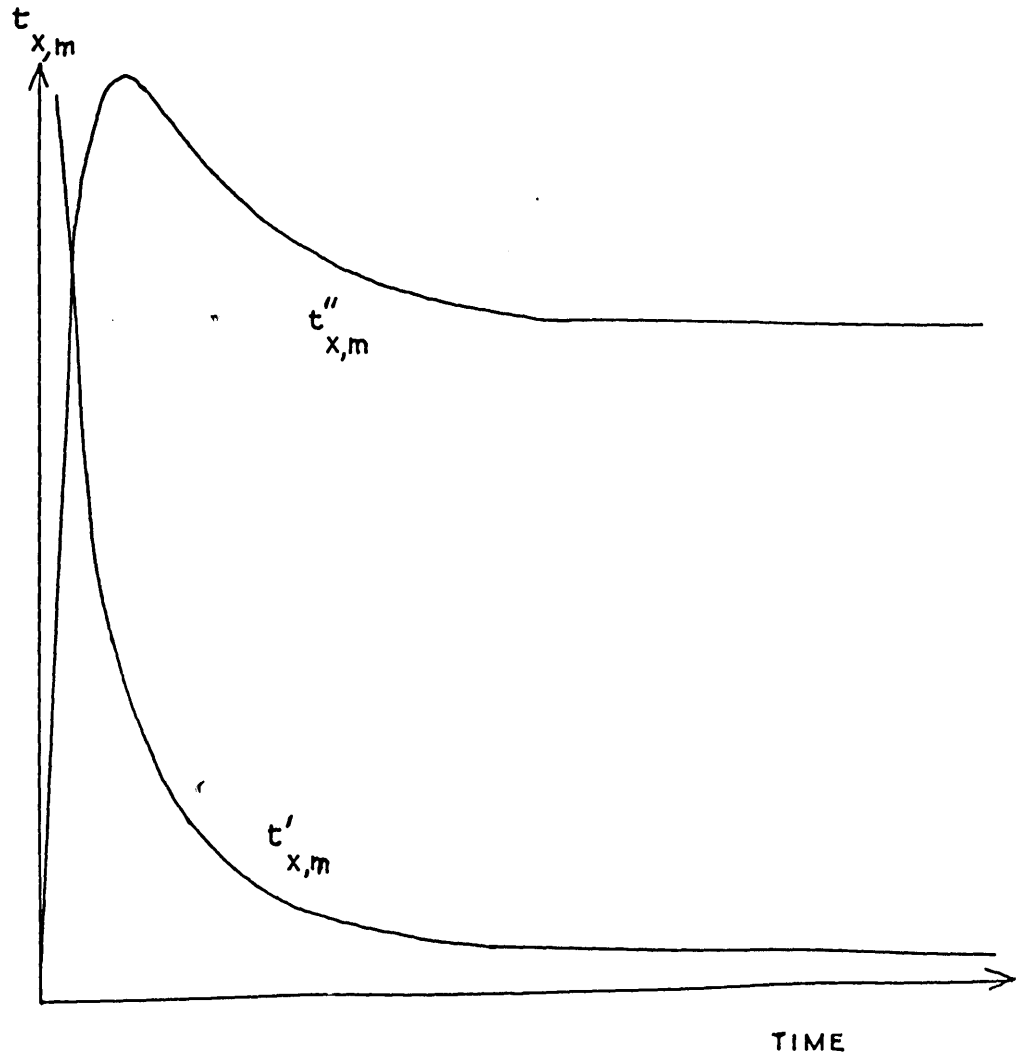

FIGURE 5.3

BURNS CASE III

that the experimental results verified (at least qualitatively) the theoretical results. The initial overshoot in figure 5.3 was shown by Burns and Willmott to decrease as the magnitude of the stepchange in decreased, giving graphs as in figure A.51. Run 50B did not correspond to a Burns and Willmott case, but is included nevertheless, to show that the agreement is good for another case. At the same time, the inclusion of this experiment completes the permutations of increases and decreases in hot and cold gas flowrates, in conjunction with an increase in inlet temperature.

The fit of simulated to experimental exit temperatures for all runs is seen to be very good for both hot and cold sides, using f = 0.85. The m.s.d. for run 51B (10.8) is the largest for any experiment presented in this thesis, but again only represents $\sim 3.3^{\circ}C$ discrepancy in $100^{\circ}C$. The hot side curve for run 52B (case II) is especially interesting, since one response can be seen 'pulling back' the other; for this case also, f = 0.85 gives a good correlation.

It is therefore concluded that the factor 0.85, which results in good correlation for step changes in t_i' and step changes in flowrate, is equally applicable to simultaneous step changes in both quantities. Burns and Willmott's theoretical results agree with the results from the regenerator system for three specific cases of simultaneous step change.

5.6 OTHER RESULTS

The effect on the simulations of using other heat transfer coefficient correlations (discussed in Chapter 2) is shown in figures 5.4 and 5.5. Run 37B (step change in t_i', $\gamma = 1$) was used, and the exit temperatures from experiment and four simulations (all with f = 1.0) are shown. It can be seen that the Denton and Heggs correlations give the best simulations, although the inclusion of an f-factor < 1 is required for a better agreement with experiment. For (Denton x 0.85) to be equal to (Heggs x f), f would be equal to ~0.92.

A similar approach can be adopted if the results of this thesis are to be applied to other regenerator systems. It is merely necessary to find, by the method described in Appendix C, the value of the f-factor applicable to the regenerator system to be studied. This value is then incorporated into the model used in this thesis, in place of the value 0.85.

Figure 5.6 shows the cold side experimental results for run 37, with the temperatures recorded at the bed top (37A), cone top (37B) and dome pipe (37C) shown on the same graph. This illustrates the effects discussed in section 4.1, explaining why the cone top thermocouple was used (heat loss/mixed flow compromise). It is seen that the closer to the bed the temperatures were measured, the higher the values recorded. No equivalent hot side graph is shown,

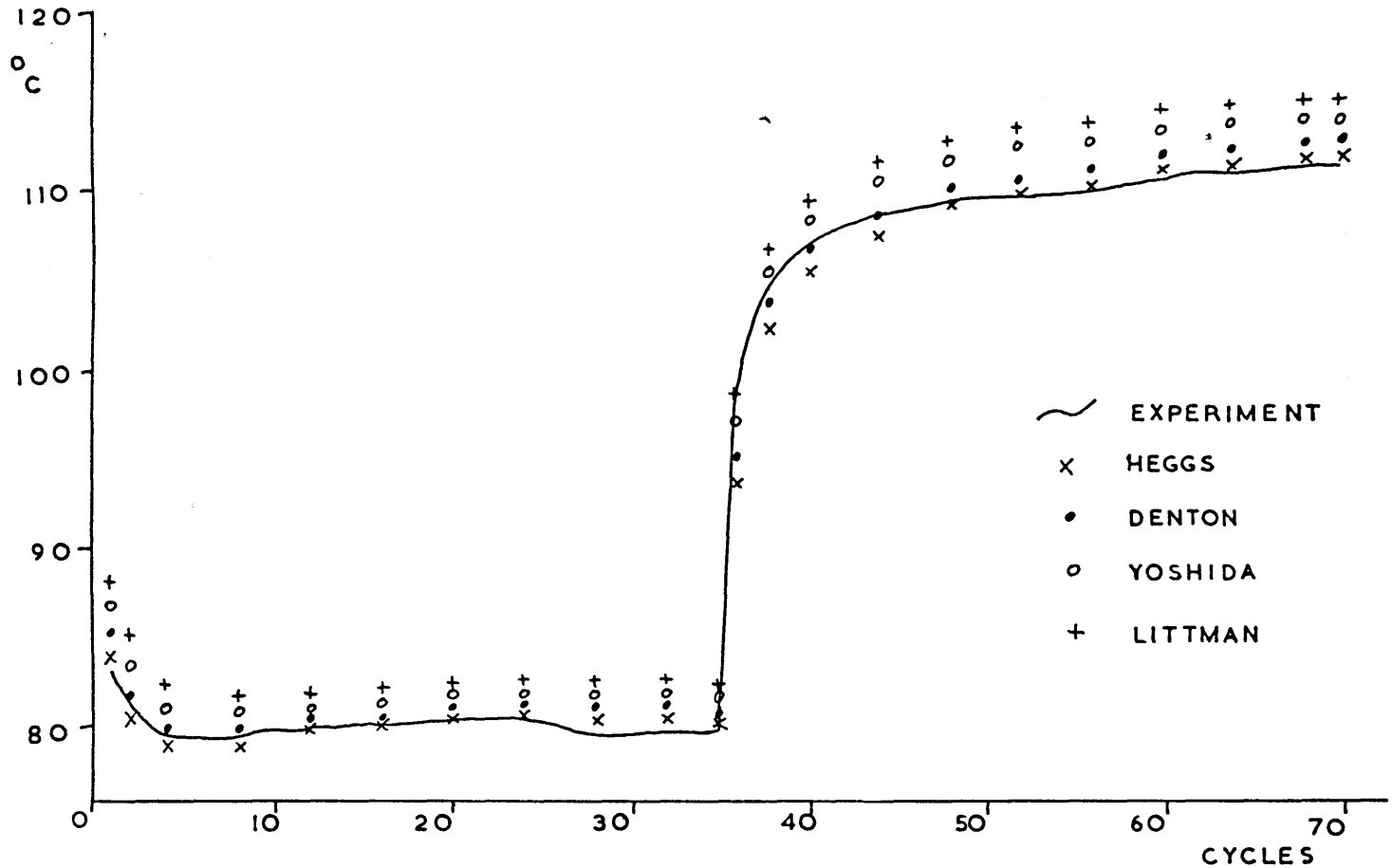

FIGURE 5.4

RUN 37B COLD GAS EXIT TEMPERATURE, SIMULATIONS WITH $f = 1.0$

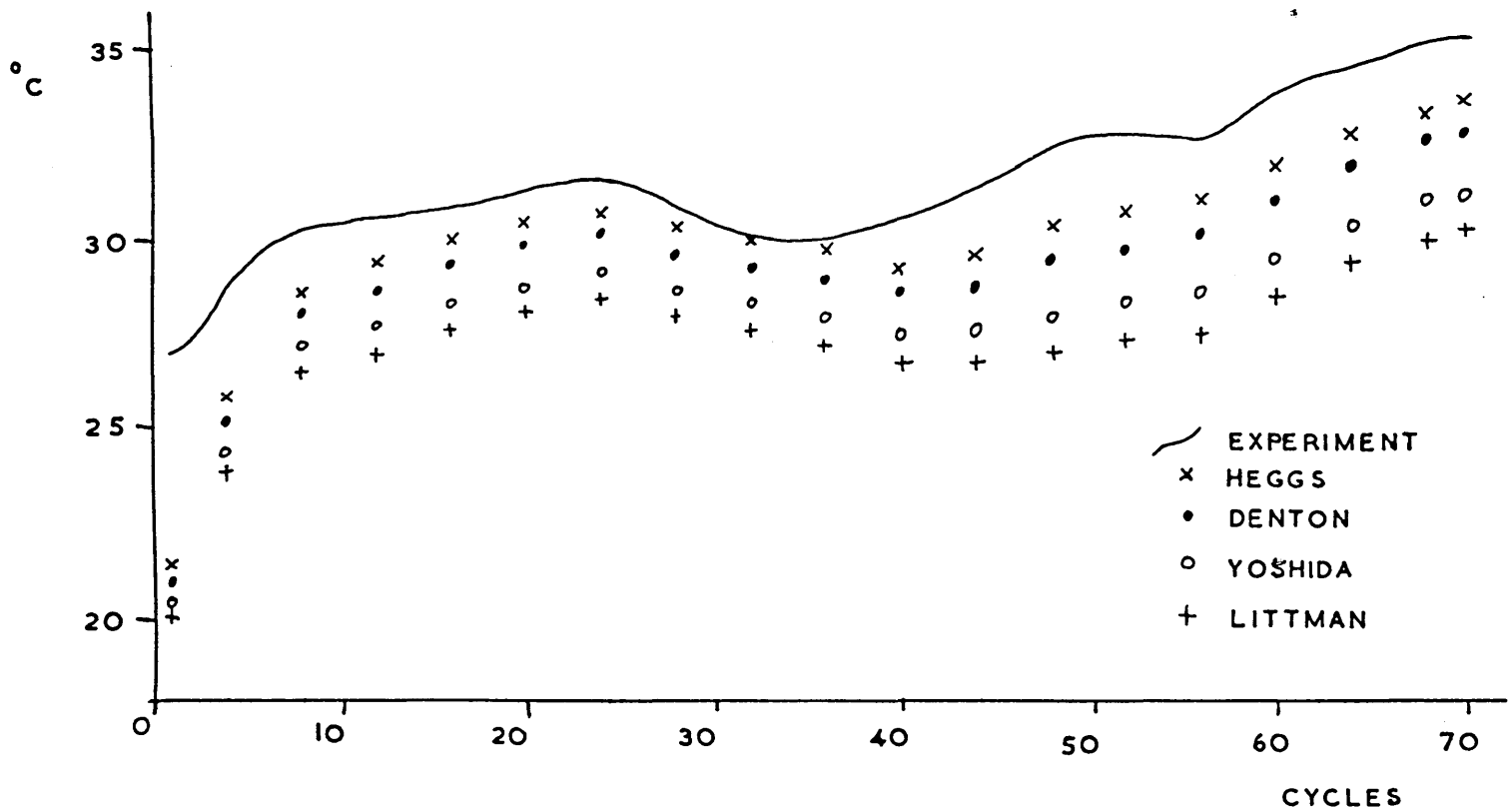

FIGURE 5.5

RUN 37B HOT GAS EXIT TEMPERATURE, SIMULATIONS WITH $f = 1.0$

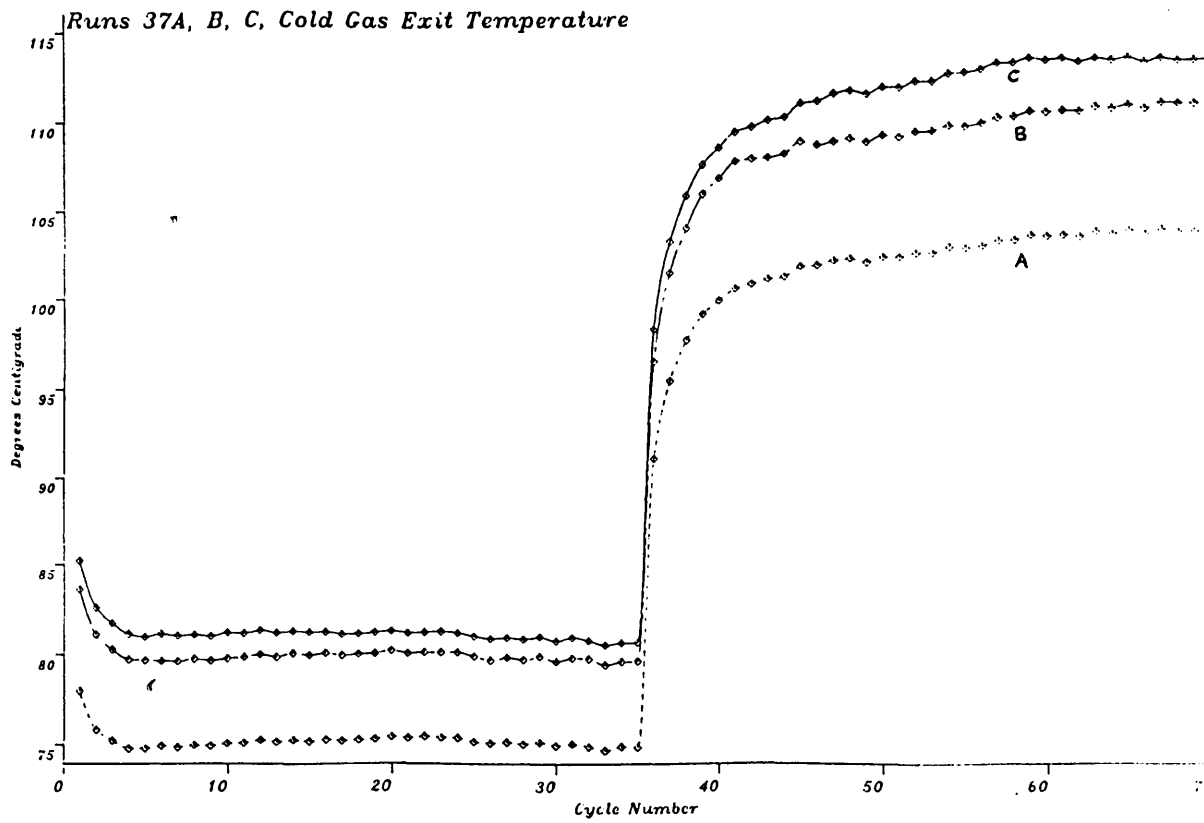

FIGURE 5.6

THERMOCOUPLE POSITIONING

since the values of $t'_{x,m}$ recorded at the orifice plate meter were rendered meaningless by heat losses in the intervening pipework. Therefore only the stack pipe thermocouples were used, and the profile recorded is shown in figure A.4.

In order to reduce the actual timescale of an experiment further, it is necessary to reduce the area to mass ratio of the packing. The reduced period Π is given by

$$\Pi = \frac{hAP}{MC} \qquad (1.36)$$

so, for given values of h, C and P, increasing the area to mass ratio A/M increases the value of Π. Green (1967) found that the total time to equilibrium, Θ, is given by

$$\Theta = 2\Pi n = k, \text{constant} \qquad (2.43)$$

for a given Λ.

Increasing Π, therefore, results in a decrease in n, i.e. fewer cycles are required to attain equilibrium. Since P was unchanged when A/M was increased, the actual time to equilibrium is reduced.

This timescale compression is most easily achieved on the rig by using packing of a lower density but still of 17mm diameter. Thus M is reduced and hence A/M is increased, <u>without</u> changing A, which would give an unwanted change in reduced length. Applying this dimensionless analysis to run 37B, figure 5.7 shows $t''_{x,m}$ against real time with the rig (a) as for this thesis, and (b) with a (realistic) 1/3 reduction in solid density. It is seen that there

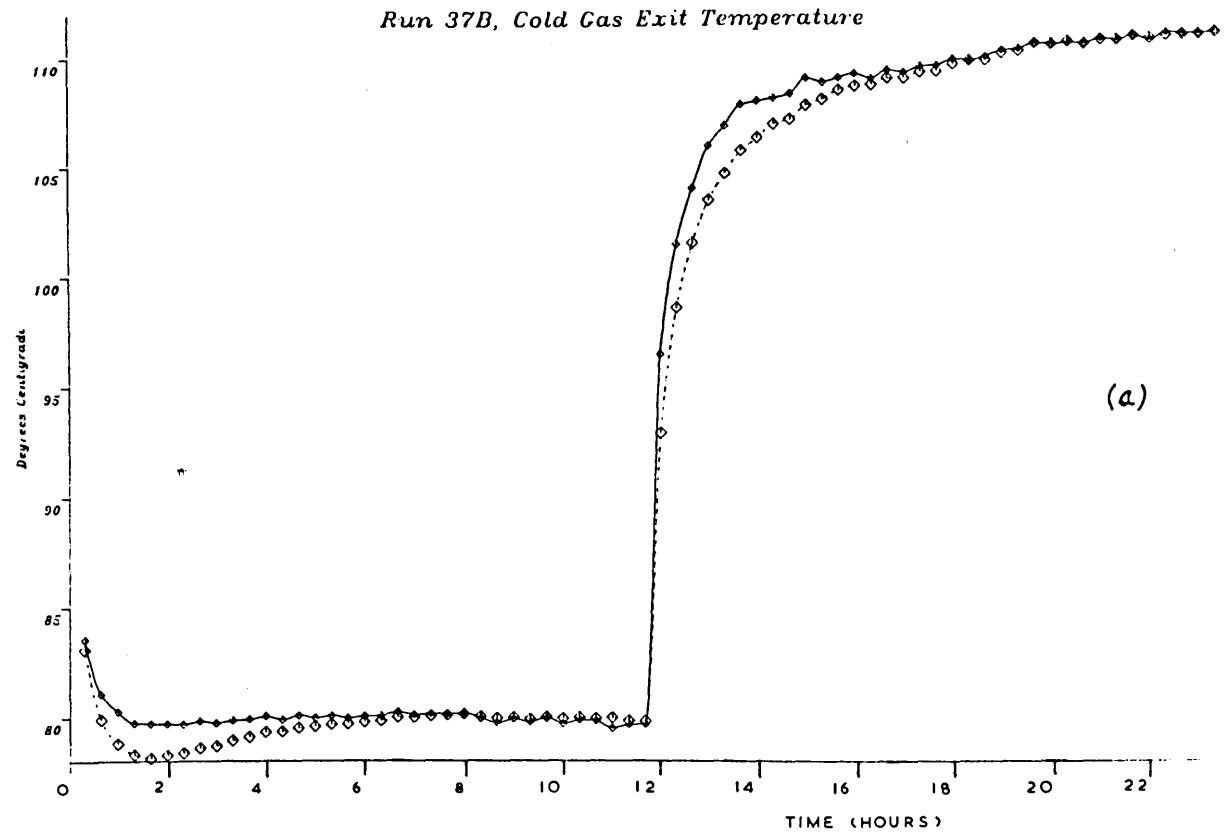

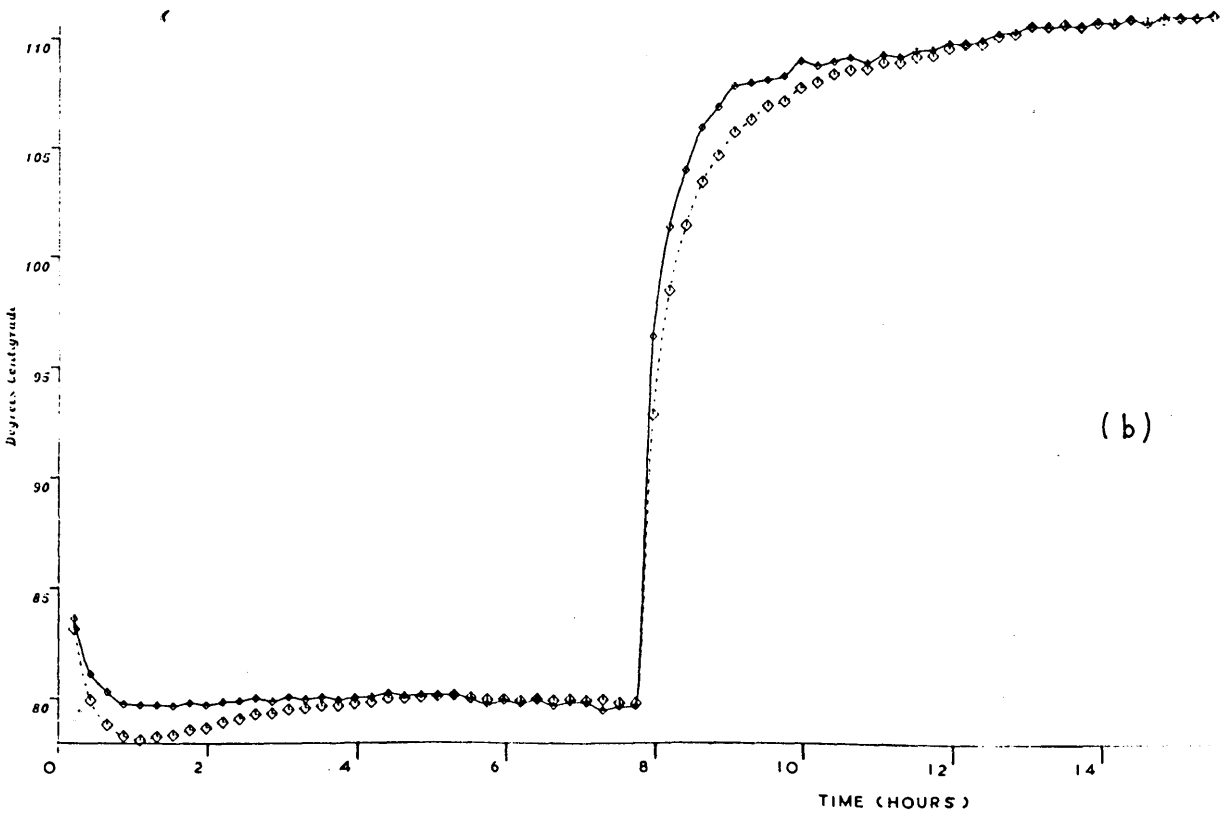

FIGURE 5.7
EXPERIMENT TIMESCALE

is a 1/3 reduction in the total time taken for the experiment. This could be reduced still further by using still lower density packings or even using hollow spheres, which also increases A/M.

CHAPTER 6

CONCLUSIONS

It is necessary, at this concluding juncture, to re-state the motivations behind this research. It has been seen that the great majority of previous work on thermal regenerators has laid emphasis on theoretical work, and cyclic equilibrium behaviour in particular. As far as experimental studies of transient behaviour are concerned, little previous work has been published; the work of Chao (1955) at the Ford Motor Co. was published in the scientific literature, and some work done at the Universities of Bradford and Leeds is available only in the form of Ph.D. theses.

Chao's work was mainly concerned with the design and description of the apparatus, and the transient response of the regenerator was not investigated in any detail. The work was restricted to startup from cold, and changes in hot gas inlet temperature. Graphs are presented for the cold gas response under these conditions, and the experimental/theoretical agreement appears, from the same graphs, to be good. No quantification of the level of agreement is, however, presented, and no analysis of the (few) experimental results is undertaken. Ajitsaria (1973) and Hollins (1981) studied only changes in gas flowrate or period duration, and moreover the results of the latter work are of doubtful validity, as discussed in Chapter 2.

The aims of this research have been, therefore, twofold. It was intended to redress the balance of previous work by demonstrating that industrial thermal regenerators can be modelled using a laboratory-scale system, and also to place previous theoretical work on a more secure basis, namely the establishment of the principle that the Willmott 2D model (1964) can be used to predict the performance of at least an experimental system for transient conditions. Indeed, this thesis has increased knowledge concerning regenerators by carrying out a (previously lacking) extensive experimental and linked theoretical investigation into the unsteady-state performance of practical regenerators for many cases.

Much work was undertaken in commissioning the experimental apparatus and improving the measurement and instrumentation techniques. Once rig development had reached a stage where accurate experiments could be performed, the response of the system to step changes in temperature and flowrate was studied. Single step increases in hot gas inlet temperature were carried out for various flowrates and for various degrees of imbalance, and single step changes in flowrate were carried out for increases and decreases in both hot and cold flowrates. Finally, simultaneous step changes in both hot gas inlet temperature and flowrate were studied.

The results of these experiments were used to develop an accurate theoretical model of the regenerators, and extensive simulations using Willmott's 2D method yielded a good correlation. Gas exit

temperatures from simulations were found to agree extremely closely with those from all categories of experiment if the Denton heat transfer coefficient correlation was used with a multiplication factor of 0.85. It should be noted that the model used by this author was also used in previous work, but operated under much easier conditions than those imposed upon it when simulating the experiments in this thesis. After much development by this author, however, the model was found to be entirely adequate.

A theoretical model of the experimental system now exists, therefore, which can be used to predict the rig's behaviour under many operating conditions. The only conditions not examined were step changes in period duration, although theory indicates that this case is approximately equivalent to flowrate step changes. Experimental and simulated cold gas exit temperatures agreed to within 1.9°C, this figure being an average over all experiments. The number of cycles taken to re-establish equilibrium after a step change was found to be the same whether experiment or simulation was used. It was also noted that stringent criteria for detecting equilibrium, as are commonly used in purely theoretical studies, are not applicable to experimental studies of this nature, mainly due to the severe effect of non-constant operating conditions which inevitably prevail. Similarly it was noted that, in experimental work, the hot side response cannot easily be normalised in many cases, and no quantification in this manner is possible. Little information can therefore be gained by studying hot side responses,

and work has to be concentrated mainly on the cold side responses. This is apparently consistent with the findings of previous experimental work at the Ford Motor Co.

The experimental results are summarised as follows. For step changes in hot gas inlet temperature under symmetric conditions ($\gamma = 1$), it was found that the responses were independent of the gas flowrates. Under unbalanced conditions ($\gamma \neq 1$), where the initial and final imbalance was the same, it was seen that the degree of imbalance has very little effect on the responses, for a fairly wide range of γ. This apparently contradicts previous theoretical work, but it has been argued in Chapter 5 that the effects observed in such theoretical studies would not be expected to be manifest in the experiments. The response of the system to changes in flowrate was seen to depend only upon the final degree of imbalance, and not upon the initial conditions or method used to attain the final state. This is consistent with previous theoretical work. The response of the experimental regenerator to simultaneous step changes has also been seen to be in good agreement with previous theoretical work, implying that a superposition principle, as discussed by Burns and Willmott (1978), is applicable to the experimental responses.

It was originally intended that the experimental results from step change experiments be used to 'tailor' various industrial control algorithms, which would then be implemented, tested and developed on the rig. The constraints of time did not, unfortunately, allow

this, but the groundwork has been done for future work. Considerable progress has been made, and the practical problems inherent in any experimental work have been overcome. In particular, an extensive period of the research was spent debugging and developing the experimental apparatus, in the areas of both hardware and software. The development of the mathematical model occupied a similar period of the research. When both the rig and the simulation program were in a satisfactory state to produce results, the physical timescale of the experiments and the associated analysis meant, however, that a larger number of experiments could not be conducted. The means to speed up future experimental work have been discussed in Chapter 5.

The experiments which were carried out and the analysis presented in this thesis provide a satisfactory and thorough study of the unsteady-state performance of an experimental thermal regenerator system. The means to extend the results obtained to other practical systems in industry have been outlined.

CHAPTER 7

FURTHER WORK

There are four directions which future work may take: improvements to the experimental apparatus and technique; improvements to the computer model; extension of the experiments carried out for this thesis; and investigation of industrial control strategies. The last area is potentially the most fruitful and should be regarded as the most important, but it is recommended that the other areas be researched first in order to improve the results of the last.

Firstly, it is recommended that the rig flowrates be re-calibrated, as described in Chapter 3, in order to improve the accuracy of flow control. The flow constants c, m, g, and O_i should be determined for each flowpath. This may also necessitate re-calibration of the heater settings if any flowrates are found to be seriously in error.

Secondly, also in the area of rig improvements, an attempt should be made to improve the flow distribution in the regenerators by reducing or removing the excess wall voidage. This could be done by lining the insides of the containers with a material such as kaowool (expensive) or household glass fibre loft insulation (cheap). Loft insulation should be capable of withstanding at least 200^{o}C and so should be suitable. Flow baffles in the form of annuli around the walls would also improve flow distribution by forcing the flow to

break off from the walls at intervals. Further improvements may also result from increasing the length to diameter ratio of the regenerators.

The alternative to removing the excess wall voidage is to incorporate it into the mathematical model, and this forms the main area of model development. Parabolic (and other) flow distributions across a regenerator can be simulated by several smaller regenerators each with uniform (but different) flowrate distributions. If these smaller regenerators are then run in parallel, the simulated results should be sufficiently close to experimental results as to reduce or even obviate the need for an f-factor. Work is already in progress in this area (Penney, 1984). The mathematical model may be further improved by incorporating the heat capacity and associated regenerative effect of the containers and pipework; this should also reduce the need for the f-factor. It can be argued, however, that the existing model, incorporating the constant f-factor 0.85, is entirely adequate. The suggested changes to the mathematical model would merely result in f becoming closer to 1.0, with no actual improvement in model accuracy over the f = 0.85 model.

If purely theoretical predictions are to be made using the computer model, it will be necessary to predict the cold gas inlet temperature. This may be done by tabulating the typical ambient temperature profile, and possibly modifying it according to observed

deviations if an experiment is proceeding in parallel. This profile is then used as the cold gas inlet temperature profile for the model.

Further experimental improvements may be made in the following ways:

i) overcome the constraint that the total gas flow over the heaters must be constant. Another heater may be installed (possibly uneconomic) or the existing heaters may be brought under the control of the computer

ii) reduce the timescale of the experiments, as discussed in Chapter 5, by increasing the area to mass ratio of the packing

iii) raise the cold gas inlet temperature slightly above ambient (say $30^{o}C$) and install a dedicated controller to hold it constant in the face of diurnal variations in ambient temperature

It is then recommended that the experiments discussed in Chapter 5 be extended as follows:

i) study step increases in t_i' ($\gamma = 1$) for a wider range of flowrates, specifically at very high and very low flowrates

ii) study step decreases in t_i' under various conditions

iii) investigate step changes in flowrate further, specifically with starting condition $\gamma \neq 1$, with final condition $\gamma = 1$ or $\gamma \neq 1$

iv) study further examples of simultaneous step changes. It could be argued, however, that the four examples already examined were chosen randomly and so may be assumed to be representative.

Similar experimental work should also be conducted with different packings, and, in addition, on regenerator systems other than the rig used in this thesis. In this way, the general applicability of the work done by this author will be determined. This may proceed in parallel with an investigation into whether the various problems which were encountered (and overcome) in this work are particular to this apparatus or are of general concern in experimental regenerator work.

Following the above work, an extensive knowledge of the transient behaviour of physical regenerator systems will exist, and this will facilitate the investigation of industrial control strategies. It is suggested that Burns' (1978) strategy be implemented on the rig, and studied as the first step toward implementing a more complete strategy such as that used by Hoogovens (Beets and Elshout, 1976).

Further work could also be done developing the staggered parallel control strategy originally developed on the rig by Smith (1983).

The advantages of physical and mathematical modelling in general are obvious; timescale compression is achieved, and, in regenerator applications, the severe problems associated with temperature and flowrate measurement in industrial plant are not encountered. As a result of establishing the value 0.85 for the f-factor over a wide range of experiments, the way is now clear for investigations to be made with the emphasis on computer simulations. The advantages of simulations over experimental studies are many, both financial and in terms of time. A large number of simulations can be run in a short time, even for extremely complex control strategies. A few key cases would also need to be investigated on physical models, to confirm the accuracy of the simulations and to ascertain the ease of practical implementation of the strategies under investigation. It should be noted, however, that much useful experience has been gained from the rig which would not have been forthcoming if simulations had been used alone. It is therefore recommended that physical and mathematical modelling proceed in parallel rather than relying on simulations alone. In this way, two independent models of industrial regenerators can be used, as opposed to merely a 'mathematical model of a physical model of a real system', which obviously incorporates a degree of redundancy.

It is hoped that the experimental and theoretical study of control strategies, in conjunction with studies of fuel enrichment strategies, will lead to an improvement in the efficiency of operation of regenerator systems.

APPENDIX A

GRAPHS OF RESULTS

Four graphs of temperature plotted against cycle number for each experiment are reproduced here. The graphs are of t''_i, t'_i, $t''_{x,m}$ and $t'_{x,m}$, in that order. The graphs present the experimental results in the chronological order in which they were conducted, i.e. from run 37B through to run 52B.

A key which applies to all graphs is reproduced first.

Key to Graphs

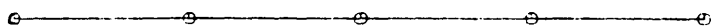

Hot gas inlet temperature

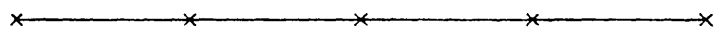

Cold gas inlet temperature

Hot gas exit temperature (experiment)

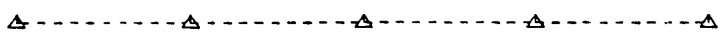

Hot gas exit temperature (simulation)

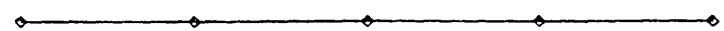

Cold gas exit temperature (experiment)

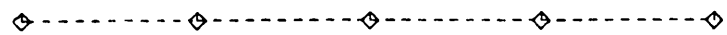

Cold gas exit temperature (simulation)

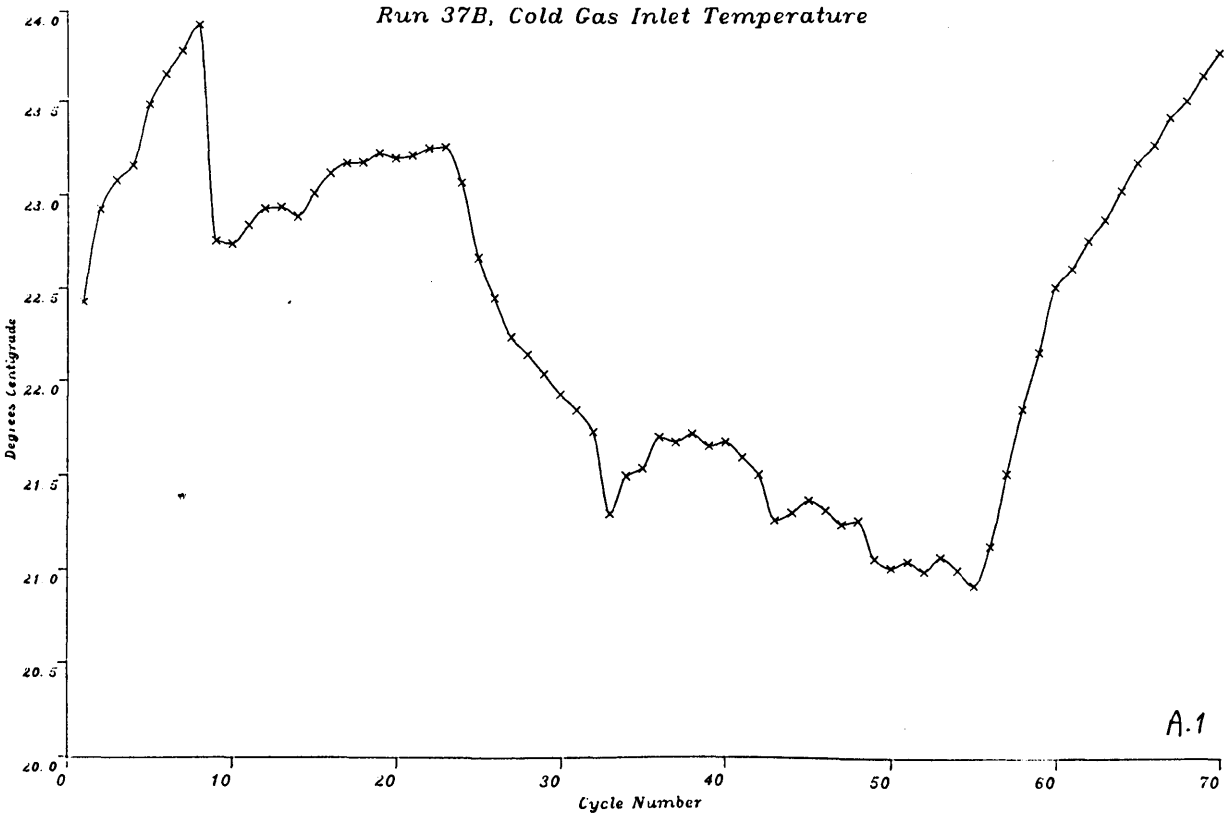
Run 37B, Cold Gas Inlet Temperature
Degrees Centigrade
24.0
23.5
23.0
22.5
22.0
21.5
21.0
20.5
20.0
0
10
20
30
40
50
60
70
Cycle Number
A.1

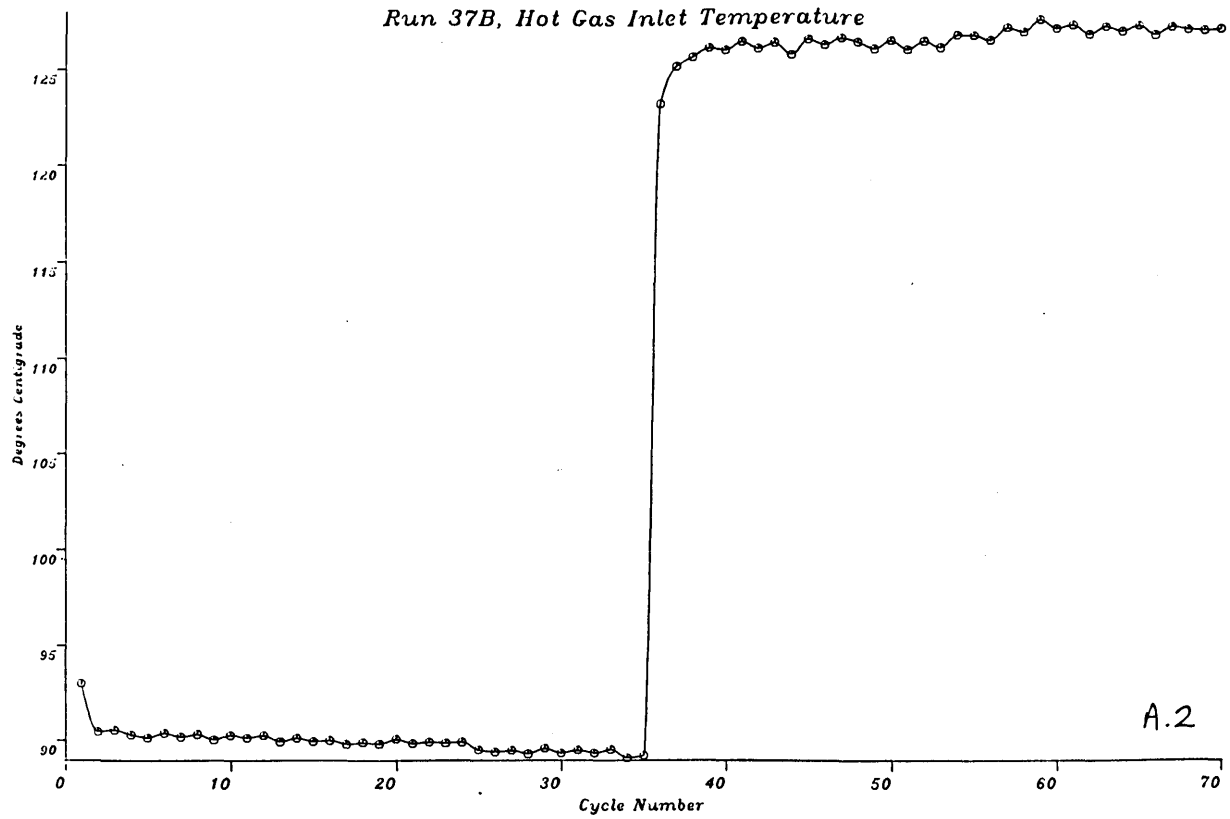
Run 37B, Hot Gas Inlet Temperature
Degrees Centigrade
125
120
115
110
105
100
95
90
0
10
20
30
40
50
60
70
Cycle Number
A.2

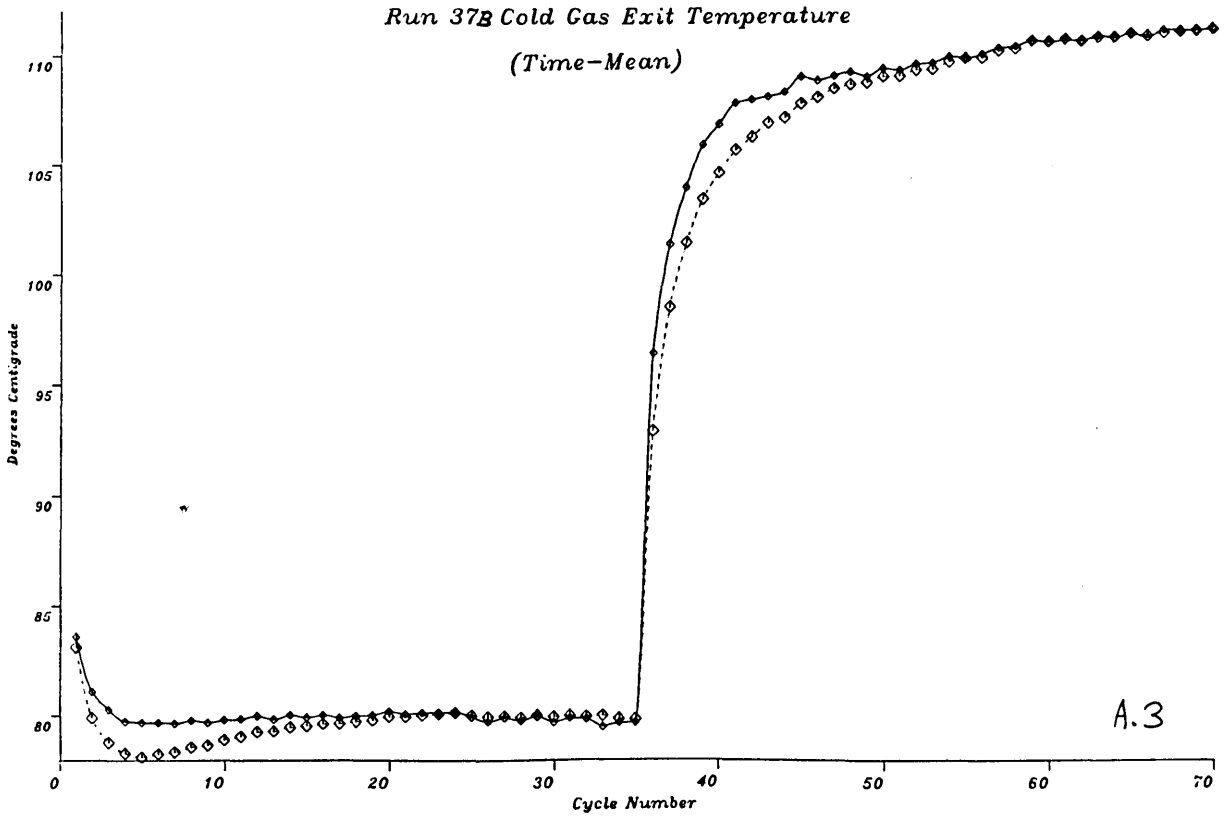
Run 37B Cold Gas Exit Temperature
(Time-Mean)
Degrees Centigrade
110
105
100
95
90
85
80
0
10
20
30
40
50
60
70
Cycle Number
A.3

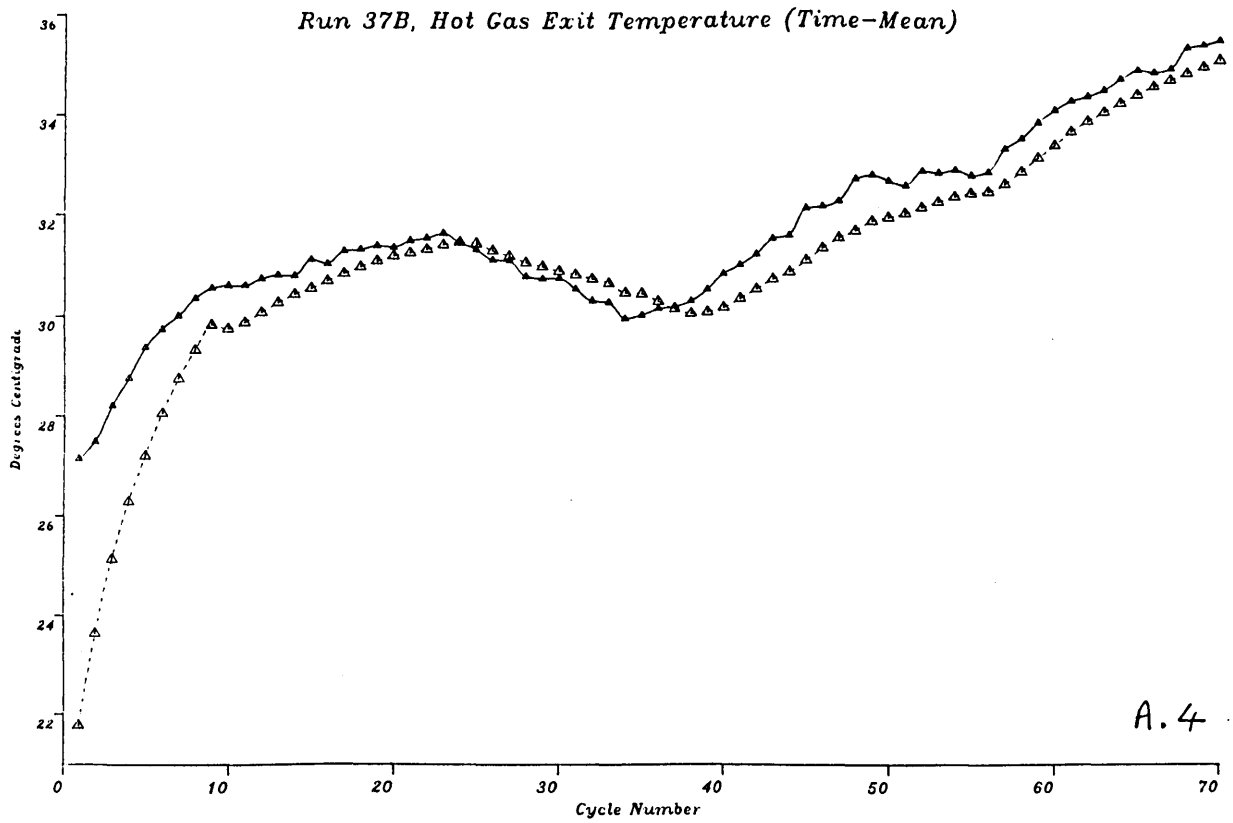
Run 37B, Hot Gas Exit Temperature (Time-Mean)
Degrees Centigrade
36
34
32
30
28
26
24
22
0
10
20
30
40
50
60
70
Cycle Number
A.4

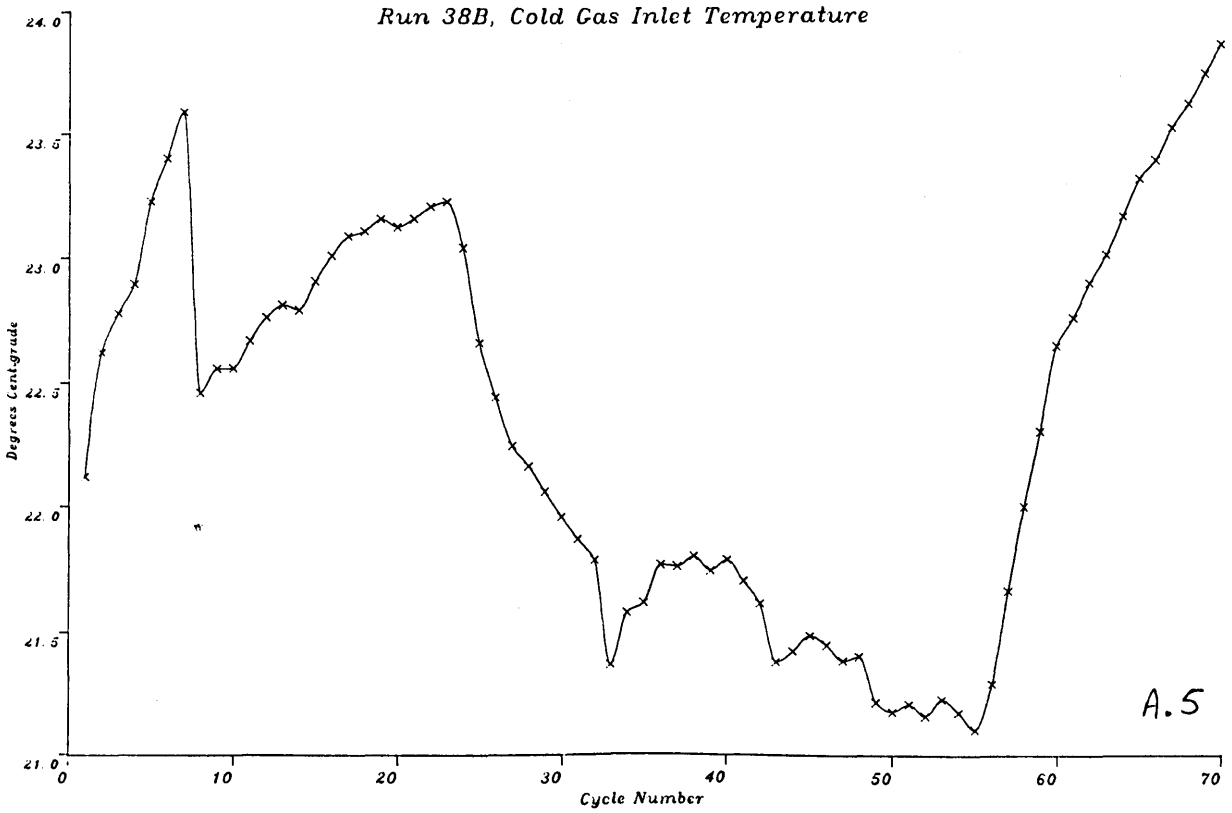
Run 38B, Cold Gas Inlet Temperature
Degrees Centigrade
24.0
23.5
23.0
22.5
22.0
21.5
21.0
0
10
20
30
40
50
60
70
Cycle Number
A.5

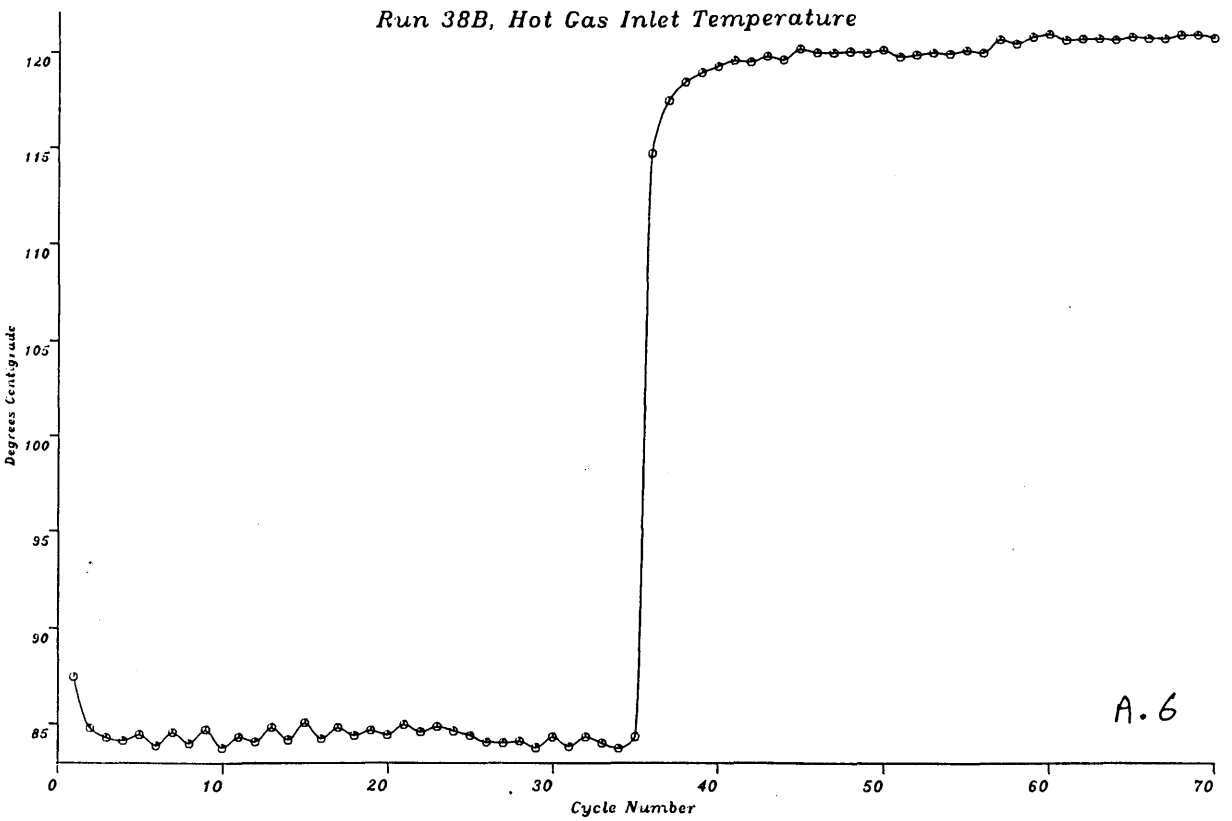
Run 38B, Hot Gas Inlet Temperature
Degrees Centigrade
120
115
110
105
100
95
90
85
0
10
20
30
40
50
60
70
Cycle Number
A.6

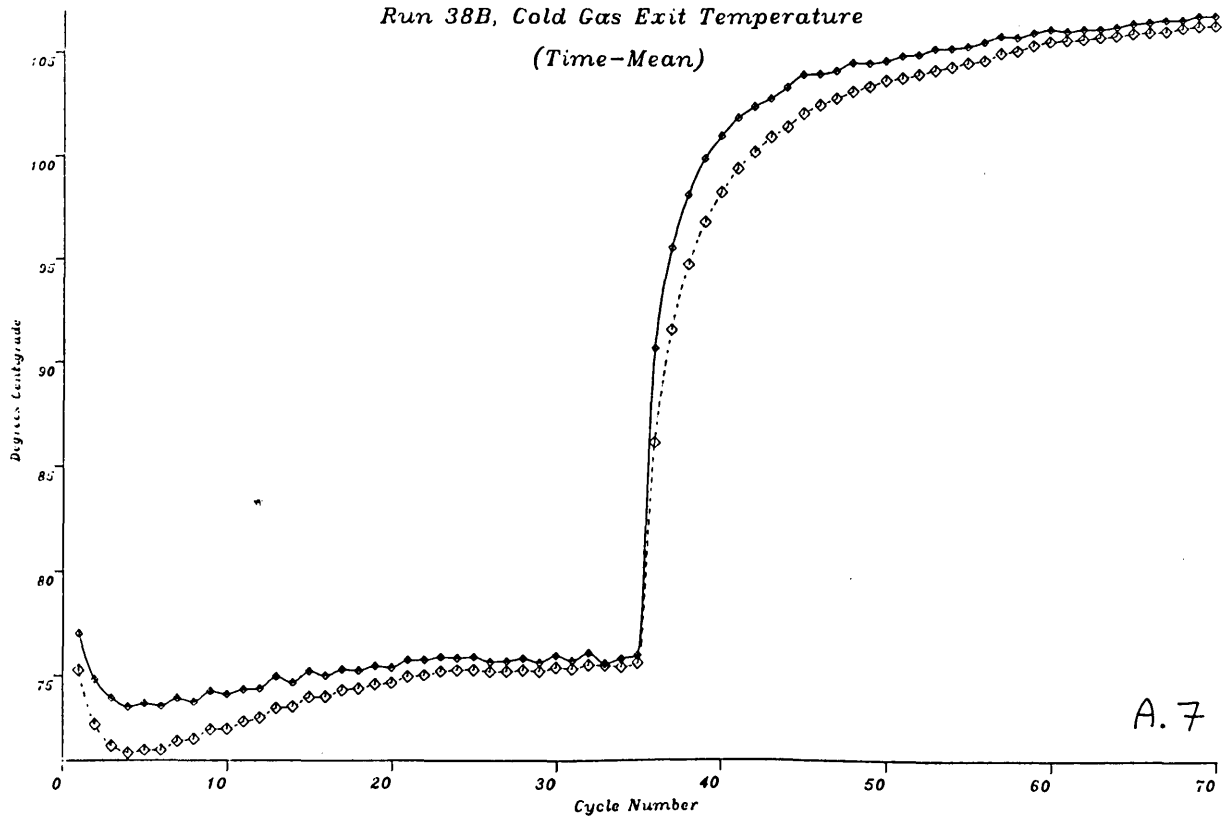
Run 38B, Cold Gas Exit Temperature
(Time-Mean)
Degrees Centigrade
100
90
80
75
0
10
20
30
40
50
60
70
Cycle Number
A. 7

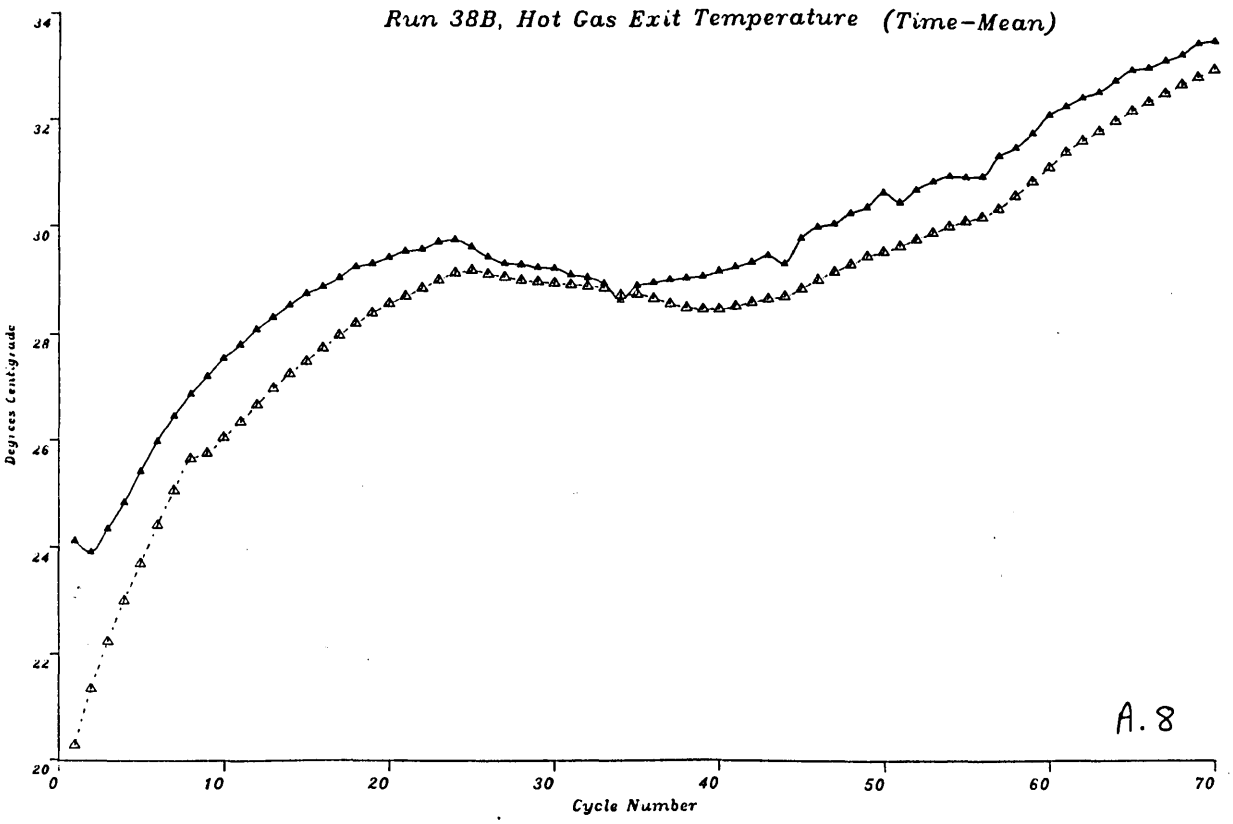
Run 38B, Hot Gas Exit Temperature (Time-Mean)
Degrees Centigrade
34
32
30
28
26
24
22
20
0
10
20
30
40
50
60
70
Cycle Number
A. 8

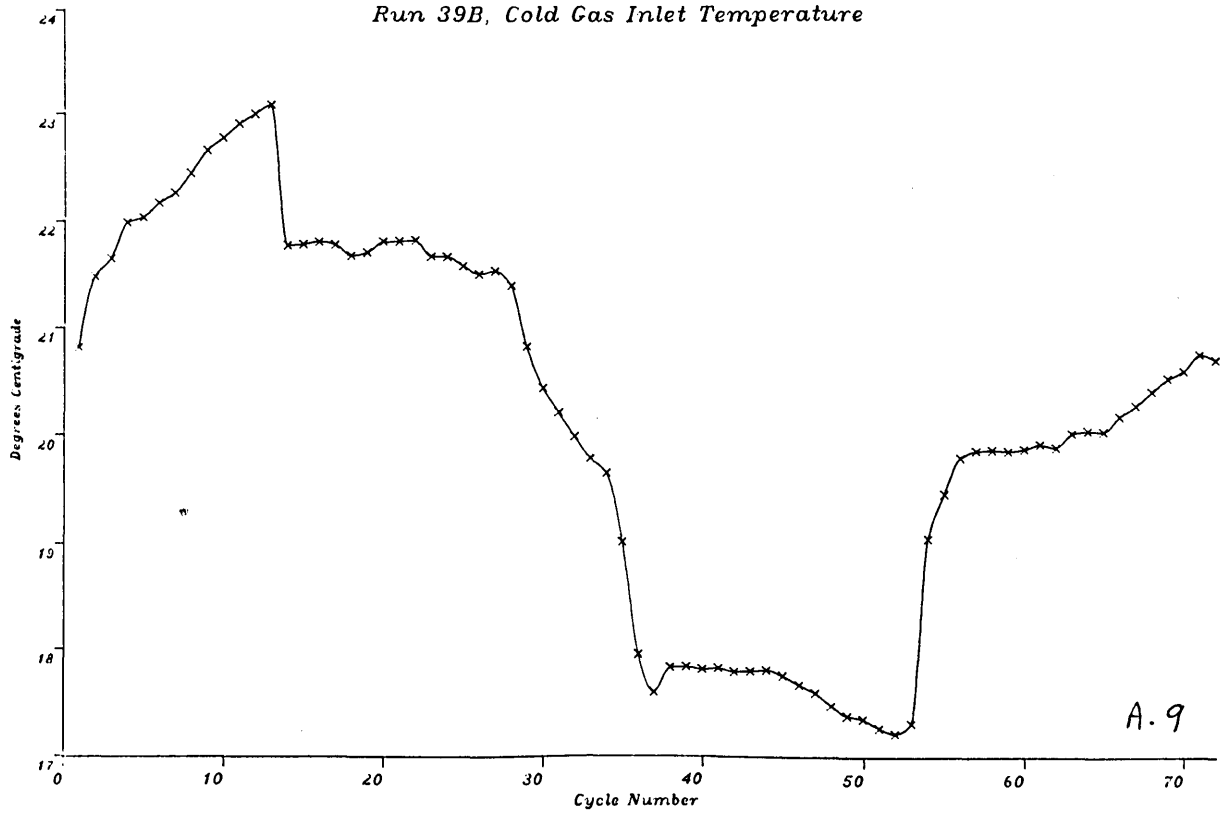
Run 39B, Cold Gas Inlet Temperature
Degrees Centigrade
24
23
22
21
20
19
18
17
0
10
20
30
40
50
60
70
Cycle Number
A.9

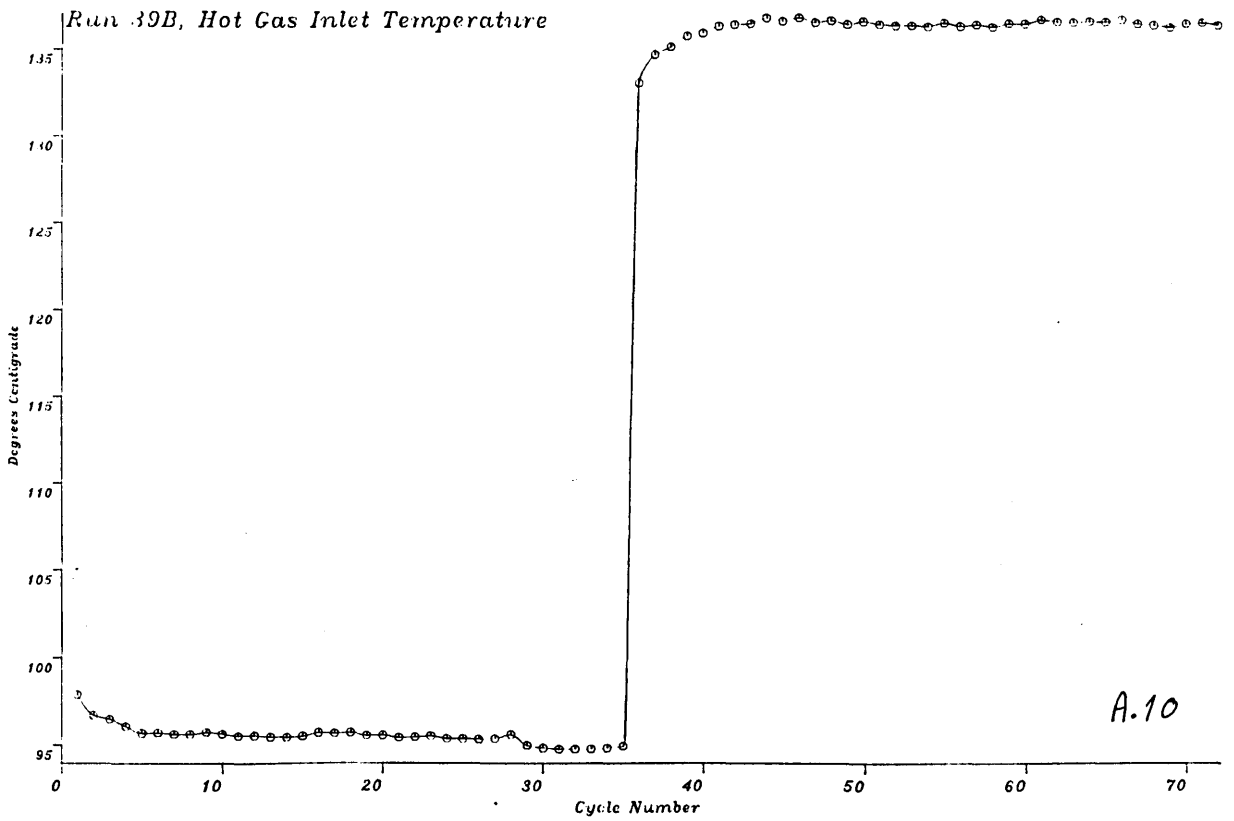
Run 39B, Hot Gas Inlet Temperature
Degrees Centigrade
135
130
125
120
115
110
105
100
95
0
10
20
30
40
50
60
70
Cycle Number
A.10

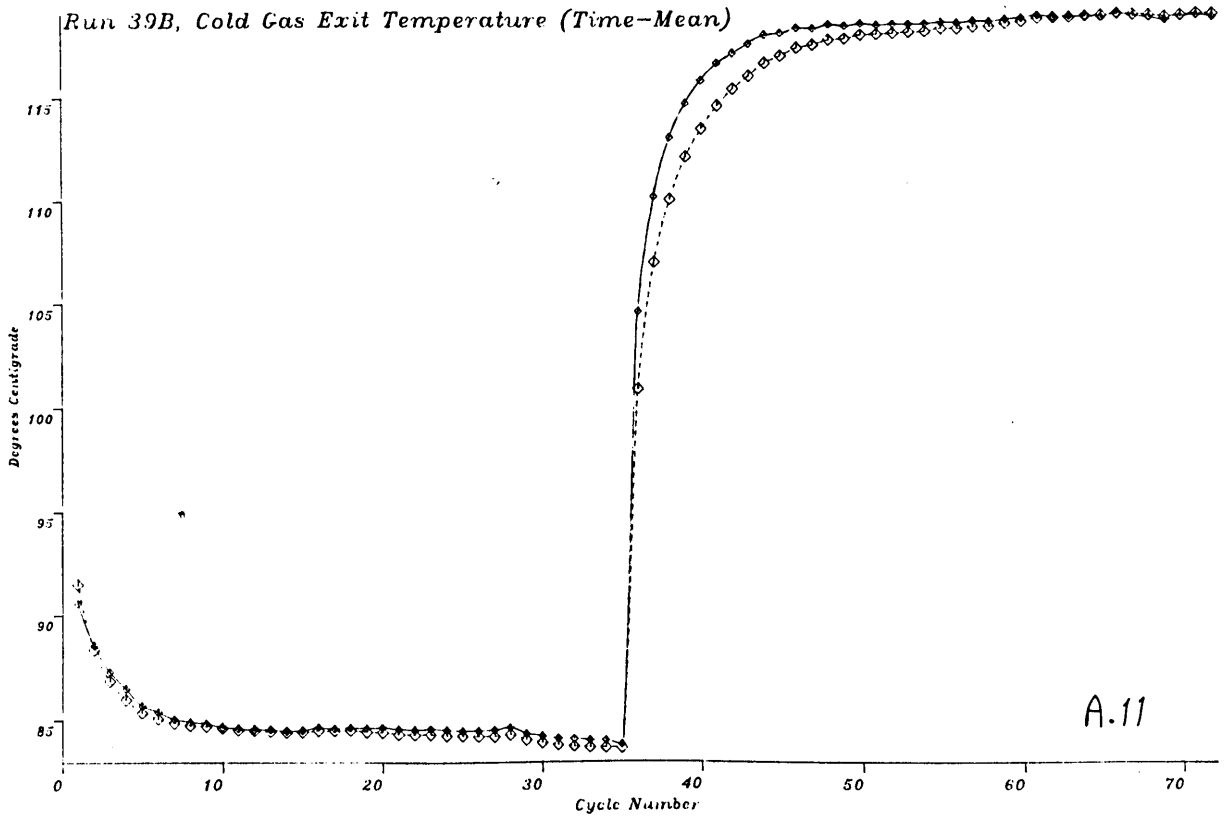
Run 39B, Cold Gas Exit Temperature (Time-Mean)
Degrees Centigrade
115
110
105
100
95
90
85
0
10
20
30
40
50
60
70
Cycle Number
A.11

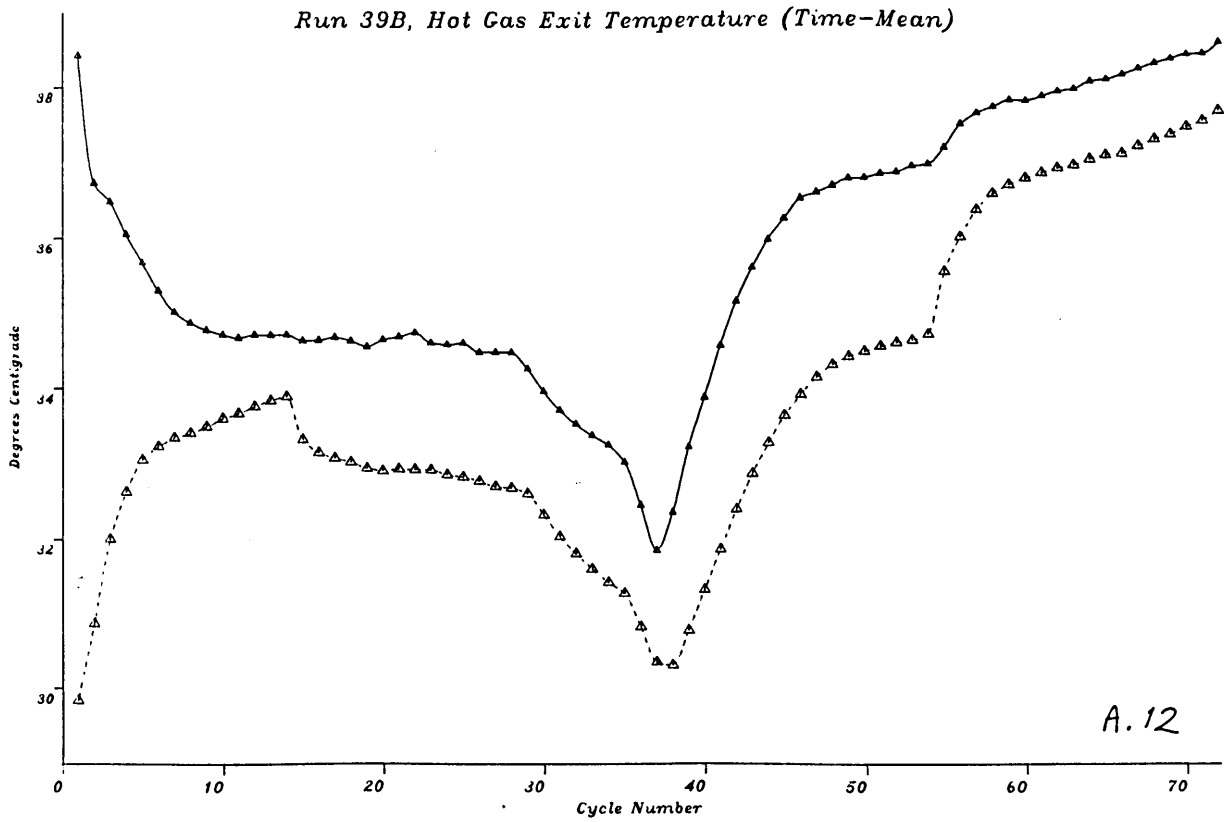
Run 39B, Hot Gas Exit Temperature (Time-Mean)
Degrees Centigrade
38
36
34
32
30
0
10
20
30
40
50
60
70
Cycle Number
A.12

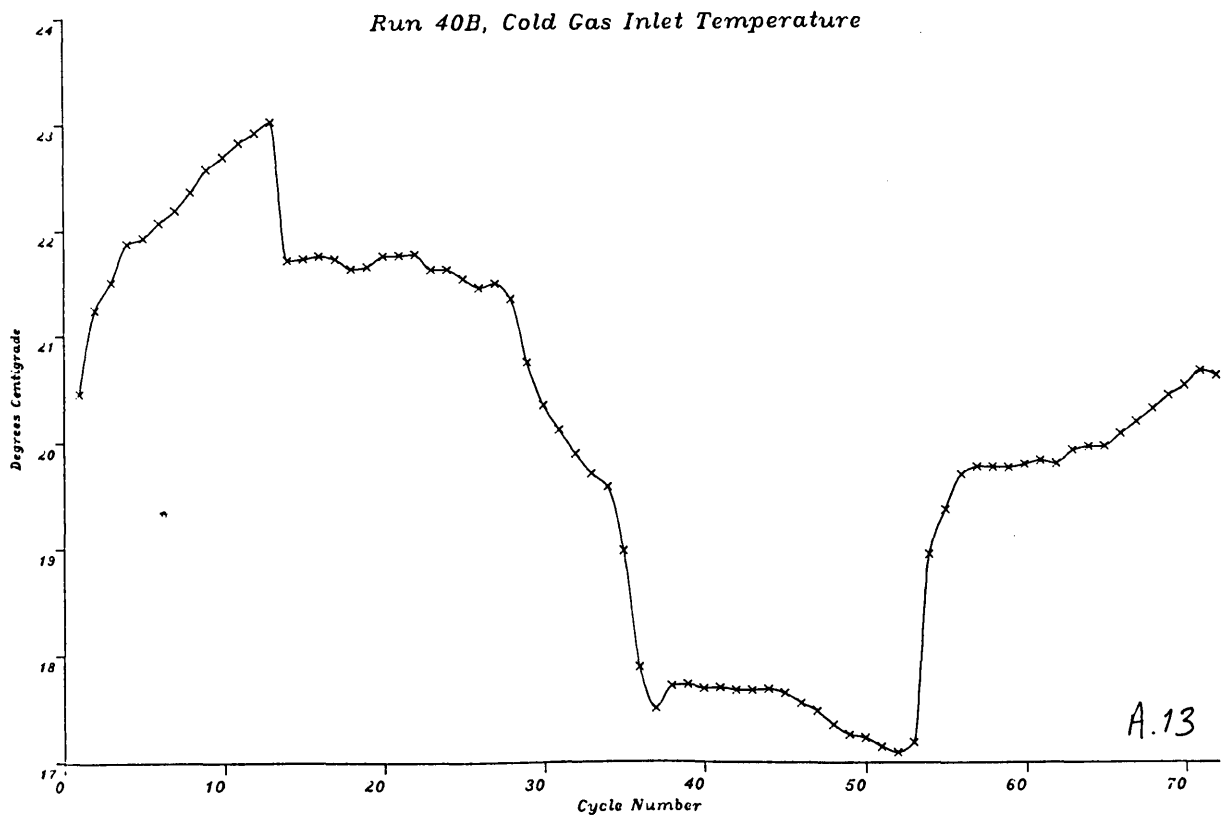
Run 40B, Cold Gas Inlet Temperature
Degrees Centigrade
24
23
22
21
20
19
18
17
0
10
20
30
40
50
60
70
Cycle Number
A.13

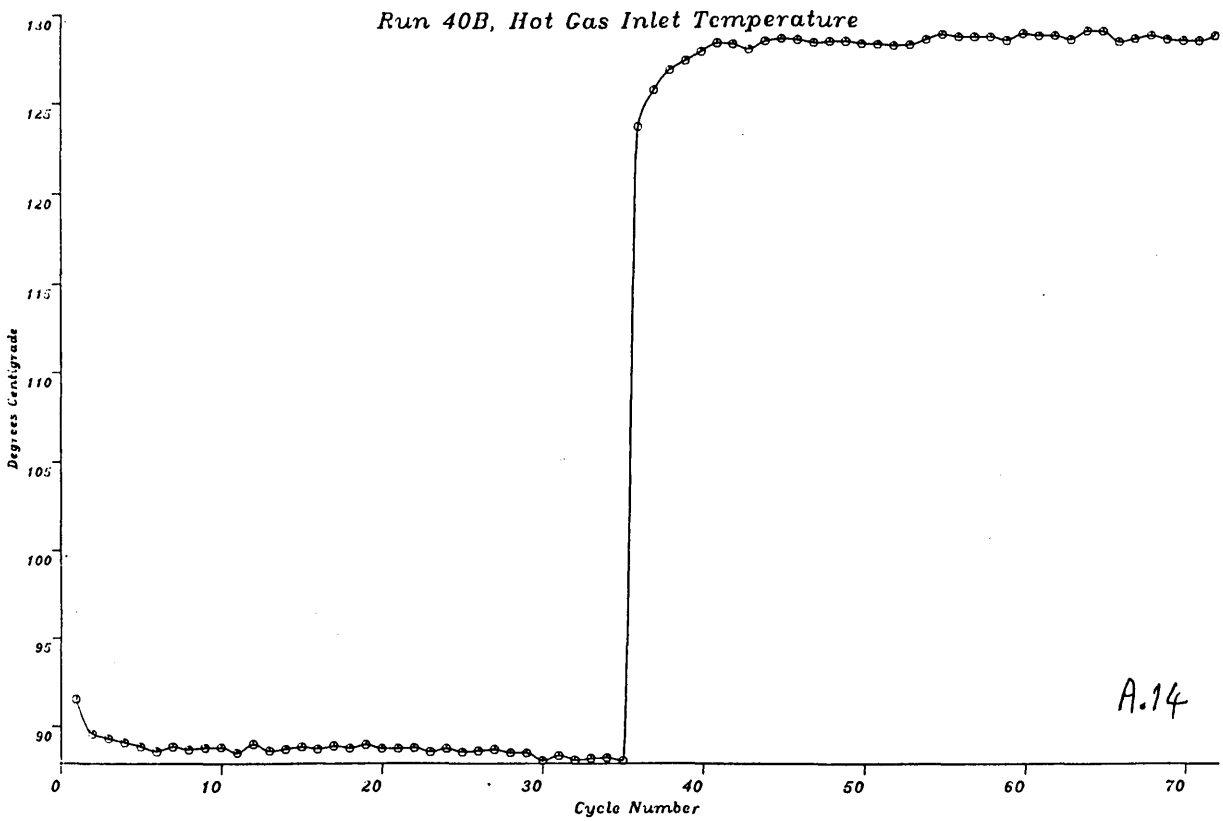
Run 40B, Hot Gas Inlet Temperature
Degrees Centigrade
130
125
120
115
110
105
100
95
90
0
10
20
30
40
50
60
70
Cycle Number
A.14

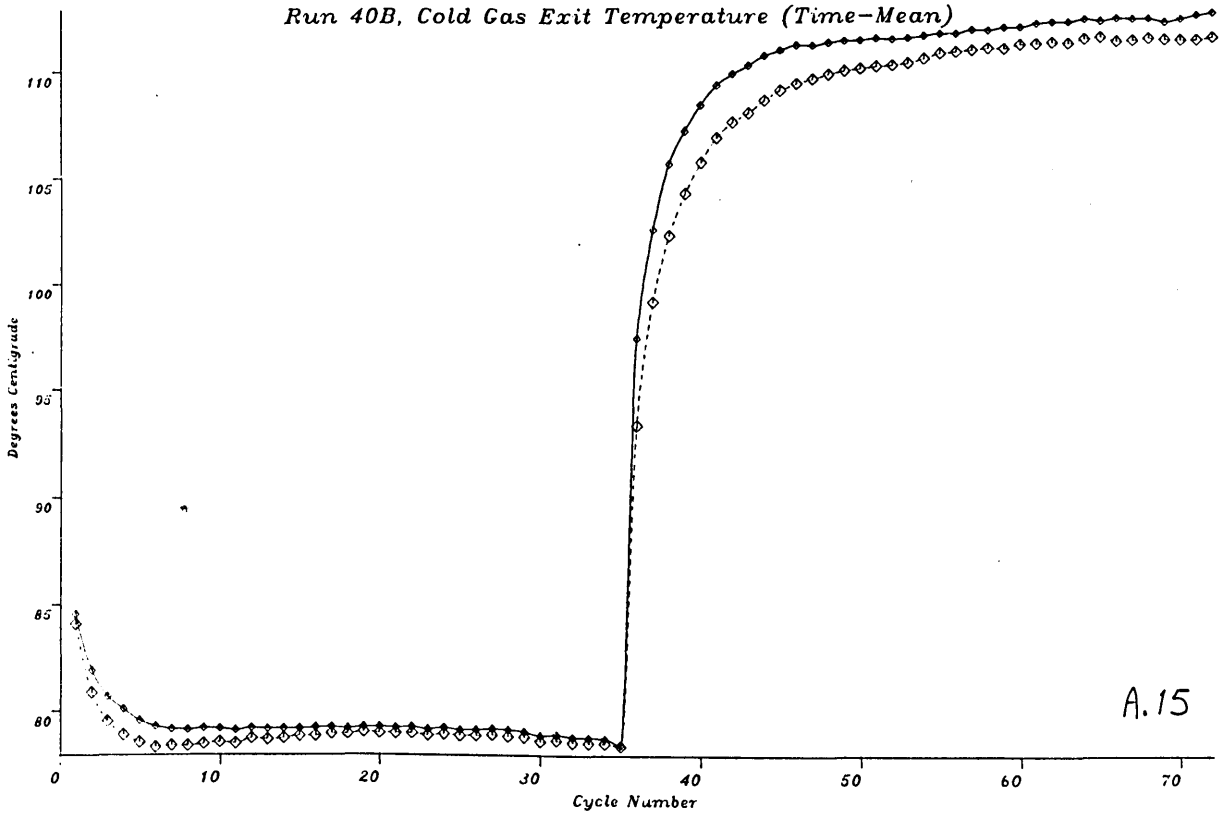
Run 40B, Cold Gas Exit Temperature (Time-Mean)
Degrees Centigrade
110
105
100
95
90
85
80
0
10
20
30
40
50
60
70
Cycle Number
A.15

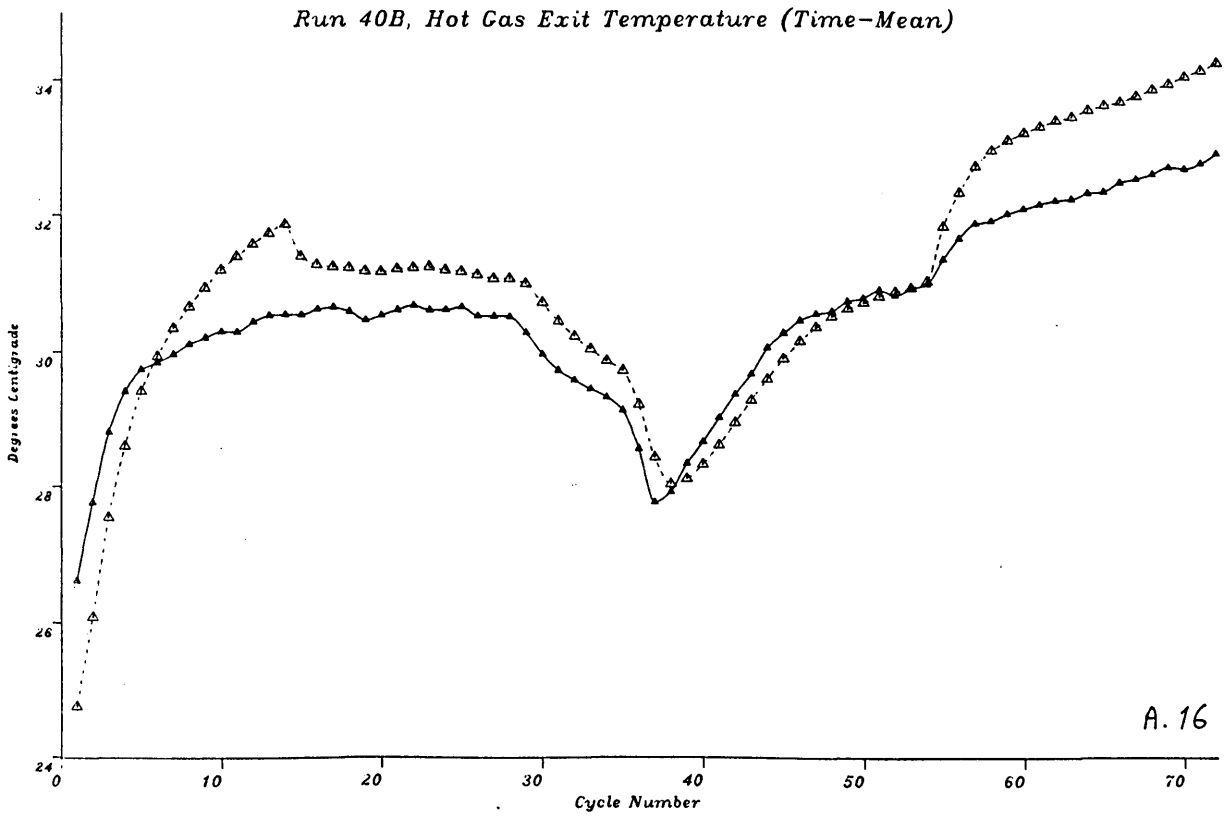
Run 40B, Hot Gas Exit Temperature (Time-Mean)
Degrees Centigrade
34
32
30
28
26
24
0
10
20
30
40
50
60
70
Cycle Number
A.16

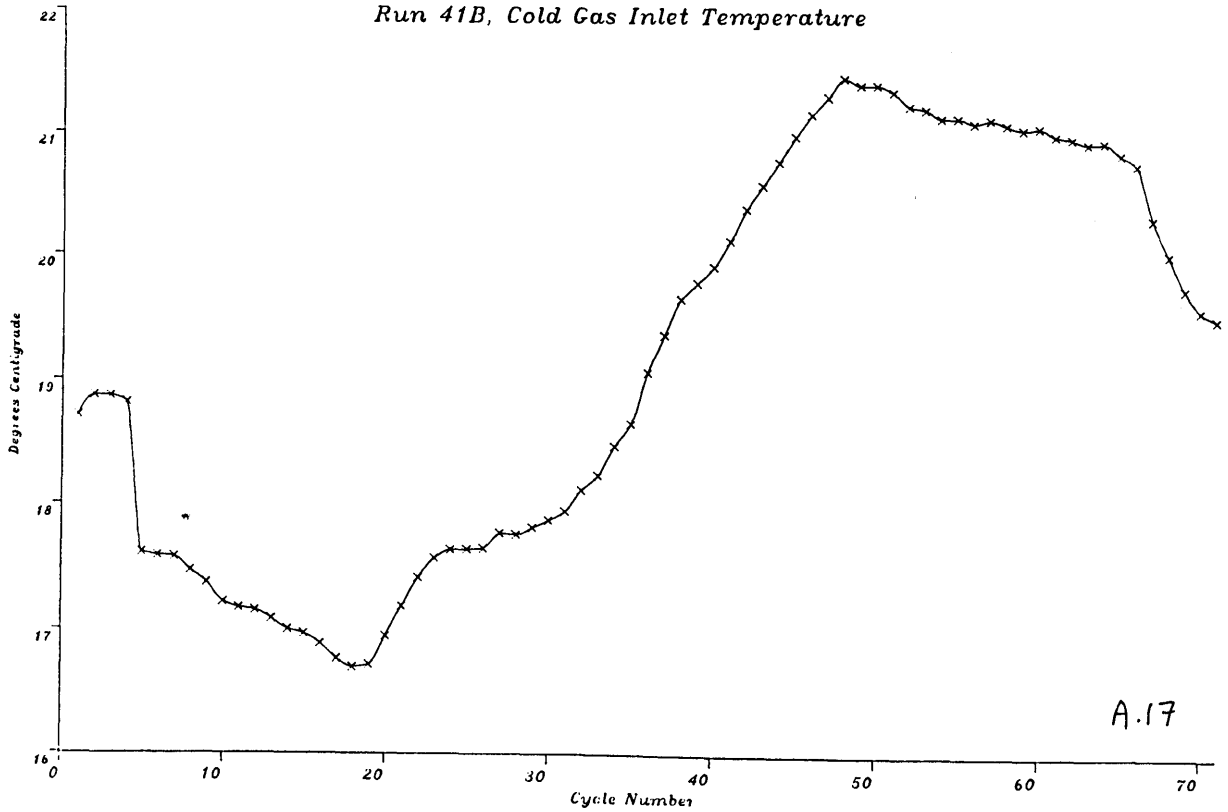
Run 41B, Cold Gas Inlet Temperature
Degrees Centigrade
22
21
20
19
18
17
16
0
10
20
30
40
50
60
70
Cycle Number
A.17

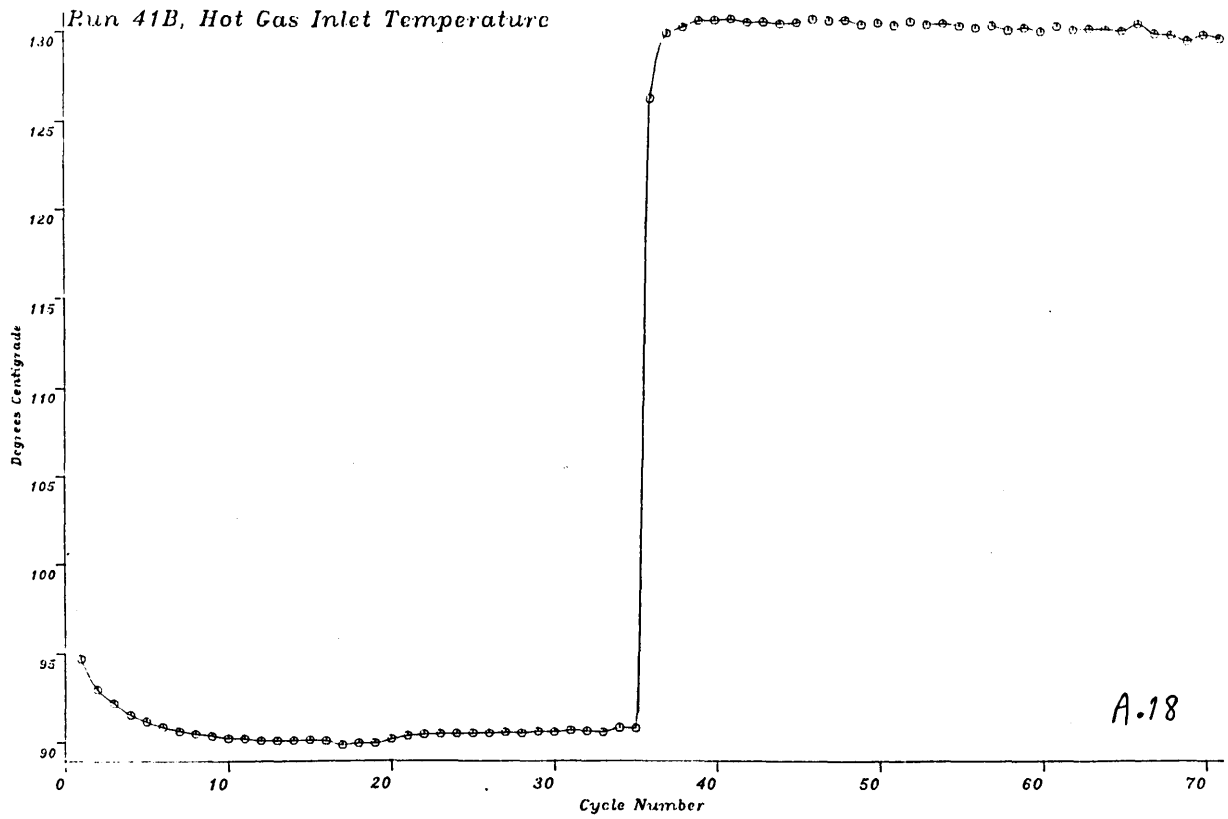
Run 41B, Hot Gas Inlet Temperature
Degrees Centigrade
130
125
120
115
110
105
100
95
90
0
10
20
30
40
50
60
70
Cycle Number
A.18

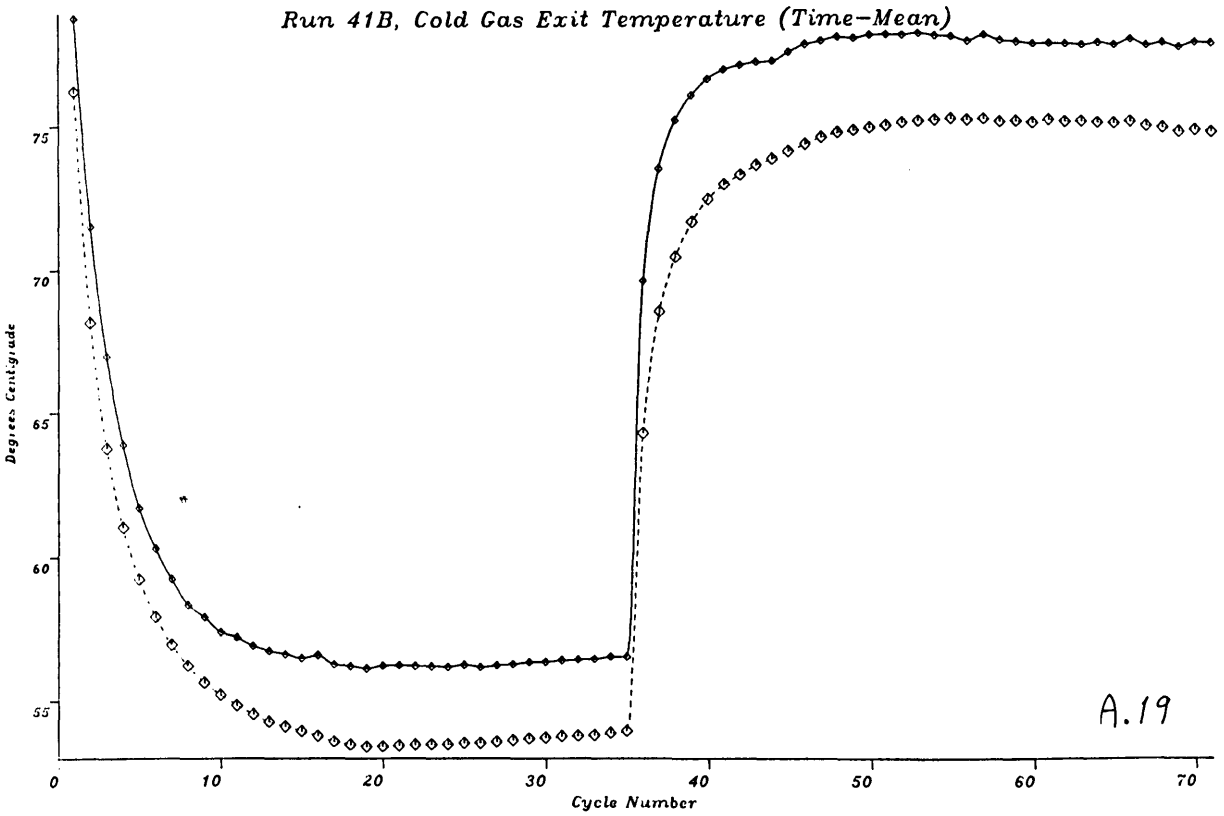
Run 41B, Cold Gas Exit Temperature (Time-Mean)
Degrees Centigrade
75
70
65
60
55
0
10
20
30
40
50
60
70
Cycle Number
A.19

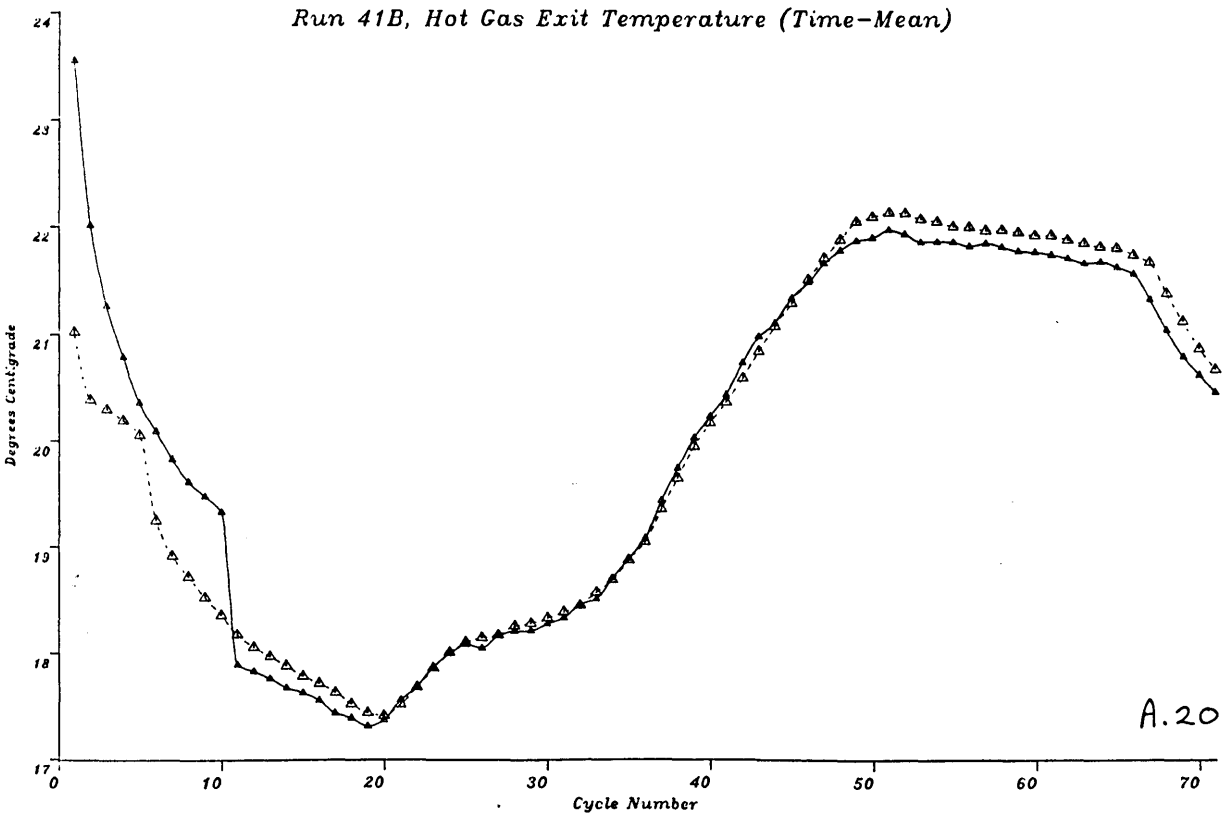
Run 41B, Hot Gas Exit Temperature (Time-Mean)
Degrees Centigrade
24
23
22
21
20
19
18
17
0
10
20
30
40
50
60
70
Cycle Number
A.20

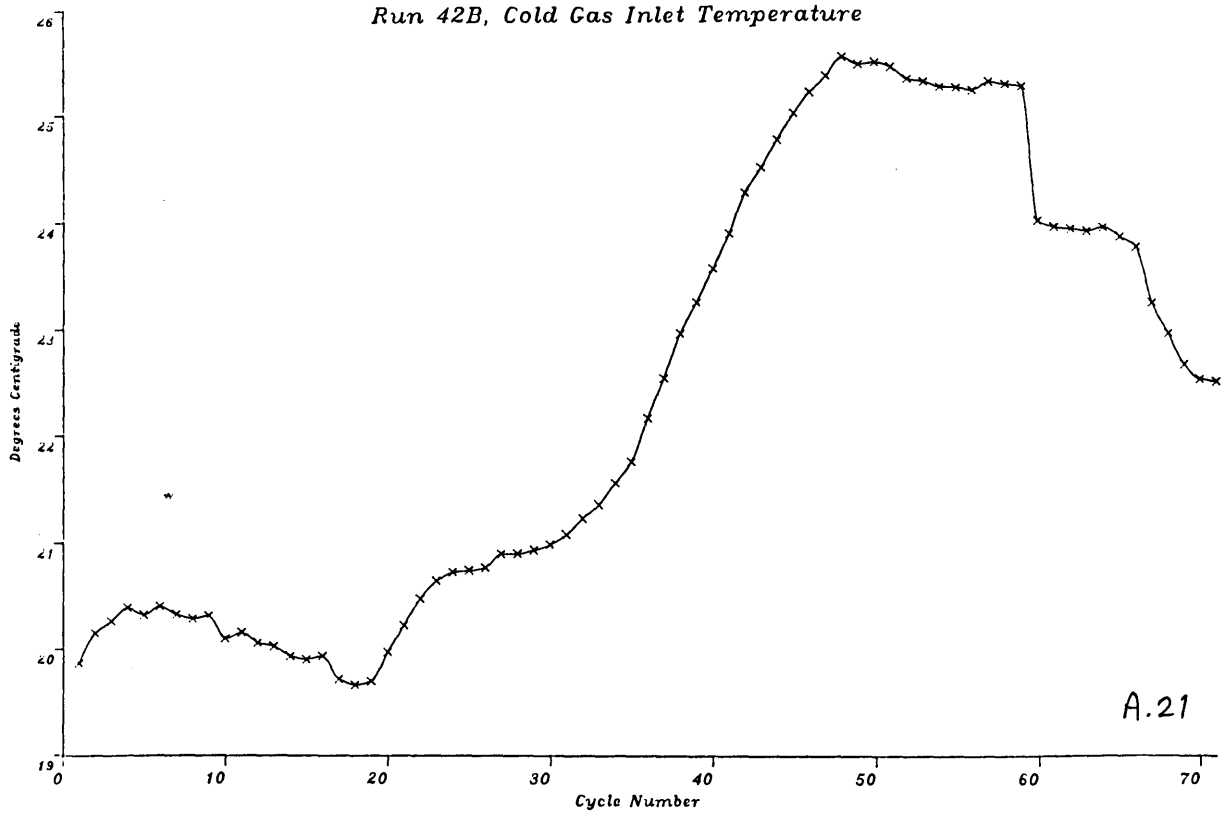
Run 42B, Cold Gas Inlet Temperature
Degrees Centigrade
26
25
24
23
22
21
20
19
0
10
20
30
40
50
60
70
Cycle Number
A.21

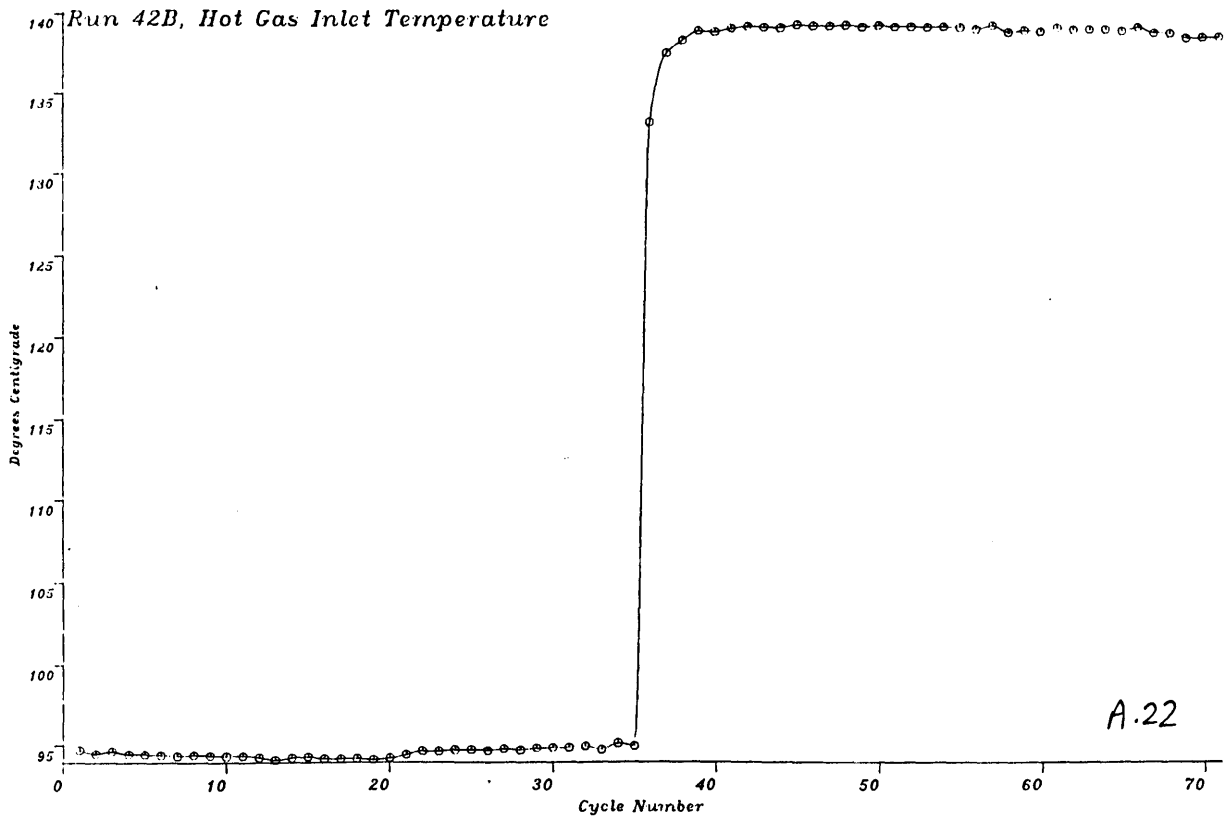
Run 42B, Hot Gas Inlet Temperature
Degrees Centigrade
140
135
130
125
120
115
110
105
100
95
0
10
20
30
40
50
60
70
Cycle Number
A.22

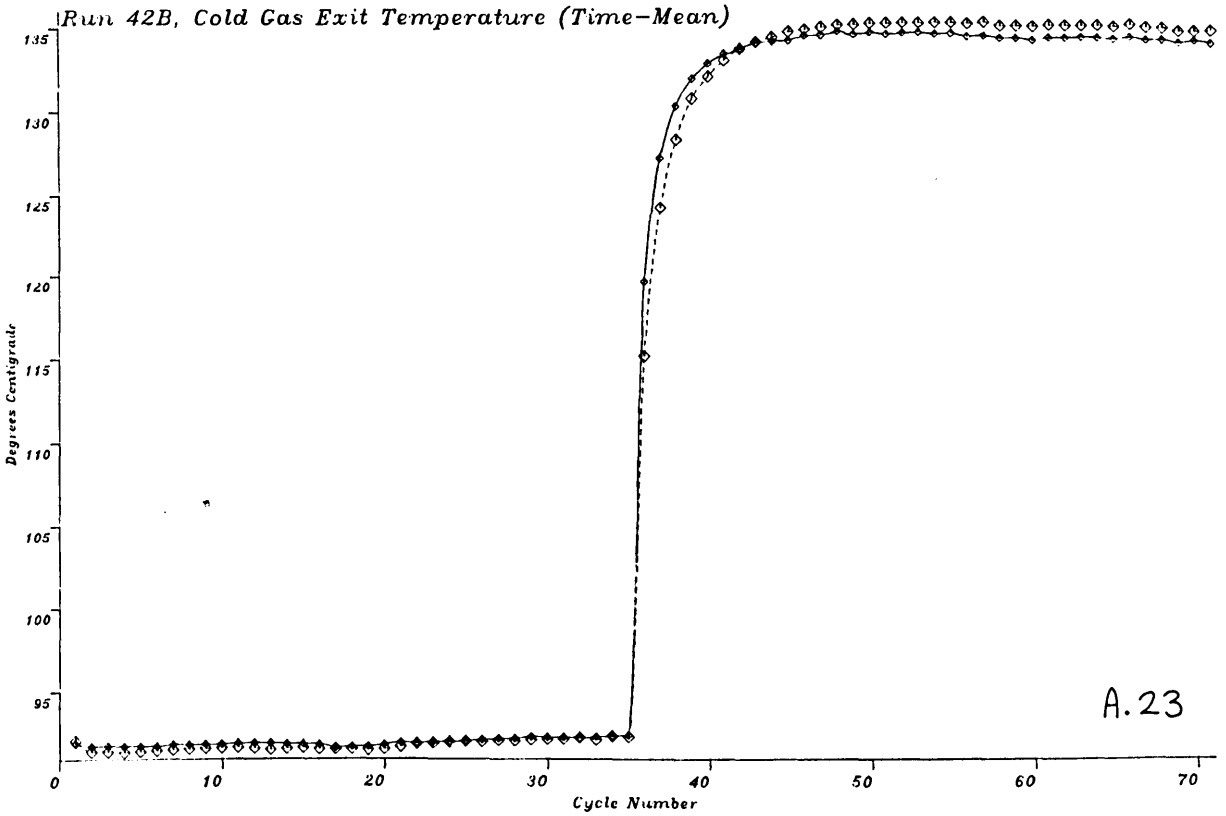
Run 42B, Cold Gas Exit Temperature (Time-Mean)
Degrees Centigrade
135
130
125
120
115
110
105
100
95
0
10
20
30
40
50
60
70
Cycle Number
A.23

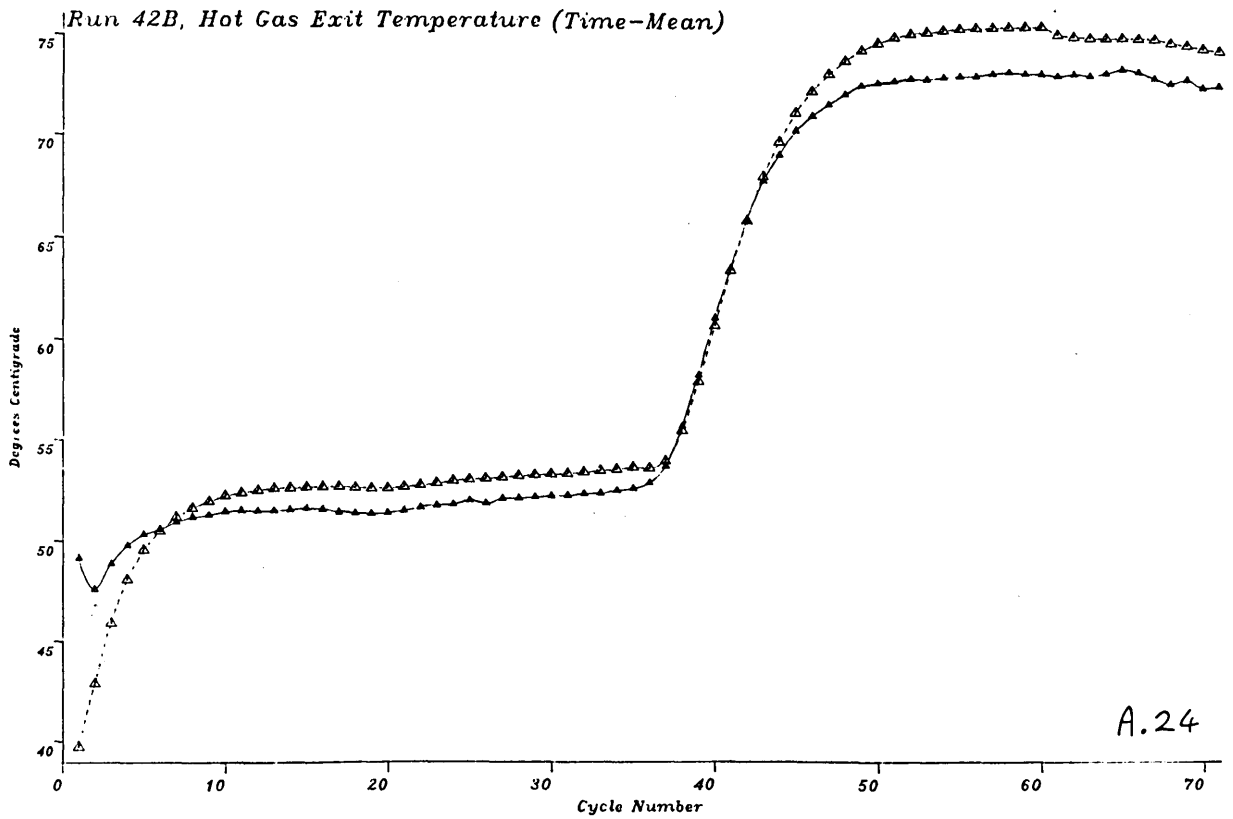
Run 42B, Hot Gas Exit Temperature (Time-Mean)
Degrees Centigrade
75
70
65
60
55
50
45
40
0
10
20
30
40
50
60
70
Cycle Number
A.24

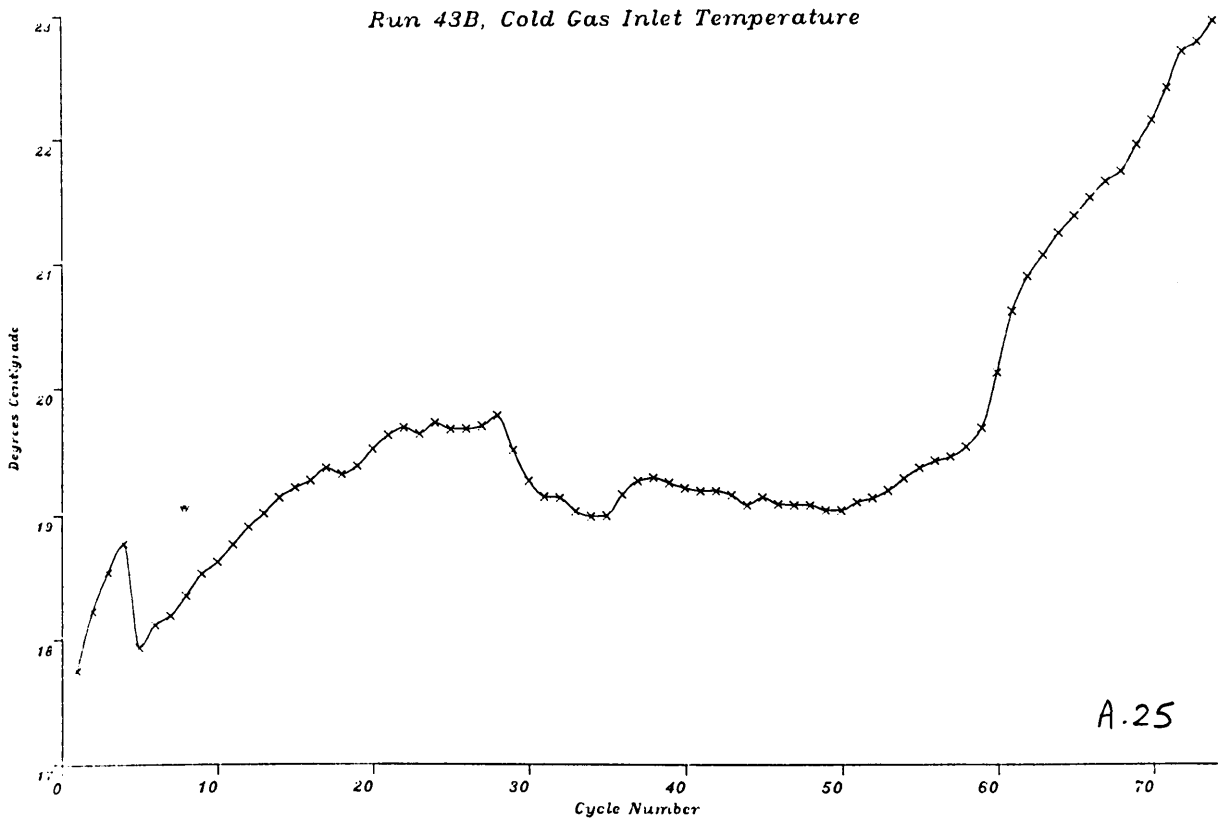
Run 43B, Cold Gas Inlet Temperature
Degrees Centigrade
23
22
21
20
19
18
0
10
20
30
40
50
60
70
Cycle Number
A.25

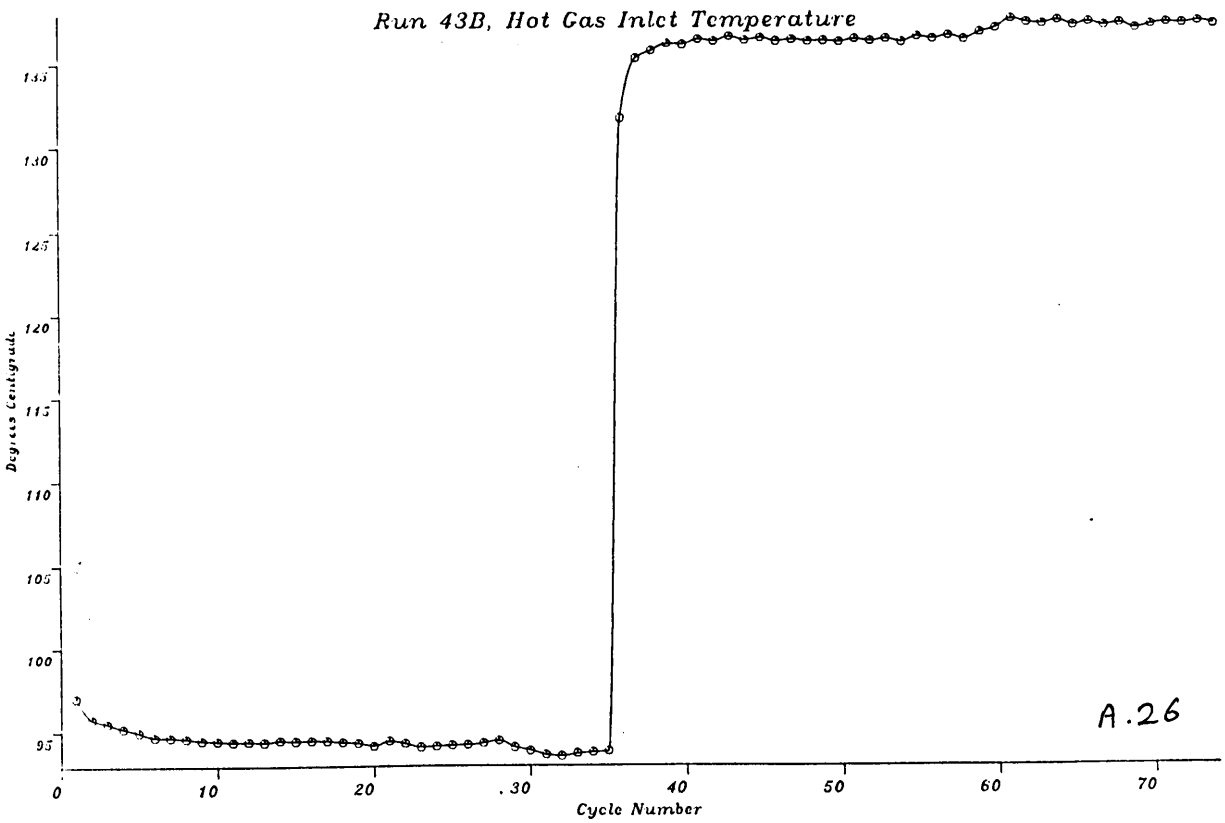
Run 43B, Hot Gas Inlet Temperature
Degrees Centigrade
135
130
125
120
115
110
105
100
95
0
10
20
30
40
50
60
70
Cycle Number
A.26

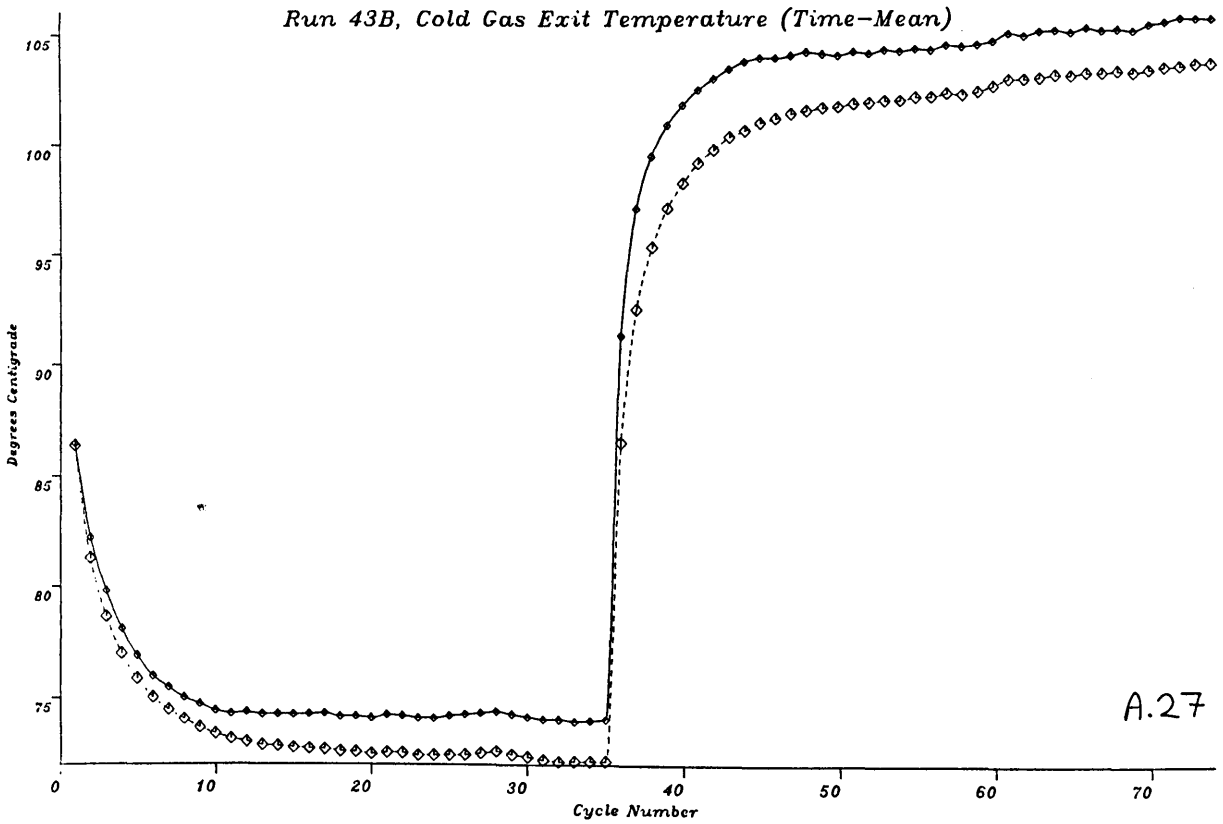
Run 43B, Cold Gas Exit Temperature (Time-Mean)
Degrees Centigrade
105
100
95
90
85
80
75
0
10
20
30
40
50
60
70
Cycle Number
A.27

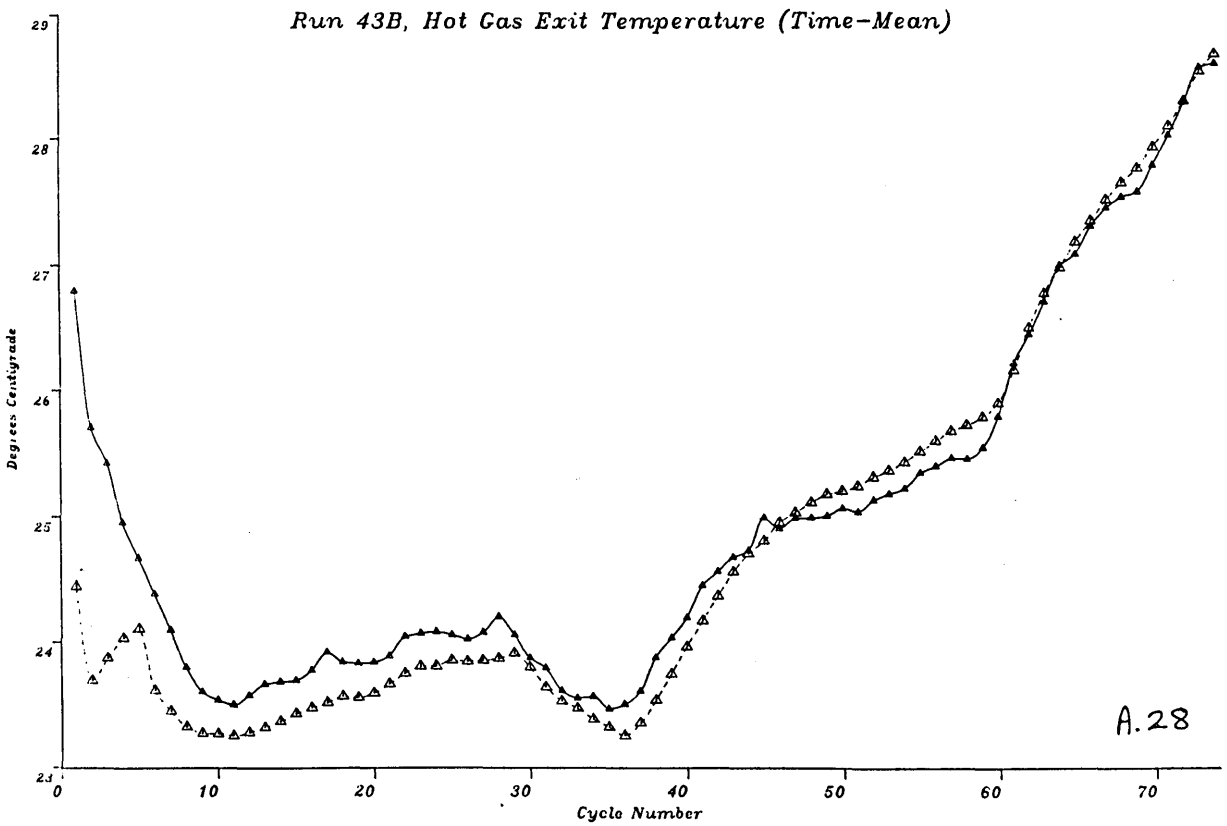
Run 43B, Hot Gas Exit Temperature (Time-Mean)
Degrees Centigrade
29
28
27
26
25
24
23
0
10
20
30
40
50
60
70
Cycle Number
A.28

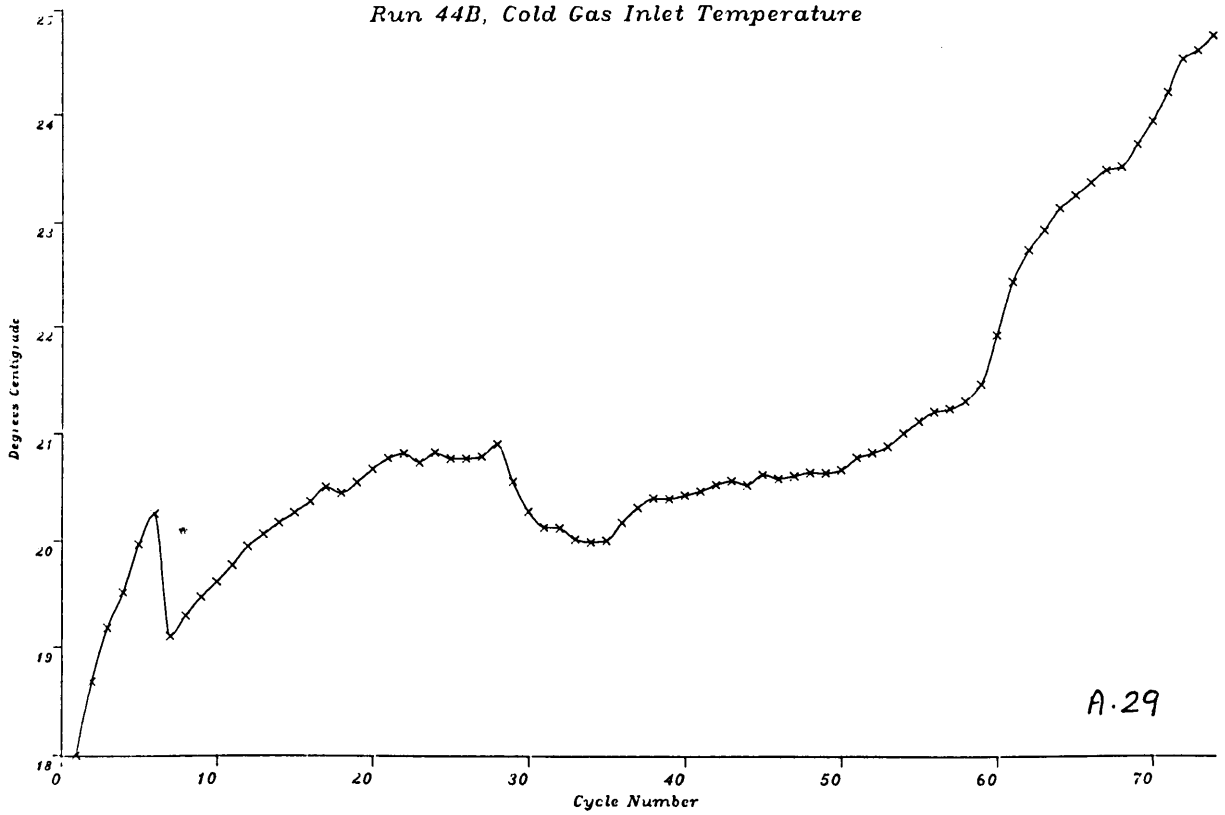
Run 44B, Cold Gas Inlet Temperature
Degrees Centigrade
25
24
23
22
21
20
19
18
0
10
20
30
40
50
60
70
Cycle Number
A.29

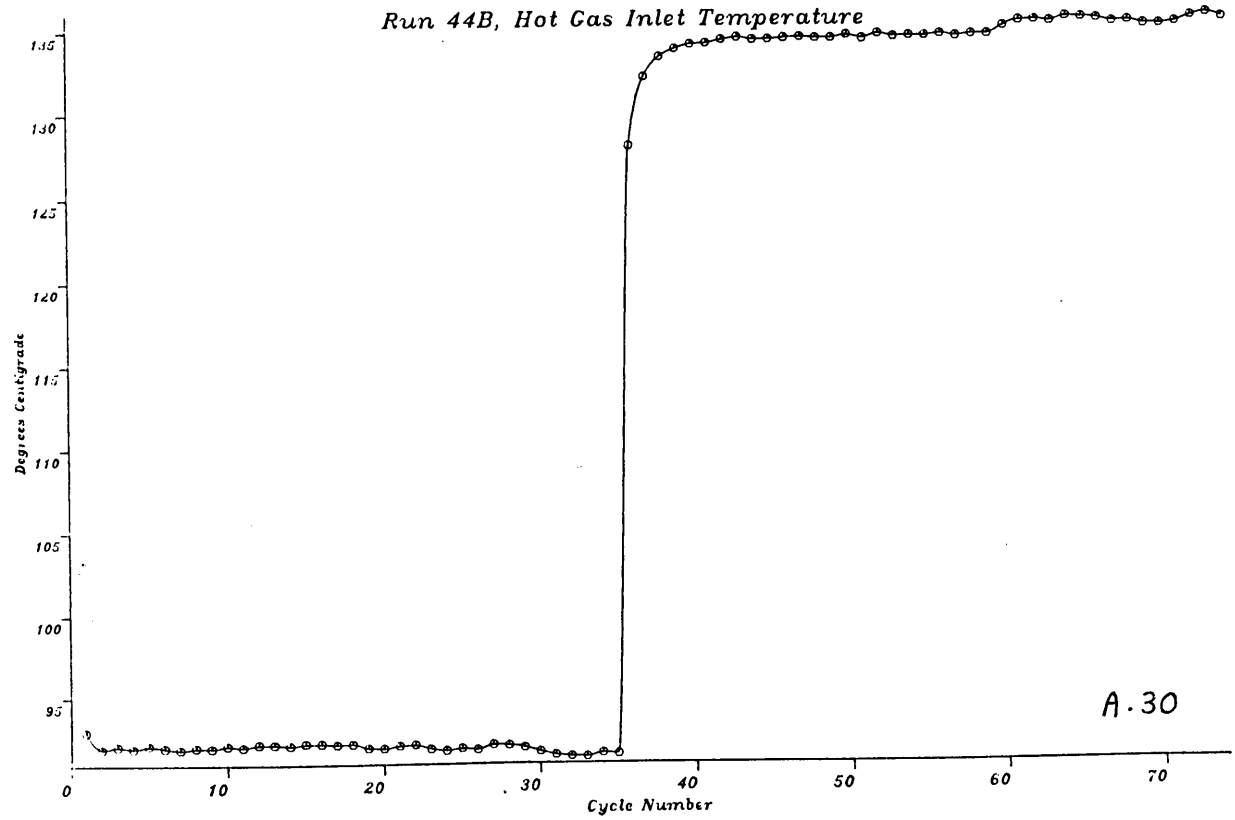
Run 44B, Hot Gas Inlet Temperature
Degrees Centigrade
135
130
125
120
115
110
105
100
95
0
10
20
30
40
50
60
70
Cycle Number
A.30

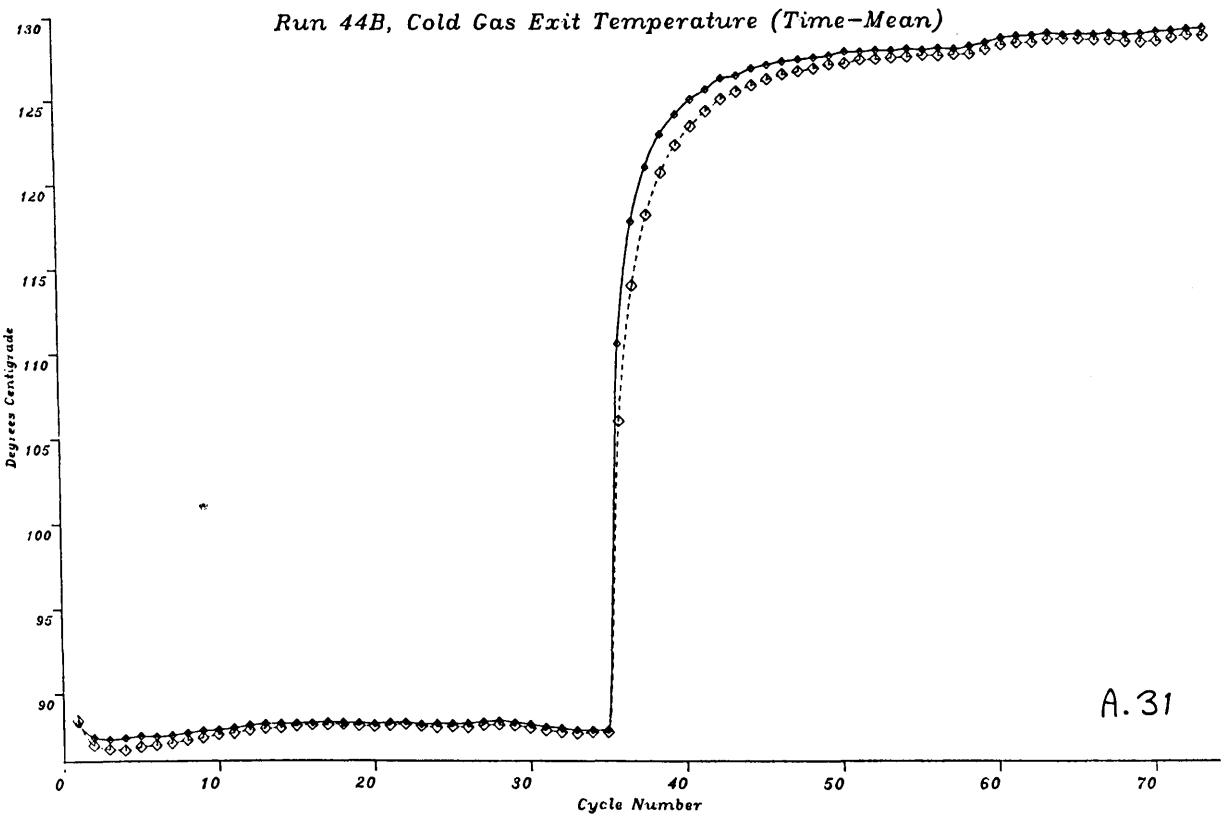
Run 44B, Cold Gas Exit Temperature (Time-Mean)
Degrees Centigrade
130
125
120
115
110
105
100
95
90
0
10
20
30
40
50
60
70
Cycle Number
A.31

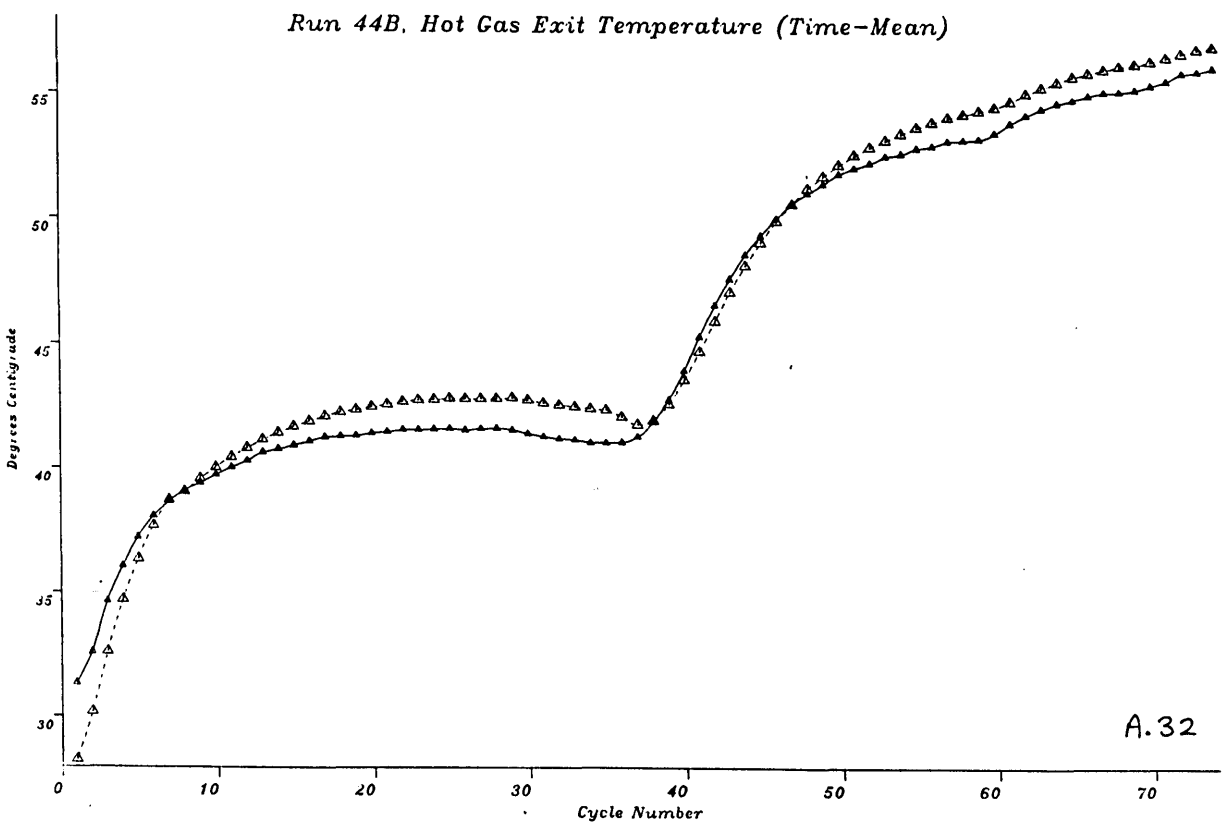
Run 44B, Hot Gas Exit Temperature (Time-Mean)
Degrees Centigrade
55
50
45
40
35
30
0
10
20
30
40
50
60
70
Cycle Number
A.32

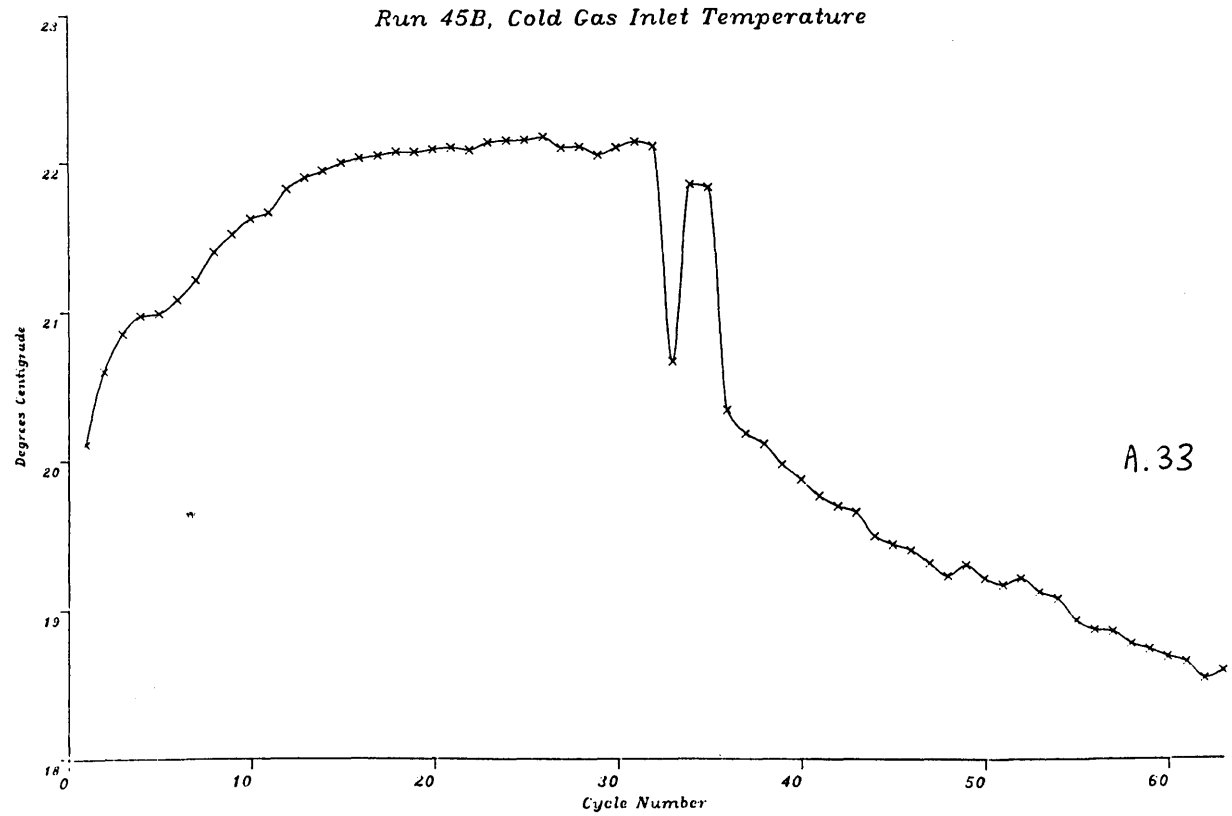
Run 45B, Cold Gas Inlet Temperature
Degrees Centigrade
23
22
21
20
19
18
0
10
20
30
40
50
60
Cycle Number
A.33

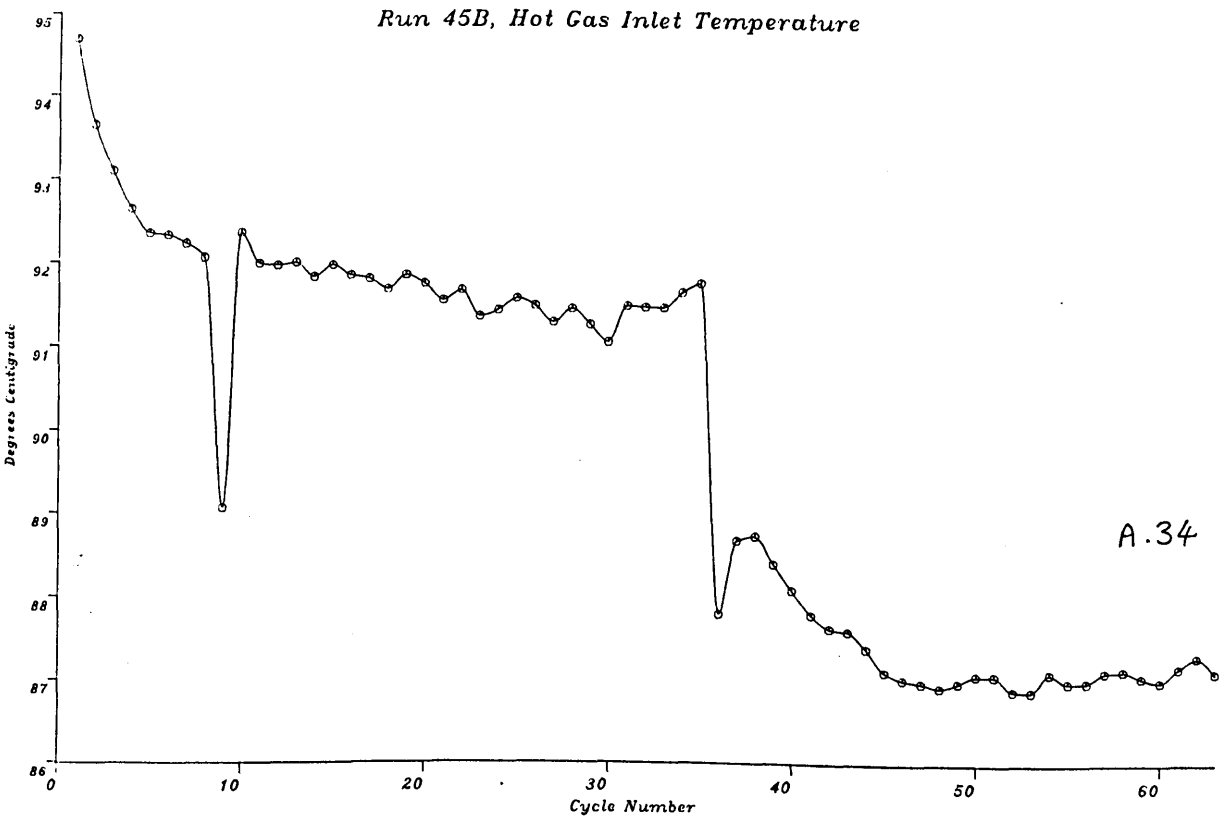
Run 45B, Hot Gas Inlet Temperature
Degrees Centigrade
95
94
93
92
91
90
89
88
87
86
0
10
20
30
40
50
60
Cycle Number
A.34

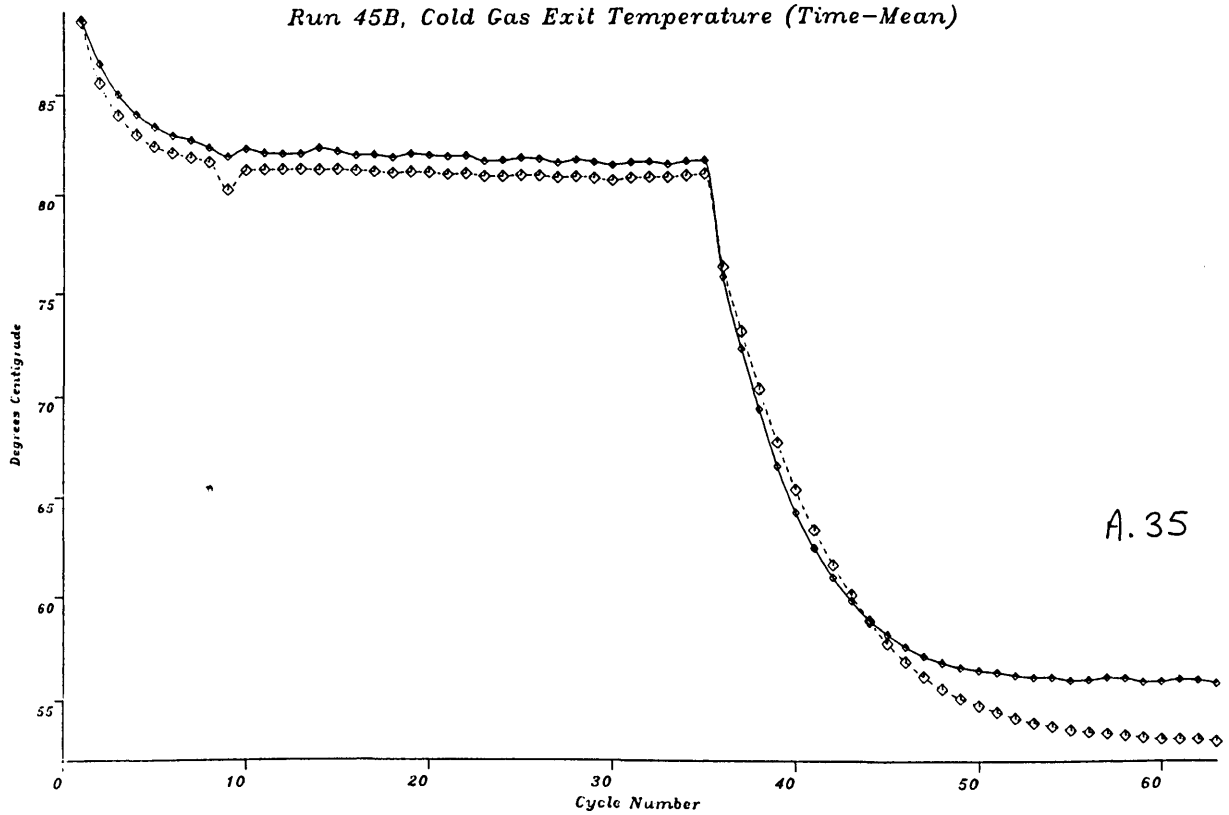
Run 45B, Cold Gas Exit Temperature (Time-Mean)
Degrees Centigrade
85
80
75
70
65
60
55
0
10
20
30
40
50
60
Cycle Number

A.35

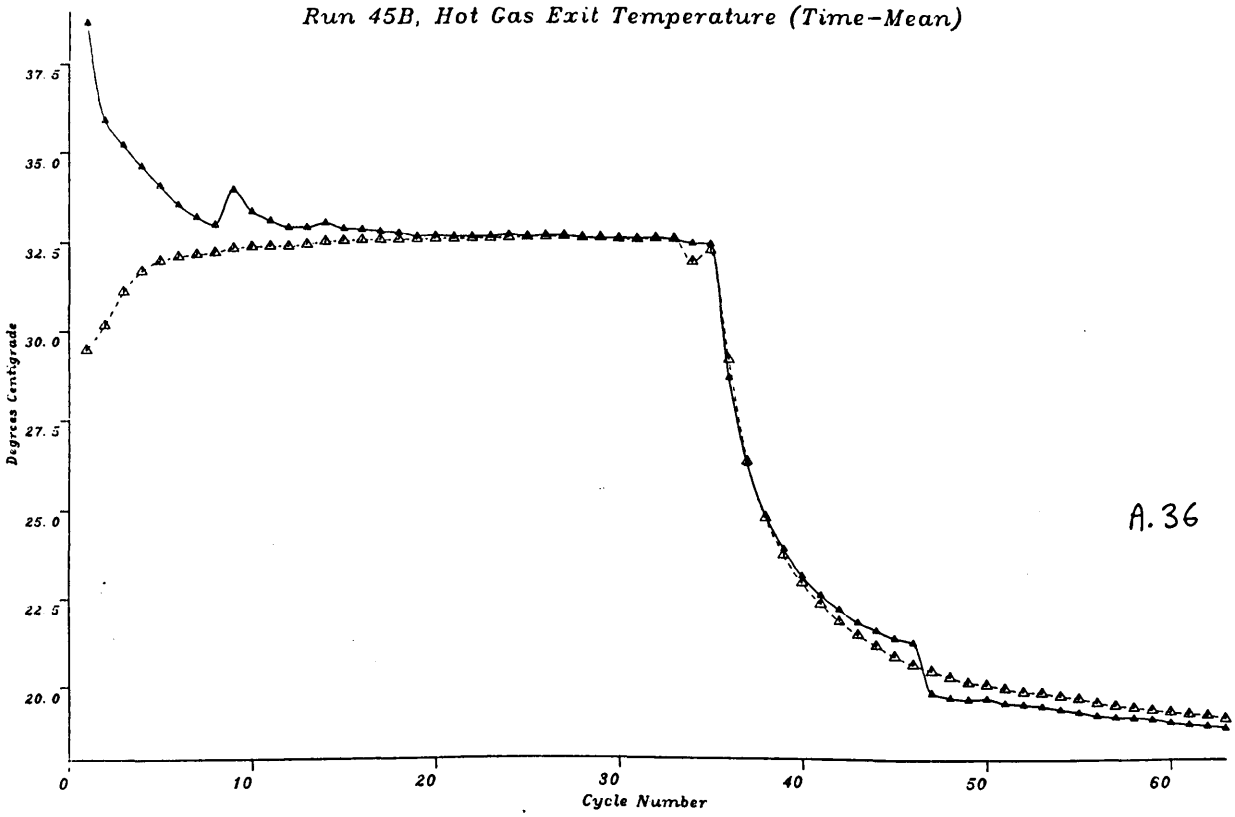
Run 45B, Hot Gas Exit Temperature (Time-Mean)
Degrees Centigrade
37.5
35.0
32.5
30.0
27.5
25.0
22.5
20.0
0
10
20
30
40
50
60
Cycle Number

A.36

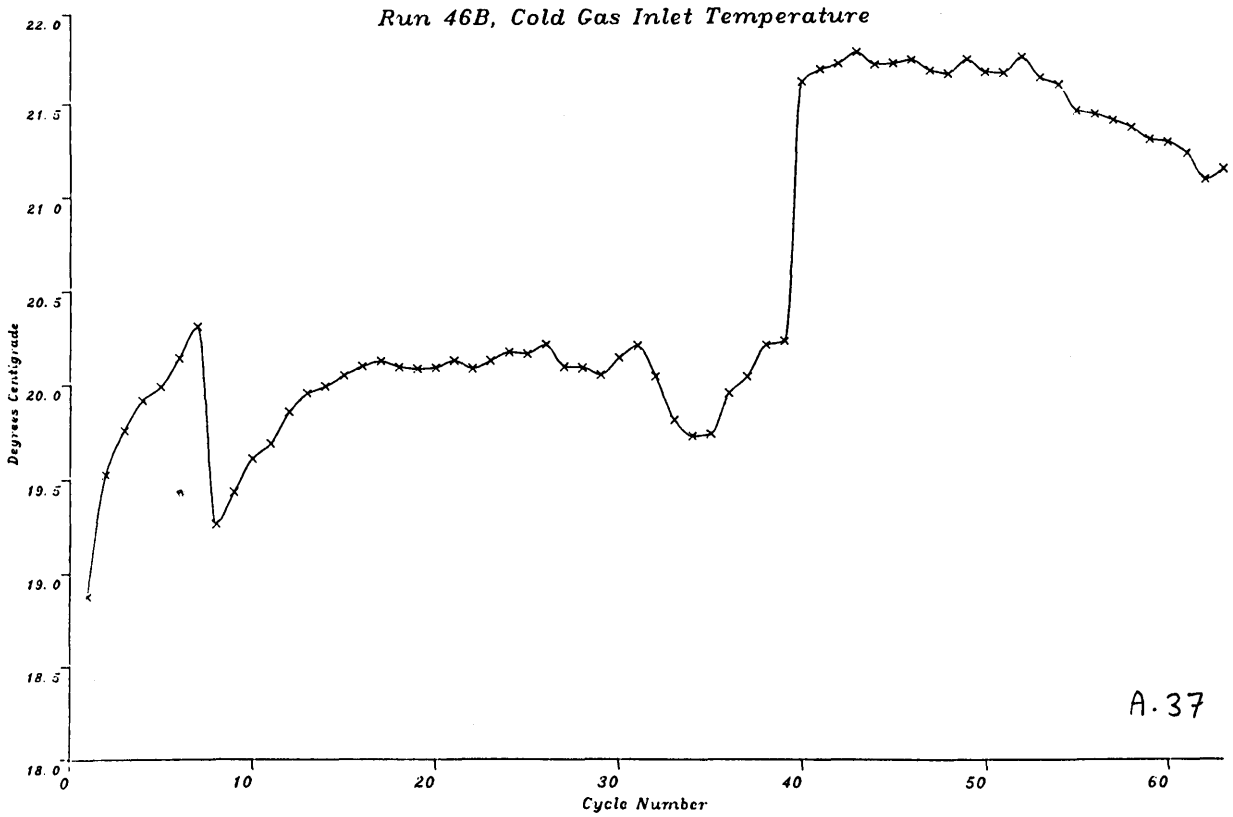
Run 46B, Cold Gas Inlet Temperature
Degrees Centigrade
22.0
21.5
21.0
20.5
20.0
19.5
19.0
18.5
18.0
0
10
20
30
40
50
60
Cycle Number
A.37

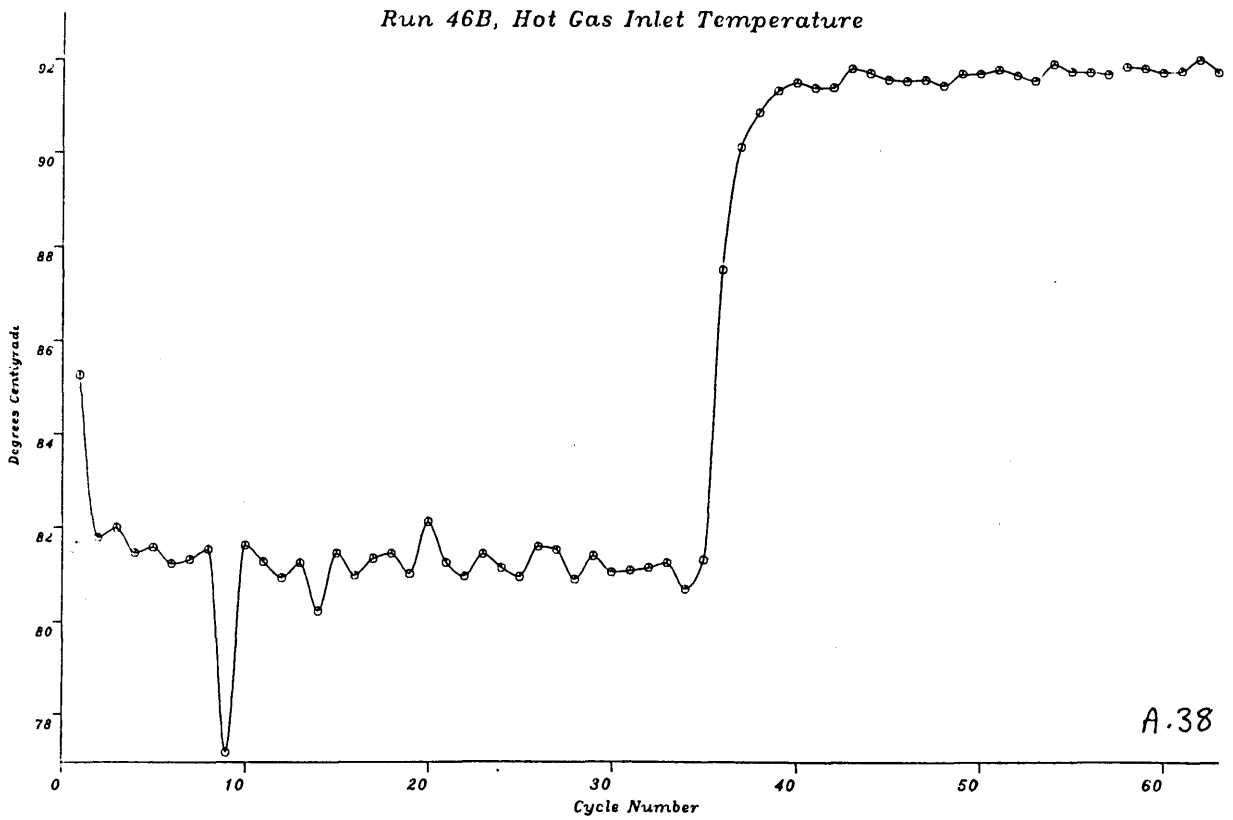
Run 46B, Hot Gas Inlet Temperature
Degrees Centigrade
92
90
88
86
84
82
80
78
0
10
20
30
40
50
60
Cycle Number
A.38

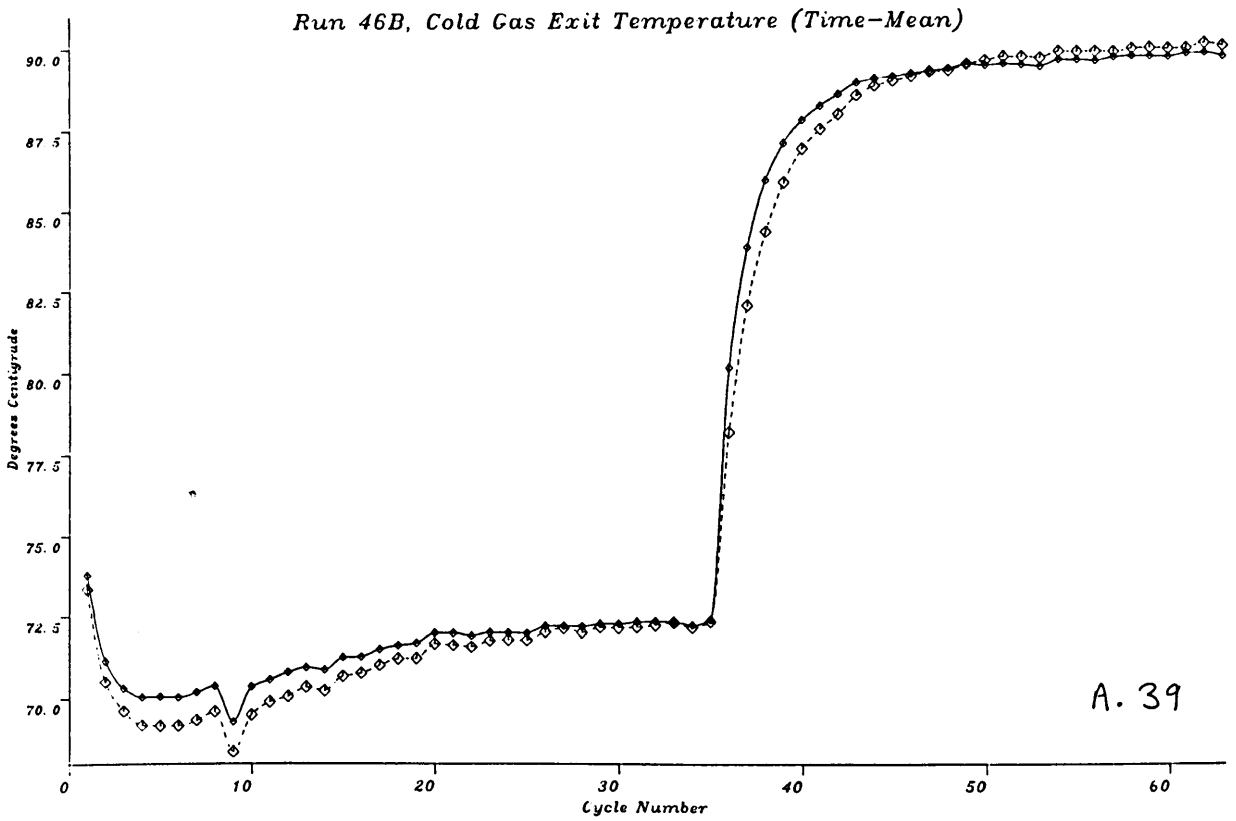
Run 46B, Cold Gas Exit Temperature (Time-Mean)
Degrees Centigrade
90.0
87.5
85.0
82.5
80.0
77.5
75.0
72.5
70.0
0
10
20
30
40
50
60
Cycle Number
A. 39

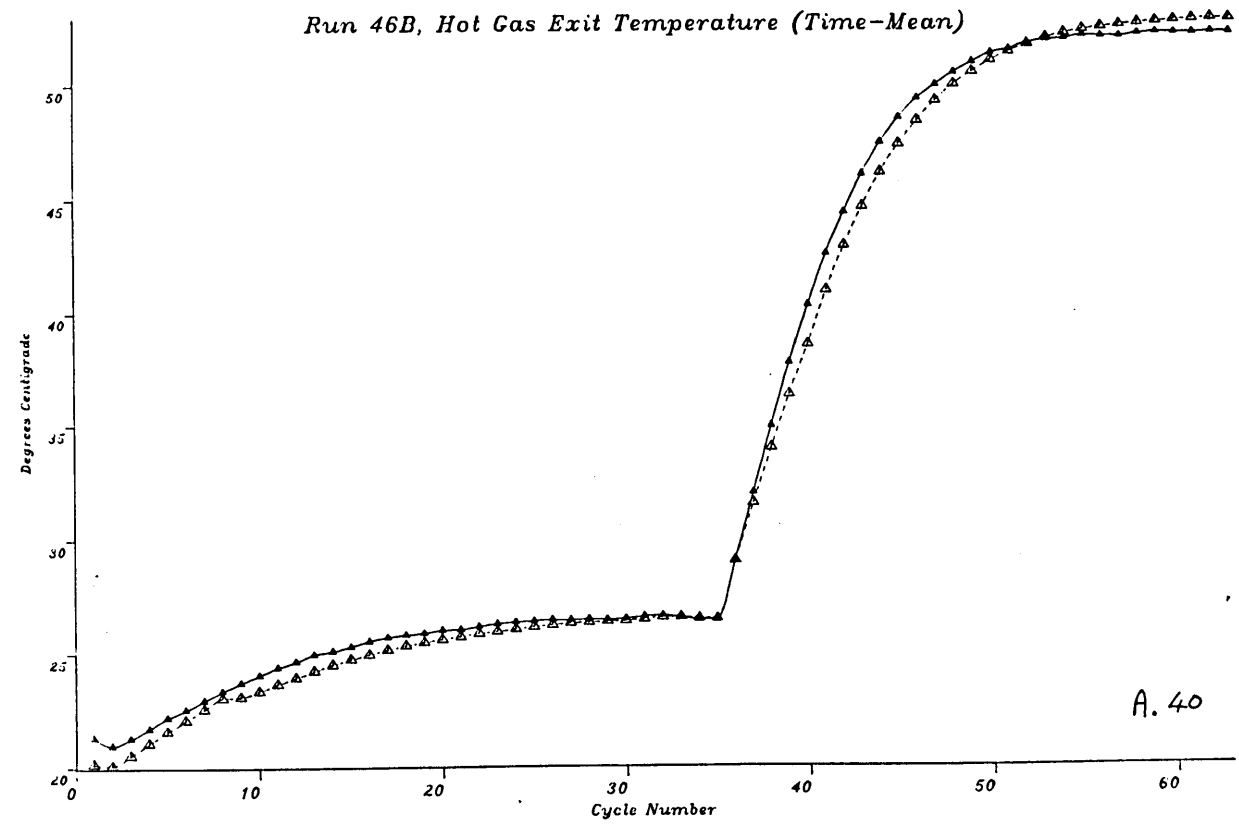
Run 46B, Hot Gas Exit Temperature (Time-Mean)
Degrees Centigrade
50
45
40
35
30
25
20
0
10
20
30
40
50
60
Cycle Number
A. 40

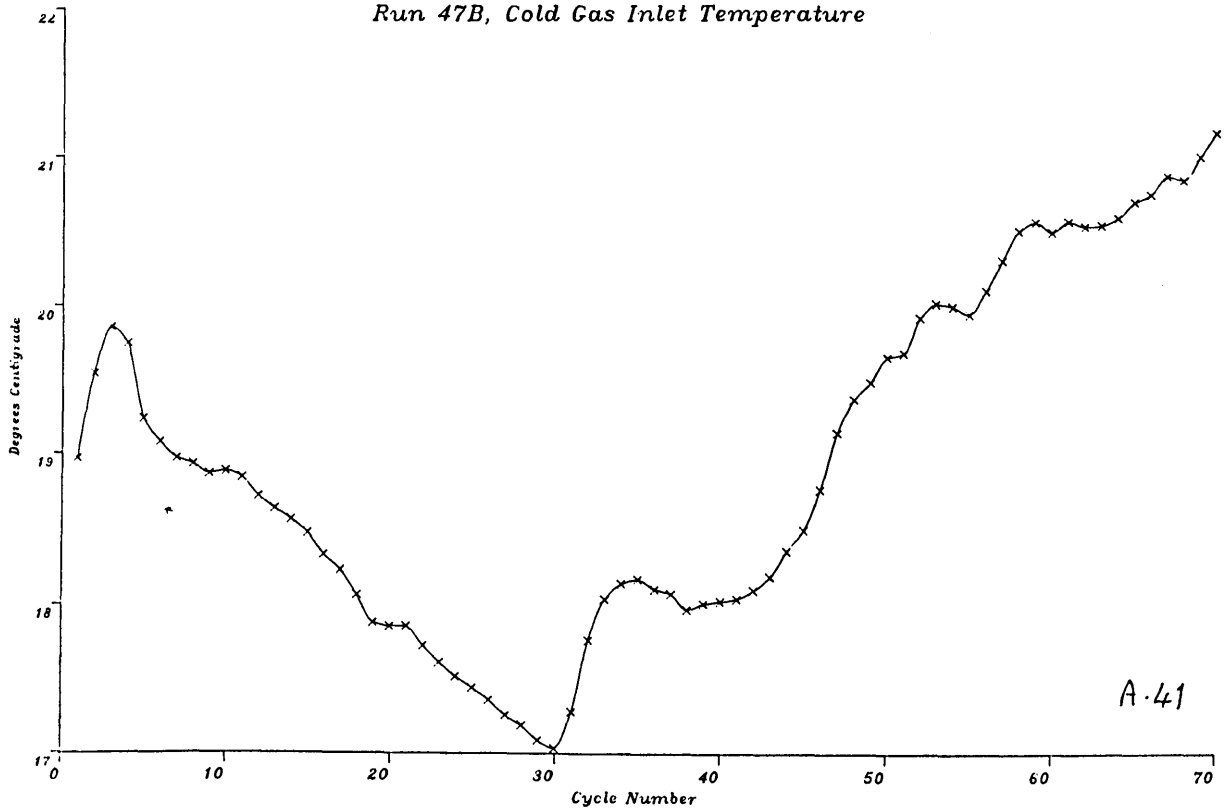
Run 47B, Cold Gas Inlet Temperature
Degrees Centigrade
22
21
20
19
18
17
0
10
20
30
40
50
60
70
Cycle Number
A·41

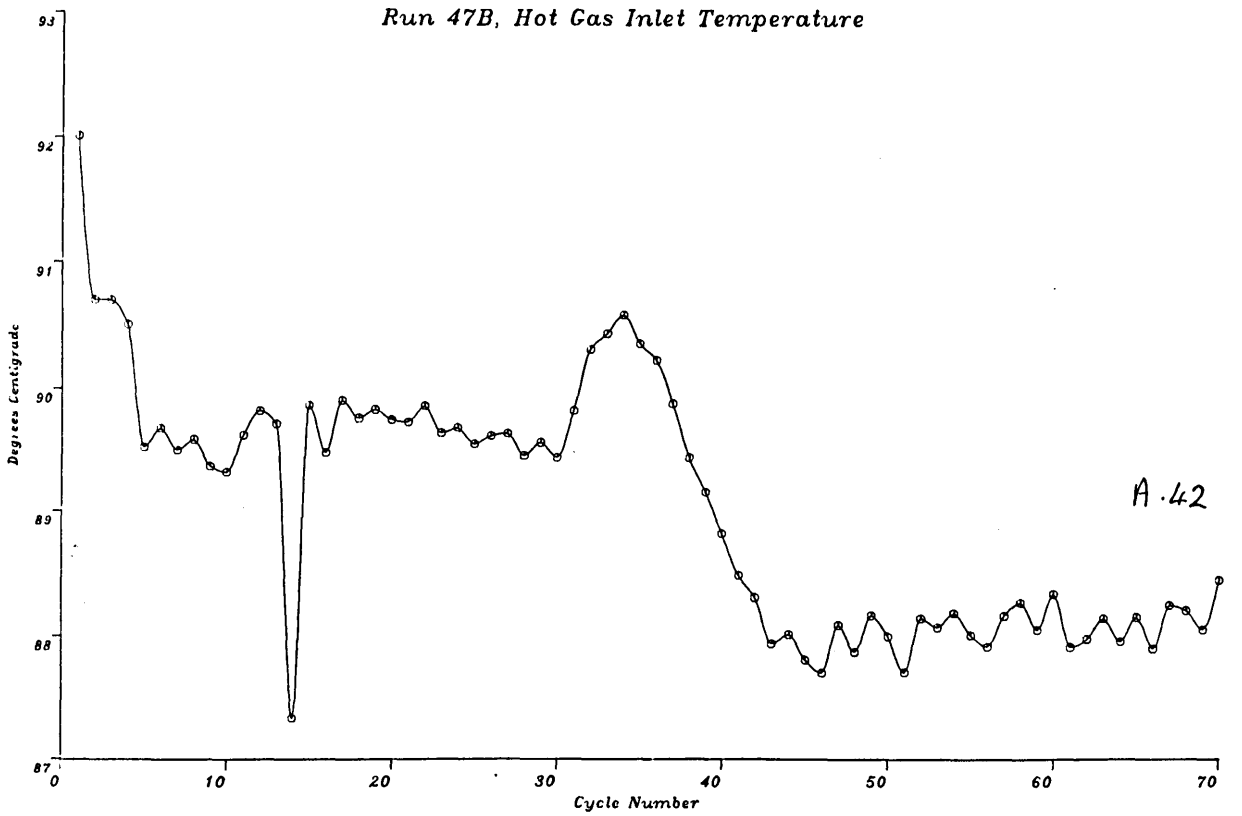
Run 47B, Hot Gas Inlet Temperature
Degrees Centigrade
93
92
91
90
89
88
87
0
10
20
30
40
50
60
70
Cycle Number
A·42

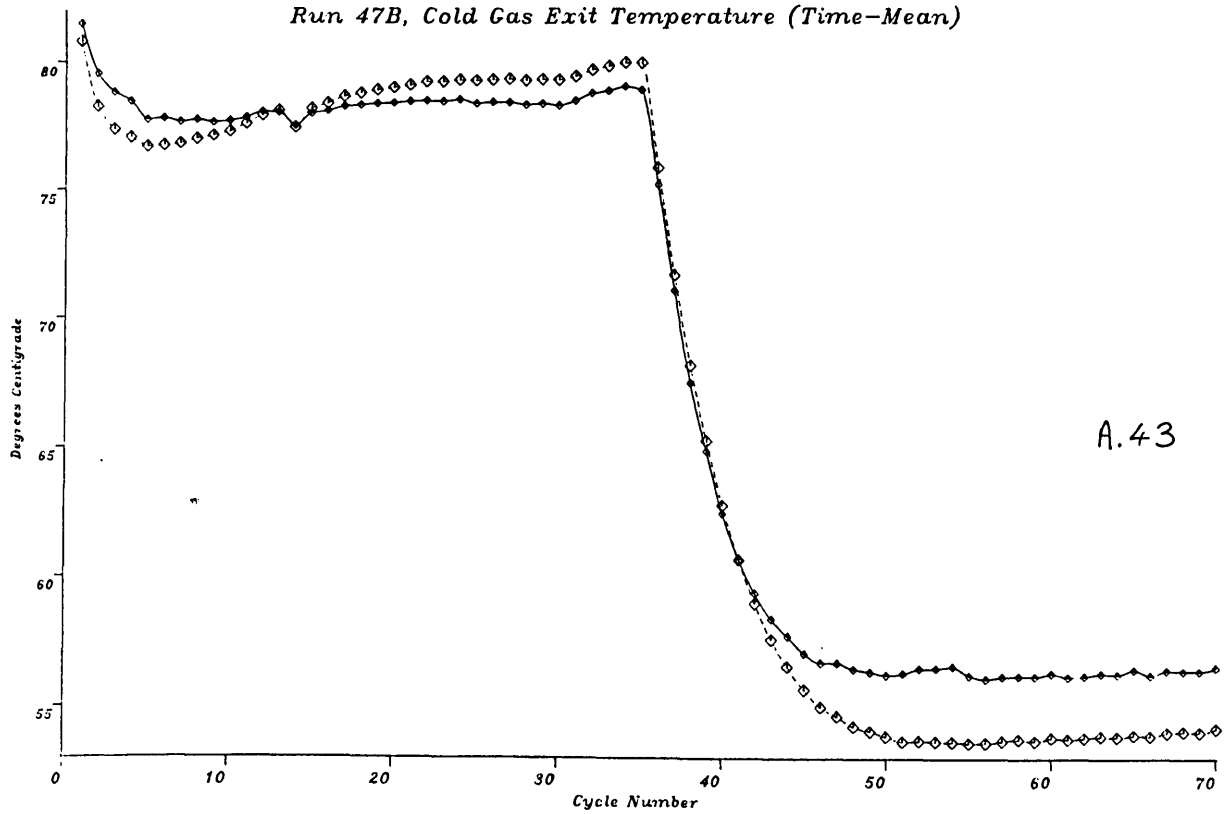
Run 47B, Cold Gas Exit Temperature (Time-Mean)
Degrees Centigrade
80
75
70
65
60
55
0
10
20
30
40
50
60
70
Cycle Number

A.43

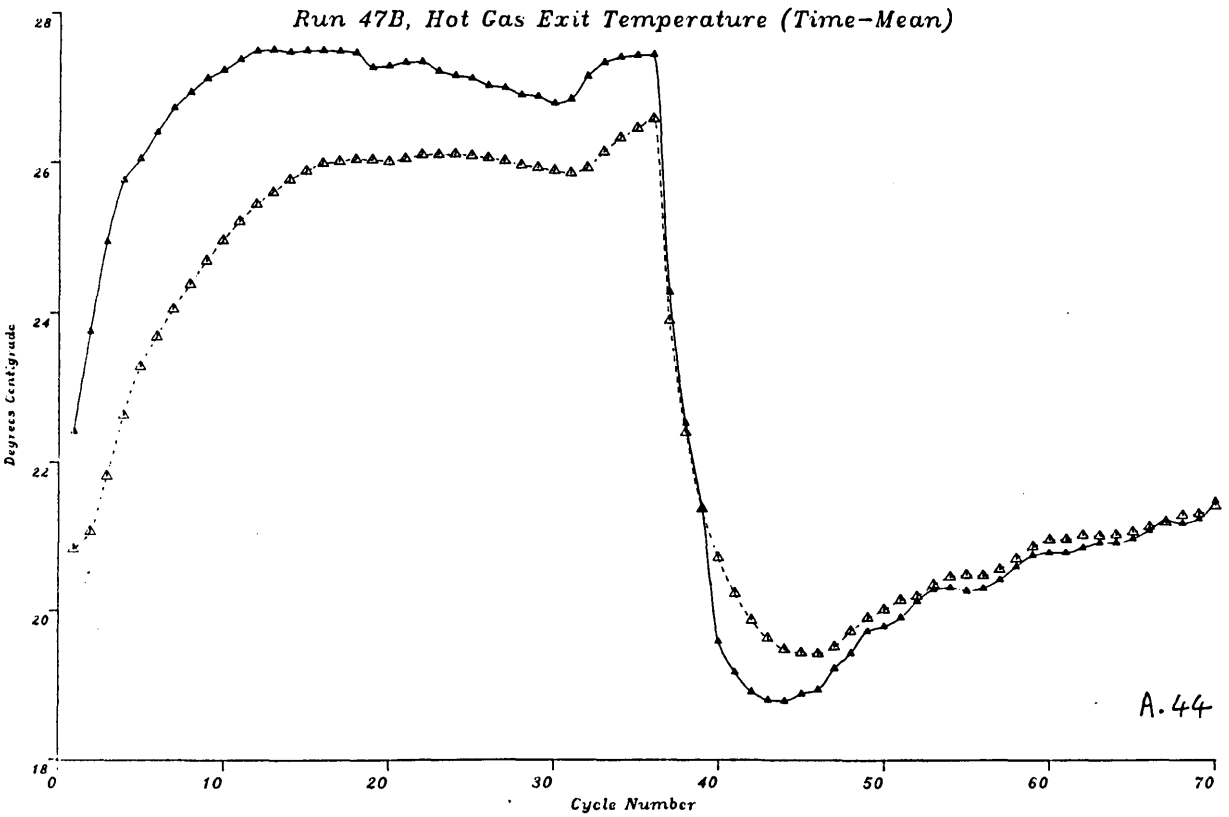
Run 47B, Hot Gas Exit Temperature (Time-Mean)
Degrees Centigrade
28
26
24
22
20
18
0
10
20
30
40
50
60
70
Cycle Number

A.44

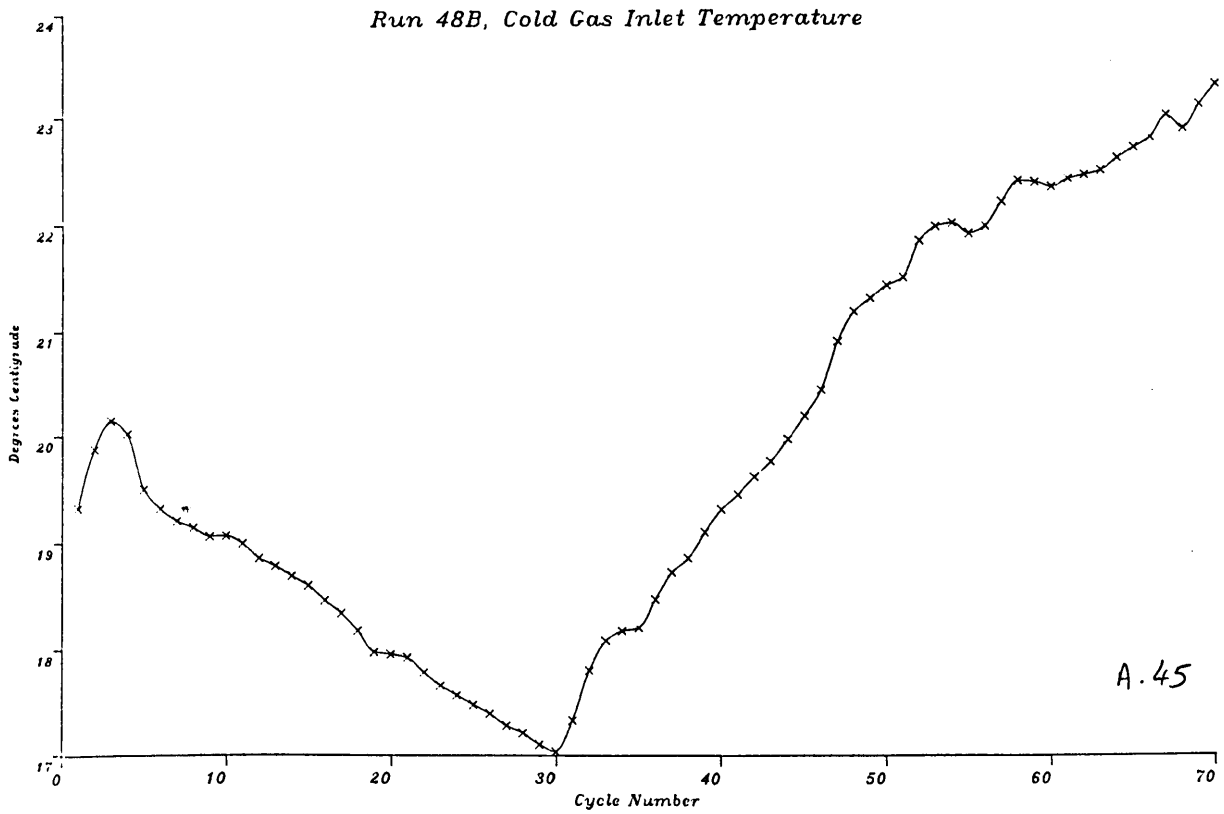
Run 48B, Cold Gas Inlet Temperature
Degrees Centigrade
24
23
22
21
20
19
18
17
0
10
20
30
40
50
60
70
Cycle Number
A.45

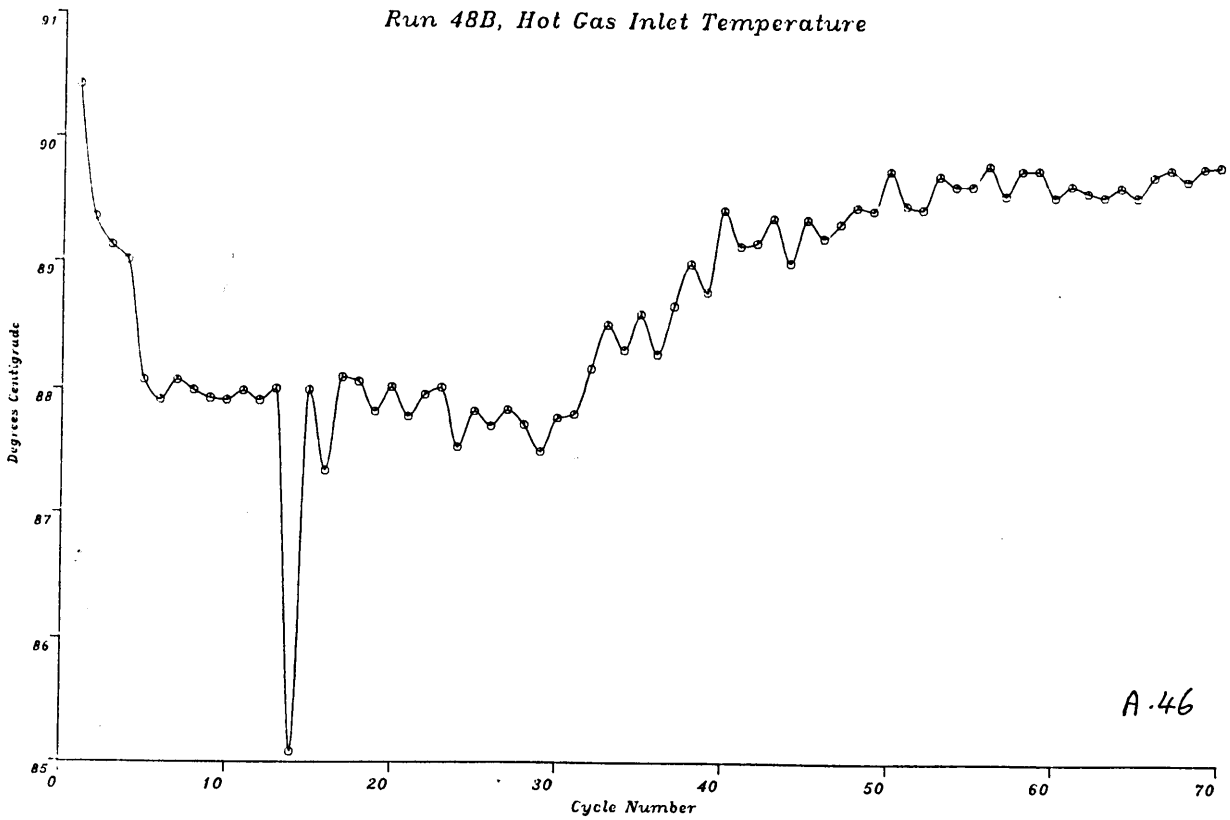
Run 48B, Hot Gas Inlet Temperature
Degrees Centigrade
91
90
89
88
87
86
85
0
10
20
30
40
50
60
70
Cycle Number
A.46

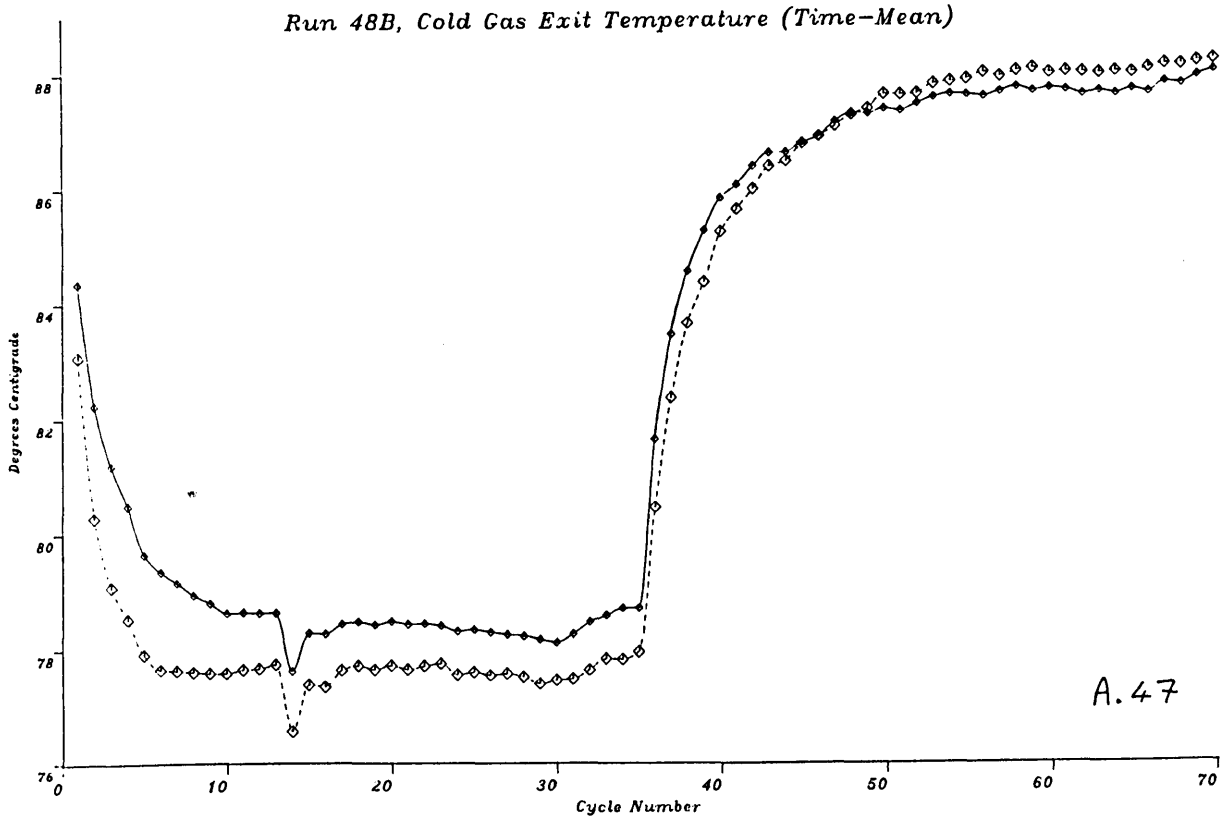
Run 48B, Cold Gas Exit Temperature (Time-Mean)
Degrees Centigrade
88
86
84
82
80
78
76
0
10
20
30
40
50
60
70
Cycle Number
A.47

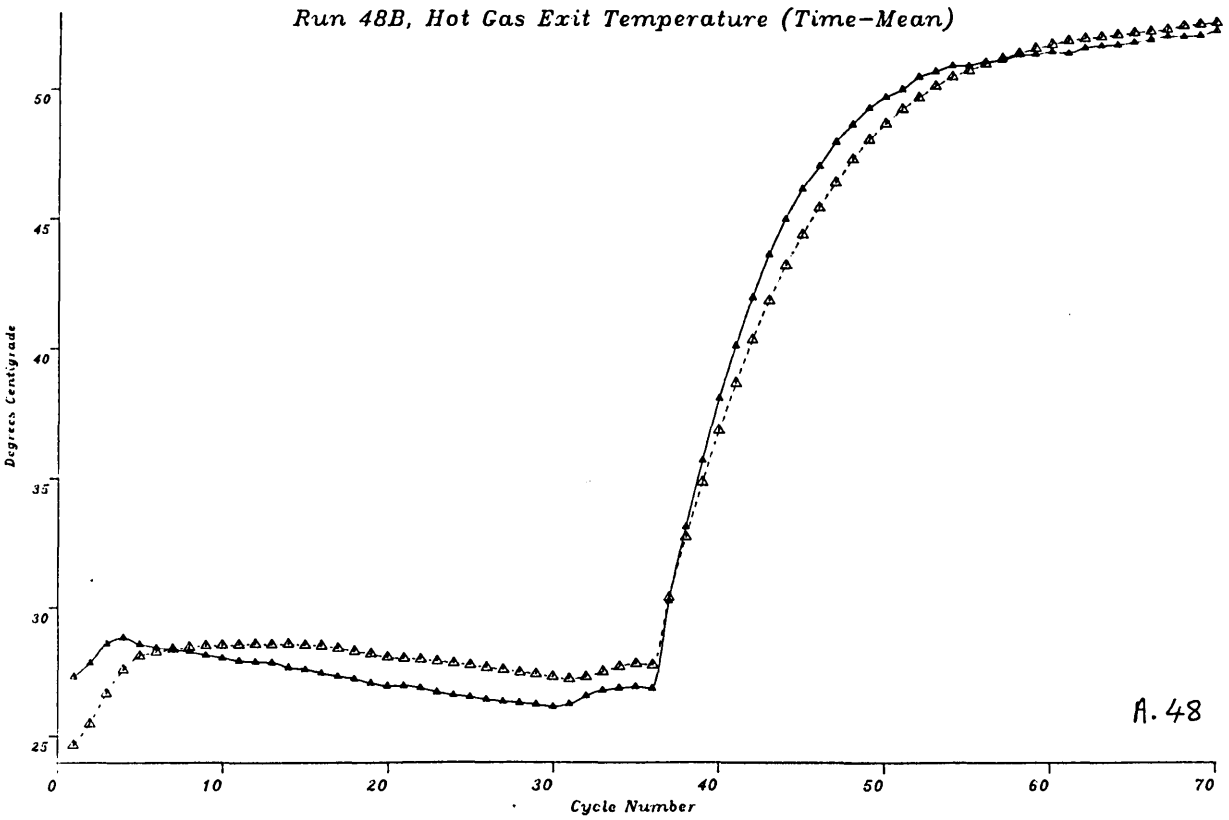
Run 48B, Hot Gas Exit Temperature (Time-Mean)
Degrees Centigrade
50
45
40
35
30
25
0
10
20
30
40
50
60
70
Cycle Number
A.48

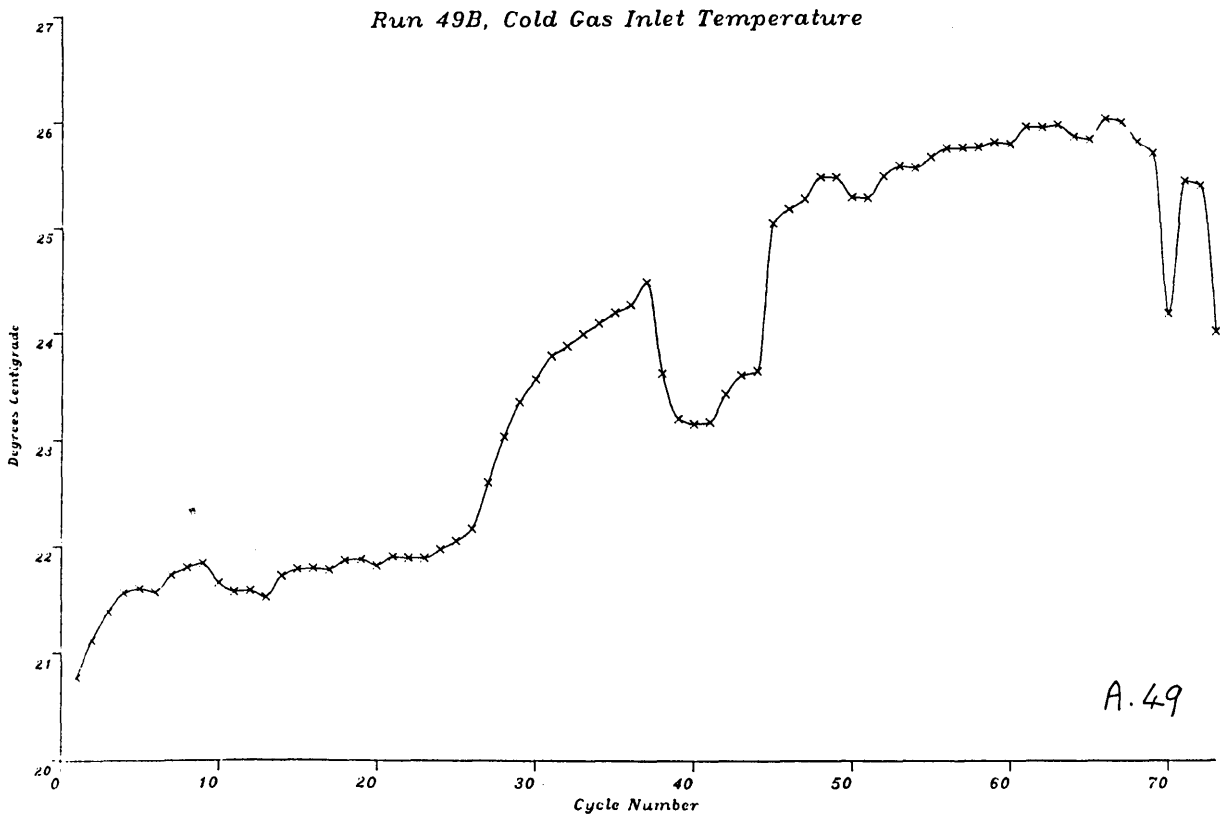
Run 49B, Cold Gas Inlet Temperature
Degrees Centigrade
27
26
25
24
23
22
21
20
0
10
20
30
40
50
60
70
Cycle Number
A.49

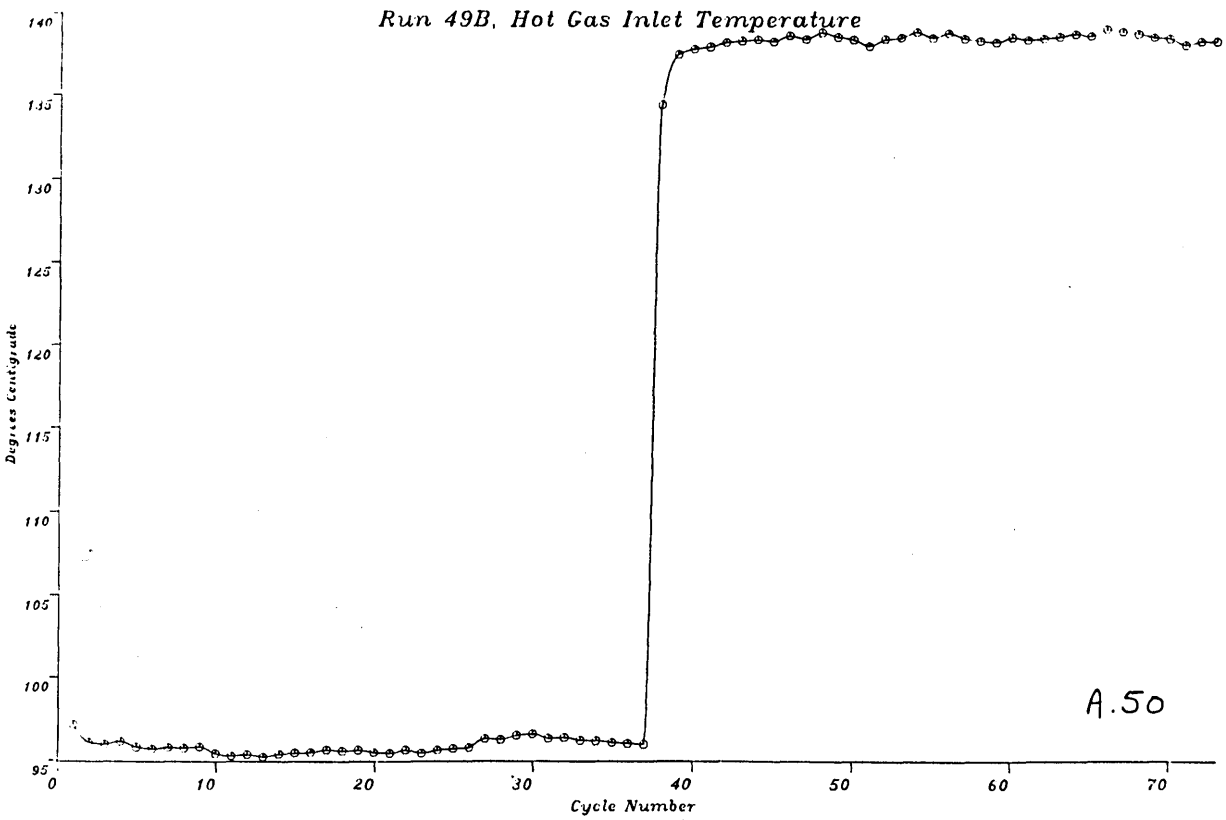
Run 49B, Hot Gas Inlet Temperature
Degrees Centigrade
140
135
130
125
120
115
110
105
100
95
0
10
20
30
40
50
60
70
Cycle Number
A.50

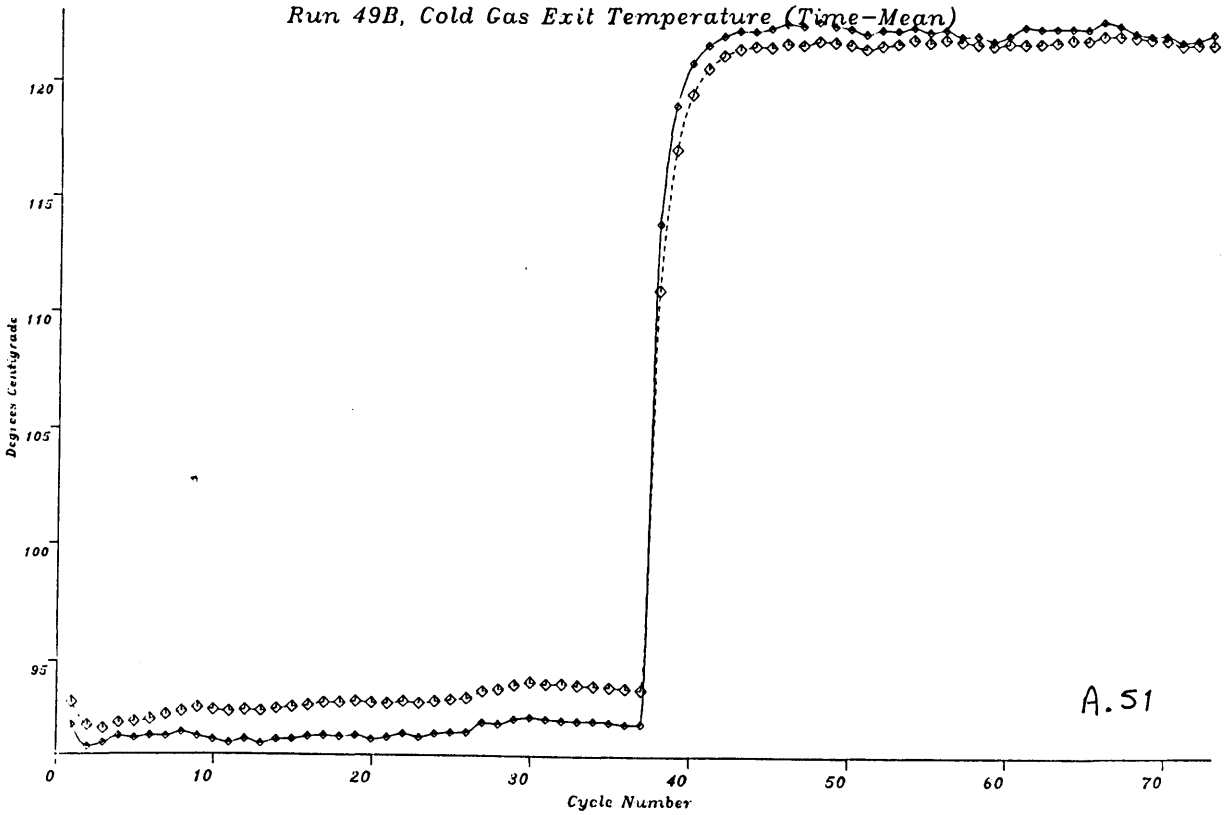
Run 49B, Cold Gas Exit Temperature (Time-Mean)
Degrees Centigrade
120
115
110
105
100
95
0
10
20
30
40
50
60
70
Cycle Number
A.51

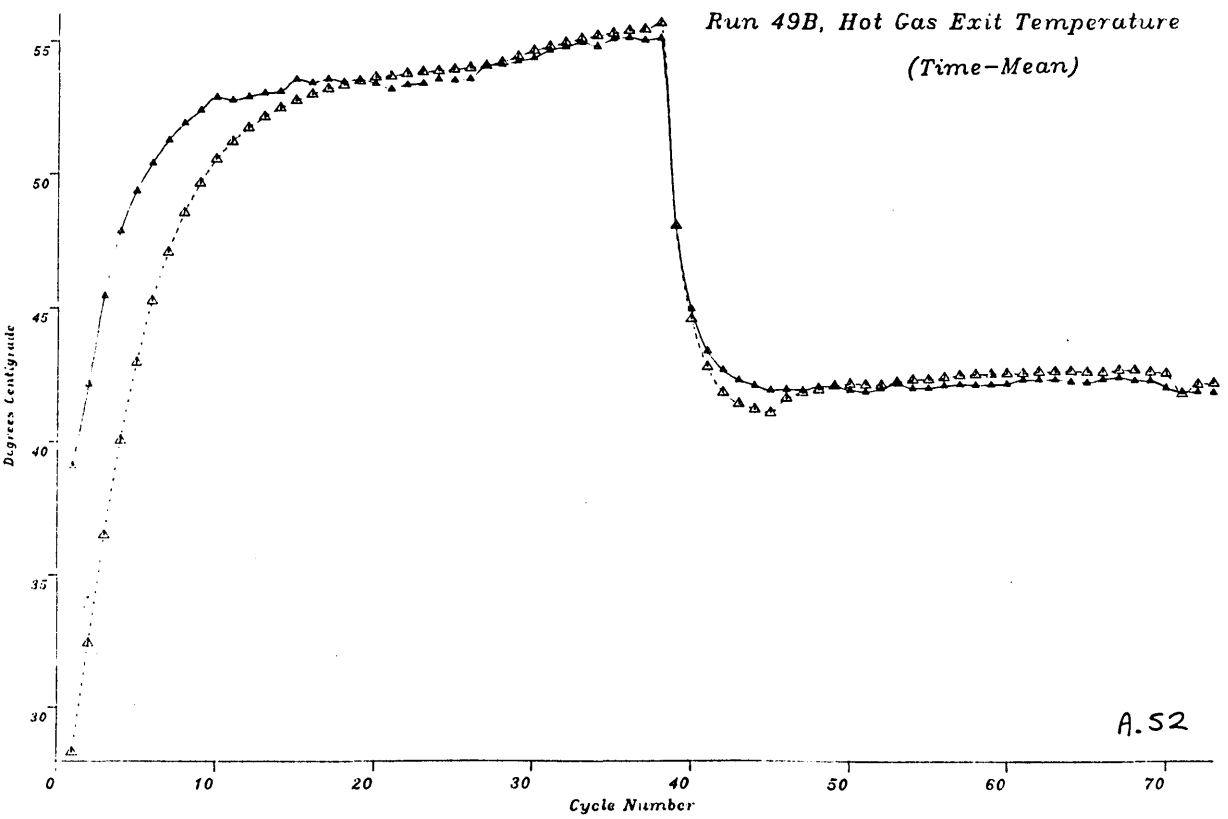
Run 49B, Hot Gas Exit Temperature
(Time-Mean)
Degrees Centigrade
55
50
45
40
35
30
0
10
20
30
40
50
60
70
Cycle Number
A.52

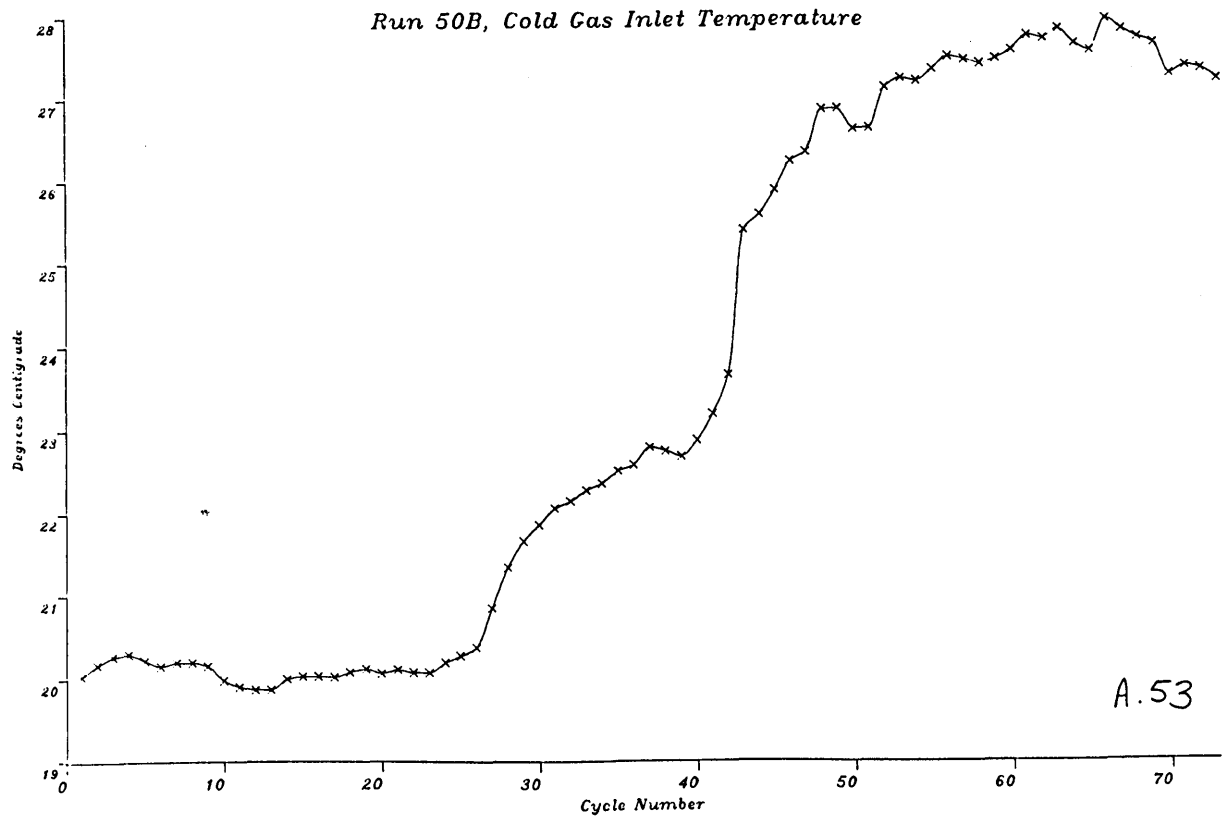
Run 50B, Cold Gas Inlet Temperature
Degrees Centigrade
28
27
26
25
24
23
22
21
20
19
0
10
20
30
40
50
60
70
Cycle Number
A.53

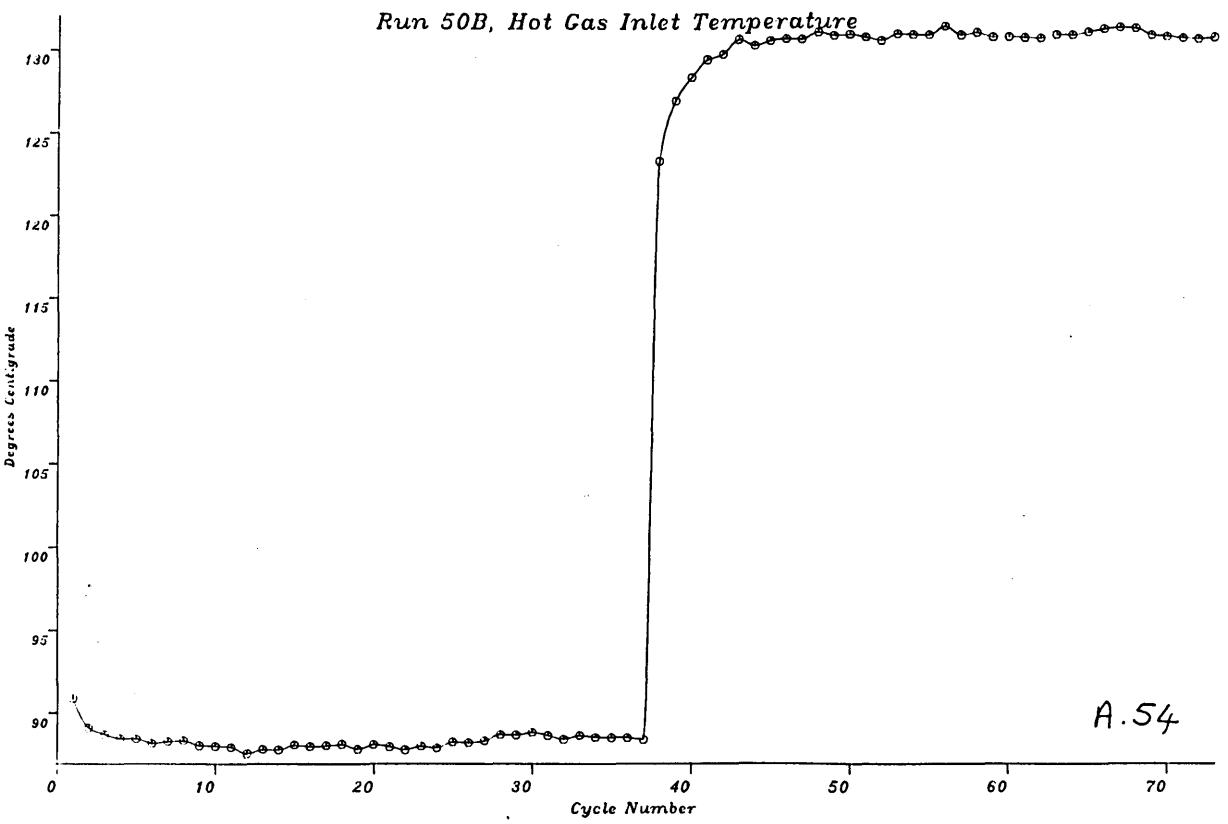
Run 50B, Hot Gas Inlet Temperature
Degrees Centigrade
130
125
120
115
110
105
100
95
90
0
10
20
30
40
50
60
70
Cycle Number
A.54

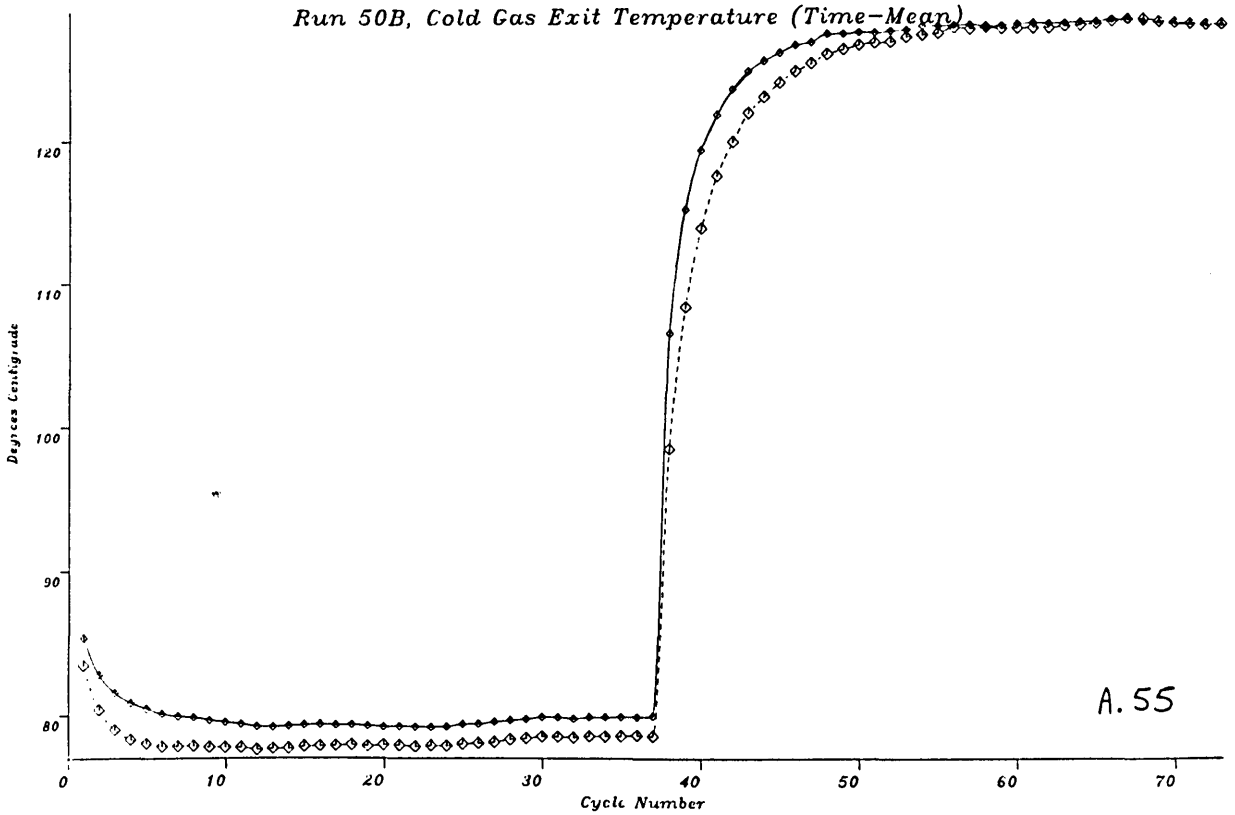
Run 50B, Cold Gas Exit Temperature (Time-Mean)
Degrees Centigrade
120
110
100
90
80
0
10
20
30
40
50
60
70
Cycle Number
A.55

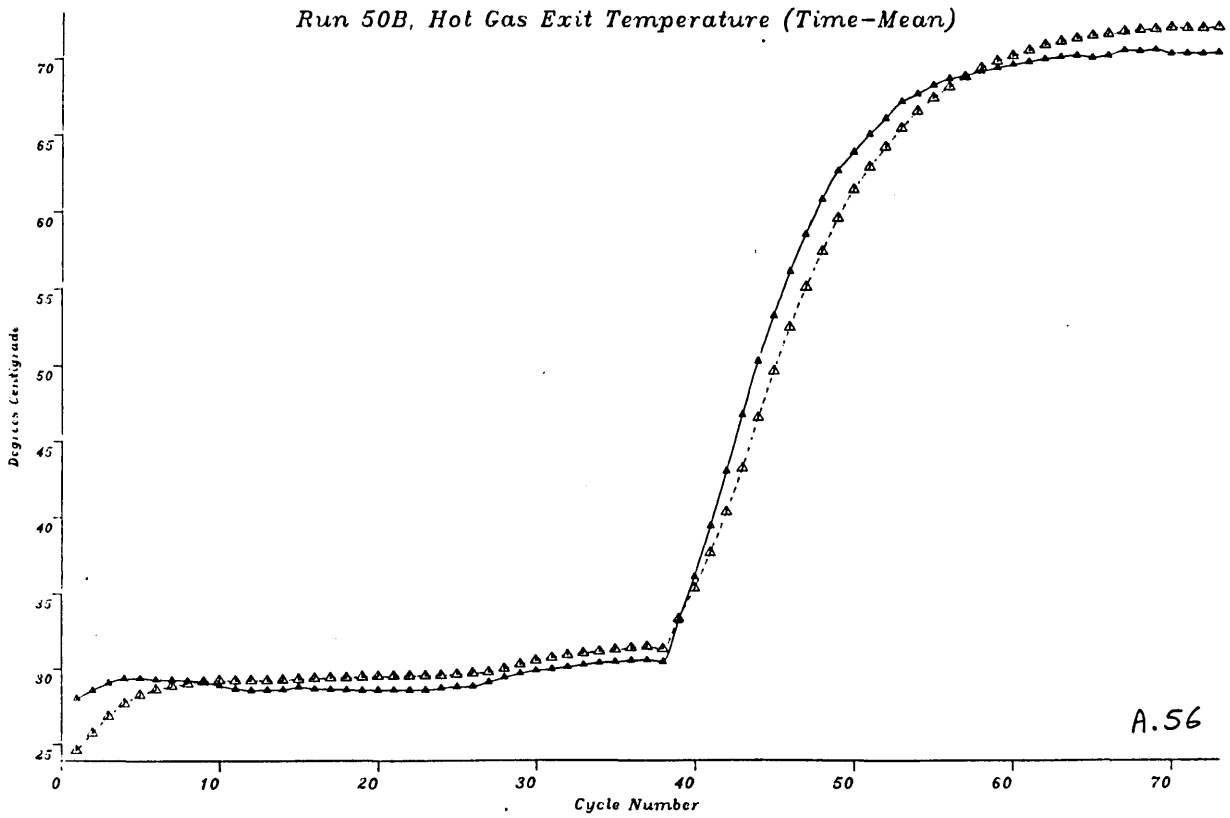
Run 50B, Hot Gas Exit Temperature (Time-Mean)
Degrees Centigrade
70
65
60
55
50
45
40
35
30
25
0
10
20
30
40
50
60
70
Cycle Number
A.56

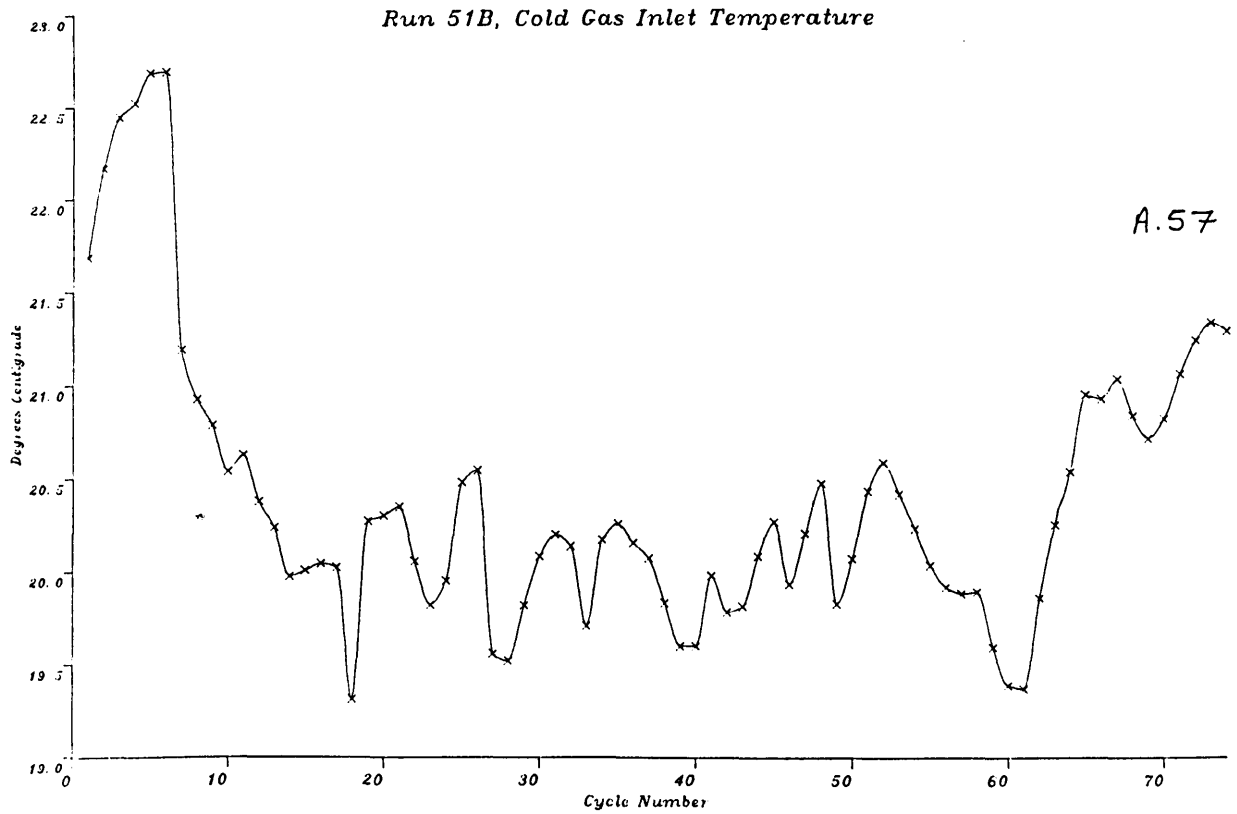
Run 51B, Cold Gas Inlet Temperature
A.57
Degrees Centigrade
23.0
22.5
22.0
21.5
21.0
20.5
20.0
19.5
19.0
0
10
20
30
40
50
60
70
Cycle Number

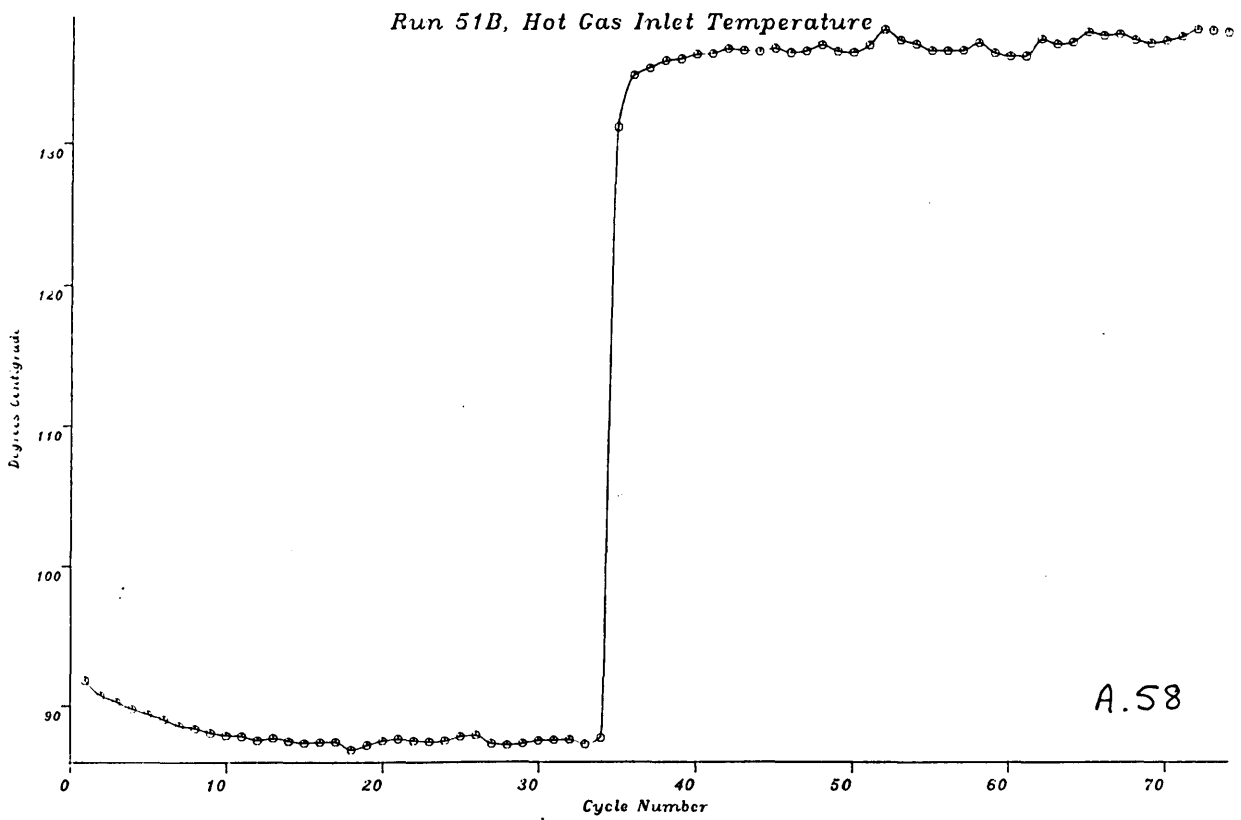
Run 51B, Hot Gas Inlet Temperature
A.58
Degrees Centigrade
130
120
110
100
90
0
10
20
30
40
50
60
70
Cycle Number

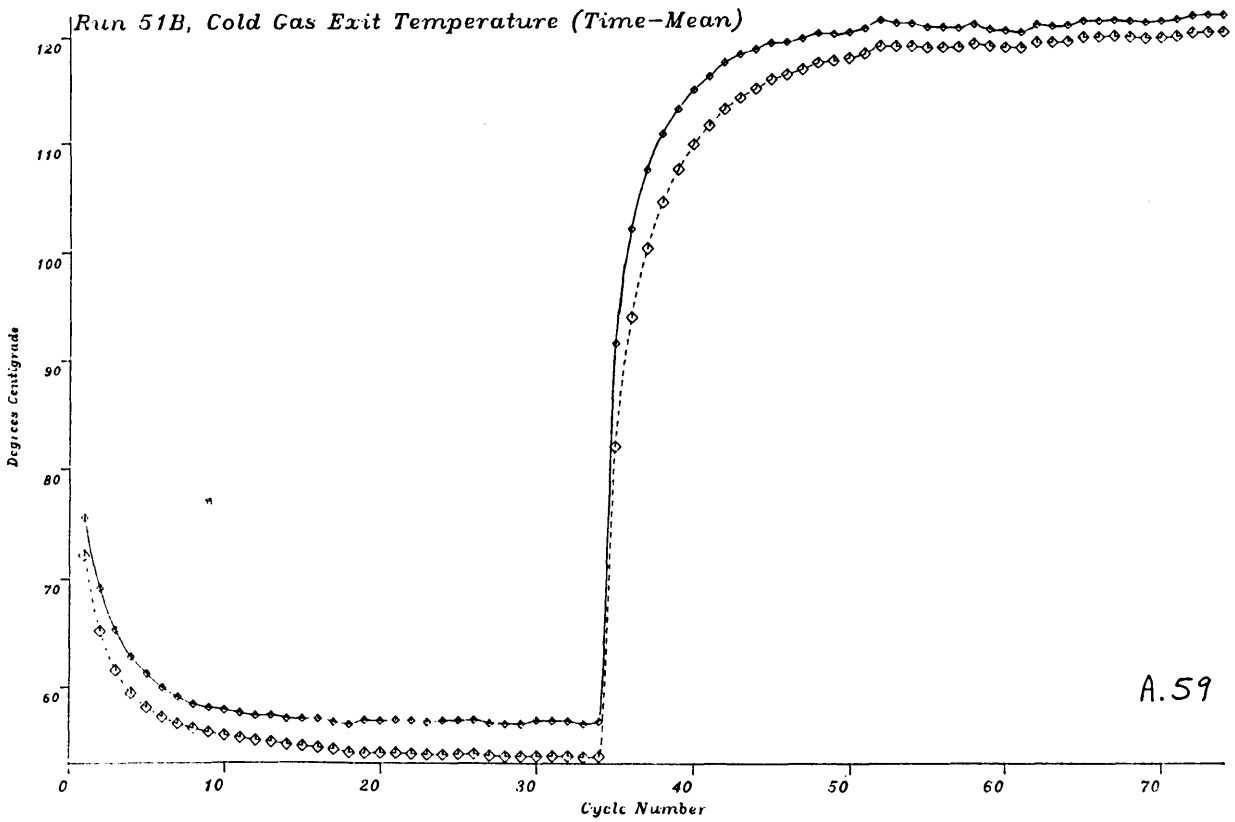
Run 51B, Cold Gas Exit Temperature (Time-Mean)
Degrees Centigrade
120
110
100
90
80
70
60
0
10
20
30
40
50
60
70
Cycle Number
A.59

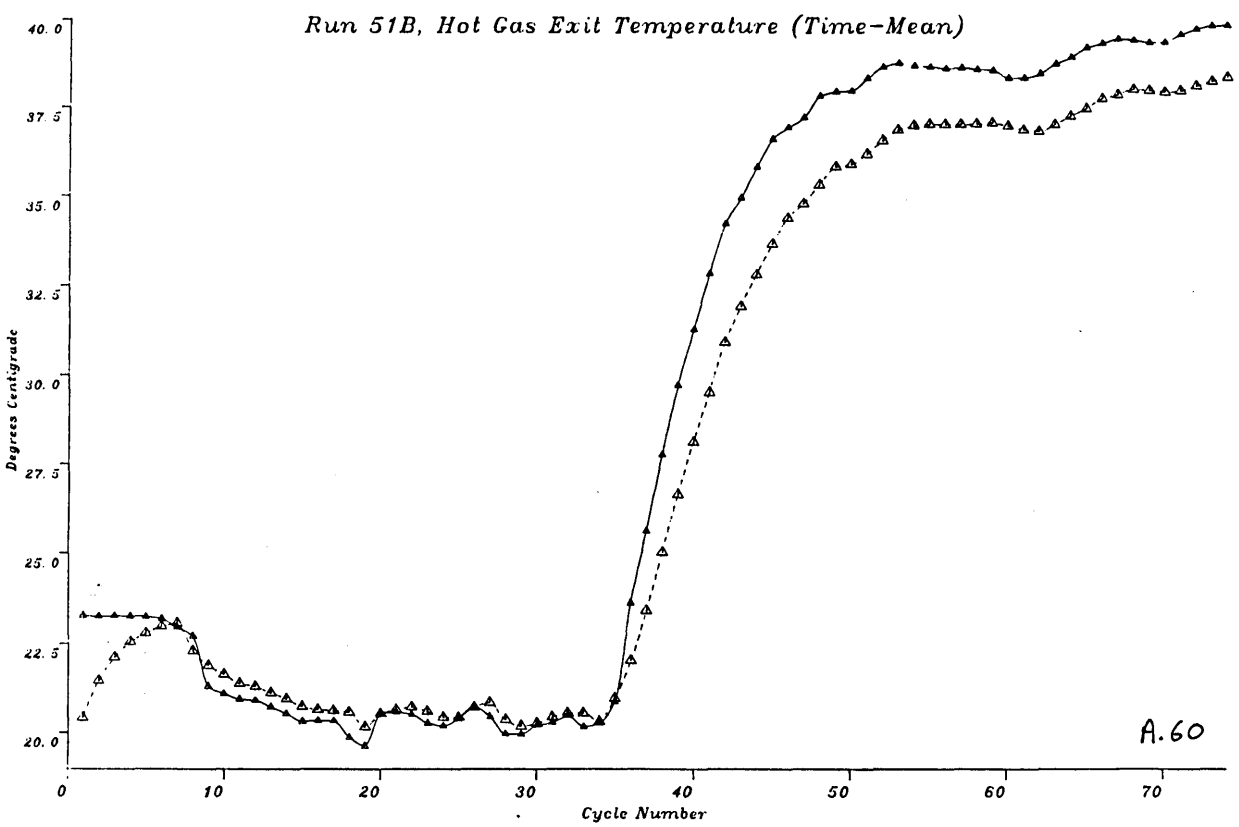
Run 51B, Hot Gas Exit Temperature (Time-Mean)
Degrees Centigrade
40.0
37.5
35.0
32.5
30.0
27.5
25.0
22.5
20.0
0
10
20
30
40
50
60
70
Cycle Number
A.60

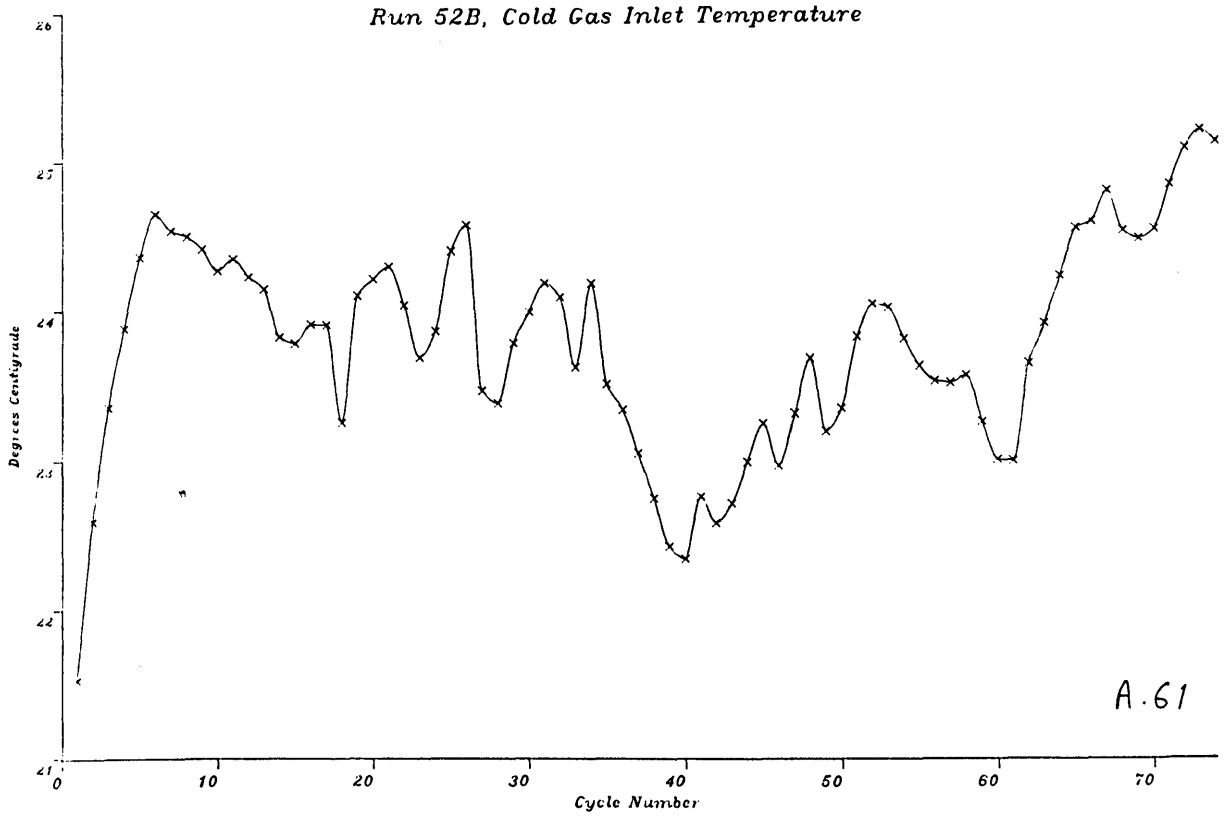
Run 52B, Cold Gas Inlet Temperature
Degrees Centigrade
26
25
24
23
22
21
0
10
20
30
40
50
60
70
Cycle Number
A.61

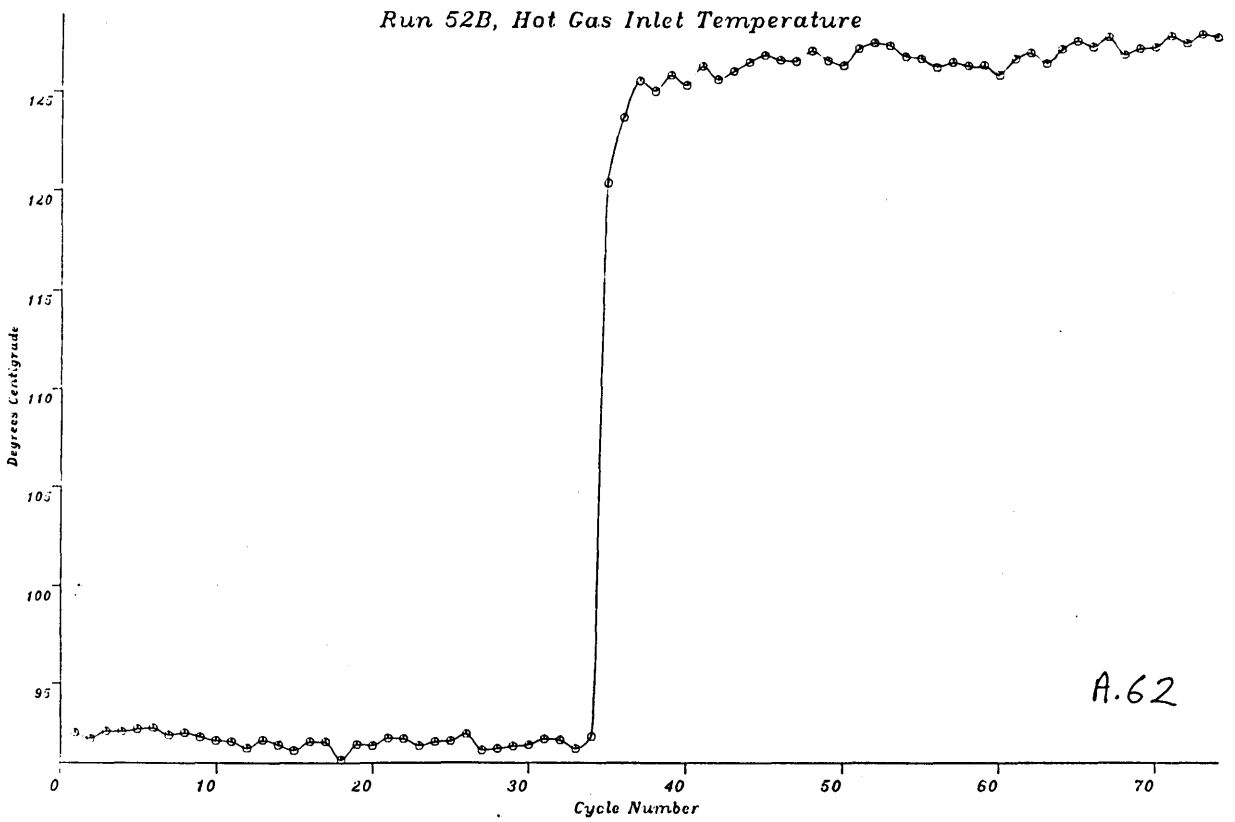
Run 52B, Hot Gas Inlet Temperature
Degrees Centigrade
125
120
115
110
105
100
95
0
10
20
30
40
50
60
70
Cycle Number
A.62

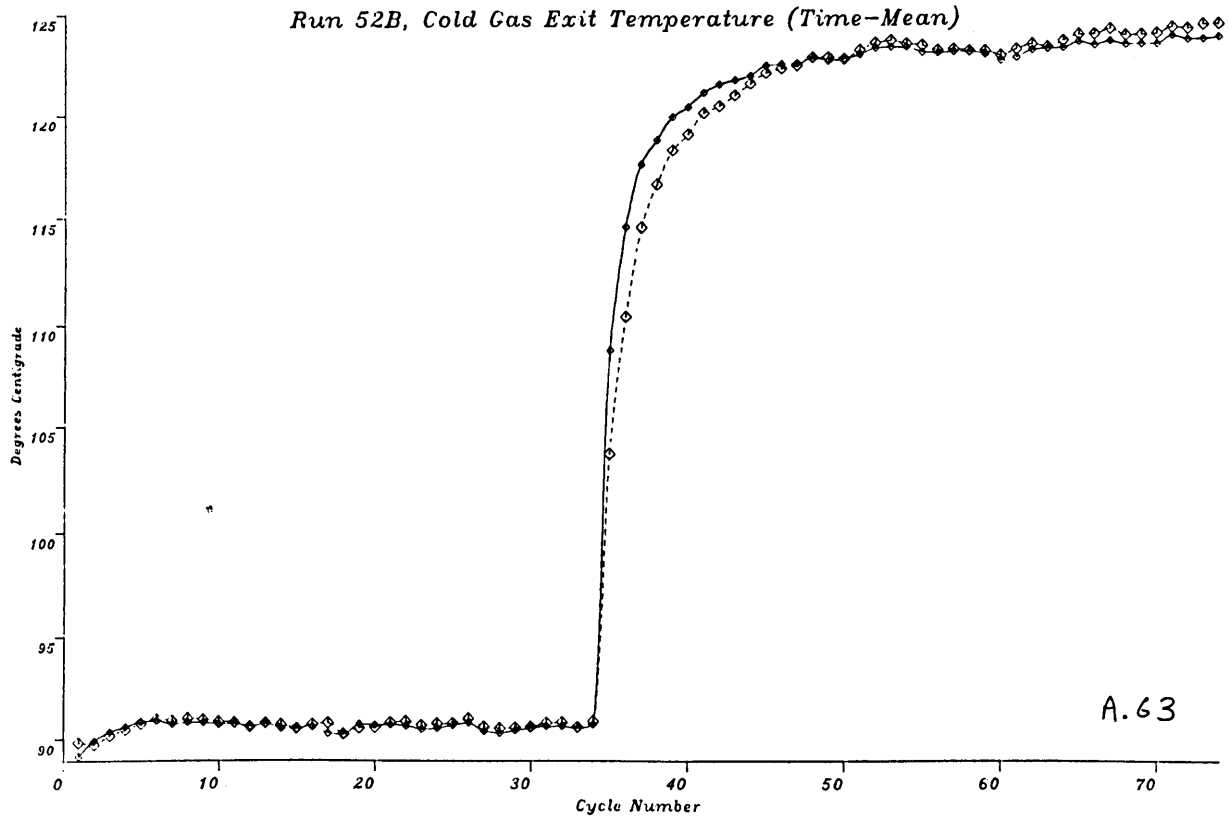
Run 52B, Cold Gas Exit Temperature (Time-Mean)
Degrees Centigrade
125
120
115
110
105
100
95
90
0
10
20
30
40
50
60
70
Cycle Number
A.63

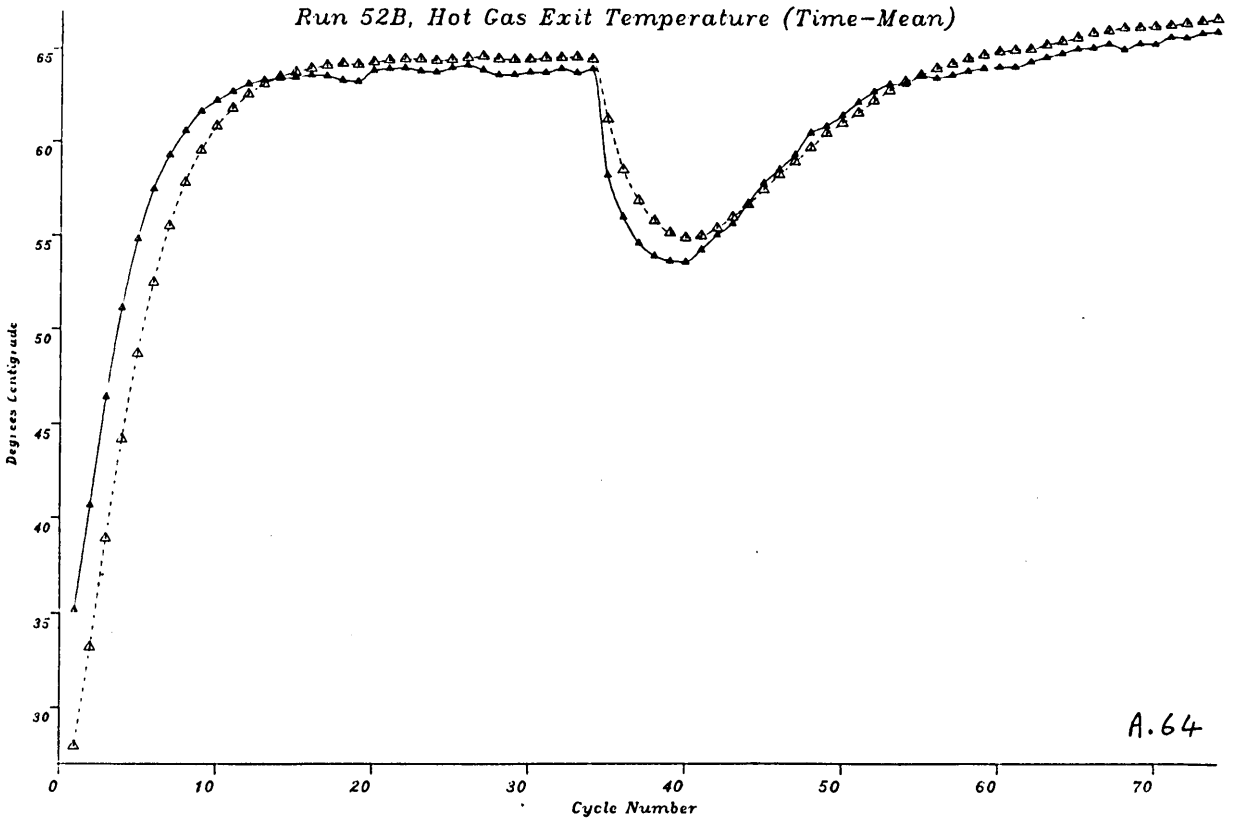
Run 52B, Hot Gas Exit Temperature (Time-Mean)
Degrees Centigrade
65
60
55
50
45
40
35
30
0
10
20
30
40
50
60
70
Cycle Number
A.64

APPENDIX B

HEAT LOSSES

The Pascal program used to produce the simulations incorporated heat losses. The effect of losses is introduced into Willmott's solution of the mathematical model as follows.

If heat loss occurs at rate $\dot{Q}$ watts, constant during a cycle, then equation 1.22 becomes

$$h A (t - T) = MC \frac{\partial T}{\partial \theta} + \dot{Q} \qquad (B.1)$$

which is equivalent to

$$\frac{\partial T}{\partial \theta} = \frac{h A}{MC} (t - T) - \frac{\dot{Q}}{MC} \qquad (B.2)$$

Making the usual substitution

$$\eta = \frac{h A \theta}{MC}$$

equation B.2 becomes

$$\frac{\partial T}{\partial \eta} = (t - T) - q \qquad (B.3)$$

where q = 'dimensionless' heat loss rate, units of temperature

$= \dot{Q}/hA$

The finite difference integration

$$T_{r,s+1} = T_{r,s} + \frac{\Delta\eta}{2}\left\{\left.\frac{\partial T}{\partial \eta}\right|_{r,s+1} + \left.\frac{\partial T}{\partial \eta}\right|_{r,s}\right\} \qquad (2.4)$$

now yields

$$T_{r,s+1}\left(1+\frac{\Delta\eta}{2}\right) = T_{r,s}\left(1-\frac{\Delta\eta}{2}\right) + \frac{\Delta\eta}{2}\left\{t_{r,s+1} + t_{r,s} - 2q\right\} \qquad (B.4)$$

which, after the substitutions made in Chapter 2, gives equation 2.11 with an additional term in q, thus:

$$T_{r,s+1} = B_1 T_{r,s} + B_2\left(t_{r,s+1} + t_{r,s} - 2q\right) \qquad (B.5)$$

The equivalent equation for the gas (derived in Chapter 2) is

$$t_{r,s+1} = A_1 t_{r-1,s+1} + A_2\left(T_{r,s+1} + T_{r-1,s+1}\right) \qquad (2.10)$$

Overall heat losses are included in the equation for the solid temperature, so there is no need for a term in q here. Substituting $t_{r,s+1}$ from 2.10 in B.5 gives

$$T_{r,s+1} = B_1 T_{r,s} + B_2\left[A_1 t_{r-1,s+1} + A_2\left(T_{r,s+1} + T_{r-1,s+1}\right) + t_{r,s} - 2q\right] \qquad (B.6)$$

which, after further collection of terms and constants becomes

$$T_{r,s+1} = K_1 T_{r,s} + K_2 t_{r,s} + K_3 T_{r-1,s+1} + K_4 t_{r-1,s+1} - 2B_2 q \qquad (B.7)$$

Hence this equation is used in place of equation 2.14, which omits the $2B_2q$ term.

The problem which remains is to determine the value of q. Consider the heat balance equation at cyclic equilibrium:

$$W'S'P'\left(t'_i - t'_{x,m}\right) = W''S''P''\left(t''_{x,m} - t''_i\right) \qquad (4.4)$$

If a heat loss of Q joules occurs over the hot-cold cycle, then

$$W'S'P'\Delta t' = W''S''P''\Delta t'' + Q \qquad (B.8)$$

For this thesis, $P' = P'' = P$ and $S' = S'' = S$, so

$$Q = S\,P\,(W'\Delta t' - W''\Delta t'') \qquad (B.9)$$

This heat is lost over 2P seconds, so the loss rate in watts is given by

$$\dot{Q} = \frac{S}{2}(W'\Delta t' - W''\Delta t'') \qquad (B.10)$$

Hence $\dot{Q}$ is found from experimental temperature data and used for the model in the form $q = \dot{Q}/hA$ in equation B.7.

It was found at a late stage of this research that the value of q used in the simulations was slightly erroneous. The simulation program evaluated h, then Λ and Π, and multiplied Λ and Π, rather than h, by the f-factor 0.85. The value of h used to find q from $\dot{Q}$ did not, therefore, incorporate the f-factor and it could be argued that q should have been 1/0.85 times the value actually used (a 17% increase). A typical value of $2B_2q$ was 0.17 (degrees Centigrade), and so a 17% increase gives $2B_2q = 0.20$. This small error in q can be ignored, as is confirmed by the discussion in section 4.1 of the effect of heat losses on the simulations.

APPENDIX C

CURVE FITTING

The program TUNER.PAS, which evaluated the heat transfer coefficient multiplication factor f, used a variable secant method to minimise the mean square difference between experimental and simulated exit temperatures. Assume that the experimental and simulated curves for $t''_{x,m}$ are as follows:

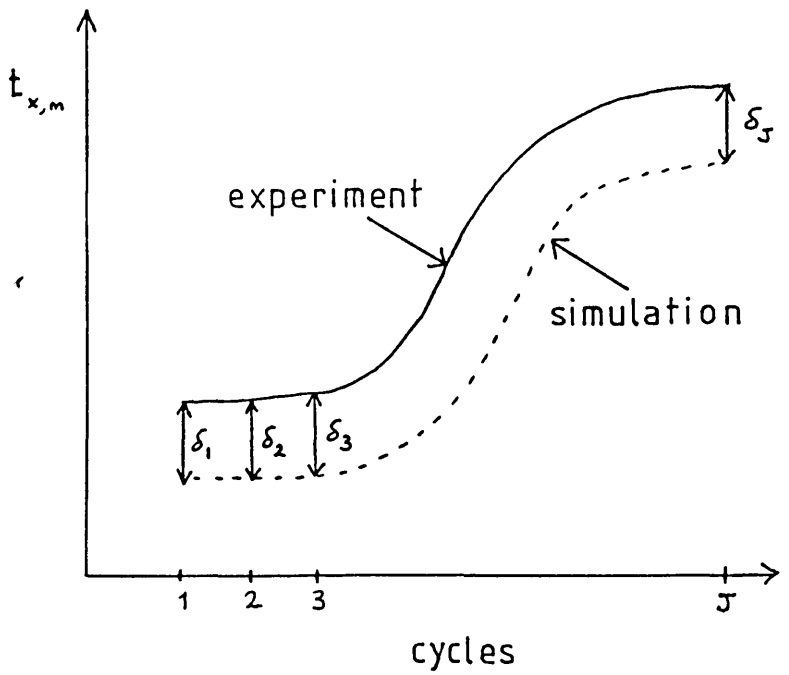

Introduce the simplifying notation $t_e = t''_{x,m}$ for experiment

$t_s = t''_{x,m}$ for simulation

For each cycle j (where $j \in \{1..J\}$), the quantity $\delta_j = t_{e,j} - t_{s,j}$ is evaluated, then squared to eliminate sign problems, and these δ_j^2 are summed over the whole run. The m.s.d., S, is given by

$$S = \frac{1}{J} \sum_{j=1}^{J} \delta_j^2 \qquad (C.1)$$

Now, if the heat transfer coefficient calculated for this simulation is multiplied by a factor f and the simulation run repeated, another S can be found. Hence a whole series of S as a function of f can be found, and the object is to find an f such that S(f) is a minimum. This is then the best fit of simulated to experimental curve.

The variable secant method for finding roots of functions assumes that S(f), $S'(f)$ and $S''(f)$ are continuous over an interval containing the root (or, in this case, the minimum). This is a valid assumption in this case, and providing that the starting value f_o is chosen sufficiently close to the root and that there is no maximum in the vicinity of the root, the iterates will converge. Graphically, the method is shown as below:

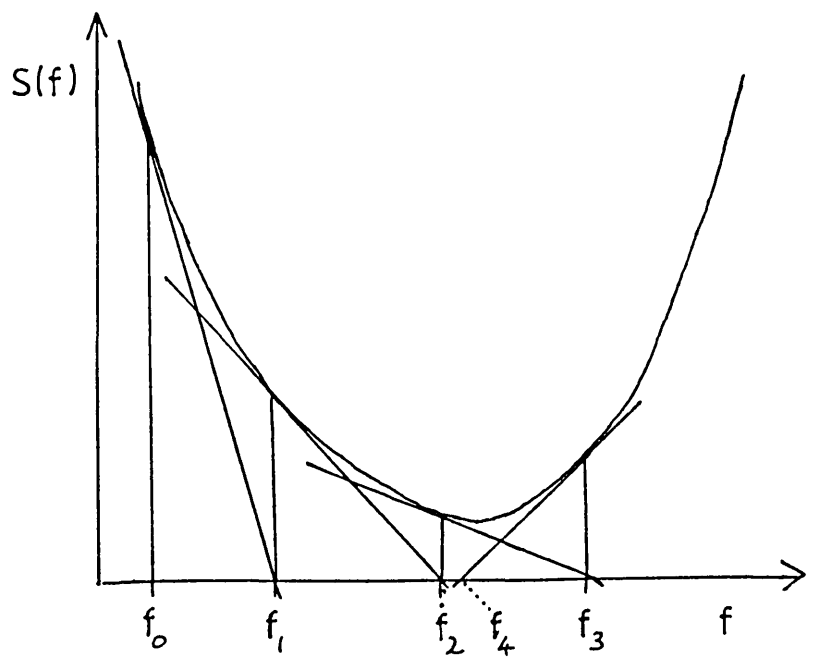

The tangent to the curve at $(f_n, S(f_n))$ is given by

$$S'(f_n) = \frac{S(f_n) - S(f_{n-1})}{f_n - f_{n-1}} \qquad (C.2)$$

and the next iterate, f_{n+1}, is given by

$$f_{n+1} = f_n - \frac{S(f_n)}{S'(f_n)} \qquad (C.3)$$

Substitution of C.2 in C.3 gives

$$f_{n+1} = f_n - S(f_n)\,\frac{f_n - f_{n-1}}{S(f_n) - S(f_{n-1})} \qquad (C.4)$$

Hence the basic procedure for minimising S, as used in the program, is as follows:

1) User inputs starting values f_0 and f_1
2) Evaluate Λ and Π, multiply by f and do a full simulation run for each starting value
3) Compute $S(f_0)$ and $S(f_1)$
4) Apply equation C.4 to find f_2
5) Multiply original Λ and Π by f_2
6) Do a simulation run
7) Compute S(f); if S(f) < (user-specified amount), then exit
8) Apply equation C.4 to find next f
9) Multiply original Λ and Π by this f; goto 6

In order to stop wild fluctuations in the iterates, the value for f computed at step 8 is not accepted if the change produced in f is greater than a user-specified fraction. In this instance, f is changed by this fraction only, and the user is informed of the trap occurrence.

This method of curve fitting is known as S_2 fitting, and was selected as being the most suitable. Alternate methods exist, such as S_∞ where the quantity to be minimised is

$$S_\infty = \max_{1..J} | t_{e,j} - t_{s,j} | \qquad (C.5)$$

i.e. the largest discrepancy is minimised. From the graphs in Appendix A it is apparent that, in many cases, S_∞ fitting would result in a smaller discrepancy in the middle portion of the curves at the expense of larger discrepancies at either end.

The program TUNER.PAS is reproduced in Appendix E.

APPENDIX D

RIG CONTROL SOFTWARE

There follow listings of two MUSIC programs, BOOT15.MUS and TRNS15.MUS. BOOT15.MUS is used to configure the system after a reload has been necessary, by defining the DLX groups and reading (from a separate papertape) the constants held in the X and Z arrays. It also allows output of these constants to the papertape punch. TRNS15.MUS is subsequently loaded, and accesses the constants whilst handling the experiment control and data recording. Despite the lack of explanatory comments in the listing (due to a memory space shortage), TRNS15.MUS is fairly straightforward once the variable usage has been understood. To this end, the usage of the X, and Z arrays and the unstructured variables A to U are now summarised. Some single elements of the X and Y array are also used as unstructured variables.

Simple (Unstructured) Variables

A regenerator number for graphical output of flowrates - set by user

B regenerator 2 bed top thermocouple (integrated reading)

C mass flowrate (std. m^3/min)

D regenerator 2 guide cone thermocouple (integrated reading)

E regenerator 1 bed top thermocouple (integrated reading)

F integral control constant for three term controller; dummy

argument for function calls; assigned 'hours' by FNE

G proportional control constant for three term controller; assigned 'minutes' by FNE

H assigned 'seconds' by FNE; temporary storage in flow control routine

I loop control variable

J counter for time-averaging of data

K loop control variable

L cycle number

M integration chopoff (seconds)

N temporary storage in flow control routine

O temporary storage in flow control routine

P derivative control constant for three term controller

Q temporary storage in flow control routine; warmup time (mins) in initialisation code

R temporary storage in flow control routine

S regenerator 1 guide cone thermocouple (integrated reading)

T reset rate (secs) for three term controller

U cold junction temperature (^{o}C) (integrated reading)

X(9) a.p.t. channel number

X(19) counter for time averaging of cold junction temperature

Y(1)-Y(4) flows 1-4, setpoints for next changeover (std. m^3/min)

Y(11)-Y(14) flows 1-4, 'snapshots' of measured mass flowrate from flow control routine

Y(21)-Y(24) flows 1-4, measured mass flowrates (integrated reading)

Y(31) regenerator 1 dome pipe thermocouple (integrated reading)

Y(32) regenerator 2 dome pipe thermocouple (integrated reading)

Y(33) regenerator 1 stack pipe thermocouple (integrated reading)

Y(34) regenerator 2 stack pipe thermocouple (integrated reading)

Y(35) regenerator 1 orifice plate (cold) thermocouple (integrated reading)

Y(36) regenerator 2 orifice plate (cold) thermocouple (integrated reading)

Y(37) regenerator 1 orifice plate (hot) thermocouple (integrated reading)

Y(38) regenerator 2 orifice plate (hot) thermocouple (integrated reading)

Various 'system variables' (preceded by '@') are also used as simple MUSIC variables in the flowrate control routine. These are as follows:

@A a.p.t. channel number

@B butterfly valve output channel number

@F flowrate correction thermocouple channel number

@N d.p.t. channel number

@S stop valve output channel number

V Array

Used by DLX for datalogging

W Array

Copy of the V array used by MUSIC; copied in line 37

X Array

Various constants for flows 0-8. For flow i:

X(i) c constants from flowrate calibration

X(i+10) m constants from flowrate calibration

X(i+20) g gradients for FF term

X(i+30) O_i intercepts for FF term

Z Array

Z contains other constants, and is also used as a workspace for the three term controller. For flow i:

Z(i) flowrate setpoint passed to three term controller

Z(i+10) last measured value of flowrate

Z(i+20) last-but-one measured value of flowrate

Z(i+30) last output to valve (FB term only)

Z(i+40) W_s saturation values of flowrate (for error trapping)

Z(i+50) orifice plate diameter (for reference)

Functions

FNA converts thermocouple millivoltage to °C, assuming 20°C cold junction temperature

FNB enables a DLX group after a specified time

FNC evaluates mas flowrate from transducer readings

FND halts a DLX group after a specified time

FNE converts 'seconds from now' to time of day F:G:H (hrs:mins:secs)

FNF assigns transducer and valve channel numbers for specified flow

FNG three term controller; evaluates FB term

FNH zeroes all time-averaged data variables

FNI evaluates time-mean for data variables

Program Description

Lines 1-18 consist of the experiment initialisation code, with checking for the condition (setpoint > saturation flow). Half-scale output is made to the two X-Y plotter channels for adjustment, and the DLX groups which control the experiment are enabled.

Lines 20-37 are the group 1 (flow control) code. This code is executed 9 times for each scan of group 1 (once for each flow), and calls FNG to evaluate the FB output. The FF term is added, the output made, and the hot and cold flowrates for regenerator 'A' are output to the X-Y plotter. 'Snapshots' of flows 1-4 are taken at lines 33-36, for later use. Finally a copy of the multiplexer data is taken in the W array.

Lines 50-58 (group 2) control output of data to the papertape punch after each cold period. The system variable @J is tested, and hence the user is informed (on the VDU) of any system crashes which have occurred. The data is averaged (line 53), then punched, and the flowrate setpoints are changed (line 56), to force a changeover by the group 1 code. The data variables are zeroed (line 57) and the integrating routine enabled for the following period.

Lines 60-66 (group 3) are the equivalent for the end of the hot period.

Lines 70-77 (group 4) perform the data averaging; every 2 seconds the current values of various thermocouple and flowrate readings (the 'snapshots' taken by group 1) are added to accumulator variables. A counter is incremented so that, at the end of each period, the accumulators can be divided by the counter to find the time-mean values.

Lines 80-82 (group 5) perform the same function for the cold junction temperature.

Lines 85-86 (group 6) print, on the VDU, information about the current state of flowrate control. This group is optionally enabled by the operator.

Lines 89-116 are the function definition block (see above).

The program listings follow.

```
5 REM " SYSTEM BOOTING SOFTWARE, VERSION BOOT15 "
10 REM " RELOAD X AND Z AND DEFINE DLX GROUPS "
15 FORJ(0,3):FORI(0,8):X(I+10*J)=INPUT1:NEXI:NEXJ
20 FORJ(4,5):FORI(0,8):Z(I+10*J)=INPUT1:NEXI:NEXJ
25 $G1 C0-54 I::2 R2 M0 J20$
30 $G2 W0-0 I:10:0 R6 M0 J50$
35 $G3 W0-0 I:10:0 R6 M0 J60$
40 $G4 W0-54 I::2 R6 M0 J70$
45 $G5 C56-56 I:1:0 R2 M0 J80$
50 $G6 W0-0 I::10 R6 M0 J85$
55 QUIT
60
80 REM " PUNCH X AND Z "
85 @P=1:FORJ(0,3):FORI(0,8):PRINT X(I+10*J):NEXI:NEXJ
90 FORJ(4,5):FORI(0,8):PRINT Z(I+10*J):NEXI:NEXJ:@P=0
95 QUIT
```

```
1 REM " EXPERIMENT CONTROL SOFTWARE, VERSION TRNS15 "
2 REM " EXPERIMENT INITIALISATION "
3 J=FNH:@J=1:Z(0)=0:FORK(10,38):Z(K)=0:NEXK
4 @P=0:PRINT"POWER UP PTP":PRINT"HOT PERIOD (MINS)":Y(6)=60*INPUT0
5 PRINT"COLD PERIOD (MINS)":Y(5)=60*INPUT0
6 PRINT"WARMUP PERIOD (MINS)":0=60*INPUT0
7 PRINT"INTEGRATION CHOPOFF (SECS)":M=INPUT0
8 PRINT"BED 1 FLOWRATES (H,C) (M^3/MIN)":Y(2)=INPUT0:Y(1)=INPUT0
9 IFGZ(Y(2)-Z(42)):GO 18
10 IFGZ(Y(1)-Z(41)):GO 18
11 PRINT"BED 2 FLOWRATES (H,C) (M^3/MIN)":Y(4)=INPUT0:Y(3)=INPUT0
12 IFGZ(Y(4)-Z(44)):GO 18
13 IFGZ(Y(3)-Z(43)):GO 18
14 Z(1)=0:Z(2)=Y(2):Z(3)=0:Z(4)=Y(4):Z(7)=Y(1):Z(8)=0:Z(5)=Y(3):Z(6)=0
15 DWOUT(20,127):DWOUT(22,127):A=99:PRINT"PENS HALF-SCALE THEN SET A"
16 T=FNE(Y(5)+Y(6)):$G2I(F):(G):(H)$:$G3I(F):(G):(H)$
17 L=FNB(2,G):L=FNB(3,0+Y(6)):L=FNB(5,0):$E1@$:QUIT
18 PRINT"FLOWRATE TOO HIGH":QUIT
19
20 REM " GROUP 1; FLOW CONTROL "
21 G=1.5:F=9:P=0:T=2
22 FORI(0,8):R=Z(I):@N=FNF(I):X(9)=V(@A):IFZ(FRA(I/2)):X(9)=0
23 C=FNC(V(@N),V(@F),X(9),X(I),X(I+10)):IFGZ(R):GO 25
24 O=0:0=0:N=0:H=0:GO 29
25 N=Z(I+10):H=Z(I+20):O=Z(I+30)
26 O=FNG(0):IFGZ(I):DBOUT(@S,0)
27 O=R/X(I+20)+X(I+30)+0:IFGZ(0-255):0=255
28 IFLZ(G):G=0
29 DWOUT(@B,Q):IFZ(R):IFGZ(I):DBOUT(@S,1)
30 Z(I+10)=C:Z(I+20)=N:Z(I+30)=0
31 IFZ(I-(2*A-1)):DWOUT(20,255*C)
32 IFZ(I-2*A):DWOUT(22,255*C)
33 IFZ(I-1):Y(11)=C
34 IFZ(I-2):Y(12)=C
35 IFZ(I-3):Y(13)=C
36 IFZ(I-4):Y(14)=C
37 NEXI:[W(@)=V(@)]:QUIT
38
50 REM " GROUP 2; END OF COLD PERIOD DATA OUTPUT "
51 @P=0:$T$:PRINT"CYCLE",L,"COMPLETED":IFZ(@J):PRINT"*** POWERFAIL FLAG ***"
52 IFZ(L):GO 56
53 F=FNI
54 @P=1:PRINT L,U:PRINT Y(21),Y(33),Y(35),E,S,Y(31)
55 PRINT Y(23),Y(34),Y(36),H,D,Y(32):@P=0
56 Z(1)=0:Z(2)=Y(2):Z(3)=0:Z(4)=Y(4):Z(7)=Y(1):Z(8)=0:Z(5)=Y(3):Z(6)=0
57 J=FNH
58 F=FNB(4,M):F=FND(4,Y(6)-M):L=L+1:QUIT
59
60 REM " GROUP 3; END OF HOT PERIOD DATA OUTPUT "
61 @P=0:PRINT"":F=FNI
62 @P=1:PRINT L,U:PRINT Y(22),E,S,Y(31),Y(33),Y(37)
63 PRINT Y(24),H,D,Y(32),Y(34),Y(38):@P=0
64 Z(1)=Y(1):Z(2)=0:Z(3)=Y(3):Z(4)=0:Z(7)=0:Z(8)=Y(2):Z(5)=0:Z(6)=Y(4)
65 J=FNH
66 F=FNB(4,M):F=FND(4,Y(5)-M):QUIT
67
70 REM " GROUP 4; TEMPERATURE INTEGRATION, BOTH PERIODS "
71 J=J+1
72 E=E+W(9):S=S+W(8):Y(31)=Y(31)+W(1)
73 Y(33)=Y(33)+W(4):Y(35)=Y(35)+W(2):Y(37)=Y(37)+W(3)
```

```
74 B=B+W(21):D=D+W(20):Y(32)=Y(32)+W(13)
75 Y(34)=Y(34)+W(16):Y(36)=Y(36)+W(14):Y(38)=Y(38)+W(15)
76 FORK(1,4):Y(20+K)=Y(20+K)+Y(10+K):NEXK
77 QUIT
78
80 REM " GROUP 5; COLD JUNCTION TEMPERATURE INTEGRATOR "
81 X(19)=X(19)+1:U=U+V(0)
82 QUIT
83
85 REM " GROUP 6; FLOW CONTROL MONITOR "
86 FORK(0,8):PRINT K,Z(K),Z(K+10),Z(K+20),Z(K+30),Z(K+40):NEXK:PRINT:QUIT
87
89 REM " FUNCTION DEFINITION BLOCK "
90 DEF FNA:IFLZ(ARG1):GO 93
91 F=-.03998+SQR(.03998^2+4*.0000324*(.02543+ARG1))
92 RETURN(F/(2*.0000324)+20)
93 ARG1=-ARG1
94 F=-.03998+SQR(.03998^2+1*.0000324*(.02543+ARG1))
95 RETURN(20-F/(2*.0000324))
96 DEF FNB:T=FNE(SEC0+ARG2):$E(ARG1)@(F):(G):(H)$:RETURN 0
97 DEF FNC:IFGZ(ARG1):GO 99
98 RETURN 0
99 RETURN(ARG4*EXP(ARG5*LOG(ARG1*(1+.0142*ARG3)/(1+.0798*ARG2))))
100 DEF FND:T=FNE(SEC0+ARG2):$H(ARG1)@(F):(G):(H)$:RETURN 0
101 DEF FNE:IFGZ(ARG1-86400):ARG1=ARG1-86400
102 F=INT(ARG1/3600):G=INT(ARG1/60-60*F):H=INT(ARG1-60*(G+60*F)):RETURN 0
105 DEF FNF:IFZ(ARG1):@D=16:@F=53:RETURN 48
106 @S=31+ARG1:@D=2*(ARG1-1):@F=3*@B+2:IFZ(FRA(ARG1/2)):@F=@F-5
107 IFNZ(FRA(ARG1/2)):@A=49:IFGZ(ARG1-4):@A=50
108 RETURN(@F+8)
110 DEF FNG:RETURN(O+G*(N-C)+F*T*(R-(C+N)/2)+P/T*(2*N-H-C))
112 DEF FNH:E=0:S=0:D=0:B=0:U=0:X(19)=0:FORK(20,40):Y(K)=0:NEXK:RETURN 0
115 DEF FN1:E=E/J:S=S/J:D=D/J:B=B/J:U=U/X(19)
116 FORK(20,40):Y(K)=Y(K)/J:NEXK:RETURN 0
```

APPENDIX E

PASCAL SIMULATION PROGRAM

The main simulation program resided in the DEC-10 file

DSKB:EXPSIM.PAS[1044,2155]

The program used to fit simulated to experimental results resided in

DSKB:TUNER.PAS[1044,2155]

The second program contained the first, almost in its entirety, packaged as PROCEDURE REGENERATE , so in order to save space and avoid repetition, only the second program is reproduced here.

To execute TUNER.PAS, the command is

/TUNER nnx

where nnx = experiment number, e.g. 37B

The execution of EXPSIM.PAS is described in the next appendix.

The structure of the program TUNER.PAS is shown overleaf. A listing of the program follows, and is self-documentary.

```
PROGRAM tuner

    FUNCTION sigma
    END sigma;

    FUNCTION raise
    external, in LIB.PAS
    END raise;

    PROCEDURE heatlossrate
    END heatlossrate;

    PROCEDURE regenerate

        PROCEDURE regparams
        calls raise
        END regparams;

        PROCEDURE cycle_once
        END cycle_once;

        PROCEDURE hot_cycle
        calls cycle_once
        END hot_cycle;

        PROCEDURE cold_cycle
        calls cycle_once
        END cold_cycle;

        PROCEDURE reverse_flow
        END reverse_flow;

        FUNCTION t_x_m
        END t_x_m;

        PROCEDURE stepsize
        END stepsize;

    calls regparams, stepsize, hot_cycle,
    t_x_m, reverse_flow, cold_cycle
    END regenerate;

calls heatlossrate, regenerate, sigma
END tuner.
```

```
PROGRAM tuner (input);

{ written by N.G. Cutland Feb 1982 and continuously modified thereafter

  Iteratively fits theoretical to experimental results, returning a multiplying
  factor, the f-factor, for the heat transfer coefficient

}

CONST lengthmax = 50;              { steps for AJW method }
      timemax = 50;                { ditto }
      maxcycles = 150;             { max no. of cycles in experimental run }
      maxsig = 1E20;               { stop overflow in PROC regenerate }
      regtest = false;             { set TRUE if debugging PROC regenerate }
      calltest = false;            { set TRUE if tracing execution sequence }
      tracetest = true;            { set TRUE if tracing behaviour of variable
                                     secant part }

TYPE profiletype = ARRAY[1..maxcycles] OF real;
     htc = (Denton, Yoshida, HandHeggs, Littman);

VAR i,                             { looper }
    iterations,                    { counter }
    max_iterns,                    { user-specified - max allowed attempts to find
                                     f-factor }
    totalcycles,                   { length of exptl run }
    m,                             { dist steps in AJW method }
    p,                             { time steps in AJW method }
    wu_durn,                       { warmup duration, multiples of hot reduced period }
    ignoredcycs,                   { no. of cycles to ignore at beginning of run }
    ans,                           { variables used to set up heat loss rate profiles... }
    cycle1,
    cycle2,
    losscycle,
    chcycle
         : integer;

    T_solid,                       { initial solid temp (uniform) }
    criterion,                     { least-square difference criterion }
    f,                             { f-factor this iteration }
    next_f,                        { proposed f-factor next iteration }
    last_f,                        { f-factor last iteration }
    S,                             { mean square difference using this f-factor }
    last_S,                        {   "    "      "      "     last     "     }
    q_h,                           { dimensionless heat loss rate, hot period }
    q_c,                           { ditto, cold period }
    period_c,                      { period durations (seconds) }
    period_h,
    hlrate,                        { heat loss rate for one cycle (watts) }
    dump,                          { skip unwanted input }
    maxchange : real;              { user-specified - max allowed single fractional change
                                     in f-factor }

    hlr,                           { heat loss rate profile (rate for each cycle) (watts) }
    W_h,                           { flowrate profiles }
    W_c,
    dlesshlr,                      { 'dimensionless' heat loss rate profile }
    h_i_prof,                      { exptly observed hot gas inlet temperature profile }
    c_i_prof,                      {   "      "    cold  "    "    "       "      "    }
    s_h_x_prof,                    { hot gas exit temp profile from simulation }

    s_c_x_prof,                    { cold  "    "    "     "      "       "     }
    e_h_x_prof,                    { experimentally observed hot gas exit temp profile }
    e_c_x_prof : profiletype;      {       "          "     cold  "   "    "      "   }

    reqd_htc : htc;                { user-specified, which h.t.c. to use }

    answer,                        { user's answers }
    h_or_c : char;                 { user-input - fit hot or cold side ? }

    input_ok,                      { flags invalid data input }
    manualoss,
    found,                         { indicates fit completed, f-factor found }
    errorflag,                     { indicates overflow imminent and causes a
                                     graceful crash! }
    hotflag : boolean;             { TRUE - fit hot side   FALSE - fit cold side }
```

```
FUNCTION sigma(init,final : integer; profile1, profile2 : profiletype;
               VAR error : boolean) : real;

{ Returns mean square difference of profile1 and profile2 over
  cycles 'init' to 'final' inclusive }

VAR i : integer;
    sig : real;

BEGIN
   IF calltest THEN writeln(tty, 'SIGMA called');
   error := false;
   i := init;
   sig := 0;
   WHILE (i <= final) AND (NOT error) DO
   BEGIN
      IF sig > maxsig - SQR(profile1[i] - profile2[i]) THEN
      BEGIN
         write(tty, '%ERROR - Overflow imminent... next sig =');
         writeln(tty, sig,' +',SQR(profile1[i] - profile2[i]));
         error := true;
      END
      ELSE sig := sig + SQR(profile1[i] - profile2[i]);
      i := i + 1;
   END;
   sigma := sig / (final - init + 1);
END;



FUNCTION raise (a,b : real) : real;   EXTERN;

{ raises a to the power b, with error trapping }


PROCEDURE heatlossrate(cyc:integer);

{ evaluates heat loss rate (W) for a given cycle }

CONST S = 1004.83;
      rho_0 = 1.2928;
      room_t = 20;
VAR flow_h,
    flow_c : real;

BEGIN
   flow_h := W_h[cyc] / 60 * rho_0 * 273/(room_t + 273);
   flow_c := W_c[cyc] / 60 * rho_0 * 273/(room_t + 273);
   hlrate := S/2 * (flow_h * (h_i_prof[cyc] - e_h_x_prof[cyc])
                  - flow_c * (e_c_x_prof[cyc] - c_i_prof[cyc]));
   IF hlrate < 0 THEN BEGIN
                         write(tty, 'Auto loss rate negative on cycle ');
                         writeln(tty, losscycle:1,' - assigned zero');
                         hlrate := 0;
                      END
   ELSE writeln(tty, 'Heat loss rate = ',hlrate,' W');
END;
```

```
PROCEDURE regenerate (factor : real);

{ alias PROGRAM expsim, packaged as a procedure}


{ Simulation of a thermal regenerator, based on Willmott's
1964 method. (J.Iron and Steel Inst.)}


{ Written by N. G. Cutland, Oct 1980
  Modified to accept step changes      1981
  Improved o/p of results    1981
  Accept continuous hot blowing warmup period Dec 1981
  O/p debugging information Dec 1981
  Accept time-varying gas inlet temps, ie modification to
  simulate experimental runs  Jan 1982
  Run with imbalance Feb 1982
  Incorporate heat losses Apr 1982
  Allow steps in flowrate via variable lambdas etc Apr 1982
  Evaluate lambda and pi every cycle from exptl data Sept 1982
  Allow user-selection of h.t.c. to use Feb 1983 and before
  Add another htc Mar 1983
  Improve heatloss treatment Oct 1983
  Packaged up as a procedure Dec 1983 (this version) }



CONST
      test = false;              { set this true when debugging program }
      dummy = 0;                 { used for padding out o/p files }

TYPE
     cyctype = (hot,cold);

VAR d_xi_c,                      { cold period length step size }
    d_xi_h,                      { ditto, hot period }
    d_eta_c,                     { cold period time step size }
    d_eta_h,                     { ditto, hot period }
    q,
    lambda_c,                    { cold period reduced length }
    lambda_h,                    { ditto, hot period }
    pi_c,                        { cold period reduced period }
    pi_h,                        { ditto, hot period }
    t_average,                   { mean of gas inlet and exit temps }
    a,                           { alpha }
    B,                           { beta }
    A1,                          { constants for eqns 7a and 9 }
    A2,
    B1,
    B2,
    K1,
    K2,
    K3,
    K4:
                real;
    r,                           { distance }
    s,                           { time }



    i,                           { general loop control variable }
    cyclenumber:                 { loop counter }
                integer;
    manualoss,                   { signifies user-input lossrates in force }
    warmup:                      { signifies warmup in progress }
                boolean;
    cycle:                       { signifies type of cycle }
                cyctype;
    t,                           { gas temperature space-time lattice }
    T_:                          { solid temperature space-time lattice }
                ARRAY [0..lengthmax,0..timemax] OF real;
```

```
PROCEDURE regparams(w_v_nom,P,t:real;reqd_htc:htc;VAR lambda,red_pi:real);

{ evaluates heat transfer coefficient, reduced length, reduced period,
  from experimental data.
  user selects which of 4 h.t.c.s to use }


CONST rho_0 = 1.2928;              { Density of air at 0 deg. c }
      room_t = 20;                 { Degrees c }
      pi = 3.14159;                { obvious }


VAR h,                             { Heat transfer coefficient }
    l,                             { Length of bed }
    D,                             { Diameter of packing particles }
    a,                             { Voidage fraction of bed }
    w_v_t,                         { Actual volume flowrate, i.e corrected to gas temp }
    V,                             { Linear velocity of gas in empty container }
    w_m,                           { Total mass flow rate of gas }
    G,                             { Mass flowrate per unit X-sectional area of
                                     empty container }
    nu,                            { Kinematic viscosity of gas }
    r,                             { Radius of bed }
    C,                             { Specific heat of packing material }
    S,                             { Specific heat of gas }
    rho_solid,                     { Density of packing material }
    rho_t,                         { Gas density at t deg. c }
    rho_room,                      { Gas density at 'room' deg. c }
    k,                             { Gas thermal conductivity }
    Re,                            { Reynolds number }
    Pr,                            { Prandtl number }
    Nus,                           { Nusselt number }
    j_H,                           { Colburn j-factor }
    SA_bed,                        { Total bed surface area for ht transfer }
    M_bed,                         { Mass of packing in bed }
    XA :                           { Cross-sectional area of empty container }
        real;



BEGIN              {regparams}
   l := 0.4;                       { m }
   D := 0.017;                     { m }
   a := 0.4125;
   r := 0.15;                      { m }
   C := 1130.44;                   { J/kg deg. c }
   S := 1004.83;                   { J/kg deg. c }
   rho_solid := 2480;              { kg/cu.m }

   { CALCULATIONS }

   XA := pi*r*r;
   M_bed := XA * l * (1-a) * rho_solid;
   SA_bed := 6/D * (1-a) * XA * l;
   rho_room := rho_0 * 273/(273+room_t);
   rho_t := rho_0 * 273/(273+t);
```

```
    w_v_nom := w_v_nom / 60;                        { convert to cu.m/sec }
    w_m := w_v_nom * rho_room;
    G := w_m / XA;
    w_v_t := w_v_nom * (273+t)/(273+room_t);
    V := w_v_t / XA;
    { NB w_m also = w_v_t * rho_t etc etc ... }
    nu := 0.0136/13 * t + 0.13;                     { deduced from Spiers P.159 }
    nu := nu / 10000;                               { convert to SI }
    k := 0.18E-4/100 * t + 0.58E-4;                 { deduced from Spiers P.224 }
    k := k * 4.1868 * 100;                          { convert to SI }
    P := P * 60;                                    { convert to secs }
    Pr := S * nu * rho_t / k;

    CASE reqd_htc OF

       Denton: BEGIN
                  Re := V * D / nu;
                  h := raise(Re, -0.3);
                  h := V * rho_t * S * 4.32 * (1-a)/D * h;
                  lambda := h * XA * l / (w_m * S);
                  re_pi := h * XA * l * P / (M_bed * C);
                  dlesshlr[cyclenumber] := hlr[cyclenumber] / (h * XA * l);
               END;

       Yoshida: BEGIN
                   Re := V * D / (6 * nu * (1-a));
                   IF Re < 50 THEN j_H := 0.91 * raise(Re, -0.51)
                              ELSE j_H := 0.61 * raise(Re, -0.41);
                   h := j_H * S * G / raise(Pr, 2/3);
                   lambda := h * SA_bed / (w_m * S);
                   red_pi := h * SA_bed * P / (M_bed * C);
                   dlesshlr[cyclenumber] := hlr[cyclenumber] / (h * SA_bed);
                END;

       HandHeggs: BEGIN
                     Re := 2/3 * D/(1-a) * V / nu;
                     j_H := 0.26 * raise(Re, -0.33) / a;
                     h := j_H * S * G / raise(Pr, 2/3);
                     lambda := h * SA_bed / (w_m * S);
                     red_pi := h * SA_bed * P / (M_bed * C);
                     dlesshlr[cyclenumber] := hlr[cyclenumber] / (h * SA_bed);
                  END;

       Littman: BEGIN
                   Re := V * D / nu;
                   Nus := 0.53 * raise(Re, 0.75);
                   h := k / D * Nus;
                   lambda := h * SA_bed / (w_m * S);
                   red_pi := h * SA_bed * P / (M_bed * C);
                   dlesshlr[cyclenumber] := hlr[cyclenumber] / (h * SA_bed);
                END;

       END;     (CASE)
END;    (regparams)
```

```
PROCEDURE cycle_once;
{ performs one cycle of operation, either hot or cold }

BEGIN
   FOR s:=1 TO p DO t[0,s]:=t[0,0];  { t[0,s] const for all s }
   FOR r:=0 TO m-1 DO t[r+1,0]:=A1*t[r,0]+A2*(T_[r+1,0]+T_[r,0]);
   FOR s:=0 TO p-1 DO T_[0,s+1]:=B1*T_[0,s]+B2*(t[0,s+1]+t[0,s]-2*q);

{ at this stage we have t[0,s] for all s, t[r,0] for all r,
T_[0,s] for all s, and T_[r,0] for all r.
Now compute all other values of t[r,s] and T_[r,s]... }

   FOR s:=0 TO p-1 DO            { do this for the whole period }
      FOR r:=1 TO m DO              { do this for the length of the reg. }
      BEGIN
         T_[r,s+1]:=K1*T_[r,s]+K2*t[r,s]+K3*T_[r-1,s+1]+K4*t[r-1,s+1]-2*B2*q;
         t[r,s+1]:=A1*t[r-1,s+1]+A2*(T_[r,s+1]+T_[r-1,s+1])
      END;



PROCEDURE hot_cycle;
{ initialises constants and heatloss rates for hot period, then calls cycle_once }

BEGIN
   a:=d_xi_h / 2.0;
   B:=d_eta_h / 2.0;     { define alpha & beta }
   A1:=(1-a)/(1+a);              { define A's B's and K's }
   A2:=a/(1+a);
   B1:=(1-B)/(1+B);
   B2:=B/(1+B);
   K1:=B1/(1-A2*B2);
   K2:=B2/(1-A2*B2);
   K3:=A2*B2/(1-A2*B2);
   K4:=A1*B2/(1-A2*B2);
   { assign heat loss rate }
   IF manualoss THEN q := q_h ELSE q := dlesshir[cyclenumber];
   { gas temp at entrance = hot gas inlet temp }
   t[0,0]:=h_i_prof[cyclenumber];
   IF test AND warmup THEN writeln(tty,'Hot_cycle called');
   cycle_once
END;



PROCEDURE cold_cycle;
{ initialises constants and heat loss rates for cold period then calls cycle_once }

BEGIN
   a:=d_xi_c / 2.0;
   B:=d_eta_c / 2.0;     { define alpha & beta }
   A1:=(1-a)/(1+a);              { define A's B's and K's }
   A2:=a/(1+a);
   B1:=(1-B)/(1+B);
   B2:=B/(1+B);
   K1:=B1/(1-A2*B2);
   K2:=B2/(1-A2*B2);
   K3:=A2*B2/(1-A2*B2);
   K4:=A1*B2/(1-A2*B2);
   { assign heat loss rate }
   IF manualoss THEN q := q_c ELSE q := dlesshir[cyclenumber];
   { gas temp at entrance = cold gas inlet temp }
   t[0,0]:=c_i_prof[cyclenumber];
   IF test AND warmup THEN writeln(tty,'Cold_cycle called');
   cycle_once
END;
```

```
PROCEDURE reverse_flow;
{ applies boundary condition between end of one period and start of another }

BEGIN
   { if warmup, continue blowing in same direction,
     otherwise reverse direction of flow }
   IF warmup THEN FOR r := 0 TO m DO T_[r,0] := T_[r,p]
   ELSE FOR r := 0 TO m DO T_[r,0] := T_[m-r,p];
END;




FUNCTION t_x_m: real;
{ evaluates the time mean exit gas temp. using Gregory's formula }

VAR sum:                { sum of exit gas temp for all time }
             real;
BEGIN
   sum:=0;
   FOR s:=1 TO p-1 DO sum:=sum + t[m,s];          { evaluate sum }
   t_x_m:=1/p*(0.5*t[m,0]+sum+0.5*t[m,p]-1/12*((t[m,p]-t[m,p-1])-(t[m,1]-t[m,0]))
   -1/24*((t[m,p]-t[m,p-1])-(t[m,p-1]-t[m,p-2])+(t[m,2]-t[m,1])-(t[m,1]-t[m,0]))
   -19/720*(((t[m,p]-t[m,p-1])-2*(t[m,p-1]-t[m,p-2])+(t[m,p-2]-t[m,p-3]))
   -((t[m,3]-t[m,2])-2*(t[m,2]-t[m,1])+(t[m,1]-t[m,0])));
        { Gregory's formula!! }
END;

      {



PROCEDURE stepsize(cyc :cyctype);
{ multiplies lambda and pi by f-factor and evaluates step sizes for the integration }

BEGIN
   CASE cyc OF
      hot : BEGIN
               lambda_h := factor * lambda_h;
               pi_h := factor * pi_h;
               d_xi_h := lambda_h / m;
               d_eta_h := pi_h / p;
            END;
      cold : BEGIN
               lambda_c := factor * lambda_c;
               pi_c := factor * pi_c;
               d_xi_c := lambda_c / m;
               d_eta_c := pi_c / p;
             END;
   END;
END;
```

```
{ ****** REGENERATE procedure body ****** }

BEGIN
   FOR r:=0 TO m DO T_[r,0]:=T_solid;     { initial temp profile }

   warmup := true;
   cyclenumber := 1;
   t_average := (h_i_prof[cyclenumber] + e_h_x_prof[cyclenumber]) / 2;
   regparams ( W_h[cyclenumber], Period_h, t_average, reqd_htc, lambda_h, pi_h );
   stepsize(hot);
   FOR i := 1 TO wu_durn DO              { warmup, continuous hot blow }
   BEGIN
      IF test THEN writeln(tty,'One warmup period');
      hot_cycle;
      reverse_flow;      { NB flow DIRECTION is not actually reversed...
                           see proc. reverse_flow }
   END;
   warmup := false;

   FOR cyclenumber := 1 TO totalcycles DO
   BEGIN
      t_average := (h_i_prof[cyclenumber] + e_h_x_prof[cyclenumber]) / 2;
      cycle := hot;
      regparams ( W_h[cyclenumber], Period_h, t_average, reqd_htc, lambda_h, pi_h );
      stepsize(hot);
      hot_cycle;
      s_h_x_prof[cyclenumber] := t_x_m;
      reverse_flow;
      t_average := ( c_i_prof[cyclenumber] + e_c_x_prof[cyclenumber] ) / 2;
      cycle := cold;
      regparams ( W_c[cyclenumber], Period_c, t_average, reqd_htc, lambda_c, pi_c );
      stepsize(cold);
      cold_cycle;
      s_c_x_prof[cyclenumber] := t_x_m;
      reverse_flow;
   END;

END;    { Regenerate }
```

```
{ *** TUNER main program *** }

BEGIN

   REPEAT
      input_ok:=true;
      writeln(tty);
      BEGIN
         write(tty,'Number of steps (distance,time) : ');
         read(tty,m,p);
         IF (m>50) OR (m<1) OR (p>50) OR (p<1) THEN
         BEGIN
            writeln(tty);
            writeln(tty,'?ERROR: 1 step min., 50 steps max.');
            writeln(tty);
            input_ok:=false
         END
      END
   UNTIL input_ok;

   write(tty,'Initial solid temp : ');
   read(tty,T_solid);

   write(tty,'Period durations (mins) , (cold, hot) : ');
   read(tty, Period_c, Period_h);

   write(tty,'Warmup duration, in multiples of Hot period duration : ');
   read(tty, wu_durn);

   write(tty, 'Number of cycles in inlet temperature profiles : ');
   read(tty, totalcycles);

   FOR i := 1 TO totalcycles DO
      read(input,dump,dump,W_h[i],h_i_prof[i],e_h_x_prof[i],dump,
                           W_c[i],c_i_prof[i],e_c_x_prof[i],dump);

   write(tty, 'Ignored cycles at beginning : ');
   read(tty, ignoredcycs);

   manualoss := false;
   write(tty, 'Heat losses; auto (1), manual (2) or zero (3) : ');
   read(tty, ans);

   CASE ans OF

      3 : FOR i := 1 TO totalcycles DO hlr[i] := 0;

      2 : BEGIN
             manualoss := true;
             write(tty, 'Dimensionless loss rates (cold, hot) : ');
             read(tty, q_c, q_h);
          END;

      1 : BEGIN
             cycle1 := 1;
             chcycle := 0;
             writeln(tty, 'Input cycle pairs, up to and including last cycle :-');
             WHILE chcycle < totalcycles DO
             BEGIN
                write(tty, 'Lossrate cycle, upto cycle : ');
```

```
                read(tty, losscycle, chcycle);
                heatlossrate(losscycle);
                FOR i := cycle1 TO chcycle DO hlr[i] := hlrate;
                cycle1 := chcycle + 1;
             END;    { WHILE }
          END;    { 3rd case }

   END;    { CASE }


   write(tty,'HTC to use; 1 = Denton, 2 = Yoshida, 3 = Mandley & Heggs, 4 = Littman: ');
   REPEAT read(tty, i) UNTIL i IN [1..4];
   CASE i OF
      1 : reqd_htc := Denton;
      2 : reqd_htc := Yoshida;
      3 : reqd_htc := MandHeggs;
      4 : reqd_htc := Littman;
   END;

   write(tty, 'Maximum allowed number of iterations : ');
   read(tty, max_iterns);

   write(tty, 'Maximum allowed single fractional change in f : ');
   read(tty, maxchange);

   write(tty, 'Evaluate f-factor for hot or cold side; (h/c) : ');
   REPEAT read(tty, h_or_c) UNTIL h_or_c IN ['h','H','c','C'];

   IF h_or_c IN ['h','H'] THEN hotflag := true ELSE hotflag := false;

   write(tty, 'Convergence criterion : ');
   read(tty, criterion);

   write(tty, 'Enter f0, f1 : ');
   read(tty, last_f, f);

   regenerate(last_f);
   iterations := 1;
   IF hotflag THEN
   last_S := sigma(ignoredcycs+1,totalcycles,e_h_x_prof,s_h_x_prof,errorflag)
   ELSE
   last_S := sigma(ignoredcycs+1,totalcycles,e_c_x_prof,s_c_x_prof,errorflag);
   IF tracetest THEN writeln(tty, 'f =',last_f,' S =',last_S);
   IF last_S <= criterion THEN
   BEGIN
      found := true;
      f := last_f;
      S := last_S;
   END
   ELSE found := false;

   WHILE (iterations < max_iterns) AND (NOT found) AND (NOT errorflag) DO
   BEGIN
      regenerate(f);
      IF hotflag THEN S := sigma(1,totalcycles,e_h_x_prof,s_h_x_prof,errorflag)
                 ELSE S := sigma(1,totalcycles,e_c_x_prof,s_c_x_prof,errorflag);
      iterations := iterations + 1;
      IF tracetest THEN writeln(tty,'f =',f,' S =',S);
      IF S <= criterion THEN found := true
      ELSE




      BEGIN
         next_f := f - (S * (f - last_f)/(S - last_S));
         last_f := f;
         last_S := S;
         IF ABS((next_f - f)/f) <= maxchange THEN f := next_f
         ELSE { don't allow wild fluctuations ...}
         BEGIN
            IF tracetest THEN writeln(tty, 'Large change in f-factor trapped');
            IF next_f > f THEN f := f + maxchange * f
            ELSE f := f - maxchange * f;
         END;
      END;
   END;
   IF NOT found THEN
   BEGIN
      writeln(tty,'No f-factor found after ',iterations:1,' iterations.');
      writeln(tty,' S =',S,', f =',last_f);
   END
   ELSE writeln(tty, 'S =',S,' after ',iterations:1,' iterations, giving f =',f);
END.
```

APPENDIX F

PROCESSING OF EXPERIMENTAL DATA

The 'help' file EXPTS.HLP is reproduced here. It contains instructions for the processing of data from the initial raw data stage up to the final plotting stage. The process is shown diagramatically in figures F.1 and F.2.

Procedure for processing experimental results is as follows:-

0) Split results into two separate files as follows:
   /SPLIT nnmm,v,switch
                        where nn and mm are the run numbers
(and input data is in file Rnnmm.DAT), v is the version i.e. A,B,C etc.,
and switch='nc' if no compilation is required.
For example, /SPLIT 74,75,b,nc will split file R7475.DAT into RES74B.DAT
and RES75B.DAT (without compiling SPLIT.PAS). Now continue with each output
file as a separate input file to the steps below.

1) Examine exptl data and note total number of cycles

Each line in file RESn.DAT has format

Cycleno. Muxtemp   Wh   thi   thx   Wc   tci   tcx

2) /PRELIM n,switch   where n = expt number, as in file RESn.DAT
                          switch = 'nc' if no compilation required, i.e. if
                                   .EXE file already exists

2a) /EXPSIM n,switch   (if a sim run is required)
    NB: steps 1 and 2 must be carried out previous to a sim run

3) /RANGE1 x,n,switch   where x = 'e' if exptl data
                                 x = 's' if sim run
   Record ranges for plotting

4) /PLOT1 n,switch   to plot experiment and sim files on one graph
   Examine graphs and note equilibrium exit temps

4a) /PLOT3 n,switch   to plot experiment files nA, nB, nC on one graph

4b) /PLOT4 n,switch   to plot experiment and sim files on graphics vdu
                         (with autoranging)

NB: The following files will be created,
    in addition to various .REL, .EXE files etc:-

XPRn.USR   (Header followed by temps)
XTn.TEM   (Temps only)
SPLOT1.LOG   (Log of SIMPLEPLOT transactions)

where X = 'E' if exptl data
      X = 'S' if sim run

Note that the programs PLOT1 and PLOT4 will plot from either or both of
'E' files and 'S' files. The program dialog requires the user to
specify which files to plot from, and providing he specifies according to
which files exist, everything will function correctly.
Hence no 'x' switch is required at step 4 or 7.

INITIAL SPLITTING :-

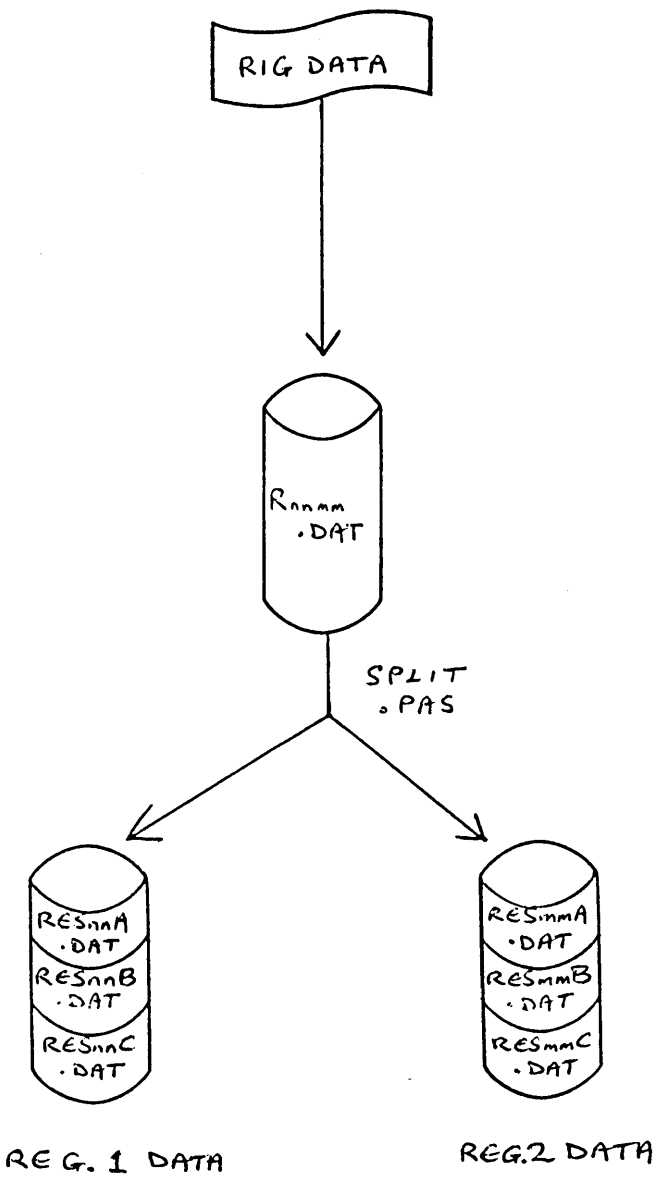

FIGURE F.1

EXPERIMENT DATA PROCESSING (1)

FOR EACH OF RESnnA.DAT,
RESnnB.DAT,
RESnnC.DAT :-

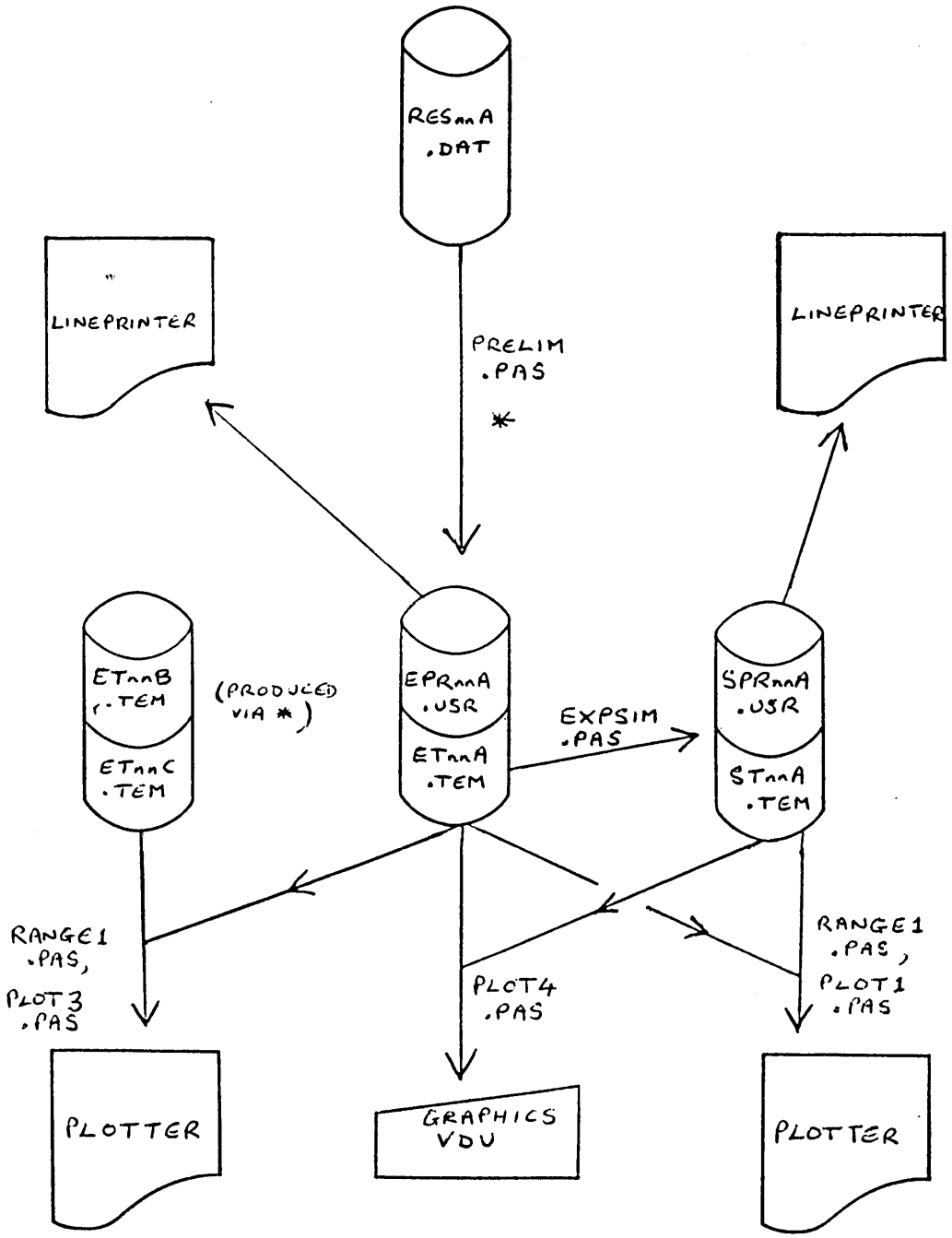

FIGURE F.2

EXPERIMENT DATA PROCESSING (2)

LIST OF REFERENCES

AFGAN and SCHLUNDER, Heat Exchangers: Design and Theory Sourcebook, McGraw-Hill, 1974

AJITSARIA N.K., Dynamic Response of Packed Bed Regenerators, Ph.D. Thesis, University of Bradford, 1973

ALLEN D.N. de G., The calculation of the efficiency of heat regenerators, Q. J. Mech. Appl. Maths, V(4), 456-461, 1952

BARKER J.J., Heat transfer in packed beds, Ind. and Eng. Chem., 57(4), 43-51, 1965

BEETS J. and ELSHOUT J., Control model for a hot-blast stoves system, International Meeting on Iron and Steel Making, Brussels, May 1976

BENENATI R.F. and BROSILOW C.B., Void fraction distribution in beds of spheres, A.I.Ch.E. J., 3, 359, 1962

BIRD, STEWART and LIGHTFOOT, Transport Phenomena, Wiley, 411, 1960

BROOKS S.F., Private communication, 1983

BURNS A., The Simulation and Control of Thermal Regenerators, D.Phil thesis, University of York, 1978

BURNS A. and WILLMOTT A.J., Transient performance of periodic flow regenerators, Int. J. Heat Mass Transfer, 21, 623-627, 1978

BUTTERFIELD P., SCHOFIELD J.S. and YOUNG P.A., Hot blast stoves, J. Iron Steel Inst., 199, 229-240, 1963

CHAO W.W., Research and development of an experimental rotary regenerator for automotive gas turbines, Proc. Am. Power Conf., 17, 358-374, 1955

CIMA R.M. and LONDON A.L., The transient response of a two-fluid counterflow heat exchanger - the gas-turbine regenerator, Trans. A.S.M.E., 80, 1169-1179, 1958

DENTON W.H., ROBINSON C.H. and TIBBS R.S., The heat transfer and pressure loss in fluid flow through randomly packed spheres, A.E.R.E Harwell report R4346(HPC35), 1963

DUNKLE R.V. and ELLUL W.M.J., Randomly-packed particulate bed regenerators and evaporative coolers, Mech. Chem. Eng. Trans. I.E. Aust, MC 8, No.2, 117-121, 1972

FURNAS C.C., Heat transfer from a gas stream to a bed of broken solids, Bull. U.S. Bureau of Mines, 1-87, 1932

GLIDDON B.J. and CRANFIELD R.R., Gas particle heat transfer coefficients in packed beds at Reynolds numbers between 2 and 100, Heat Transfer, 15(4), 481-482, 1970

GREEN D.R., Some Aspects of Hot Blast Stove Development and Operation, M.Sc. thesis, UMIST, 1967

HARTREE D.R., Numerical Analysis, OUP, 114, 1958

HAUSEN H., Berechnung der Steintemperature in Winderhitzern, Arch. Eisenuttes, 10, 474-480, 1938/1939

HAUSEN H., Vervollstandigte Berechnung des Warmeaustausches in Regeneratoren, Z. Ver. Deutch. Ing., Beiheft Verftk No.2, 31-43, 1942

HAUSEN H., Warmeaubertragung im Gegenstrom, Gleichstrom und Kreuzstrom, Springer-Verlag, Berlin, 1950

HAUSEN H., Heat Transfer in Counterflow, Parallel Flow and Cross Flow, McGraw-Hill, (Ed. A.J. WILLMOTT), 1983 (Translation of Hausen, 1950)

HAYNES A.B., The Simulation and Control by Digital Computer of a Thermal Regenerator, D.Phil thesis, University of York, 1973

HEGGS P.J. and HANDLEY D., Momentum and heat transfer mechanism in regular shaped packing, Trans. Inst. Chem. Eng., 46, 1968

HEGGS P.J. and MITCHELL S., The transient response of counterflow thermal regenerators, Regenerative and Recuperative Heat Exchangers, HTD Vol. 21, ASME, 1981

HENRICI P., Elements of Numerical Analysis, Wiley, 70-74, 1964

HILTON R.J., Private communication, 1983

HINCHCLIFFE C.E. and WILLMOTT A.J., Lumped heat-transfer coefficients for thermal regenerators, Int. J. Heat Mass Transfer, 24, 7, 1229-1236, 1981

HOLLINS S.J., Development of an apparatus to investigate the thermal characteristics of regenerative heat exchangers, Ph.D thesis, University of Leeds, 1981

HOLSTEIN C. and SANNA D., Conduite automatique d'une batterie de Cowpers, Societe Lorraine de Laminage Continu (SOLLAC), 1978 (English translation N.G. CUTLAND 1980)

ILIFFE C.E., Thermal analysis of the contra-flow regenerative heat exchanger, J. Inst. Mech. Engrs, 159, 363-372, (War Emergency Issue no. 44), 1948

JAKOB M., Heat Transfer, Vol. 2, Wiley, 1957

JEFFRESON C.P., Feedforward control of blast furnace stoves, Automatica, 15, 149-159, 1979

KAN O., Automatic control system for hot blast stoves, Fuji Electrical Review, 14, 127-132, 1968

KATSURA K. and ISOBE T., Automatic control and automatic changing of hot blast stoves, Tetsu-to-Hagane Overseas, 5(1), 1965

KNEPPER W.A. and CAMPBELL W.W., Temperature distribution in the blast furnace stove, blast furnace, coke oven and raw materials, Conf. Amer. Inst. Min. Met. and Pat. Engrs., 1-6, 1958

KULAKOWSKI and ANIELEWSKI, Application of the closed methods of computer simulation to nonlinear regenerator problems, Archiwum Automatyki i Telemechaniki, 24, 49, 1979

KWAKERNAAK H., STRIJBOS R.C.W. and TIJSSEN P., Optimal operation of thermal regenerators, IEEE Trans. Aut. Cont., 14, 728-731, 1969

KWAKERNAAK H., TIJSSEN P. and STRIJBOS R.C.W., Optimal operation of blast furnace stoves, Automatica, 6, 33-40, 1970

LITTMAN H., BARILE R.G. and PULSIFER A.H., Gas-particle heat transfer coefficients in packed beds at low Reynolds numbers, Ind. and Eng. Chem. Fund., 7(4), 554-561, 1968

LITTMAN H. and SLIVA D.E., Gas-particle heat transfer coefficients in packed beds at low Reynolds numbers, Heat Transfer, VII, 1970

LONDON A.L., BIANCARDI F.R. and MITCHELL J.W., The transient response of gas-turbine plant heat exchangers - regenerators, intercoolers, precoolers and ducting, A.S.M.E. J. of Eng. for Power, 81, 433-338, 1959

LONDON A.L., SAMPSELL D.F. and McGOWAN J.G., The transient response of gas-turbine plant heat exchangers - additional solutions for regenerators of the periodic-flow and direct-transfer types, A.S.M.E. J. of Eng. for Power, 86, 127-135, 1964

MEEK R.M.G., Measurement of heat transfer coefficients in randomly packed beds by the cyclic method, N.E.L. Report no. 54, 1962

MICRO CONSULTANTS, DLX/MUSIC v.3 manual, 1979

MITCHELL S., Investigation of the factors affecting the operation of thermal regenerators, Ph.D. thesis, University of Leeds, 1982

NAHAVANDI A.N. and WEINSTEIN A.S., A solution to the periodic-flow regenerative heat exchanger problem, Appl. Sci. Res., A10, 335-348, 1961

NUSSELT W., Die Theorie des Winderhitzers, Z. Ver. Deutch. Ing., 71, 1927

PENNEY M.E., Private Communication, 1984

RAZELOS P. and BENJAMIN M.K., Computer model of thermal regenerators with variable mass flow rates, Int. J. Heat Mass Transfer, 21, 735-743, 1978

SAUNDERS O.A. and FORD H., Heat transfer in the flow of gas through a bed of solid particles, J. Iron and Steel Inst., 141, 291-316, 1940

SCHLUNDER E.U., Transport phenomena in packed bed reactors, Chem. Reaction Eng. Rev., ACS Symposium Series No. 72, 1978

SCHMIDT F.W. and WILLMOTT A.J., Thermal Energy Storage and Regeneration, McGraw-Hill, 1981

SCHUMANN T.E.W., Heat transfer to a liquid flowing through a porous prism, J. Franklin Inst., 208, 405-416, 1929

SCHWARTZ C.E. and SMITH J.M., Flow distribution in packed beds, Ind. and Eng. Chem., 45, 6, 1209-1218, 1953

SHEARER C.J., Measurement of heat transfer coefficients in low-conductivity packed beds by the cyclic method, N.E.L. Report no. 55, 1962

SMITH A.D., Implementation of Staggered Parallel and Bypass Main on the Experimental Thermal Regenerator, Final Year Project Report, University of York, 1983

SPIERS H.M., Technical Data on Fuel, World Power Conf., 6th ed., 1962

STANWORTH J.E., Physical Properties of Glass, OUP, 1950

STIKKER U.O. and BROEKHUIS H., Automatic control of a hot stove system, Journees Intern. de Siderurgie, 1970

STRAUSZ I., Automatic control of a hot stove system at a blast furnace by use of a digital computer, Q. J. Aut. Cont. (Belgium), 1, 15-20, 1970

THOMAS R.J., Improved Computer Simulations of a Thermal Regenerator, D.Phil thesis, University of York, 1972

TIPPLER W., A simple theory of the heat regenerator, Shell Technical Report ICT/14, 1947

TOULOUKIAN Y.S., series editor, Thermophysical Properties of Matter, TPRC Data Series, Vol. 2, 1970

WEATH R.C., chief editor, CRC Handbook of Chemistry and Physics, 64th ed., CRC Press, 1983-1984

WILLMOTT A.J., Digital computer simulation of a thermal regenerator, Int. J. Heat Mass Transfer, 7, 1291-1302, 1964

WILLMOTT A.J., Simulation of a thermal regenerator under conditions of variable mass flow, Int. J. Heat Mass Transfer, 11, 1-11, 1968

WILLMOTT A.J., The regenerative heat exchanger computer representation, Int. J. Heat Mass Transfer, 12, 997-1014, 1969a

WILLMOTT A.J., Simulation of a thermal regenerator under conditions of variable flow, Int. J. Heat Mass Transfer, 12, 1105-1115, 1969b

WILLMOTT A.J., Computer Simulations of a Thermal Regenerator, Ph.D. thesis, University of Manchester, 1971

WILLMOTT A.J. and BURNS A., The recuperator analogy for the transient performance of thermal regenerators, Int. J. Heat Mass Transfer, 22, 1107-1115, 1979

WILLMOTT A.J. and WRAITH A.E., The modelling and regulation of a regenerator system under varying operating conditions, York Computer Science Report, 50, 1982

ZUIDEMA P., Non-stationary operation of a staggered parallel system of blast furnace stoves, Int. J. Heat Mass Transfer, 15, 433-442, 1972